AMYLOID PRECURSOR PROTEIN PROCESSING AND REDOX BALANCE IN THE DEVELOPMENT OF ALZHEIMER'S DISEASE

RICHARD J ELSWORTHY

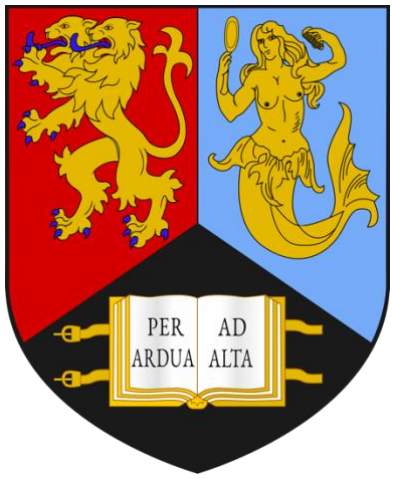

A thesis submitted to the University of Birmingham for the degree of DOCTOR OF PHILOSOPHY

School of Sport, Exercise and Rehabilitation Sciences

College of Life and Environmental Sciences

University of Birmingham

23/06/2020

ABSTRACT

Alzheimer's Disease (AD) is the leading cause of dementia and is characterised by progressive and irreversible neurodegeneration. The societal increase in average lifespan and trends in the prevalence of obesity are both associated with an increased risk of AD. Despite advancements in our understanding of the biochemical processes underlying AD, such as perturbed Amyloid- β Precursor Protein (AβPP) processing and disrupted redox homeostasis, finding new treatments that can prevent the neurodegenerative process has proved difficult. Recently, there has been growing interest in the 'a disintegrin and metalloproteinase' -10 (ADAM10) enzyme as both a biomarker for detecting AD and as a potential avenue for intervention. ADAM10 has been shown to have a favourable role in AβPP processing, therefore, strategies aimed at increasing ADAM10 enzymatic activity may hold therapeutic benefits.

The thesis presented contains four empirical research chapters (chapters 3-6). In chapter 3, the research was focused on measuring peripheral markers associated non-amyloidogenic platelet AβPP processing, inflammation and oxidative stress in people who may be 'at risk' of AD. This research showed that lowered platelet ADAM10 and elevated markers of oxidative stress were associated with advancing age and obesity. However, there was no change in the AβPP isoform ratio. Lowered platelet ADAM10 has been previously shown to be predictive of AD and worsening cognitive function, this research suggests ADAM10 may a useful tool in determine people 'at risk' of AD.

Research in chapter 4 focused on the characterisation of markers associated with AβPP processing and redox balance in induced pluripotent stem cell (iPSC) models carrying one of two *PSEN1* mutations (L286V and R278I) compared to a healthy control line. The main findings demonstrated that AβPP processing was altered towards the pro-amyloidogenic

pathway, with increased Aβ secretion, reduced ADAM10 protein levels and a lower AβPP ratio in both *PSEN1* mutations. Further, markers of oxidative stress were typically elevated in *PSEN1* mutations. These features are consistent characteristics identified in people with AD and therefore, this '*in vitro'* model represents a functional system to study the early pathological features of AD.

Work in chapter 5 investigated the functionality of the Serotonin-4 receptor (5HT4r) in the healthy control and L286V mutation carrying iPSC cortical models. This work extended to assess whether 5HT4r modulation affected ADAM10 activity. Detection of the 5HT4r by a polyclonal antibody (ab60359, Abcam) using both western blotting and immunocytochemistry showed positive staining for the receptor at the predicted molecular weight. Functional neuronal depolarisation was detected using a calcium tracking probe as a result of agonist / antagonist incubation. Treatment with the 5HTr agonist, Prucalopride, significantly increased ADAM10 activity in L286V cells, but not healthy controls.

Finally, chapter 6 focused on the effect of continuous treatment with a Selective serotonin reuptake inhibitor (SSRI), Citalopram, on ADAM10 activity, Aβ-peptide generation and redox balance in the L286V PSEN1 mutation and healthy control iPSC models. Treatment with Citalopram significantly increased ADAM10 activity and reduced markers of oxidative stress in iPSC-derived cortical cell models carrying *PSEN1* mutations. Differential effects on Aβ generation were shown in control cells, with a reduction in Aβ generation at a dose of 0.8μM and elevated Aβ generation at 10μM. However, there were no changes in Aβ generation in L286V mutation carrying cells. This data suggests that treatment with Citalopram may hold protective effects on processes underlying AD, possibly, through the modulation of ADAM10 activity.

The research presented in this thesis highlights the potential role for ADAM10 in the early development of AD and demonstrates a therapeutic role of SSRIs in modifying ADAM10 expression and correcting redox imbalance in an iPSC-derived cortical cell model of AD. Further research aimed at improving our understanding of how ADAM10 is regulated across the lifespan and whether it is a useful biomarker for assessing risk of AD is needed. Mechanistically the association of ADAM10 with other membrane receptors, and the impact of this colocalisation on ADAM10 activity should be further investigated.

ACKNOWLEDGEMENTS

I would like to thank the following people for their support throughout my PhD, without them I would not have been able to complete this research.

Firstly, thank you to Dr Sarah Aldred for guiding me throughout this project, allowing me the freedom to develop my own research ideas and shape my PhD, whilst challenging me to become a better academic.

I would also like to thank Dr Eric Hill and Dr Melissa Grant for welcoming me into their labs and providing valuable resources for me to progress my research.
Further, I would like to thank the guys over at Aston University, Ally, James, Marianne and Adele. You were never too busy to help me, giving up your own time, and I appreciate that.

I would also like to thank Emily Fisher for her support over the last four years as a fellow PhD student, swimming partner and most importantly as a friend who I could always count on.

Finally, I would like to thank my family and friends at home. Their continuous love and support made the whole journey easier. I would especially like to thank my parents for supporting me, for always listening to me and showing interest in my work, even if they didn't understand half the things I was talking about.

PUBLICATIONS

Elsworthy RJ, Aldred S. 2019. Depression in Alzheimer's Disease: An Alternative Role for Selective Serotonin Reuptake Inhibitors? *Journal of Alzheimer's Disease*, 69: 651-661.

Elsworthy RJ, Aldred S. 2020. The Effect of Age and Obesity on Platelet Amyloid Precursor Protein Processing and Plasma Markers of Oxidative Stress and Inflammation. *Experimental Gerontology,* 110838.

Fisher, E., Wood, S. J., Elsworthy, R. J., Upthegrove, R., & Aldred, S. (2020). Exercise as a protective mechanism against the negative effects of oxidative stress in first-episode psychosis: a biomarker led study. Translational Psychiatry, 10, 254.

CONTENTS

PUBLICATIONS ..... **v**

LIST OF FIGURES ..... **xii**

LIST OF TABLES ..... **xvii**

ABBREVIATIONS ..... **xviii**

CHAPTER 1 - INTRODUCTION **1**

1.1 The global burden of Dementia 1

1.2 Alzheimer's Disease 1

1.3 Familial Alzheimer's Disease 2

1.3.1 The APP gene *3*

1.3.2 PSEN1 and PSEN2 genes *4*

1.4 Late-onset Alzheimer's Disease 4

1.4.1 Non-modifiable risk factors for LOAD *5*

1.4.2 Modifiable Risk Factors for LOAD *7*

1.5 The Neuropathological Features of Alzheimer's Disease 8

1.5.1 Intracellular neurofibrillary tangles *10*

1.5.2 Extracellular amyloid plaques *11*

1.6 Processing of the amyloid precursor protein 12

1.6.1 The non-amyloidogenic AβPP processing pathway *14*

1.6.2 ADAM10 ..... *14*

1.6.3 Soluble AβPP- α *15*

1.6.4 The amyloidogenic AβPP processing pathway *16*

1.6.5 BACE-1 ..... *16*

1.6.6 Soluble AβPP-β *17*

1.6.7 Amyloid-β *18*

1.6.8 The γ-secretase protein complex *21*

1.7 Oxidative Stress and Alzheimer's Disease 22

1.7.1 Mitochondria, reactive oxygen species and Aβ *24*

1.7.2 Lipid, protein and DNA damage in Alzheimer's disease *25*

1.8 The Diagnosis of Alzheimer's Disease 28

1.8.1 Clinical assessment *29*

1.8.2 Brain imaging *31*

1.8.3 Fluid biomarkers *32*

1.8.4 Platelets in Alzheimer's disease *34*

1.8.5 The importance of early diagnosis *36*

1.9 Treatment for Alzheimer's Disease 36

1.9.1 Treatments directly targeting Aβ *37*

1.9.2 BACE-1 and γ-secretase inhibitors *38*

1.9.3 Targeting ADAM10: a therapeutic option? *39*

1.10 An Alternative Role for Selective Serotonin Reuptake Inhibitors for the Treatment of Alzheimer's Disease? 42

1.10.1 Mechanisms of action *43*

1.11 Modelling the Brain Using Induced Pluripotent Stem Cells 47

1.11.1 Presenilin mutations as viable model to study AD? *48*

1.12 Research Aims 49

CHAPTER 2 - GENERAL METHODS 52

2.1 Culturing Protocol of iPSC's: From Stem Cell to Cortical Networks 52

2.1.1 Preparation and coating of Geltrex™ *54*

2.1.2 Thawing, expansion and maintenance of HiPSC's *54*

2.1.3 Passage of HiPSC's *55*

2.1.4 Freezing HiPSC's for cryopreservation in liquid nitrogen *55*

2.1.5 Induction of HiPSC's to HNSC *56*

2.1.6 Freezing HNSC's for cryopreservation in liquid nitrogen *57*

2.1.7 Thawing and expansion of HNSC's *58*

2.1.8 Spontaneous differentiation of HNSC's into neuron and astrocyte co-cultures *58*

2.1.9 Preparation of cellular fractions and media collection *59*

2.2 Live Cell Assays 59

2.2.1 Fluo-4AM imaging *59*

2.2.2 MitoSOX Red assay *60*

2.3 Methods of Assessing Protein Expression 60

2.3.1 Immunocytochemistry *60*

2.3.2 Determination of protein concentration *61*

2.3.3 Western blotting *62*

2.4 Plate-based Assays 62

2.4.1 Interleukin-6 ..... *62*

2.4.2 ADAM10 enzyme activity *63*

2.4.3 Quantification of Amyloid-β peptides 1-40 and 1-42 in cell media *64*

2.4.4 Quantification of Amyloid-β oligomers in cell media *65*

2.4.5 Total 8-isoprostanes *65*

2.4.6 Protein carbonyls *66*

2.4.7 Total antioxidant capacity *68*

2.4.8 Succinate dehydrogenase activity (MTT) assay *68*

2.5 Statistical Analysis 69

CHAPTER 3 - THE EFFECT OF AGE AND OBESITY ON PLATELET AMYLOID PRECURSOR PROTEIN PROCESSING AND PLASMA MARKERS OF OXIDATIVE STRESS AND INFLAMMATION 70

3.1 Background 70

3.1.1 Inflammation and oxidative stress in ageing 70

3.1.2 Inflammation and oxidative stress in obesity 72

3.1.3 Alzheimer's disease in ageing and obesity 73

3.2 Methods 75

3.2.1 Participants 75

3.2.2 Blood collection 76

3.2.3 SDS-PAGE and Western blotting 76

3.2.4 Plate-based Assays 77

3.2.5 Statistical Analysis 77

3.3 Results 78

3.3.1 Participant characteristics 78

3.3.2 Inflammation 79

3.3.3 Oxidative stress 80

3.3.4 Platelet AβPP processing markers 82

3.4 Conclusion 84

CHAPTER 4 - CHARACTERISATION OF AβPP PROCESSING AND REDOX BALANCE IN SPONTANEOUSLY DIFFERENTIATED HUMAN iPSC-DERIVED NEURON AND ASTROCYTE CO-CULTURES CARRYING PSEN1 GENE MUTATIONS 88

4.1 Background 88

4.2 Methods 93

4.2.1 Culturing and neuralisation of iPSC's to HNSCs 93

4.2.2 Expansion and spontaneous differentiation of HNSC's 93

4.2.3 Cell characterisation using ICC 94

4.2.3 SDS-PAGE and Western blotting 94

4.2.4 Plate-based assays 95

4.2.5 Statistical Analysis 95

4.3 Results 95

4.3.1 Immunocytochemical cell characterisation 95

4.3.2 ADAM10, AβPP and Aβ are altered in PSEN1 mutations 99

4.3.3 Redox balance is perturbed in cocultures carrying PSEN1 mutations 103

4.4 Conclusion 105

CHAPTER 5 - THE 5HT4 RECEPTOR IN iPSC-DERIVED NEURON AND ASTROCYTES 110

5.1 Background 110

5.2 Methods 113

5.2.1 Cell culture and immunodetection of 5HT4r 113

5.2.2 Calcium imaging 113

5.2.3 ADAM10 activity 114

5.2.4 Statistical Analysis 115

5.3 Results 115

5.3.1 Immuno-based detection of 5HT4r 115

5.3.2 Functional 5HT4r respond to selective agonists 117

5.4 Conclusion 121

CHAPTER 6 - THE EFFECT OF CITALOPRAM TREATMENT ON AβPP PROCESSING AND REDOX BALANCE 124

6.1 Background 124

6.2 Methods 126

6.2.1 Optimising Citalopram treatments 126

6.2.2 Longitudinal delivery of Citalopram treatments 126

6.2.3 ADAM10 activity 127

6.2.4 AβPPr measured by Western Blotting 127

6.2.5 Mitochondrial ROS production 127

6.2.6 Plate-based assays 128

6.2.7 Statistical Analysis 128

6.3 Results 129

6.3.1 Optimisation of Citalopram doses 129

6.3.2 AβPP processing 130

6.3.3 Oxidative stress 134

6.4 Conclusion 138

CHAPTER 7 - GENERAL DISCUSSION 141

REFERENCES 152

LIST OF FIGURES

Figure 1 - Diagrammatic representation of the trafficking and processing of AβPP from intracellular compartments to the cell membrane. Major AβPP cleavage sites of ADAM10 and BACE-1 activity are shown and represent the 'non-amyloidogenic' and 'amyloidogenic' pathways respectively. 13

Figure 2 - ROS cascade starting from the initial generation of Superoxide anions. Propagation of oxidative molecules is dependent on interaction with antioxidant enzymes (green) or the oxidation of other biomolecules (Red). Myeloperoxidase (MPO, Blue) is an enzyme that forms part of the microbial defence system not covered in this thesis. 28

Figure 3 - Diagrammatic representation of the therapeutic targets SSRI's may positively effect that are altered in both depression and AD. 47

Figure 4 - Diagrammatic outline of research chapters presented in this thesis. 51

Figure 5 - Effect of age (years) and BMI (kg/m^2) on plasma markers of inflammation and oxidative stress. **A**, Plasma IL-6 (pg/ml) compared between groups. **B**, Concentrated plasma 8-isoprostane (pg/ml) compared between groups. **C.** ROC analysis for predictive capacity of plasma IL-6 (solid line) and isoprostanes (dashed line) to distinguish between obese and non-obese participants. **D**, ROC analysis for predictive capacity of plasma protein carbonyls (solid line) and isoprostanes (dashed line) to distinguish between young and old participants. * indicates a significant difference between corresponding groups... 81

Figure 6 - Effect of age (years) and BMI ($kg.m^2$) on platelet protein levels of AβPP isoforms and ADAM10 measured via western blotting in a sub sample of participants (Young/Lean n=8, Young with obesity n=6, Old/Lean n=8, Old with obesity n=7). **A**, Platelet protein levels of mADAM10 (AU) normalised to Actin compared between groups. **B**, Platelet protein levels of proADAM10 (AU) normalised to Actin compared between groups. **C.** Platelet protein levels of AβPP (AU) analysed at the ratio between upper and lower band compared between groups. **D**, Images of western blotting for AβPP (Upper box), ADAM10 (middle) and Actin as a control protein (Lower box). *significantly lower than Young/Lean # significantly lower than Young/Obese 83

Figure 7 – Confocal microscopy images of iPSC's with ICC staining taken at 40x magnification. fAD iPSCs were fixed at in PFA and stained for **A**. DAPI nuclear stain. **B.**

Oct4 (green) **C.** Sox2 (red) **D.** Merge showing co-expression of DAPI, Oct4 and Sox2. (Scale bars to 50µm). 96

Figure 8 – Confocal microscopy images of HNSC's with ICC staining taken at 20x magnification. NPCs were fixed in PFA at day 7 following neural induction. The white box indicates an exemplar neural rosette formation **A**. DAPI nuclear stain. **B.** Pax6 (green) **C.** Sox2 (red) **D.** Merge showing co-expression of DAPI, Pax6 and Sox2. (Scale bars to 100µm). 97

Figure 9 – Confocal microscopy images of radial glia in co-culture with ICC staining taken at 40x magnification. Formation of immature astrocytes at day 20 **A**. DAPI nuclear stain. **B.** S100β (green) **C.** GFAP (red) **D.** Merge showing co-expression of DAPI, S100β and GFAP. (Scale bars to 100µm). 98

Figure 10– Confocal microscopy images of neuron and astrocytic co-culture with ICC staining taken at 40x magnification. Neuron and astrocyte co-cultures at day 45. **A**. DAPI nuclear stain. **B.** S100β (green) **C**. TUJ1 (red) **D**. Merge showing co-expression of DAPI, S100β and TUJ1. (Scale bars to 100µm). 99

Figure 11 - Graphs showing the individual data points for cell lysate replicates (45 days old) analysed via western blotting relative to total protein densitometry. Cell lysates from healthy control (n=5), L286V (n=5) and R278I (n=3) were separated using SDS-PAGE electrophoresis followed by western blotting. Densitometry was quantified using Licor C-digit and image studio software. **A & B.** mADAM10 and ProADAM10 expression (AU) normalised to total protein densitometry which can be seen on the right. Representative blot images show both the immature 85kDa proADAM10 and mature/active 68kDa mADAM10 detected by Ab1997 antibody corresponding to table above. **B.** AβPPr quantified by the ratio of bands at 130kDa to 110kDa. Representative blotting images of AβPP bands detected using Mab348 antibody corresponding to table above. *Significantly different to matched Cell Line ($p<0.05$) **($p<0.01$) 101

Figure 12 - Graphs showing the individual data points for media concentration replicates of **A.** Aβ1:40 and **B.** Aβ1-42 (pg/ml) analysed via ELISA in Healthy control (n=5), L268V (n=5) and R278I (n=3) at day 45 post neural induction. **C.** Shows the sum of Aβ1:40+1:42 peptides to give total amyloid Aβ1:40 and 1:42 secretion. **D.** The ratio of Aβ1:42 to

Aβ1:40 is shown in Arbitrary units (AU). **E.** Aβ oligomers (ng/ml) (n=3 for each cell line) *Significantly different to matched Cell Line ($p<0.05$) **($p<0.01$).....102

Figure 13 - Graphs showing the individual data point replicates for markers of redox balance in cell lysates (45 days old) normalised to cellular protein content. **A.** Protein carbonylation in healthy control (n=7), L286V (n=7) and R278I (n=3) measured via ELISA (mg/ml) B. Total 8-isoprostanes in immunopurified lysate preparations from healthy control (n=4), L286V (n=4) and R278I (n=3) quantified by ELISA (pg/mg/ml) **C**. Cellular antioxidant capacity relative to ascorbic acid measured in healthy control (n=7), L286V (n=7) and R278I (n=3) using colorimetric assay (µg/mg). Regression analysis between markers of oxidative stress and AβPP processing. **D.** Protein carbonylation (mg/ml) and mADAM10 expression (AU) measured via ELISA and Western blot respectively. **E.** Protein carbonylation (mg/ml) and AβPPr (AU) measured via ELISA and Western blot respectively. *Significantly different to matched Cell Line ($p<0.05$) **($p<0.01$) 104

Figure 14 – Diagram showing the potential interaction of 5HT4 receptor with ADAM10 at the cell membrane. Agonist binding, shown here by 5HT, stimulates ADAM10 activity and therefore, increases non-amyloidogenic AβPP processing.....112

Figure 15 – ICC images of control cells 45 days post differentiation taken at 40x magnification (scale bars at 50µm) and protein expression via western blotting. **A1** - DAPI (blue) nuclear stain. **A2** - 5HT4r (green). **A3** - AβPP (red). **A4 -** Merge of A1, A2 and A3 to show co-staining. B. Two identical bands ~ 44kDa after detection with anti-5HT4r antibody in 20µg cell lysate (n=2). Right panel shows identical samples after detection with secondary antibody only. 116

Figure 16 – Traces displaying baseline adjusted relative fluorescence (RFU) of Fluo-4AM calcium binding averaged over time in five ROIs (N=3). In all conditions from 0-5 minutes aCSF was perfused over cells to allow for baseline measurements **A.** Shows a calcium trace at baseline followed by 5HT (20µM) perfusion (blue line) and then aCSF (red line). **B.** Shows a calcium trace at baseline, with Prucalopride (10µM) (blue line), Prucalopride and 5HT (red line) and Prucalopride, 5HT and GR113808 (50µM) (green line). **C.** Shows a calcium trace at baseline, with GR113808 (blue line) and GR113808 and Prucalopride (red line). 118

Figure 17 – Comparison of ADAM10 activity measured via FRET assay in iPSC derived neuron and astrocyte co-cultures (day 45 post induction). **A.** Baseline ADAM10 activity in control cells (n=6) compared to treatment with 5HT (n=2), Prucalopride (n=6) and GI254023X (n=2). **B.** Baseline ADAM10 activity in L286V cells compared to L286V cells treated with 5HT (n=2) and Prucalopride (n=6). Al treatments were for 2 hours prior to assay. *Significantly different to matched condition. 120

Figure 18 – Percentage viability after treatment with Citalopram (μM) measured via MTT assay in control cells at 45 days post differentiation. Each dose was replicated 3 times **A.** Sigmoidal four-parameter variable slope of percentage viability against $\log^{10}$ Citalopram concentration (μM). Red line shows IC50. **B.** Bar graph representation of percentage viability to highlight significant decrease from baseline shown by * ($p<0.05$), (n = 3). 129

Figure 19 – Data displaying ADAM10 activity and APPr in control (solid bars) and L286V (spotted bars) cells after continuous treatment with 0μM (n=5), 0.8μM (n=2), 5μM (n=2), 10μM (n=2) of Citalopram for 45 days post differentiation. ADAM10 activity (n=3 all conditions) measured via FRET assay (**A&B**) and AβPPr measured by western blotting (**C&D**). Example loading of western blots in L286V cells displayed in **E**. *Significantly different to 0μM treatment condition. 131

Figure 20 - Data displaying Aβ secretion into spent media from control (solid bars) and L286V (spotted bars) cells after continuous treatment with 0μM (n=5), 0.8μM (n=2), 5μM (n=2), 10μM (n=2) of Citalopram for 45 days post differentiation. **A-D** shows data for control cells, **E-F** shows data for L286V cells. *Significantly different to 0μM treatment condition. 133

Figure 21 – Figures displaying MitoSOX Red assay data in cells 45 days post differentiation (N=3). **A.** Change in fluorescence over time in control (AX0018) cells at basal rates. Red line depicts the change in fluorescence (RFU) with the addition of with H_2O_2 (100μM) indicating increased ROS production. **B.** Comparison of basal ROS production from MitoSOX Probe binding between control and L286V (n=3). **C-D**. Change in ROS generation after being treated continuously for 45 days with Citalopram at different doses (μM) *Significantly different to L286V cells under no treatment condition ($p<0.05$) (**$p<0.01$)..... 135

Figure 22 – Figures displaying markers of oxidative stress data in cell lysates 45 days post differentiation after different treatments with Citalopram, 0μM (n=7) 0.8μM (n=2), 5μM (n=2) and 10μM (n=2). **A-B** Protein carbonylation (mg/ml) in Control cells (Left, solid bars) and L286V cells (Right, spotted bars). **C-D** Total 8-isoprostanes (pg/mg/ml) in Control cells (Left, solid bars) and L286V cells (Right, spotted bars). **E-F** Antioxidant capacity (μM/mg) in Control cells (Left, solid bars) and L286V cells (Right, spotted bars). *Significantly different to L286V cells under no treatment condition ($p<0.05$) (**$p<0.01$). 137

LIST OF TABLES

Table 1 - Information on cell lines used for modelling Alzheimer's disease and healthy control 52

Table 2 - Neural induction media (NIM) made by the addition of small molecule signalling pathway inhibitors to Essential 6 as a base medium. 57

Table 3 - Characteristics and comparison of the participant sample 79

Table 4 – aCSF constituents used for baseline calcium signalling measurements and experimental compounds. 114

ABBREVIATIONS

5HT - Serotonin

5HTr – Serotonin Receptor

aCSF – Artificial Cerebrospinal Fluid

AD – Alzheimer's Disease

ADAM10 – 'a disintegrin and metalloproteinase' 10

APOE – Apolipoprotein E

AU – Arbitrary Units

Aβ – Amyloid-beta

AβPP – Amyloid-β Precursor Protein

AβPPr -Amyloid-β Precursor Protein ratio

BACE1 – Beta Amyloid Cleaving Enzyme-1

BCA – Bicinchoninic Acid

BMI – Body mass index

CDR – Clinical Dementia Rating

CNS – Central Nervous System

CSF - Cerebrospinal fluid

CT – Computerised tomography

CTF – C-Terminal Fragment

fAD – Familial Alzheimer's Disease

FRET – Fluorescence Resonance Energy Transfer

HNSC – Human Neural Precursor Cell

ICC – Immunocytochemistry

IL-6 - Interleukin-6

iPSC – Induced Pluripotent Stem Cell

JNK - C-jun N-terminal kinase

LOAD – Late-onset Alzheimer's Disease

mADAM10 – Mature ADAM10

MCI – Mild Cognitive Impairment

MAPT - Microtubule-Associated Tau

MMSE – Mini Mental State Examination

MRI – Magnetic resonance imaging

MTT – 3-(4,5-dimethylthiazol-2-yl)-2,5-diphenyltetrazolium bromide

NF-κB - Nuclear Factor κ-light-chain-enhancer of activated B cells

NIM – Neural Induction Media

NMDA - N-Methyl-D-Aspartate

NMM - Neural Maintenance Media

NPC – Neural Progenitor Cell

PBS – Phosphate Buffered Saline

PET – Positron emission tomography

ProADAM10 – Prodomain-intact immature ADAM10

PRP – Platelet-rich Plasma

PrP^{C} – Cellular Prion Protein

PS1 – Presenilin protein 1

PSEN1 – Presenilin 1 (gene)

PSEN2 – Presenilin 2 (gene)

REDOX – Reduction/Oxidation

RFU – Relative Fluorescence Units

ROS – Reactive Oxygen Species

RT – Room Temperature

sAβPP-α – Secreted Amyloid-β Precursor Protein α

sAβPP-β - Secreted Amyloid-β Precursor Protein β

SDS-PAGE – Sodium dodecyl sulphate – Poly Acrylamide Gel Electrophoresis

SSRI – Selective Serotonin Reuptake Inhibitor

TBST – Tris Buffered Saline with Tween20

TSPAN – Tetraspanin

CHAPTER 1 - INTRODUCTION

1.1 The global burden of Dementia

Dementia is an umbrella term used to describe a number of neurocognitive disorders as a result of brain disease or injury and is characterised by memory loss, personality changes, and impaired reasoning (Hugo and Ganguli, 2014). Ageing is the greatest risk factor for developing dementia (Prince et al., 2016) and currently a third of older people die with a form of dementia. With worldwide trends for life expectancy increasing, the prevalence of dementia is predicted to triple by 2050 (Livingston et al., 2017). However, this does not mean dementia is a normal part of ageing. Advancements in our understanding of the pathological processes underlying specific types of dementia will enable us to delay or even prevent the onset of symptoms. The trajectory of the dementia-associated symptoms is often variable between individuals which can significantly impact quality of life. Some individuals may experience more neuropsychiatric symptoms such as depression and anxiety, whereas others may experience severe short-term memory loss or amnesia (Jahn, 2013). Nonetheless, dementia is debilitating for a number of years prior to death (Melis et al., 2019). In addition, associated economic burden will be unsustainable unless action to prevent and treat dementia is taken.

1.2 Alzheimer's Disease

Alzheimer's disease (AD) is the leading cause of dementia affecting around 5% of people over the age of 60 years old and as many as 50% over the age of 85 years old. AD is characterised by progressive and irreversible neurodegeneration. Typically, AD presents as set of mild symptoms including changes in mood, short term memory loss, difficulty maintaining conversation, confusion and agitation. Onset of the first symptoms is often

preceded by a period known as mild cognitive impairment (MCI), although MCI is not pre-AD, i.e. it is not a certainty that people with MCI will go on to develop AD. Although the observed cognitive decline in MCI is greater than that associated with normal ageing it may never progress to AD and in some cases can fully reverse (Petersen et al., 2019). The progression of symptoms in AD can vary between individuals however, life expectancy is around 3-10 years from the onset of symptoms.

The first documented case of what is now known as AD was in 1907 by a German scientist called Alois Alzheimer. He published findings of a patient who had developed 'rapid memory loss and became disorientated in space and time' named Auguste D. (Small and Cappai, 2006, Alzheimer et al., 1995). Post-mortem examination revealed widespread atrophy of the brain, extracellular plaques and intracellular tangled proteins. This was the first documented case of what is now known as AD. The features described by Alois Alzheimer are now considered hallmarks of the AD brain and have been identified as the core neuropathology of AD. As previously mentioned, the onset of AD symptoms typically arises later in life, however, there have been numerous documented cases of AD-related symptoms and matching pathology in individuals at much younger ages. Familial AD (fAD) is caused by known genetic origins with symptoms becoming apparent much earlier on in life. The more common type of AD, late-onset AD (LOAD) however, is a multifactorial disease with a combination of non-modifiable and modifiable risk factors contributing (*see 1.4.1 and 1.4.2 respectively).*

1.3 Familial Alzheimer's Disease

fAD is a rare hereditary condition making up around 5% of all AD diagnoses (Mendez, 2019). The symptoms of fAD develop between the ages of 30-65 and therefore fAD

is commonly termed ‘early-onset AD’. fAD is caused by a number of possible gene mutations to either chromosomes 21 (Patterson et al., 1988), 14 (Del-Favero et al., 1999) or 1 (Levy-Lahad et al., 1995). These autosomal-dominant gene mutations are often fully penetrant and have been highly informative in the search for the cause of AD (Nikolac Perkovic and Pivac, 2019).

1.3.1 The APP gene

The *APP* gene codes for the Amyloid-β Precursor Protein (AβPP) located on chromosome 21. Although the physiological roles of AβPP are not fully understood it is thought to play a crucial role in neurodevelopment, acting as a cell signalling protein. Within the amino acid sequence of AβPP is the Aβ region. This is a key site for gene mutations that can significantly alter the breakdown of AβPP, increase the aggregation potential of Amyloid-β peptides generated towards oligomeric forms and alter γ-secretase processing resulting in different lengths of Aβ peptides (Goate and Hardy, 2012). The first mutations to the *APP* gene were discovered in families with fAD and all mutations occurred at the carboxyl end of the Aβ region which is located in the transmembrane portion of AβPP (Chartier-Harlin et al., 1991, Murrell et al., 1991). Since then there have been multiple pathogenic mutations to the *APP* gene identified, some even on the same amino acid residues, which all lead to fAD. These mutations tend to be on exons 16 and 17 which encode the Aβ peptide. More recently, duplication of the *APP* locus has been shown to cause fAD (Rovelet-Lecrux et al., 2006). This placed the AβPP and the Aβ peptide in the spotlight for the majority of future AD research.

1.3.2 PSEN1 and PSEN2 genes

Despite the discovery that mutations to the *APP* gene caused fAD there were still cases of families without the *APP* gene mutation who presented with similar cognitive deficits and neurological lesions. This quickly led to the identification of a mutation on chromosome 14 (Schellenberg et al., 1992). Such mutations were found to be on the Presenilin-1 (*PSEN1*) gene locus and are the most common cause of fAD (Clark et al., 1995). There are now known to be over 200 *PSEN1* mutations which, unlike the localisation of *APP* mutations to the Aβ region, are spread throughout the translated protein.

At the same time *PSEN1* mutations were being uncovered, a third candidate gene mutation for fAD was proposed. The Presenilin-2 (*PSEN2*) gene located on chromosome 1 was identified as a homologous protein sequence to the *PSEN1* gene (Levy-Lahad et al., 1995). However, *PSEN2* gene mutations are incredibly rare with only 12 known missense mutations leading to fAD. In some cases, *PSEN2* mutations are only partially penetrant for fAD (Sherrington et al., 1996). The newly discovered *PSEN1* and *PSEN2* were determined to belong to a family of conserved genes that coded for Presenilin proteins 1 (PS1) and 2 respectively (Rogaev et al., 1995). The Presenilin proteins are a critical subunit of an enzyme responsible for the breakdown of AβPP and has added significant weight to the inclusion of altered Aβ peptide generation in AD pathology.

1.4 Late-onset Alzheimer's Disease

LOAD is the more prevalent type of AD accounting for more than 95% of cases. In contrast to fAD, LOAD is a multifactorial disease with both modifiable and non-modifiable risk factors contributing to an individual's risk. Although LOAD by definition is a progressive irreversible neurodegenerative disease the onset and development of symptoms

can be delayed by adhering to a 'neuro-protective' lifestyle and such 'modifying' risk of development (Xu et al., 2015).

1.4.1 Non-modifiable risk factors for LOAD

The risk of a person developing LOAD is affected by several risk factors that are non-modifiable, that is, things that an individual cannot change. Of these, ageing is the single greatest risk factor and symptoms of LOAD typically become apparent after the age of 65 years old (Winblad et al., 2016). The risk of LOAD increases approximately 2-fold every 5 years above the age of 65 (Corrada et al., 2008, Plassman et al., 2007, Lobo et al., 2000). The association of increasing age with LOAD is thought to be due to several hallmark biological processes of ageing including genomic instability, telomere attrition, cellular senescence, stem cell exhaustion, mitochondrial dysfunction and a loss of proteostasis (for a comprehensive review see (Hou et al., 2019)). The brain is particularly susceptible to age related degeneration as it is mainly comprised of post-mitotic cells. Therefore, under increased cellular stress cells have limited regenerative capacity and will be more likely to enter an apoptotic fate (Castillo-Morales et al., 2019). However, it is important to consider that LOAD is not part of normal ageing and many of the 'ageing hallmarks' can in fact be attenuated by engaging in healthy behaviours across the lifespan. In addition to ageing, an individual with a family history of LOAD is at a greater risk of AD themselves. This is due to a combination of two factors: hereditary genetic risk that a person may carry; and the environment that a person is exposed to. Unlike monogenic fAD gene mutations, the genetic risk factors for LOAD are not causal in nature, meaning a person may carry a gene that predisposes a greater risk for AD but never experience clinical symptoms. The most well studied genetic risk factor for LOAD is the Apolipoprotein E (*APOE*) gene. The *APOE*

protein is found in both peripheral and central tissues and is involved in immunoregulation, cell growth (Belloy et al., 2019) and is known to play a critical role in cholesterol transport (Mahley, 1988). There are three isoforms of the *APOE* gene, *APOE* e2, *APOE* e3 and *APOE* e4 and each person carries a combination of two alleles (Zannis et al., 1982). The *APOE* e3 gene is the most commonly carried. Carrying one or two copies of the *APOE* e2 variant is associated with a person having a decreased risk of developing LOAD. In contrast, carriers of the *APOE* e4 allele are at an increased risk of developing LOAD (van der Lee et al., 2018, Corder et al., 1993, Strittmatter et al., 1993). Carrying two copies of the *APOE* e4 gene can increase the risk of LOAD by 50% compared to those carrying at least one copy of the *APOE* e2 variant. This translates into an 18-23 year difference in age of onset (van der Lee et al., 2018). Early genome-wide association studies (GWAS) consistently identified *APOE* as a significant risk factor for LOAD, however, these were in relatively small sample sizes (>2000 participants) (Neuner et al., 2020). More recently, larger GWAS studies have highlighted over 20 genetic risk factors affecting an individual's susceptibly to developing LOAD (Kunkle et al., 2019, Marioni et al., 2018). Functionally, these are genes involved in cholesterol and lipid metabolism, endocytosis, and immune responses (Rezazadeh et al., 2019) with a number being particularly enriched in astrocytes, microglia and myeloid cells (Pimenova et al., 2018). From this data it is becoming more apparent of a role of the immune system in the development of AD rather than a secondary immune response (Jansen et al., 2019). There are also novel genes identified that are functionally associated with AD such as rare coding variants effecting *ADAM10* and *APH1B* which encode for enzymes involved with AβPP processing (Kunkle et al., 2019).

However, the role of other identified genes is not as strongly associated with LOAD onset as that of *APOE* and this is currently a key area of research to assess preclinical LOAD

risk. The interaction between these genetic risk factors are thought to contribute to the heterogenous development of LOAD and can be grouped into a polygenic risk score (Chaudhury et al., 2019).

1.4.2 Modifiable Risk Factors for LOAD

Although a person's genetic makeup can increase their susceptibility to LOAD, engaging in a healthy 'neuroprotective' lifestyle can delay or even prevent cognitive symptoms developing (Edwards Iii et al., 2019). Modifiable risk factors represent measures a person can take to minimise their risk of LOAD, such as regular exercise and a nutritionally balanced diet (Sampaio et al., 2019, Vassilaki et al., 2018, McGurran et al., 2019). These modifiable lifestyle choices have a direct effect on brain health via improved cerebral blood flow and vessel health, increased synaptic plasticity and regulation of neurotrophic factors (Cabral et al., 2019, Jackson et al., 2016). In addition, lifestyle choices can significantly impact common comorbid diseases that increase the risk of LOAD such as obesity and the metabolic syndrome, cardiovascular disease and diabetes (Green and Smith, 2018, Alford et al., 2018).

Obesity has been of particular research interest as there is a growing prevalence worldwide and a significant correlation with and increased risk of LOAD (Anstey et al., 2011). Therefore, a growing percentage of the population are becoming at greater risk of poor cognitive health in later life. Obesity is a multifactorial condition resulting in abnormal adipose tissue accumulation throughout the body and is associated with metabolic dysfunction. The increased risk of LOAD as a result of obesity is not caused by a single mechanism, but more globally through increased adipokine secretion, increased insulin resistance and chronic inflammation (Picone et al., 2020, Forny-Germano et al., 2018). These

can all increase oxidative stress and cellular dysfunction leading to neurodegeneration and associated co-morbidities such as diabetes and cardiovascular disease which can further increase the risk of LOAD. (Kacířová et al., 2020). There has been some debate regarding the link between obesity and AD in later-life. The late-life obesity paradox pulls from evidence showing that people who have a higher body mass index in late-life may be protected from cognitive decline and LOAD (Sun et al., 2020, Ma et al., 2019). However, this data is limited to metabolically healthy obese individuals and may be explained by disease related weight-loss prior to cognitive symptoms being recognised. The link between mid-life obesity and LOAD is more established (Berti et al., 2018, Elsworthy and Aldred, 2020, Chuang et al., 2016). Metabolic dysfunction, as a result of poor lifestyle choices highlight the importance of promoting a healthy lifestyle as a preventative measure across the lifespan rather than once cognitive symptoms are present, as this is likely too late to significantly impact disease progression (Palta et al., 2019, Zotcheva et al., 2018, Lamb et al., 2018). Research has also highlighted poor mental health, reduced sleep quality and reduced education as risk factors for LOAD (Wang et al., 2017a, Wang and Holtzman, 2020, Almeida et al., 2019).

1.5 The Neuropathological Features of Alzheimer's Disease

Although the causal onset of LOAD and fAD are different, both can be described generally by shared neuropathological features of the AD brain. Since the discovery of an accumulation of extracellular Aβ plaques and intracellular tau neurofibrils in the AD brain, significant progress has been made in our understanding of these two cardinal lesions. Initially accumulating in cognitively healthy individuals the presentation of both elevated Aβ and tau deposition are associated with future cognitive decline. However, there is not always consistent correlation between the amount of Aβ, tau deposition and the severity of AD

symptoms (Sperling et al., 2019). Several other neuropathological features have also been characterised as in the AD brain (Doan et al., 2017, Sivera et al., 2019). These include morphological changes in the brain, in particular a reduction in the hippocampal and temporal lobe volume, as well as synapse degeneration (DeTure and Dickson, 2019). These most strongly associate with the rate of cognitive decline and are most pronounced at later stages of AD (Andreotti et al., 2017, Halliday, 2017). There is also great interest in the atrophy and loss of function in specific cell types. Neuronal loss has been extensively researched and is shown to contribute to the significant reduction in brain volume and associated with disease progression (Theofilas et al., 2018). An accumulation of granule containing vacuoles in the cytoplasm of neurons containing proteins associated with tau pathology, autophagy and signal transduction pathways are also commonly seen in AD (Köhler, 2016). As our understanding of the role glial cells play in maintaining neuronal homeostasis and aiding neurotransmission evolves, it appears that astrocyte function may be a critical component in mediating the neurodegenerative process (Garwood et al., 2017, Jones et al., 2017). Reactive astrocytes and activated microglial are able to contribute to neuroinflammation which has been identified in the AD brain. Regional hypometabolism and altered glucose metabolism have also been detected using brain scanning techniques. Part of this may be explained by the loss of neurons or via synaptic degeneration which are highly energy demanding sites to maintain (Perez Ortiz and Swerdlow, 2019) (for further detail see *1.6.1 Mitochondria, reactive oxygen species and Aβ*).

The inaccessibility of the human brain makes investigation incredibly difficult, however, the significant progress has been made in our understanding of the pathological features underlying AD.

1.5.1 Intracellular neurofibrillary tangles

The key constituent of neurofibrillary tangles has been identified as hyperphosphorylated Tau. These intracellular lesions are also present in other neurodegenerative diseases, known as Tauopathies (Iqbal et al., 2005). Encoded by the Microtubule-Associated Tau (*MAPT*) gene, Tau is an important protein for stabilising microtubules and supporting the axonal transport of molecules (Caillet-Boudin et al., 2015). Tau has also been implicated in neurogenesis and maintaining neuronal activity (Wang and Mandelkow, 2016). However, the post-translational phosphorylation of Tau renders it to a non-native aggregation state. Additionally, Tau hyperphosphorylation can enable to shift of Tau from the axon into the soma and dendritic cell compartments, areas in which Tau is maintained at low concentrations in healthy cells (Ittner and Ittner, 2018). This shift in Tau localisation has been shown to interfere with post-synaptic signalling and the redistribution of mitochondria, leading to respiratory dysfunction and cellular degeneration (Cheng and Bai, 2018, Wang and Mandelkow, 2016). The propagation and transmission of neurofibrillary Tau throughout the brain has been closely linked to cognitive symptoms of both AD and other Tauopathies such as Parkinson's disease and frontotemporal dementia (Del Tredici and Braak, 2019). The classification of Tau localisation in the brain is known as Braak staging (Braak et al., 1996). In addition to Tau in the brain, total Tau and hyperphosphorylated Tau can also be quantified in Cerebrospinal fluid (CSF) and has become useful diagnostic tool for AD (Pase et al., 2019). Despite the correlation of brain and CSF Tau with the symptoms of AD, its use for detecting pre-clinical AD alone is currently limited. However, there is evidence of a relationship between elevated tau and a faster rate of cognitive decline and therefore, may be useful for improving the accuracy of biomarker panels to detect AD (Betthauser et al., 2020, Racine et al., 2016).

1.5.2 Extracellular amyloid plaques

The identification of a 4kDa Amyloid peptide in the core of the extracellular plaques seen in the AD brain, identified as Aβ placed this peptide at the centre of AD research (Glenner and Wong, 1984). Perhaps the strongest evidence of a role for Aβ in AD came from the fact that AβPP mutations and *PSEN1*/2 mutations alter the production of Aβ and caused fAD. The 'Amyloid Cascade Hypothesis' (Hardy and Higgins, 1992) postulated that Aβ could either directly damage neurons or may increase the vulnerability of neurons to other excitotoxic damage. This was supported by the apparent disruption to calcium homeostasis after exposure of neurons to Aβ peptides (Yang et al., 2012). Despite strong evidence of Aβ plaques forming in AD brains an apparent lack of correlation between Aβ plaque load and cognitive decline led many to question if Aβ has a causative role in AD. In addition, Aβ plaques can be seen in cognitively healthy brains with no obvious symptoms or diagnosis of AD. Instead, oligomeric species of Aβ have been found to possess greater cytotoxic properties and correlate much more closely with synaptic dysfunction and degeneration (Haass and Selkoe, 2007). Aβ oligomers can arise from the aggregation of Aβ peptides or can dissociate from larger, more stable, Aβ complexes/ plaques (Yang et al., 2017b). The increased solubility of these Aβ oligomers enables them to move more freely in the extracellular space where they can interact with cell membranes and disrupt synapse function (Li and Selkoe, 2020). This increased mobility may also explain the 'prion-like' spread of Aβ through the brain (Katzmarski et al., 2020).

Together, hyperphosphorylated Tau and oligomeric Aβ are considered the fundamental lesions of the AD brain. It is widely accepted that their interaction has the capacity to cause significant neurodegeneration. In fact, the extracellular accumulation of Aβ can lead to intracellular tau misfolding, a process which precedes tau toxicity (Rudenko et al.,

2019). Further, cells expressing a higher ratio of Aβ1-42:Aβ1-40 also display a significant increase in pathogenic tau accumulation (Kwak et al., 2020). Despite this, it is not so clear as to what causes AD in the first instance, and why some brains remain cognitively healthy even with the presence of these pathological hallmarks (Gulisano et al., 2018). However, the fact remains that this neuropathology is present in AD and plays a role in the disease. In order to understand AD, it is therefore necessary to fully characterise the role of Aβ in the pathogenesis of AD, and potentially develop effective treatments against Aβ. Thus, it is essential that we gain a better understanding of the processes underpinning Aβ biochemistry.

1.6 Processing of the amyloid precursor protein

Over 30 years ago a full-length protein, AβPP, was identified and shown to contain the amino acid sequence for the Aβ peptide. At this time AβPP was predicted to function as a glycosylated cell membrane receptor and its breakdown resulted in the generation of Aβ (Kang et al., 1987). AβPP has multiple functions which are critical for physiological processes (Müller et al., 2017). The single-pass membrane protein has a key role in signalling information about extracellular conditions into intracellular compartments. This can have fundamentally different actions on gene regulation, central nervous system development and synapse maintenance (Goodger et al., 2009, Plummer et al., 2016). AβPP is expressed as multiple isoforms: AβPP695, AβPP751 and AβPP770 arise as product of alternate splicing. Each isoform is differentially expressed depending on the tissue but are all processed in the same way. In the brain, AβPP695 is the predominate isoform and is crucial to neuronal growth and maturation, especially during development (Coronel et al., 2019). In peripheral tissue the longer AβPP751 and AβPP770 isoforms are expressed. Post-translational modifications, such as glycosylation, are known to mediate AβPP trafficking through the

secretory and endo-lysosomal pathways. N-glycosylated AβPP (Immature AβPP) is held in the endoplasmic reticulum, whereas, the modification of O-glycosylation sites promotes AβPP (mature AβPP) movement to the cell membrane (Wang et al., 2017b, Hoffmann et al., 2000). Mature O-glycosylated AβPP is also more likely to be held in the cell membrane (Chun et al., 2015b). Each of the AβPP isoforms are proteolytically cleaved in two distinct processing pathways which are highly dependent on the cellular trafficking of AβPP and the activity of three key enzymatic interactions (see figure 1). This consecutive shedding process is named 'regulated intramembrane proteolysis' and is typically associated with signalling pathways (Lichtenthaler et al., 2011).

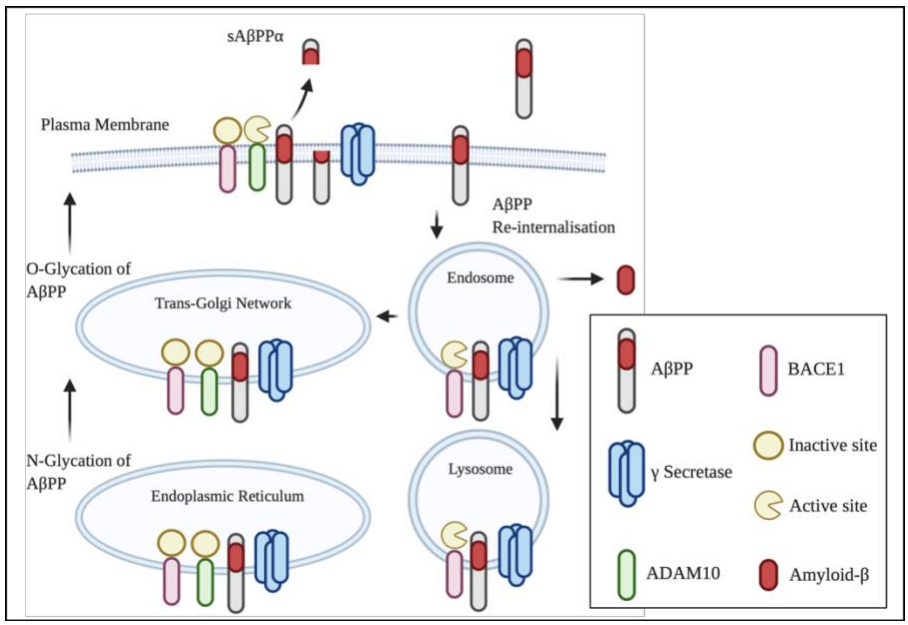

Figure 1 - *Diagrammatic representation of the trafficking and processing of AβPP from intracellular compartments to the cell membrane. Major AβPP cleavage sites of ADAM10 and BACE-1 activity are shown and represent the 'non-amyloidogenic' and 'amyloidogenic' pathways respectively.*

1.6.1 The non-amyloidogenic AβPP processing pathway

The non-amyloidogenic processing pathway is initiated by α-secretase enzymatic cleavage of AβPP through the Aβ region. This prevents the formation of Aβ peptides. The primary site of α-cleavage is at the cell membrane resulting in the release of the N-terminal fragment sAβPPα into extracellular compartments. The remaining intramembrane C-terminal fragment consisting of 83 amino acids can then be further cleaved by the γ-secretase enzyme to release a truncated Aβ peptide known as P3 and the AβPP intracellular domain (Haass et al., 2012).

1.6.2 ADAM10

Several zinc metalloproteinases are members of the 'a disintegrin and metalloproteinase' (ADAM) family and are known to possess α-secretase activity. This includes ADAM9, ADAM10, ADAM17 and ADAM19 (Allinson et al., 2003, Qian et al., 2016). Whilst the cleavage of AβPP can be shared between multiple ADAMs, in neurons, ADAM10 appears to be the major physiologically relevant α-secretase (Postina et al., 2004, Kuhn et al., 2010). The ADAM10 zymogen (proADAM10|) undergoes prodomain cleavage by proprotein convertase enzymes, PC7 and Furin (Anders et al., 2001). This generates the catalytically active, mature ADAM10 (mADAM10) enzyme. Blocking this process can significantly reduce membrane expression of ADAM10 (Seifert et al., 2020) and lower sAβPPα secretion (Anders et al., 2001). The maturation of ADAM10 is regulated during trafficking to the cell membrane, where it is most active, by a series of Transmembrane-4 superfamily proteins known as Tetraspanins (TSPAN). In particular, a sub-group known as the C8-TSPANs have been of particular interest (Matthews et al., 2017). These partner proteins have been shown to direct the interaction of ADAM10 with AβPP at the cell

membrane and can either have inhibitory or promoting effects on non-amyloidogenic AβPP processing depending on the C8-TSPAN/ADAM10 pairing (Matthews et al., 2017, Seipold and Saftig, 2016). The upregulation of ADAM10 activity and therefore, non-amyloidogenic AβPP processing, significantly blunts the formation of Aβ peptides. This suggests that both pathways are able to compete for AβPP substrates (Postina et al., 2004). In addition, the secretion of sAβPPα is associated with neuroprotective effects. Mutations to the *ADAM10* gene that attenuate enzymatic activity are shown to associate with susceptibility to LOAD (Kim et al., 2009). Therefore, the modulation of ADAM10 could be a target for therapeutic intervention in AD.

1.6.3 Soluble AβPP- α

The N-terminal fragment, sAβPPα, has been implicated in a number of neuroprotective processes to act as a cell signalling molecule. These effects include neurogenesis, maintaining synaptic function and supporting the formation of neuronal networks (Yuan et al., 2017, Kögel et al., 2012). The generation of sAβPPα is thought to be protective in the adult brain, and even more so in the aged brain. This is supported by evidence that in AβPP deficient mice, the addition of exogenous sAβPPα can rescue long term potentiation and have beneficial effects on memory (Hick et al., 2015). In both cell and animal models, treatment with sAβPPα has also been shown to reduce Aβ toxicity, tau hyperphosphorylation and inhibit Beta-site AβPP Cleaving Enzyme-1 (BACE-1) activity (Peters-Libeu et al., 2015, Deng et al., 2015).

1.6.4 The amyloidogenic AβPP processing pathway

The cleavage of AβPP, resulting in the liberation of Aβ peptides is termed Amyloidogenic processing. The initiating event in this pathway is the interaction of AβPP with BACE-1. This cleavage event occurs in the trans Golgi network and endosomal pathways where BACE-1 possesses high activity releasing the N-terminal fragment, soluble AβPP-β, leaving the Aβ-containing C-terminal fragment C99 anchored to the membrane (Chun et al., 2015a, Haass et al., 2012). Subsequent cleavage by the γ-secretase enzyme, liberates the Aβ-peptide and the AβPP intracellular domain.

1.6.5 BACE-1

BACE-1 is a type-1 transmembrane protein with aspartyl protease activity and is the mediating factor in amyloidogenic AβPP cleavage (Cole and Vassar, 2007, Vassar, 2001). This was shown by the homozygous knockout of the BACE-1 gene abolishing Aβ production (Cai et al., 2001, Luo et al., 2001). The BACE-1 protein is translated into a zymogen and requires prodomain cleavage by a Furin-like protease to enable its enzymatic activity (Bennett et al., 2000). BACE-1 is then transported along the secretory pathway where it preferentially sits close to lipid rafts. This is a primary site for AβPP cleavage (Ehehalt et al., 2003). Interestingly, altered lipid raft composition and elevated membrane cholesterol have been shown in both fAD and LOAD where BACE-1 activity is highest (Cho et al., 2019, Fabelo et al., 2014). Although BACE-1 and AβPP are present at the cell membrane it is during reinternalization through the endosomal pathway that AβPP cleavage and therefore Aβ generation is greatest (Sun and Roy, 2018, Das et al., 2013). This may be due to the low pH where BACE-1 is most active (Vassar, 2001). BACE-1 is expressed in many tissues with the highest levels found in brain and pancreas (Vassar et al., 1999, Marcinkiewicz and Seidah,

2000). BACE-1 expression and activity is increased in the brain and CSF of people with AD above that seen in normal ageing (Zetterberg et al., 2008, Yang et al., 2003, Li et al., 2004), however, the mechanisms relating to the elevation in BACE-1 are poorly understood. Elevated BACE-1 activity may be related to the incidence of *APOE* e4 allele occurrence, however this relationship has only been identified in a small number of cases (Roses, 1994, Ahmed et al., 2010). Therefore, changes in BACE-1 activity more likely reflect the disease process and have become a key target for AD therapeutics and biomarker research. In addition to BACE-1 there is another β-site cleaving enzyme, BACE-2. BACE-2 is predominately expressed in peripheral tissue and is also a type-1 transmembrane protein. BACE-2 is 75% homologous to BACE-1 (Sun et al., 2005) and is also present in the brain, although mainly in astrocytes as opposed to the neuronal expression of BACE-1 (Voytyuk et al., 2018b). BACE-2 can cleave AβPP at the β-site as its name suggests and this is demonstrated by residual BACE activity after BACE-1 knockout (Cai et al., 2001, Luo et al., 2001). However, BACE-2 has a preference for cleavage within the Aβ region preventing the liberation of full Aβ peptides. Therefore, BACE-1 is considered the major enzyme in the generation of Aβ peptides.

1.6.6 Soluble AβPP-β

The secreted sAβPP-β N-terminal protein that is released following BACE-1 cleavage of full length AβPP, has been shown to lack the neuroprotective effects that have been seen for sAβPP-α (Hick et al., 2015). Despite only differing by 16 amino acids from sAβPP-α , sAβPP-β is conformationally very different (Gralle et al., 2006). In fact, sAβPP-β may be more toxic than Aβ in stimulating synaptic and memory deficit in animal studies (Tamayev et al., 2012). However, a physiological role of sAβPP-β during neurodevelopment has been

suggested in synaptic pruning and regulated cell death through Caspase3 and 6 protein activation in central and peripheral neurons (Nikolaev et al., 2009). Interestingly, sAβPP-β may also affect stem cell differentiation by reducing neuron formation in favour of astrocyte development (Kwak et al., 2006).

1.6.7 Amyloid-β

The neurotoxic effect of Aβ peptides has been perhaps the most widely studied phenomenon in AD research. The generation of Aβ, following sequential cleavage of AβPP by BACE-1 and then γ-secretase (see section *1.6.5*), can result in peptides of different amino acid lengths (Steiner et al., 2018). Aβ peptides of differing lengths have been identified from Aβ1-37 to Aβ1-43. Most commonly, Aβ1-40 is produced and is considered the most physiologically normal Aβ peptide. In fact, the regulated release of Aβ1-40 may have benefits for the brain including aiding in fighting infection, maintaining the blood brain barrier integrity and regulating synaptic functions (Brothers et al., 2018). Conversely, the loss of regulated Aβ production, in combination with poor clearance is deleterious in the brain. The main component of extracellular amyloid plaques is the Aβ1-42 peptide and therefore, research into the Aβ1-42 peptide as the key pathological protein in AD has been of interest (Festa et al., 2019, Finder et al., 2010). This interest in Aβ1-42 in AD has been fuelled by the finding that fAD mutations are associated with an increased Aβ1-42:Aβ1-40 ratio (Xu et al., 2016, Arber et al., 2019). Despite the peptides only differing by two amino acids at the C-terminal end, there have been a number of differences identified between Aβ1-40 and Aβ1-42 in relation to their metabolism and propensity for aggregation (Qiu et al., 2015, Nirmalraj et al., 2020).

Crucially, Aβ1-42 is able to more rapidly aggregate at lipid membranes, forming oligomeric Aβ species and accumulating in endocytotic vesicles (Zheng et al., 2017). Aβ1-42 has been shown to more easily propagate from smaller tetra- and hexameric oligomers to larger aggregates when compared to more resistant Aβ1-40 tetramers (Bernstein et al., 2009). The aggregation of Aβ into annular assemblies can result in wide-ranging molecular weight complexes, dependent on peptide number and interaction with membrane lipids (Sakono and Zako, 2010). This has raised significant interest in the structure-toxicity relationship of different size Aβ oligomers and evidence suggests that both smaller trimers and larger dodecamers can have toxic effects (Huang and Liu, 2020). Other factors can also impact oligomerisation and aggregation; for example the interaction of Aβ with transition metal ions (Rana and Sharma, 2019), interaction with membrane microdomains enriched for cholesterol and sphingolipids (Rushworth and Hooper, 2010) and alterations in plasma membrane constituents such as sphingomyelin and the monosialganglioside GM1 (Amaro et al., 2016), can all impact Aβ oligomerisation.

The aggregation of Aβ peptides into extracellular plaques was originally suggested as a mechanism of neurodegeneration and became a hallmark feature of the AD brain. Yet, the presence of amyloid plaques is poorly associated with cognitive deficits and amyloid plaques are present in cognitively healthy brains in older age (Haller et al., 2019, Caselli et al., 2010). The appearance of such ‘intermediate’ oligomeric forms of Aβ that appear to be particularly toxic to neurons has provided a new area of investigation for the role of Aβ in the pathology of AD (Lesné et al., 2008, Kim et al., 2003). In fact, the structural organisation of Aβ oligomers into extracellular fibrils has been considered as an adaptive protective mechanism against oligomeric Aβ toxicity in the brain (Salahuddin et al., 2016). However, Aβ oligomers have also been shown to diffuse from Aβ fibrillar plaques (Koffie et al., 2009) and exert

cytotoxic effects which are associated with synapse loss and cognitive decline, which suggests amyloid plaques are not fully innocuous (Pickett et al., 2016). Aβ oligomers can exert cytotoxic effects by disturbing intracellular processes, for example; the internalisation of extracellular Aβ peptides, in addition to the generation of Aβ peptides at organellar membranes such as, mitochondria, trans-golgi network, endoplasmic reticulum and the endosomal/lysosomal pathways, can all increase the intracellular pool of Aβ oligomers (Lee et al., 2017). Intracellular Aβ oligomers have been implicated in elevating endoplasmic reticulum stress, calcium ion dyshomeostasis, mitochondrial damage and a loss of proteostasis leading to apoptosis (Umeda et al., 2011, Resende et al., 2008, Poon et al., 2013, Calvo-Rodriguez et al., 2019) and thus are able to significantly disrupt cellular function. Further, Aβ oligomers can cause cellular damage by interacting directly in extracellular compartments. Such mechanisms include; the direct binding to, and disruption of, the plasma membrane (Sciacca et al., 2012, Hong et al., 2014); the formation of pores in the membrane that can lead to dysregulated permeability (Drews et al., 2016, Peters et al., 2016) and binding to receptors to influence signal transduction (Smith and Strittmatter, 2017). This multitude of interactions highlights the potential for Aβ oligomers to have widespread cytotoxic effects throughout the brain.

The ability of Aβ oligomers to trigger synaptic dysfunction suggests synaptic receptors may be important binding sites or targets for modulation of cell signalling (Smith and Strittmatter, 2017). Some examples of these include; glutamate, insulin, nerve growth factor and acetylcholine receptors (Smith and Strittmatter, 2017, Zhang et al., 2017, Mroczko et al., 2018). Notably, the cellular prion protein (PrP^C) has a selective, high affinity for Aβ oligomer binding and appears to have a primary role in Aβ cytotoxicity (Salazar and Strittmatter, 2017, Kudo et al., 2012). The treatment of hippocampal neurons with

extracellular Aβ oligomers can increase the surface expression of the PrP^C by limiting its endocytosis (Caetano et al., 2011). Further, binding of Aβ oligomers to the PrP^C may modulate the surface expression of nearby post-synaptic receptors which could have profound downstream effects on cell signal transduction and Tau phosphorylation (Caetano et al., 2011, Um et al., 2012, Larson et al., 2012). The role of PrP^C in mediating Aβ oligomer toxicity has highlighted a potential avenue for therapeutic research in AD. Increasing PrP^C shedding and thus, reducing Aβ oligomer binding, has been shown to prevent associated cytotoxicity (Jarosz-Griffiths et al., 2019). This shedding activity has been attributed to ADAM10 (Linsenmeier et al., 2018) (see section *1.6.2*). Therefore, increasing ADAM10 activity and shedding of PrP^C may be of therapeutic benefit.

1.6.8 The γ-secretase protein complex

The final cleavage event in both the non-amyloidogenic and amyloidogenic AβPP processing pathways is catalysed by the γ-secretase enzyme. In the amyloidogenic pathway the C99 fragment enters the active site of γ-secretase and undergoes stepwise carboxyl trimming. This sequentially cuts the Aβ region down from Aβ1-49, known as the ε-cleavage site. Changes in this process enable the release of the multiple Aβ peptides (Steiner et al., 2018). γ-secretase is comprised of four subunits and is an intramembrane aspartyl protease. These subunits consist of Presenilin, Presenilin Enhancer-2 (PEN2), Anterior Pharynx-defective-1 (APH-1) and Nicastrin. In addition to AβPP, γ-secretase also cleaves a number of other functionally important type-1 transmembrane proteins within the lipid bilayer (Zhang et al., 2014). Some of the more well studied substrates include Notch, E-cadherin and TREM2, although over 140 substrates have so far been proposed (Güner and Lichtenthaler, 2020). In particular Notch has been widely studied for its role in cellular development and cell fate

determination. The substrates identified for γ-secretase suggest roles in embryonic development, adult tissue homeostasis, signal transduction and protein degradation (Güner and Lichtenthaler, 2020) and may also mediate some of these effects through non-proteolytic functions. Altered calcium dynamics and defects in autophagic/lysosomal processes are disrupted in neurons carrying *PSEN1* mutations (Lee et al., 2010, Bezprozvanny and Hiesinger, 2013, Zhang et al., 2010). This highlighs a diverse acting repertoire of γ-secretase substrates.

The catalytic subunit, Presenilin, is encoded by the *PSEN1* and *PSEN2* genes and therefore, exists in two isoforms. The mutations to these genes can affect the function of γ-secretase causing fAD. γ-secretase interacts with multiple intramembrane proteins in addition to AβPP and there has been a great deal of interest in trying to understand how these substrates are recognised for cleavage (Wolfe, 2020, Zhou et al., 2019). This is particularly important for AD as limiting γ-secretase activity can prevent Aβ production, yet, knockout or broad inhibition of γ-secretase activity is associated with severe side effects (Bursavich et al., 2016). The Nicastrin subunit has been attributed with the role of 'gatekeeper' for substrates entering the γ-secretase complex for cleavage. The remaining two subunits are much less studied. APH-1 helps form a scaffold for the γ-secretase protein complex and PEN2 aids the maturation of the enzyme (Carroll and Li, 2016).

1.7 Oxidative Stress and Alzheimer's Disease

The generation of reactive oxygen species (ROS) occurs as a part of aerobic life and have a fundamental role in physiological functions, such as cell signalling and as enzymatic catalysts (Sies and Jones, 2020). A major source of ROS comes from oxidative phosphorylation in mitochondria (Lanzillotta et al., 2019) (see section 1.7.1). This process

leaks the superoxide anion radical which is highly reactive and can easily interact with other molecules and if not quenched, can form an oxidising cascade (see figure 2). Under normal conditions ROS production is balanced by efficient antioxidant systems, that can stabilise oxidising molecules and prevent an excessive accumulation of oxidised biomolecules. This is known as redox balance (Zhao and Zhao, 2013). However, in pathological conditions this balance is disrupted towards a pro-oxidant state, overwhelming antioxidant defence and leading to oxidative stress (Oswald et al., 2018).

The involvement of chronic oxidative stress in the pathogenesis of AD is now widely accepted as a component of the neurodegenerative process seen in the brain (Yaribeygi et al., 2018, Butterfield, 2018). Whether oxidative stress is a causal feature, or a consequence of a pathogenic cascade in AD is not so clear. The presence of increased transition metals, capable of catalysing ROS production, elevated lipid and protein oxidation end products and a reduction in energy metabolism all provide direct evidence that the brain is under oxidative stress in AD (Perry et al., 2002, Butterfield and Halliwell, 2019). In addition, Aβ can lead to ROS generation through direct interaction with transition metals and activating nearby immune cells (Sies and Jones, 2020). One of the major consequences of this interaction is the potential for surrounding cell membrane disruption resulting in cell death (Cheignon et al., 2018). These findings led to the proposal of the 'Oxidative Stress Hypothesis of Alzheimer's disease' (Markesbery, 1997). Oxidative stress has also been implicated in the 'Two-hit Hypothesis' of AD (Zhu et al., 2004) by which oxidative insults and mitotic abnormalities can increase cell susceptibility to further damage and redox stress. A key challenge of understanding the involvement of oxidative stress in AD has been to determine both the mechanisms of redox imbalance and where the source of this redox imbalance is localised. Potential sources of ROS could be from respiratory and vascular systems, genetic variations, a

build-up of transition metals, nutrient stress or even Aβ accumulation (Smith et al., 2000, Tan et al., 2018, Guzik and Touyz, 2017). Interestingly, the link between ROS generation and Aβ accumulation may be in part explained by a ROS-Aβ feedback loop in mitochondria (Leuner et al., 2012).

1.7.1 Mitochondria, reactive oxygen species and Aβ

Evidence for a role of dysfunctional mitochondria in AD was initially developed from the detection of regional hypometabolism using brain scanning techniques. A reduction in brain glucose consumption was first noted and can be explained by a combination of reduced glycolysis and neuronal or synaptic degeneration (Perez Ortiz and Swerdlow, 2019). Mitochondria are key organelles in the respiratory chain where adenosine triphosphate is produced to fuel metabolic processes. Although a highly efficient system, there is a small but consistent production of superoxide anions from the electron transport chain during this process. This physiologically normal superoxide production is quenched by a highly effective superoxide dismutase antioxidant enzyme system (Lalkovičová and Danielisová, 2016). Even if superoxide is able to interact with other molecules to generate radicals such as hydrogen peroxide, hydroxyl radicals, and nitric oxide radicals there are specific antioxidant systems to limit further oxidation of biomolecules. Catalase, Glutathione peroxidase and the thioredoxins are some of the more well studied endogenous antioxidant enzymes that prevent such biomolecular oxidising cascades from damaging the cell under normal physiological conditions (Mecocci et al., 2018). However, in AD this balance between ROS production and antioxidant defence systems appears to be shifted and the resulting altered redox status significantly increases the susceptibility of neurons to the cell death cascade (Angelova and Abramov, 2018). Interestingly, it has been suggested that this imbalance is due to elevated

ROS production as opposed to changes in the 'first line' endogenous antioxidant enzymes (Zabel et al., 2018). Dysregulated oxidative phosphorylation in AD and other neurodegenerative diseases has highlighted the role of mitochondria in maintaining proper neuronal function. This led to the proposal of the 'mitochondrial cascade hypothesis' which places mitochondria at the centre of the AD pathological process (Swerdlow and Khan, 2004). This hypothesis suggests that Aβ is produced as a response to elevated ROS which in turn oligomerises and leads to the generation of more ROS. Cells under oxidative stress are then subject to programmed cell death and improper cell cycle re-entry. The incorporation of mitochondrial dysfunction into this hypothesis does provide a defining role for ageing in AD pathology (Swerdlow and Khan, 2004).

1.7.2 Lipid, protein and DNA damage in Alzheimer's disease

Whilst ROS production is detectable in real-time, consistent measurement *in vivo* is difficult. Instead stable oxidative end-products are a more informative marker of biomolecular damage and can be measured in peripheral tissue. The oxidation of proteins, lipids and DNA are commonly used markers to quantify oxidative stress as end products of redox cascades (see figure 2). Elevated oxidation of nuclear and mitochondrial DNA has been implicated in AD. The oxidized nucleoside 8-hydroxy-2'-deoxyguanosine is a product of oxidative modification to the purine guanosine and can significantly limit mitochondrial biogenesis and further increase ROS leakage from oxidative phosphorylation (Strobel et al., 2019). As neurons are considered post-mitotic cells, nuclear DNA oxidation can also be particularly deleterious (Abolhassani et al., 2017) and can even result in DNA strand breaks (Shanbhag et al., 2019).

Lipid oxidation has been widely studied in AD due to the high polyunsaturated fat content of the brain and, as a potential mechanism for Aβ-induced oxidative stress (Butterfield and Boyd-Kimball, 2018b). By-products of Lipid oxidation are elevated early on in the pathology of AD and have also been reported in preclinical AD brain (Singh et al., 2010). The most common markers of which are malondialdehyde, 4-hydroxy-2-nonenal and lipid hydroperoxides (Butterfield et al., 2006b, Di Domenico et al., 2017, Butterfield, 2018, Perluigi et al., 2009). Lipid peroxidation has been shown to be elevated in synaptic and mitochondrial fractions in the frontal cortex of people with AD (Ansari and Scheff, 2010). The relative instability of early lipid peroxidation markers has proved a significant challenge to quantifying oxidative stress. However, F_2-isoprostanes, a product of arachidonic acid oxidation, and other prostaglandin-like markers are more stable (Milne, 2017). Such markers are elevated in AD brain and have been associated with worse cognitive function (Camfield et al., 2019, Praticò et al., 1998). Therefore, F_2-isoprostanes may represent a useful marker for assessing oxidative damage to lipids. Lipid peroxidation has also been monitored in peripheral fluid compartments, including blood plasma and urine. Although evidence for elevated plasma lipid peroxidation in AD has been found (Peña-Bautista et al., 2018), the results are less clear-cut. This is potentially due to the poor clearance of oxidised lipids from the brain in AD (Montine et al., 2002, Peña-Bautista et al., 2020). Despite this, conditions associated with metabolic dysfunction, such as obesity, are more clearly associated with plasma lipid peroxidation (van 't Erve et al., 2017) products and may provide a valuable tool in determining ‘at risk’ groups for AD.

Cholesterol is another lipid molecule that is susceptible to oxidation and the formation of oxysterols can occur through interaction with ROS or through enzymatic reactions seen in mitochondria. These oxygen-modified cholesterol molecules have a greater ability to

transport through cellular organelles disrupting membrane fluidity and are linked to a reduced capacity for glucose uptake in neurons (Testa et al., 2016, Gamba et al., 2019). Lipids are a crucial component of cell membrane bilayers forming the barrier between intra and extracellular space. Lipid oxidation within the cell membrane can significantly impact the fluidity and permeability of a cell leading to elevated Aβ uptake and altered intramembrane protein functioning (Bharadwaj et al., 2018). This is particularly important in AD as not only are the AβPP processing enzymes inserted into the membrane, but Aβ oligomers are able to induce further lipid oxidation creating a Aβ uptake-membrane oxidation loop (Murray et al., 2005, Oku et al., 2017). In fact, lipid oxidation has been associated with an elevation in BACE-1 activity (Tamagno et al., 2006, Borghi et al., 2007). Lipid disruption via ROS interaction may also limit ADAM10 activity, by reducing co-localisation with AβPP at the cell membrane and promoting reinternalization into the endosomal pathway. Although this has not been confirmed, treatment of neuronal cells with mild doses of hydrogen peroxide has previously caused an increase in AβPP/BACE-1 co-localisation and an increase in the BACE1 cleavage (Tan et al., 2013). The generation of lipid peroxyl radicals can further interact with proteins and significantly alter their structure and function. Some of the more well characterised protein oxidation mechanisms occur through carbonylation, nitration, glycoxidation and through protein-bound lipid oxidation products (Tramutola et al., 2017). Protein carbonylation modifications represent a stable marker of direct amino acid interaction with ROS and have been widely reported to be elevated in AD (Butterfield and Boyd-Kimball, 2018b). Further, measuring specific protein oxidation products has been linked with an ability to distinguish people with AD to healthy participants (Aldred et al., 2010, Sultana et al., 2010). This is likely to represent functional changes to proteins during the progression of AD. Increased protein oxidation has also been linked to a reduction in pre and post synaptic

proteins as well as being implicated in the disruption of several mitochondrial enzymes involved in energy metabolism (Reed et al., 2008, Scheff et al., 2016). Despite this, evidence for oxidative damage to proteins in peripheral tissues is limited, but with further research, may provide a useful source of early diagnosis and prognosis of AD (Di Domenico et al., 2011).

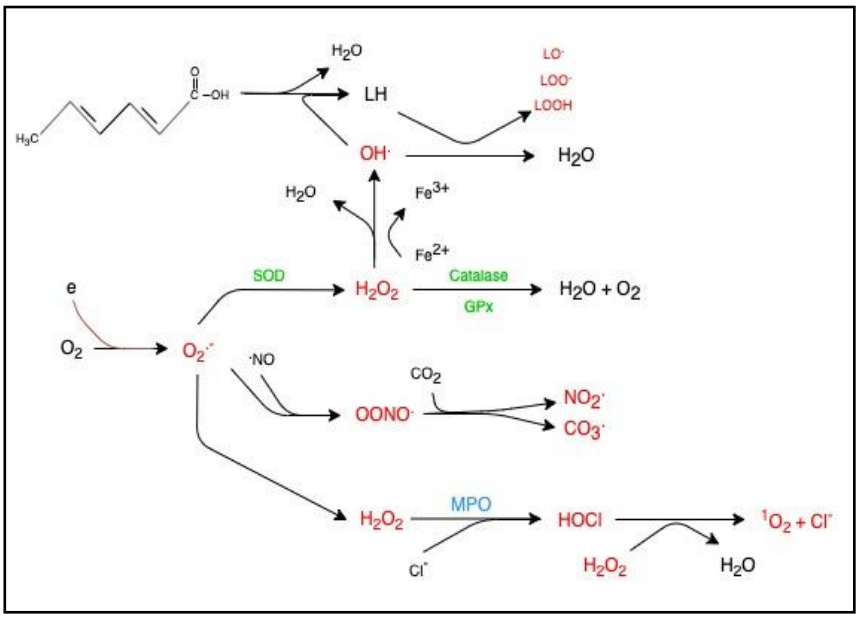

Figure 2 - *ROS cascade starting from the initial generation of Superoxide anions. Propagation of oxidative molecules is dependent on interaction with antioxidant enzymes (green) or the oxidation of other biomolecules (Red). Myeloperoxidase (MPO, Blue) is an enzyme that forms part of the microbial defence system not covered in this thesis.*

1.8 The Diagnosis of Alzheimer's Disease

Both fAD and LOAD are pathologically and clinically similar, although fAD is related to a more aggressive onset and progression (Marshall et al., 2007, Day et al., 2016). In the early stages, individuals may display forgetfulness, changes in mood and agitation. This can then advance into a more noticeable decline in cognitive function, sleep disturbances and

often the individual will require support with everyday living (Li et al., 2014, Hallikainen et al., 2018). Ultimately, both fAD and LOAD are fatal with a loss of voluntary muscle action, significant loss of both short- and long-term memory and the inability to carry out essential daily tasks. The key distinguishing factor between these conditions are the autosomal dominant gene mutations and significantly earlier age of onset in people with fAD. Therefore, determining a definitive diagnosis of fAD can be reached from genetic screening. It is also highly likely that one of the individual's parents will have fAD. In contrast, the multifactorial nature of LOAD makes diagnosis significantly more difficult. With symptoms typically presenting after the age of 65 it is not uncommon for people with LOAD to have comorbid disease with overlapping symptoms. As such, getting a definitive diagnosis of AD is currently only possible during *post-mortem* examination (de Jager et al., 2010, Thal and Braak, 2005). However, there are several approaches that can be used to give a 'probable' diagnosis of LOAD *ante*-mortem, including clinical assessment of presenting symptoms and studying key physiological changes using scanning techniques and monitoring biomarkers.

1.8.1 Clinical assessment

The symptoms of LOAD develop over a number of years as the disease progresses. The initial diagnosis of 'probable LOAD' is given after the assessment of dementia-related symptoms using cognitive measures such as the Mini Mental State Examination (MMSE) and Clinical Dementia Rating (CDR) (Folstein et al., 1975, Hughes et al., 1982). Although these tests are useful for monitoring cognitive dysfunction their ability to discriminate between LOAD and other dementias is limited. In addition, cognitive tests lack the sensitivity to detect small changes in cognitive function. The refinement and adjustment of cognitive testing methods has been subject to ongoing research with different aspects of cognition being

monitored as well as the inclusion of new technology, such as virtual environments (Matías-Guiu et al., 2017, Seitz et al., 2018, Fernandez Montenegro and Argyriou, 2017). Despite better accuracy of cognitive diagnostic tools, they suffer a fundamental flaw when considering treatment options. The physiological and biochemical changes during LOAD development are likely to have been progressing for as many as 30 years prior to any clinical symptoms (Vos et al., 2013). Evidence of such pre-symptomatic changes has been found by monitoring biomarkers in people with fAD, who will inevitably develop AD, but are yet to present symptoms. Changes in CSF markers, such as a decrease in Aβ1-42, elevated t-tau and p-tau181 and elevated oligomeric Aβ have been detected (Ringman et al., 2012a, Ringman et al., 2012b, O'Connor et al., 2020). Further, atrophy of the brain has been detected in people with fAD prior to clinical symptoms, although this is typically closer to diagnosis, around 3-5 years prior (Kinnunen et al., 2018, Weston et al., 2016, Ridha et al., 2006). From this evidence, it is apparent that a state of 'accelerated brain ageing' is present in fAD. The closeness in pathological and symptomatic features between fAD and LOAD suggest these preclinical changes are likely to occur in both cases, and the evidence from people with fAD can inform future investigations into pre-symptomatic stages of LOAD (Vlassenko et al., 2012). Identifying the pathological changes prior to symptoms is perhaps one of the significant challenges to our understanding of LOAD. There is a growing consensus that treating LOAD will only be possible if we are able to detect the onset of the disease process far earlier than currently possible (Rafii and Aisen, 2019). Therefore, a greater understanding of how the key pathological processes underlying AD manifest, develop and ultimately lead to severe neurodegeneration is needed. Further, the development of highly sensitive markers to measure and highlight those at risk of LOAD in pre-clinical stages, enabling preventative measures to be implemented is crucial.

1.8.2 Brain imaging

Advancements in brain imaging and detection sensitivity of biomarker analysis have significantly increased our ability to diagnose 'probable' AD. Computerised tomography (CT) and magnetic resonance imaging (MRI) scans have enabled the detection of intracranial lesions and regional atrophy of the brain in areas such as, the hippocampus and medial temporal structures. Thus, enabling doctors to rule out non-AD dementias (Frisoni et al., 2010). Positron emission tomography (PET) has improved our ability to visualise the brain. PET has additional advantages due to the ability to detect specific metabolic changes in the brain using radioactive tracers, for example, alterations in blood glucose metabolism can be measured using 18F-fluorodeoxyglucose. This has been successfully used to diagnose dementia and even help differentiate between AD and non-AD dementia. Altered glucose metabolism measured via 18F-fluorodeoxyglucose is considered one of the core markers of the AD brain (Garibotto et al., 2017, Pagani et al., 2015). PET scans can also be used to detect pathological lesions in the brain. Florbetapir F18 and Pittsburgh Compound-B have both been used to successfully bind to Aβ peptides in the brain, giving accurate measurement of Aβ plaque content (Yang et al., 2012). However, Aβ is present in cognitively healthy brains and as such, quantification of Aβ alone has limited diagnostic value and is limited by a lack of agreed cut-off value to distinguish Aβ-negative (or "Aβ-normal") to Aβ-positive brains (Villeneuve et al., 2015). Therefore, PET scans using Aβ binding agents are unable predict the severity of cognitive decline alone (Khosravi et al., 2019). Despite this, PET remains a useful tool in distinguishing AD from non-AD dementias. This insight can significantly speed up the diagnosis process and reduce the number of hospital visits for the patient (Carswell et al., 2018).

1.8.3 Fluid biomarkers

Fluid based biomarkers of AD are much sought after as a diagnostic tool as a reliable and accessible marker of disease would represent a more cost effect approach to diagnosing and monitoring progression of AD than brain imaging techniques (O'Bryant et al., 2017). CSF is arguably the most representative biofluid as it is directly linked to the brain and contains brain metabolites drained from the brain itself (Zetterberg and Blennow, 2018). As Aβ peptides and Tau protein filaments are key hallmarks of AD pathology they have often been a focal point of biomarker research. Quantification of CSF Aβ1-42 and the ratio of Aβ1-42:Aβ1-40 peptides have been shown to be altered in AD and observed changes correlate with imaging measures (Lewczuk et al., 2017, Pannee et al., 2016). As Aβ clearance is reduced from the brain parenchyma in LOAD, lower values of Aβ are seen in the CSF compared to people without LOAD. Typically this is also combined with and elevation in Aβ1-42, which is thought to be more toxic and prone to oligomerisation, and hyperphosphorylated Tau (Ghidoni et al., 2018). In addition, total protein levels of Tau and hyperphosphorylated Tau have been found to be elevated in CSF from people with LOAD (Ghidoni et al., 2018). These markers are generally in agreement with PET scanning outcomes, however, too many individual cases show a lack of correlation for widespread reliance on CSF assessment alone in clinical settings (Pannee et al., 2016, Leuzy et al., 2016). In addition to quantifying proteins that represent hallmark features of AD there is also evidence that CSF can be used to identify novel biomarkers. By assessing the presence of markers from specific cell type activation such as, glial cells as well as markers of synaptic dysfunction and neuronal death, it is possible to distinguish between AD and non-AD brain associated diseases in CSF. However, these data are typically only validated in small sample sizes (Sandelius et al., 2019, Morenas-Rodríguez et al., 2019, Jacobs et al., 2019). This is in

part due to the invasive nature of drawing CSF from participants which severely limits its use as a research tool.

The ability to take a routine blood sample and assess a person's risk of LOAD would revolutionise AD research. Thus, perhaps the most sought-after biomarker for AD would be something that is easily detectable in the blood. However, there are several considerations that must be overcome in order to develop a tool that would enable specific and reliable diagnosis. Often, only a low concentration of analyte is available in the blood due to the restricted passing of biomolecules across the blood-brain barrier (Zetterberg and Blennow, 2018). Added to this blood proteins are subject to degradation, can be masked by endogenous heterophilic antibodies which would influence detection by immunochemical methodologies and many of the proteins present in blood that may be associated with disease are of non-cerebral origin (Zetterberg, 2019). However, progress has been made in measuring both specific markers of AD hallmark pathology, and panels of candidate biomarkers. Initially, Aβ peptides measured in blood plasma were found to lack the consistency shown with CSF measurements and therefore, were not able to accurately distinguish people with AD (Olsson et al., 2016). However, the development of ultrasensitive single-molecule arrays has significantly increased the potential for plasma Aβ to be used clinically (Janelidze et al., 2016). In fact, this methodology has been used to detect changes in the ratio of plasma Aβ peptides in people with subjective memory complaints, prior to the classical clinical symptoms associated with AD (Verberk et al., 2018, Vergallo et al., 2019, Chatterjee et al., 2019). It is also possible to detect tau protein in plasma, and plasma Tau is elevated in people in the later stages of AD (Zetterberg et al., 2013, Pase et al., 2019). Elevated plasma Tau appears to be associated with a faster rate of cognitive decline in people with AD (Mielke et al., 2017) and perhaps is an interesting area for future investigation. In addition, the

development of more sensitive assays for plasma Tau may recognise further value for its use a diagnostic tool, as seems to be the case with plasma Aβ peptides (Tatebe et al., 2017). This may also answer questions over its use for detecting the earlier disease stages of AD when plasma tau is at low levels. Research studies have also identified panels of plasma protein biomarkers that appeared associated with AD (Ray et al., 2007). This research provided considerable promise at the time as all markers identified were related to inflammation and immune signalling which are perturbed in AD. Yet, these often-promising findings of high sensitivity for distinguishing AD from cognitively healthy individuals are hindered by a lack of reproducibility when applied to other cohorts (Marksteiner et al., 2011). There is a need for better pre-analytic sample preparation and study design standardisation to enable progress in using plasma biomarker panels to detect AD (O'Bryant et al., 2015).

1.8.4 Platelets in Alzheimer's disease

Platelets are anucleate cells that are most commonly associated with thrombus formation and are critical for haemostasis (Yun et al., 2016). Upon activation through mechanical stress or agonist interaction with platelet glycoprotein-coupled surface receptors, platelets secrete a multitude of adhesion and signalling proteins effecting plasma concentrations (Yun et al., 2016). Platelets became interesting in AD research due to the presence of inflammatory cytokines in the secretome and the discovery that platelets possess the full enzymatic machinery to generate Aβ peptides though AβPP processing in the same way that cortical cells in the brain do. In addition, the finding that platelet activation is elevated in people with AD suggested platelets may represent a surrogate source of biomarkers in isolation from the plasma protein matrix (Stellos et al., 2010). Platelet activation has also been linked to elevated lipid peroxidation which may be elevated in AD

prior to clinical symptom onset (Ciabattoni et al., 2007). However, methodological limitations do exist as preparation of a platelet sample from blood plasma can in itself cause activation of the platelets, and therefore a notable source of variability in using platelets in AD research comes from activation status during sample preparation. Platelets are metabolically active cell fragments containing numerous functional organelles including endoplasmic reticulum, Golgi apparatus and mitochondria. In people with AD, mitochondrial respiration is perturbed in intact platelets and this mitochondrial dysfunction may lead to further activation (Fišar et al., 2019). The co-expression of AβPP processing enzymes in addition to neurotrophic growth factors and neurotransmitters found in platelets presents an excellent opportunity to study these, and other markers of AD. Given these characteristics, platelets offer an excellent opportunity for AD research, when compared to the less accessible or costly alternatives, for example CSF, brain imaging and post mortem tissue (Kermani and Hempstead, 2019, Tajeddinn et al., 2016).

Early studies looking at the platelet markers of AβPP processing focused on detection of AβPP at differing molecular weights. AβPP of 120-130kDa represent the mature protein which has been post-translationally modified though N- and O- glycosylation during trafficking to the cell membrane (Schedin-Weiss et al., 2014). Shorter immature AβPP at 110kDa are more likely to interact with BACE-1 intracellular vesicles and thus are likely to follow the amyloidogenic pathway. The ratio of mature to immature AβPP (AβPPr), 130/120:110kDa has been shown to decrease in people with AD (Bram et al., 2018, Colciaghi et al., 2004, Borroni et al., 2010). Similarly, the cleaved sAβPP-α segment is decreased in people with AD, indicating a reduction in non-amyloidogenic AβPP cleavage. Also, sAβPP-β is elevated in AD and to a greater extent in MCI (Yun et al., 2019). This may be explained by altered AβPP maturation or alterations in ADAM10 activity (Colciaghi et al., (2002). In a

study investigating this further, ADAM10 expression was decreased in very mild and mild AD compared to healthy controls (Colciaghi et al., 2004), suggesting that a decrease in ADAM10 activity is associated with cognitive decline. Indeed more recently ADAM10 expression has been used to predict scores in assessments of cognitive function (Manzine et al., 2014, Manzine et al., 2013). Due to the prodromal nature of AD development, it may be possible to detect changes in platelet AβPPr and ADAM10 expression prior to clinical symptoms of dementia.

1.8.5 The importance of early diagnosis

Being able to detect the onset of pathological changes associated with AD disease pathology prior to the clinical manifestation of symptoms is crucial to the progression of AD research. It is possible that perturbed biochemical processes occur over 30 years in advance of any cognitive symptoms (Dong et al., 2017, Palmqvist et al., 2019). This period is known as prodromal AD. Therefore, the need for better biomarkers to identify those who have underlying pathological changes or prodromal AD is crucial to enable the discovery of effective and early intervention (Frisoni et al., 2017). It is thought that treatments aimed at prodromal 'at risk' populations may be more effective than after a clinical diagnosis is given (van Dyck, 2018).

1.9 Treatment for Alzheimer's Disease

Alzheimer's disease is the only leading cause of death that has no available disease modifying treatment. Currently, the majority of treatment options are concerned with management of symptoms and have modest effects in mild to moderate stages of AD (Reynolds, 2019). These treatments inhibit the cholinesterase enzyme and/or act as N-Methyl-

D-Aspartate (NMDA) receptor antagonists. In some cases, these treatments can alleviate memory complaints, reduce anxiety and improve motivation, resulting in the continued ability to carry out daily activities (Mueller et al., 2018, Kishi et al., 2017). Cholinesterase inhibitors under the names, Donepezil, Galantamine and Rivastigmine, work by inhibiting the breakdown of the neurotransmitter acetylcholine therefore, increasing the level of acetylcholine in the brain (Birks, 2006). Memantine regulates the interaction of glutamate with NMDA receptors in order to prevent perturbed calcium transport in neurons which can lead to cell death (Kishi et al., 2017). Additionally, a combination of Memantine and Donepezil can be prescribed in more severe cases of AD. An important consideration is that none of these approved treatments target the underlying AD pathology directly. Therefore, any treatment effects will only have limited effects on the rate of neurodegeneration or aid in symptom management. However, some more recent improvements in the understanding of how AβPP is processed to generate Aβ led to the first trials of novel treatments that use monoclonal antibodies and secretase inhibitors to blunt Aβ accumulation (Reynolds, 2019).

1.9.1 Treatments directly targeting Aβ

In line with the dominating theory that Aβ is a key pathological feature leading to the neurodegeneration seen in AD, treatments targeting the clearance of Aβ were developed. Over the last 20 years, drugs to prevent aggregation of Aβ, in addition to mono- and polyclonal antibodies designed to remove Aβ, have been subject to clinical trials. Early attempts to increase amyloid clearance using immunotherapy solubilised fibrils effectively in animal models, yet treatment in humans was associated with severe side effects and lacked any effect on clinical symptoms (Robinson et al., 2004, Maarouf et al., 2010). In some cases, this was due to the release of soluble oligomeric Aβ from plaques which holds greater cytotoxic

potential. In addition, completely removing Aβ, which is a physiologically normal protein, may have negative implications downstream of its function (Smith et al., 2002). There have been a number of clinical trials aimed at developing safer antibodies which target soluble forms of Aβ in the early stages of AD (Rosenblum, 2014, Satlin et al., 2016). However, most trials have shown a lack of effect in mild to moderate AD (Honig et al., 2018, Ostrowitzki et al., 2017). Perhaps the most promising treatment, Aducanumab, which is a potent anti-oligomeric Aβ antibody, is the first treatment to show a correlation between reduction of Aβ load and improved cognitive symptoms in humans. However, there was also a dose dependant association with blood brain barrier disruption resulting in vasogenic oedema and several reports of other severe adverse events (Ferrero et al., 2016).

1.9.2 BACE-1 and γ-secretase inhibitors

Another strategy that has been investigated, targeted towards blunting Aβ production, is concerned with the prevention of Aβ generation from AβPP. BACE-1 inhibitors are designed to block the enzymatic activity of BACE-1. Despite being demonstrated as potent inhibitors, many of the compounds that were first developed lacked specificity for the BACE-1 enzyme, were unable to penetrate the blood brain barrier or were associated with severe side effects (Hills and Vacca, 2007). However, with advancements in drug design, screening and improved methods of delivery, these limitations are being overcome and BACE-1 inhibitors are now in advanced clinical trials (Moussa-Pacha et al., 2020, Gabr and Abdel-Raziq, 2018). Similarly, the development of γ-secretase inhibitors has been met with significant issues (Doody et al., 2013). The potent effects seen in cell and animal models have not been replicated in human trials. This is in part due to the fact that many of the side effects alter essential physiological processes, such as notch signalling (Henley et al., 2014, De Strooper,

2014). Interestingly, Semagacestat which was recently under phase III testing has been shown to act as a pseudo-inhibitor of γ-secretase, in which enzymatic activity is not inhibited per se, but instead alters substrate preference (Tagami et al., 2017). This highlights the importance of understanding the mechanisms of action and physiological side effects of enzyme inhibitors before proceeding with clinical trials (Barão et al., 2016). Alternatively, rather than blocking enzyme activity, it is possible that controlled modulation of these enzymes may hold therapeutic potential, currently γ-secretase and BACE-1 modulators are undergoing clinical trials (Voytyuk et al., 2018a).

1.9.3 Targeting ADAM10: a therapeutic option?

As described above, ADAM10 protein expression and activity is reduced in AD, leading to increased availability of AβPP as a substrate for BACE-1 and Aβ generation (Postina et al., 2004). This is supported by the identification of missense mutations to the ADAM10 gene where people were seen to also have elevated Aβ and AD phenotype (Suh et al., 2013, Andrews et al., 2020). Importantly, ADAM10 cleavage of AβPP is associated with production of the neuroprotective fragment sAβPP-α. Therefore, it is feasible that strategies to increase ADAM10 activity or even promote the co-localisation of ADAM10 with AβPP will prevent AβPP cleavage by BACE-1 and thus may be a therapeutic option for AD. In rodent models, pharmacological modulation of ADAM10 activity using natural compounds has been shown to result in neuroprotective effects and reduce Aβ burden (Meineck et al., 2016, Manzine et al., 2019). However, there is very little evidence in humans. Currently, there is only one phase 2 trial assessing the dose-efficacy of ID1201, which is a fruit extract aimed at promoting α-secretase activity and reducing inflammation in patients with mild AD. Otherwise, the development of treatments that target ADAM10 or α-secretase activity are

sparse. One explanation for this is the associated side effects of promoting broad spectrum increases in α-secretase activity. ADAM10 is involved in the shedding of a number of membrane-bound proteins and can interfere with several pathways such as Notch signalling, inflammatory cytokine release and cell adhesion. In addition, ADAM10 is linked to a number of disease pathologies. Whilst upregulation may benefit AD, this could be detrimental in cancer progression, atherosclerosis and arthritis (Wetzel et al., 2017). Therefore, any strategy to target ADAM10 must either restore 'normal' physiological activity levels or be specific to cell or tissue expression.

Recently it has been shown that the co-localisation of ADAM10 with the TSPAN proteins is crucial for regulating ADAM10 maturation and trafficking. The repertoire of C8-TSPAN expression (TSPAN5, 10, 14, 15, 17 and 33) differs between cell types and may indicate selective substrate shedding. Further, the interaction between ADAM10 and the six C8-TSPANS form distinct molecular scissors directing cleavage preference towards specific substrates (Matthews et al., 2017). ADAM10 is involved with a large number of substrates, yet there appears no distinct amino acid sequence or position from the membrane for cleavage to occur (Noy et al., 2016). Instead, it is possible that the C8-TSPAN proteins modulate the conformation of ADAM10 and locate the metalloprotease domain at a position favouring a certain substate (Matthews et al., 2017). Perhaps the most well characterised ADAM10 substrate effected by C8-TSPAN expression is N-cadherin. Overexpression of TSPAN15 can significantly increase cleavage compared to other C8-TSPANS (Jouannet et al., 2016, Noy et al., 2016). This is further supported by TSPAN15 knockdown reducing N-cadherin cleavage (Jouannet et al., 2016). Similarly, Notch cleavage is also upregulated by TSPAN5 and 14, yet, TSPAN15 and 33 knockdowns can significantly promote notch cleavage, opposite to that seen for N-cadherin cleavage (Jouannet et al., 2016, Dornier et al., 2012).

ADAM10 mediated AβPP cleavage has also been demonstrated to be regulated by TSPANs (Xu et al., 2009). However, both promoting (Prox et al., 2012) and inhibiting (Jouannet et al., 2016) effects have been identified for various C8-TSPANs which may reflect the different cell types and their repertoire of TSPANs. Further, evidence of non-C8-TSPANs have been shown to influence AβPP cleavage (Seipold et al., 2017), yet, their interaction with ADAM10 is reliant on co-immunoprecipitation studies and diminish under stringent conditions (Dornier et al., 2012). Thus, this effect on ADAM10 activity is likely to be an interaction between multiple TSPANs. The potential to promote specific ADAM10 activity towards AβPP in neurons without the impacting physiological signalling processes is perhaps a key target for this line of research. As our understanding of how Aβ propagation and aggregation influences the pathogenesis of AD, more therapeutic avenues for targeting the ADAM10/TSPAN interaction may become apparent. Recent evidence showing ADAM10 cleavage of the PrP^c, which in turn, prevents Aβ oligomers binding to the cellular membrane (Jarosz-Griffiths et al., 2019) may be one such avenue should ADAM10 cleavge of PrP^c be mediated by C8-TSPANs.

The development of small molecules and antibodies that can interfere with negative regulators or promotors of ADAM10/C8-TSPAN interaction may hold therapeutic benefit. The relative redundancy observed between members of the TSPAN network may allow for partial inhibition of ADAM10 activity without abolishing other physiologically critical processes (Matthews et al., 2017). Further, the organisation of nanoclusters of homogenous TSPAN proteins at the cell membrane may be one area for influencing membrane protein interactions. These interactions may provide an explanation for current phenomena, such as the ADAM10 promoting action of cholesterol depletion. C8-TSPANs have an identified cholesterol binding pocket that when depleted induces a conformation change which may in

turn influence ADAM10 co-localisation at the cell membrane (Matthews et al., 2017, Kojro et al., 2001).

TSPAN mediated chaperone function can also provide scaffolding for ADAM10 interaction with cell surface receptors and intramembrane proteins. This physical interaction has been demonstrated with γ-secretase forming a multi-secretase complex at the plasma membrane (Chen et al., 2015) and was modified by TSPAN12, in addition to C8-TSPANs 5, 14 and 17. Kockdown of TSPAN5 and 14 decreased mature ADAM10 levels and ADAM10 associateion with γ-secretase . In contrast, mature ADAM10 associated to the γ-secretase secretase complex was reduced in TSPAN 12 and 17 knockdown but did not alter ADAM10 maturation (Chen et al., 2015). Although current research is limited, there is a possibility of targeting specific aspects of ADAM10 activity without compromising its association with other substrates.

ADAM10 activity has also associated with agonist binding to members of the glycoprotein-coupled 5-hydroxytryptamine receptors (5HTr), notably the 5HT4, 5HT6 and 5HT7 receptors (Cochet et al., 2013, Chen et al., 2015). Interestingly, agonist stimulation of the 5HT4r increases ADAM10 activity and is linked to an increase in sAβPPα secretion. This may in part, explain the beneficial impact of modulating Serotonin levels in AD and highlights a potential avenue for drug targets aimed at increasing ADAM10 activity and warrants further investigation.

1.10 An Alternative Role for Selective Serotonin Reuptake Inhibitors for the Treatment of Alzheimer's Disease?

"this section is taken verbatim from the following publication in which I am principal author (Elsworthy and Aldred, 2019)".

Depression is a common co-morbidity seen in people with AD (Zhao et al., 2016). Although effective in treating depression the prescription of Selective Serotonin reuptake inhibitors (SSRI) may not always be efficacious for alleviating depressive symptoms in AD. However, interest in the effectiveness of SSRI's for treatment of cognitive decline has been gaining attention. Current research suggests that long-term treatment with SSRI's may delay the progression from MCI to AD (Pelton et al., 2016, Bartels et al., 2018). In fact SSRI treatment has been associated with a reduced mortality rate at two-year follow up, although this effect dissipates after four years (Sepehry et al., 2016). However, those receiving long term treatment may have had an earlier onset of depression-related symptoms. Those who only receive SSRI treatment later in life may instead have depressive symptoms reflecting an early manifestation of AD and therefore, are more likely to develop to clinically significant AD. This raises an important consideration. Effective treatment of major depression with SSRI's can induce neurogenesis and reverse hippocampal atrophy (Eliwa et al., 2017, Dale et al., 2016). However, once the clinical symptoms of AD become apparent the associated neurodegeneration is irreversible. Therefore, the treatment of AD with SSRI's is not curative or necessarily able restore a loss of function, but may delay the disease process and crucially, prolong cognitive function into older age. In order to achieve this therapeutic effect, SSRI's must act through mechanisms that interfere with aberrant pathological processes seen in people with AD and there is emerging evidence to support this effect.

1.10.1 Mechanisms of action

One mechanism that may contribute to the beneficial effects of SSRI treatment for AD is the regulation of Aβ-production and accumulation. Further, it is possible that SSRI treatment has a positive effect on the α-cleavage of AβPP via ADAM10, which would lead to

production of the neuroprotective sAβPP-α. Interestingly, platelet ADAM10 expression can increase with use of SSRI's in people with AD (Bianco et al., 2016b). If this effect is confirmed and is mirrored in the brain, then SSRI use in AD could have implications for the progression of neurodegeneration seen in AD. If the accumulation of Aβ could be slowed by SSRI's increasing the non-amyloidogenic cleavage of AβPP then further Aβ accumulation could be prevented.

Further to this, reduced neuroinflammation and elevated brain-derived neurotrophic factor are all potential mechanisms by which SSRI treatment may contribute to the delayed progression of AD (Bartels et al., 2018). AD is a multifactorial disease. Both increased oxidative stress and a chronic low-grade inflammation are associated with AD (Tramutola et al., 2017, Forloni and Balducci, 2018). Neuroinflammation has been implicated in the progression of AD by increasing amyloidogenic processing of AβPP, resulting in elevated Aβ and increasing the susceptibility of cells to neurodegenerative processes (Minter et al., 2016). SSRI's can reduce peripheral inflammatory markers such as Interleukin-6 (IL-6), C-reactive protein and Tumour necrosis factor-α and prevent microglia activation in the brain (Alboni et al., 2016). This is of particular relevance to AD as the blood brain barrier is more susceptible to leakage of cytokines into the brain. In addition, the anti-inflammatory effect of SSRI's is reflected in the brain by preventing elevated serotonin reuptake from the synapse as a result of elevated cytokine signalling or, by direct action on reducing cytokine production (Kempuraj et al., 2017, Jeon and Kim, 2016). This highlights a possible therapeutic mechanism of action in slowing the global inflammatory response seen as a result of AD progression (Gałecki et al., 2018). Further, SSRI's may also be effective in lowering oxidative stress. This may be due to either increased endogenous antioxidant protein expression, or through possible antioxidant properties of the drugs itself suggesting alternative protective action (Lee et al., 2013, Chang

et al., 2015). Higher levels of blood plasma F2-Isoprostane at baseline have also been associated with a poorer treatment response for depression (de Antonio Corradi et al., 2017, Lindqvist et al., 2017). All the current research assessing the ability of SSRI's to alter inflammation and oxidative stress has been conducted in animal models or in participants with depression alone, and therefore, given the potential interactions in pathologies between depression and AD, studies are needed to explore the effects of SSRI's in people with depression and AD.

As SSRI's may alter the processing of AβPP, and therefore the generation of Aβ, they are a potential candidate treatment to delay the progression of AD. Elevated serotonin signalling has been associated with decreased interstitial fluid Aβ peptide and Aβ plaque load (Sheline et al., 2014). In addition, SSRI use over a 5-year period has been associated with lower Pittsburgh compound-b Aβ load in cognitively healthy participants using SSRI's (Sheline et al., 2014, Cirrito et al., 2011). SSRI's have also been shown to modulate the Aβ peptide species generated and therefore can reduce the toxicity associated with oligomeric forms of Aβ (Aboukhatwa and Luo, 2011). This may also have downstream benefits on tau-hyperphosphorylation by minimising the potential for Aβ-tau cross talk (Nisbet et al., 2015). SSRI's may also help by reducing synergistic toxic effects of Aβ and hyperphosphorylated tau and the associated synaptic and neuronal dysfunction seen in people with AD (Wu et al., 2018, Nisbet et al., 2015). In fact, this effect has been demonstrated in primary rodent neurons (Wang et al., 2016b).

Some of the possible mechanisms by which SSRI's could alter the processing of AβPP are via altered AβPP expression or increased trafficking of AβPP to the cellular membrane, increased ADAM10 activity and/or reduced BACE-1 activity. The majority of work to explore these mechanisms has taken place *in vitro* or in animal models, nevertheless sAβPP-α

increased 3.4-fold after treatment with Citalopram, a commonly used SSRI, which precludes the formation of Aβ (Pákáski et al., 2005). This data is supported by the finding that agonists of the serotonin receptor lowered Aβ in brain interstitial fluid but had no effect on gene expression, suggesting that AβPP processing is altered at protein level in the cell cytoplasm, with ADAM10 being the most likely candidate for upregulation. In support of this, broad pharmacological inhibition of α-secretases prevented the action of Citalopram and led to increased Aβ in brain interstitial fluid (Fisher et al., 2016). Elevated expression of ADAM10 has also been shown in response to Fluoxetine administration in a triple-transgenic mouse model of AD. This alteration in enzyme activity was further supported by an increase in sAβPP-α and C83 protein fragments. The effects of Fluoxetine were ascribed to maintaining or rescuing Wnt/ β-catenin signalling pathways through the phosphorylation of GSK3β and direct action on β-catenin expression, which are thought to be altered in AD (Huang et al., 2018). The therapeutic effects of Fluoxetine on preventing neuron degeneration, synapse dysfunction and for attenuating memory loss have also been well documented in mice (Ma et al., 2017, Sun et al., 2017a). Increased platelet ADAM10 expression has also been reported in participants with AD who were taking various SSRI medication (Bianco et al., 2016b) and this may be mediated by alterations in TSPAN5, which is known to alter the trafficking of ADAM10 in platelets (Gupta et al., 2016).

Together, there is a strong case warranting further research into the use of SSRI medication as a treatment option to delay the progression of AD, targeting multiple mechanisms of action (see figure 3).

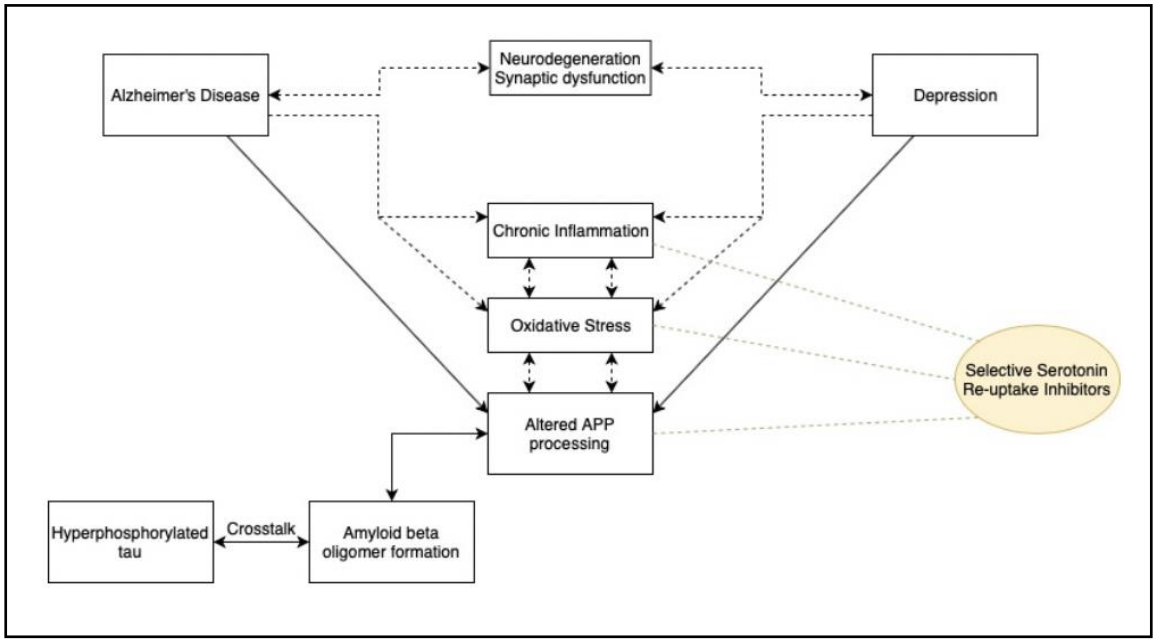

Figure 3 - Diagrammatic representation of the therapeutic targets SSRI's may positively effect that are altered in both depression and AD.

1.11 Modelling the Brain Using Induced Pluripotent Stem Cells

Advances in stem cell biology have enabled new methodologies with the unique ability to manipulate the human central nervous system (CNS), and have allowed the exploration of regenerative medicine and disease modelling with greater relevance to human tissue than previously possible (Shi et al., 2012). The ability to isolate embryonic stem cells from the inner cell mass of human and mouse blastocysts enabled research into the early cellular developmental stages and enabled the identification of key genetic factors that, when expressed, maintain pluripotency. In addition, the induction of an embryonic-like state by replacing nuclear material, or fusion of differentiated cells with embryonic stem cells, highlighted the potential for reprogramming somatic cells (Gurdon et al., 1958, Cowan et al., 2005).

The 2012 Nobel prize in physiology or medicine was awarded to Sir John B. Gurdon and Shinya Yamanaka for the discovery 'that mature cells can be reprogrammed to become pluripotent'. This research culminated in the identification of four key factors, Oct3/4, Sox2, cMyc and Klf4. These factors are since known as the Yamanaka Factors (Takahashi and Yamanaka, 2006, Takahashi et al., 2007). By reprogramming somatic cells to express these transcription factors, a state of pluripotency can be achieved.

By reprogramming human cells back to a state of induced pluripotency it is possible to direct differentiation towards neural precursor cells and ultimately into single cell types or neuron and astrocyte co-cultures by utilising dual SMAD inhibition-based protocols (Shi et al., 2012, Chambers et al., 2009). These electro-physiologically active networks represent a closer model of human brain tissue than previously used models (Hill et al., 2016). The potential to probe human derived CNS networks is of great interest for developing our understanding of, and exploring the effect of interventions on, the pathological processes underlying AD. The presentation of key biochemical features, including elevated Aβ oligomers, hyperphosphorylated tau-protein and increased oxidative stress by these induced pluripotent stem cell (iPSC) neural networks derived from people with AD, suggests this model may be a useful tool in studying the progression of AD (Kondo et al., 2013, Hossini et al., 2015). Crucially, it has been shown that tissue reprogrammed from patients with AD into cortical neurons exhibit phenotypes that are observed *in vivo* (Israel et al., 2012).

1.11.1 Presenilin mutations as viable model to study AD?

Although fAD and LOAD differ in age of onset and underlying genetic contribution to disease progression, the similarities in pathology and biochemical dysfunction make modelling fAD mutations informative for both aetiologies. Neuron and astrocyte co-cultures

derived from human iPSC's carrying *PSEN1* mutations do exhibit pathological features associated with AD during development. Neural progenitor cells (NPC) with a *PSEN1* mutation have been reported to differentiate prematurely, have decreased proliferation and an increased propensity to apoptosis (Yang et al., 2017a). Prior to differentiation NPC's carrying a *PSEN1* mutation have elevated Aβ42/40 ratio, suggesting this is an early event in familial AD development (Sproul et al., 2014). Further, iPSC derived neurons expressing *PSEN1* mutations have been found to exhibit dysfunctional endocytosis linked to an accumulation of β-C-terminal fragments, which could be rescued using BACE-1 inhibitors (Kwart et al., 2019). Astrocytes may also play a role in the pathogenesis of AD, not only by a reduced capacity to support surrounding neurons, but also by directly secreting cytotoxic peptides. Astrocytes derived from iPSC's that carry a *PSEN1* mutation have shown increased Aβ production and dysregulated calcium homeostasis. In addition, astrocytes may have an altered cytokine profile and increased oxidative stress markers, which are considered major features underlying the progression of AD (Oksanen et al., 2017). Elevated oxidative stress and altered mitochondrial function are evident prior to the appearance of Aβ and tau pathology in iPSC derived neurons from people with AD (Birnbaum et al., 2018, Hawkins and Duchen, 2019). This suggests that oxidative stress may be an early event in the development of AD. Further to this, evidence of *PSEN1* mutations altering mitochondrial function may lead to elevated superoxide generation and may compromise cellular redox status (Sarasija and Norman, 2018).

1.12 Research Aims

The overarching aim of this research was to investigate whether differences in markers associated with AβPP processing and redox balance could be detected in both '*in vivo'*

populations at risk of AD and in iPSC-derived cortical cell models of AD. From this, the potential beneficial effects of SSRI treatment on AβPP processing and redox balance were investigated in the iPSC-derived cortical model platforms.

Research in chapter 3 focused on whether alterations in blood-based markers of inflammation and oxidative stress, in addition to platelet ADAM10 protein expression and the AβPPr could be detected in people who may be considered at risk of AD, but who are cognitively healthy. The prodromal developmental nature of LOAD provided the rationale for looking at these markers at a critical time period for intervention and prevention of LOAD. In addition, this research also aimed to assess the utility of platelets as a marker for AβPP processing in 'at risk' populations. The potential identification of robust markers in those at risk for AD may enable targets for identifying risk response to therapeutic treatments, when typical cognitive testing is not appropriate.

The research presented in chapters 4, 5 and 6 aimed to investigate the utility of iPSC-derived cortical cells, carrying *PSEN1* mutations, as models for investigating the effect of SSRI treatment on AβPP processing and redox balance. Initially in chapter 4, iPSC cell cultures carrying either the *PSEN1* mutation L286V or R278I were characterised in comparison to a healthy control line for markers associated with AβPP processing, Aβ generation and oxidative stress. Next, research in chapter 5 aimed to investigate whether the 5HT4r is present and functional in the iPSC-derived cortical models as a potential avenue for SSRI treatment effects. Further, the 5HT4r agonist modulation was investigated for its effect on ADAM10 activity. Finally, in chapter 6 research aimed to test the therapeutic actions of the SSRI, Citalopram, on markers associated withβPP processing and cellular redox balance.

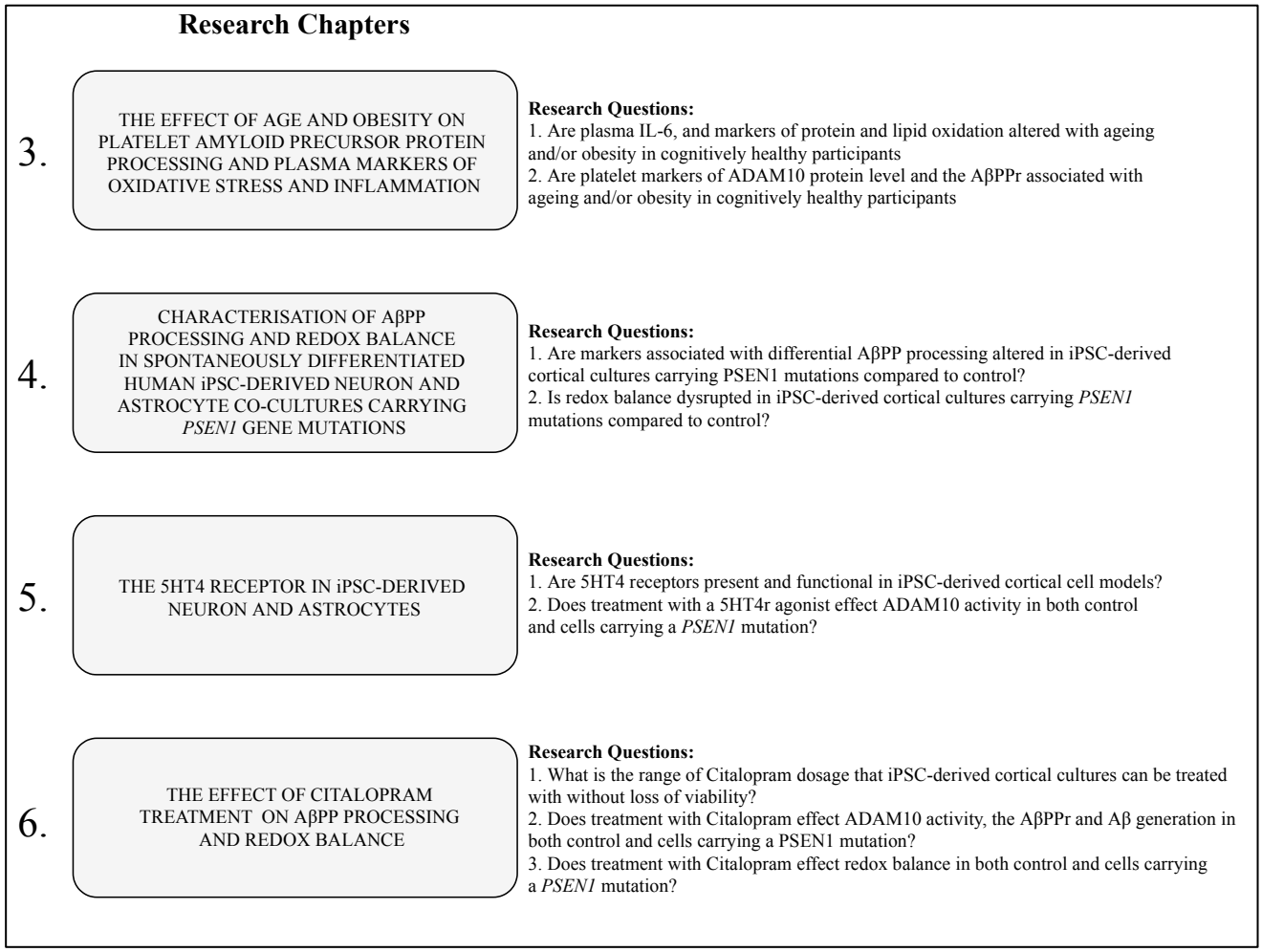

Figure 4 - Diagrammatic outline of research chapters presented in this thesis.

CHAPTER 2 - GENERAL METHODS

2.1 Culturing Protocol of iPSC's: From Stem Cell to Cortical Networks

The protocol for culturing and differentiating Human iPSC's (HiPSC) was kindly supplied by and adapted from the lab of Dr Eric Hill at Aston University. For the cell lines 'Control' (AX0018), and L286V (AX0112) methods of cell culture begin at section 2.1.7 (*Thawing and expansion of HNSC's*) as they are supplied as Human Neural Stem Cells (HNSC's) from Axol Bioscience, Cambridge, UK. Further information and characterisation of all the cell lines used can be found in *table 1*.

Table 1 - *Information on cell lines used for modelling Alzheimer's disease and healthy control*

	Ax0018	**Ax0112**	**R278I**
Diagnosis	Healthy Control	Familial AD	Familial AD
Sample type	Dermal Fibroblast	Dermal Fibroblast	Dermal Fibroblast
Donor sex	Male	Female	Male
Age at sampling (yrs)	74	38	60
Age of onset (yrs)	n/a	39	58
Karyotype	Normal	Normal	Normal
Reprogramming method	Episomal Vector	Episomal Vector	Episomal Vector (Okita et al., 2011)
Induction method	Monolayer – Axolbio NIM (Shi et al., 2012)	Monolayer – Axolbio NIM (Shi et al., 2012)	Monolayer – NIM (Shi et al., 2012)
Mutation	None	PSEN1 (L286V)	PSEN1 (R278I)
APOE status	ε2/ ε2	ε3/ ε3	ε2/ ε4

AX0018

Reprogrammed human dermal fibroblasts as defined by Shi et al., 2012 (Shi et al., 2012) from a healthy donor. This line has been used as a healthy control in previous research looking at the phosphorylation of APP and Sortilin-related receptors (Zollo et al., 2017, Poulsen et al., 2017).

Information on this cell line can be found at this link:

https://www.axolbio.com/shop/product/human-ipsc-derived-neural-stem-cells-male-3353

AX0112

Reprogrammed human dermal fibroblasts as defined by Shi et al., 2012 (Shi et al., 2012) from a donor carrying the PSEN1 L286V mutation. This is an autosomal dominant, missense mutation causing fAD. This line has been used as a model of AD in previous research looking at the phosphorylation of APP and Sortilin-related receptors (Zollo et al., 2017, Poulsen et al., 2017). This mutation has been identified in a number of fAD cases and is associated with extrapyramidal features, myoclonus and progressive memory impairment consistent with a clinical diagnosis of AD.

Information on this cell line and mutation can be found at these links:

https://www.axolbio.com/shop/product/human-ipsc-derived-neural-stem-cells-alzheimer-s-disease-patient-psen1-l286v-2805

https://www.alzforum.org/mutations/psen1-l286v

R278I

This line was kindly gifted by Dr Selina Wray, UCL. Reprogrammed 'in house' by human dermal fibroblasts as defined by Shi et al., 2012 (Shi et al., 2012) from a donor carrying the PSEN1 R278I mutation. This is an autosomal dominant, missense mutation causing fAD. This line has been used in previous research to investigate the specific effects of fAD mutations on Aβ (Arber et al., 2019).

This mutation has been identified in a number of fAD cases and is associated with early language impairment and progressive memory impairment consistent with a clinical diagnosis of AD.

Information on this mutation can be found at this link:

https://www.alzforum.org/mutations/psen1-r278i

2.1.1 Preparation and coating of Geltrex™

Geltrex™ LDEV-Free hESC-qualified Reduced Growth Factor Basement Membrane Matrix (ThermoFisher Scientific, A1413201) was used to enhance the attachment and growth of HiPSC's. Initially, Geltrex™ (200ul) was thawed overnight (4°C) and diluted in pre chilled (4°C) Dulbecco's Modified Eagles Serum (20ml, DMEM, Sigma-Aldrich, SLM-241). Immediately after dilution, DMEM (1ml) was then added to a 6-well multiwell plate (Corning, CA, USA) and spread evenly over the surface of the plate. The plate was then incubated at 37°C for 1 hour. The remaining unbound solution was then aspirated and Essential-8 media (E8 Media, ThermoFisher Scientific, A15170001) supplemented with Rho-associated protein kinase (ROCK) inhibitor (10µM) was added and placed back into the incubator until cells were ready to be plated.

2.1.2 Thawing, expansion and maintenance of HiPSC's

After preparing the plate with *Geltrex™*, pre-warmed E8 media (4ml) and ROCK inhibitor (10µM) was added to a 15ml centrifuge tube (Corning, CA, USA). Next, HiPSC's were rapidly thawed by placing the cryovial in a 37°C water bath and removed when only a small number of ice crystals were present. Thawed cells were then transferred to the centrifuge tube and centrifuged for 3 minutes at room temperature (300xg). The supernatant was then aspirated, and the cell pellet was re-suspended in E8 media and ROCK inhibitor (10µM/ml). The cell suspension was then added to the pre-prepared Geltrex™ coated plate and incubated at 37°C in a 5% CO_2/95% air atmosphere for 24-hours. Finally, a full replacement of E8 media and ROCK inhibitor (10µM/ml) was then carried out. In order to maintain and expand the HiPSC's, daily E8 media only (2ml) without ROCK inhibitor replacement was carried out.

2.1.3 Passage of HiPSC's

Initially, HiPSC's were checked using phase contrast microscopy (EVOS XL Core, Invitrogen) for colony size and changes in morphology suggesting off target differentiation. Areas of differentiation were removed via cell scraping. Media was then aspirated from the remaining cells and washed using D-PBS without calcium and magnesium (1ml/well). Ethylenediaminetetraacetic acid (EDTA) was added to the wells (0.5mM) and incubated for 5 minutes (37°C) or until edges of the cell colonies began to lift. EDTA was then aspirated and E8 media (2ml) was added to detach cells before transferring into a 15ml centrifuge tube. Cell containing tubes were centrifuged (300xg) for 3 minutes at room temperature. Supernatant was then removed, and the cell pellet was resuspended in 3ml E8 media. Cells were then added to pre-prepared Geltrex™ coated plates and incubated at 37°C in a 5% CO_2/95% air atmosphere. Subsequent feeding was carried out every 24 hours using E8 media.

2.1.4 Freezing HiPSC's for cryopreservation in liquid nitrogen

Once HiPSC expansion had been completed and cells were ready for differentiation, subcultures were frozen in liquid nitrogen for longer term storage. Spent medium was aspirated from each well and cells were washed twice with D-PBS (1ml/well). EDTA (1ml) was added to each well and the plate was incubated (37°C) for 5 minutes. EDTA was then aspirated and E8 media (2ml) was added to the wells, gently detaching cells, before transferring into a 15ml centrifuge tube. The cell suspension was then centrifuged (300xg) for 3 minutes before aspirating the supernatant. The cell pellet was resuspended in E8 media (0.5ml/well) and added to a cryovial containing cell freezing media (0.5ml E8, 20%DMSO) and placed in a precooled (4°C) Mr Frosty™ Freezing Container (ThermoFisher Scientific,

5100-0001). Cells were then transferred to a freezer (-80°C) for 24hours. Finally, cryovials were transferred to liquid nitrogen for long term storage.

2.1.5 Induction of HiPSC's to HNSC

The induction of HNSC's from of HiPSC's was carried out once colonies reached 80% confluency. Spent media was removed from HiPSC cultures and washed twice with D-PBS. Cells were detached using (1ml) Accutase™ (Stem Cell technologies, 07922) and incubated (37°C) for 5 minutes followed by gentle pipetting to loosen cell colonies. The cell suspension was then added to a centrifuge tube (15ml) with DMEM (4ml) and centrifuged (200xg) for 5 minutes at room temperature. The supernatant was removed, and the cell pellet was resuspended in E8 media (1ml) with 10µM ROCK inhibitor. The cell suspension was added to Geltrex^{TM} coated wells and incubated overnight (37°C). E8 media was exchanged daily until cells reached 100% confluency as a continuous monolayer.

At this point, cell media was removed and Neural Induction Media (NIM) was added (see table 1 for constituents). A full media exchange with NIM was carried out for a further 9 days. Cell morphology was monitored for the appearance of a multi-layered, phase dark patterning under a microscope (EVOS XL Core, Invitrogen). At day 11, spent media was removed and cells were washed twice with D-PBS before Accutase™ (1ml) was added and incubated (37°C) for 5 minutes. Cells were detached from the culture plastic to from small clusters before resuspension in a centrifuge tube with DMEM (4ml). Cells were centrifuged (200xg) for 5 minutes to pellet cells. The resulting supernatant was then removed, and cells were resuspended in Axol^{TM} Neural maintenance medium (2ml, NMM) AX0031, Axol Bioscience, Cambridge, UK) with 10µM ROCK inhibitor. Cells were incubated for 48hr before a full media exchange with NMM, this was performed every other day for 5 days. To

ensure proper neural induction, cultures were checked for rosettes forming around 12-14 days. At day 17 onwards, cells were passaged 2:1 as described above and maintained with NMM exchange every other day.

Table 2 - *Neural induction media (NIM) made by the addition of small molecule signalling pathway inhibitors to Essential 6 as a base medium.*

Component	**Amount**
Gibco™ Essential 6™ medium (ThermoFisher Scientific, A1516401	50ml
XAV939 (Stem Cell Technologies, 72672)	10µl
LDN193189 (Stem Cell Technologies, 72147)	0.5µl
Sb431542 (Stem Cell Technologies, 72232)	50µl

2.1.6 Freezing HNSC's for cryopreservation in liquid nitrogen

After neural induction of HiPSC's confluent cell culture wells were frozen in liquid nitrogen for longer term storage. Cells were washed with D-PBS and detached from plates using Accutase™ (1ml) as previously described. Following centrifugation (200xg) for 5 minutes cells were resuspended in NMM (2ml) and an aliquot (20µl) was taken for cell counting using Trypan blue (0.4%, T8154**,** Sigma-Aldrich) live/dead exclusion. NMM was added to cell suspension to adjust cells concentration (approx. 4-6 million/ml). Cryovials were filled with NMM (0.5ml, 20%DMSO) and cells suspension (0.5ml) was added (2-3million viable cells, 10% DMSO). Cells were placed in a precooled (4°C) Mr Frosty™ Freezing Container. Cells were then transferred to a freezer (-80°C) for 24hours. Finally, cryovials were transferred to liquid nitrogen for long term storage.

2.1.7 Thawing and expansion of HNSC's

Prior to thawing and expansion of HNSC's, multiwell plates were coated with poly-L-ornithine (20µg/mL) and incubated in a 5% CO_2/95% air atmosphere for 2 hours (37°C), then rinsed twice with sterile dH_20. Laminin was dissolved in sterile dH_20 (10 µg/ml) added to wells (200 µl/cm^2) then incubated at overnight (37°C). Prior to cell seeding, wells were washed with D-PBS without magnesium or calcium. Next, cryovials containing neutrally induced HiPSC's were removed from liquid nitrogen and thawed in a water bath (37°C) until only a small ice crystal was present. Cells were transferred into a centrifuge tube (15ml) containing warm NMM (5ml, 37°C). The resulting cell suspension was centrifuged (200xg) for 5 minutes. The resulting supernatant was removed, and the cell were resuspended in NMM with ROCK inhibitor (10µM/ml) to adjust concentration of cells to allow seeding at 100,000 cells/cm^2. Cells were incubated for 24hr before a full media exchange with NMM every other day. Once 80% confluency was reached, cells were passaged as before. Briefly, cells were dissociated using Accutase™(1ml), pelleted and resuspended in NMM with ROCK inhibitor (10µM/ml). After 24hrs cell media was exchanged for an equal volume of NMM which was exchanged every other day.

2.1.8 Spontaneous differentiation of HNSC's into neuron and astrocyte co-cultures

Prior to passage, plates were coated as previously described using poly-L-ornithine (20µg/mL) and Laminin dissolved in sterile dH_20 (10 µg/ml). For immunocytochemistry, ethanol-sterilised glass coverslips (13 mm) were added into 12-well plates before coating. Following cell passage with Accutase™ (1ml) and resuspension in NMM with ROCK inhibitor (10µM/ml) HNSC's were seeded at a density of 150,000 cells/cm^2. After 24hrs, media was exchanged for NMM with Fibroblast growth Factor 2 (10ng.ml) (FGF2, Sigma-

Aldrich) for 48hrs. Media was then exchanged for NMM every other day. Cells were allowed to spontaneously develop for 40 days. To confirm characterisation of cell phenotype, cell morphology and Immunocytochemical staining was performed (*see chapter 4*).

2.1.9 Preparation of cellular fractions and media collection

After maturation of the cells for 40 days, conditioned NMM was aspirated and transferred into a 15ml Amicon® ultra-15 centrifugal filter unit (3kDa pass filter) and concentrated by centrifugation for 40 minutes (4°C). Concentrated media was then stored (-80°C) for later experiments. Cells were then washed with D-PBS without magnesium or calcium. For whole cell lysates, ice-cold lysis buffer (200 mM NaCl, 10 mM EDTA, 10 mM Na_2HPO_4, 0.5% NP40, 0.1% SDS, 1x Thermo Halt protease inhibitors 78429 and 5μM GI254023X, pH 7.4) was added to the cells and incubated for 10 minutes at room temperature on a plate shaker (500rpm) to dissociate cells from plate. GI254023X (5μM) was added as a potent and selective ADAM10 inhibitor and has been shown to prevent post-lysis autocatalytic degradation of the ADAM10 enzyme and thus, improve protein detection (Brummer et al., 2018). Cells were then transferred to a microcentrifuge tube and subjected to one freeze thaw cycle. Lysates were centrifuged (10,000xg) for 5 minutes to remove debris and the supernatant was aliquoted and stored (-80°C) with fresh protease inhibitors until further use.

2.2 Live Cell Assays

2.2.1 Fluo-4AM imaging

To detect cellular calcium dynamics, cells mounted onto 13mm glass coverslips were incubated with the labelled calcium indicator Fluo-4AM (ThermoFisher Scientific, F14201)

in culture medium for 45 minutes (10μM, 37°C). Cell were then washed twice with fresh culture medium and incubated for 5 minutes (37°C) to allow for de-esterification of AM esters. Imaging was performed using a fluorescence microscope (Nikon Eclipse FN1) with a 20x objective. Fluo-4AM fluorescence was excited at 488nm and captured every 2 seconds to create a time-lapse (Hamamatsu Orca Flash V2). The fluorescence was calculated from five regions of interest containing approximately 3-10 cells using Fiji software (ImageJ, NIH).

2.2.2 MitoSOX Red assay

Cells were stained with MitoSOX Red mitochondrial superoxide indicator (M36008, Invitrogen) at a final concentration of 5μM. Cells were incubated (37°C) for 10 minutes. Images were taken to monitor real-time fluorescence over 5 minutes (Baseline, 150 seconds, 300 seconds). Quantification of the fluorescence intensity that oxidized the MitoSOX reagent was performed with Fiji (ImageJ, NIH) and averaged for three independent experiments.

2.3 Methods of Assessing Protein Expression

2.3.1 Immunocytochemistry

Cell media was exchanged for an equal volume of NMM prior to fixing to remove cell debris. For fixing, 4% paraformaldehyde in D-PBS was added to wells in an equal volume to cell media and left for 5 minutes at room temperature (RT). The solution was aspirated and 4% PFA (1ml) was added for a further 5 minutes (RT). Cells were then washed twice with D-PBS. To prevent non-specific binding of antibodies, cells were incubated in blocking buffer (1% BSA, 0.05% Tween and D-PBS) for 1hr (RT). For intracellular targets, 0.2% (v/v) Triton X-100 was added to blocking buffer instead of Tween. The cells were then stained with primary antibodies dissolved in blocking buffer for 1 hour, with gentle agitation (RT). Cells

were washed three times for 5 minutes in blocking buffer. Then, secondary antibody dissolved in block buffer was added for 1 hour in the dark (RT). Cells were washed three times for 5 minutes in block buffer followed by 1 minute in dH_2O. Cells were mounted to slides using Prolong™ Diamond antifade Mountant with DAPI (P36966, Invitrogen). Cells were imaged using a confocal microscope with a 20x/40x/100x objective (Nikon A1R Inverted Confocal/TIRF microscope) and analysed using NIS-Elements software (Nikon).

2.3.2 Determination of protein concentration

Protein concentration of cell samples was determined using the Bicinchoninic acid (BCA) protein assay (Smith et al., 1985) to enable standardisation of assays. This colorimetric method uses the reduction of Cu^{+2} to Cu^{+1} in an alkaline solution by commonly found amino acids cysteine or cystine, tyrosine, and tryptophan and the universal protein backbone. Initially, lyophilised Bovine serum albumin (BSA, Sigma, Poole, UK) was dissolved in dH_2O to give a final concentration of 1mg.ml. Cell lysates and media were diluted (0.2 – 1.0mg.ml) in lysis buffer (see above). Next, standards were prepared by diluting BSA with dH_2O ranging from 0 – 1mg.ml. Sample or standard (10µL) was added to the appropriate well/s and covered until later use. Copper sulphate (Sigma, Poole, UK) was mixed with BCA in a 50:1 ratio to obtain the necessary volume and added to each well (200µL). The plate was then incubated at 37°C for 30 minutes and protected from light. The absorbance of the plate was then read at 540nm (Fluostar Omega, BMG Labtech) and sample concentrations (mg.ml) were calculated (Omega MARS, BMG Labtech).

2.3.3 Western blotting

The protocols used for SDS-PAGE and western blotting were adapted from (Manzine et al., 2013) with minor modifications. Samples (5-20µg) were mixed 1:1 with Laemmli sample buffer (S3401, Sigma-Aldrich) and heated for 5 minutes at 95°C. After cooling, samples were loaded into 10 well- SDS- PAGE gels (8-10%). Molecular weight markers were also loaded to give context to gel running and transfer (Amersham ECL Rainbow Marker, RPN 756E). Vertical gel electrophoresis was carried out for 1hr at RT (TetraBlot Module, Bio-Rad) or until appropriate separation between molecular weight markers was achieved. Gels containing separated proteins were then transferred to nitrocellulose membranes (Amersham protran 0.2µm) using the Mini Trans-Blot Cell transfer system (Bio-Rad) for 1 hour (4°C). Membranes were blocked with 5% skim milk powder in Tris Buffered Saline with 0.1% Tween (TBST) for 1 hour. After blocking membranes were washed three times in TBST. Membranes were then incubated in the primary antibody overnight (4°C). Membranes were washed five times with TBST followed by incubation with the corresponding secondary antibodies. After, the membranes were developed using ECL substrate (Clarity Western, Bio-Rad) according to manufacturer instruction and imaged using C-digit scanner (Licor). Finally. Bands were quantified using Image Studio (Licor).

2.4 Plate-based Assays

2.4.1 Interleukin-6

IL-6 was measured using a human IL-6 immunoassay (HS600C, Quantikine HS ELISA, R&D systems) following manufacturer's instructions. IL-6 standards were prepared from a dilution series ranging from 0 to 10pg/ml to create an 8-point standard curve. Standard or sample (100µL) was added to the appropriate wells with assay diluent (100µL) and this

was left to bind at room temperature with gentle orbital shaking (500 ± 50rpm) for 2 hours. The plate was then washed 6 times with wash buffer (400µL) before human IL-6 conjugate (200µL) was added and incubated for 2 hours as previously described. Following a second wash step, substrate solution (50µL) was added and allowed to bind for 60 minutes on the benchtop, followed by the addition of the amplifier solution with a 30-minute incubation without shaking. Finally, stop solution (50µL) was added and the absorbance was read at 490nm with 650nm wavelength corrections (Fluostar Omega, BMG Labtech). Linear regression was used to calculate IL-6 (pg/ml) in samples.

2.4.2 ADAM10 enzyme activity

ADAM10 activity was measured via fluorometric FRET assay following manufacturer's instructions (AS-72226, Sensolyte 520, Anaspec). Cells were seeded (15,000 cells/well) onto 96 well plates coated with poly-L-ornithine (20µg/ml) and Laminin (10 µg/ml) and cultured as previously described for 40 days. Next, purified ADAM10 enzyme (positive control), assay buffer (negative control) and was added to appropriate wells. In addition, standards (50µL) were serially diluted and added to wells using the 5-FAM peptide (0 - 5µM). Next, ADAM10 substrate solution (50µL) was added to each well and mixed gently for 30 seconds. The Plate was then incubated at 37 ^{O}C for 45 minutes and read at fluorescence intensity ex/em= 490nm/520nm (Fluostar Omega, BMG Labtech). Linear regression was used to calculate sample ADAM10 activity in relative fluorescence units (RFU) compared to 5-FAM peptide. Data was then normalised to total protein of each sample from BCA protein assay.

2.4.3 Quantification of Amyloid-β peptides 1-40 and 1-42 in cell media

To determine the amount of Aβ 1-40 and 1-42 solid-phase, enzyme-linked immune-absorbent assays were carried out according to manufacturer's instruction (ThermoFisher, KHB3481, KHB3441). The Human Aβ 1-40 and 1-42 solid-phase sandwich ELISA are designed to measure the amount of the target bound between a matched antibody pair. These assays have an analytical sensitivity of <10 pg/mL and are reported to detect a concentration range of 15.6-1000 pg/mL of Aβ 1-40 and 1-42. Initially, standards were prepared by serially diluting the corresponding synthetic 1-40 or 1-42 Aβ peptide (0pg/ml – 500pg/ml) and adding to appropriate wells (50µL). Collected cell media, diluted 1:1 with assay medium, was added (50µL) to the microplate with the pre-coated target-specific antibody. The kit corresponding Aβ detection antibody conjugated to biotin was also added to the remaining wells (50µL) and incubated for 3 hours at room temperature. Each well was then washed four times with wash buffer (1x, 300µL). Anti-rabbit IgG HRP was added to each well (100µL) and incubated for 30 minutes in the dark at room temperature. Wells were washed as previously described and stabilised chromogen (TMB) was added (100µL) following a further 30-minute incubation in the dark at room temperature. Finally, stop solution was added to each well (100µL) and the absorbance was read at 450nm (Fluostar Omega, BMG Labtech). Linear regression was used to calculate sample Aβ (pg/ml) as signal intensity is directly proportional to the concentration of the target protein.

2.4.4 Quantification of Amyloid-β oligomers in cell media

To quantify the amount of Aβ oligomers in spent media, a solid-phase, enzyme-linked immune-absorbent assays were carried out according to manufacturer's instruction (ThermoFisher, KHB3491). The Human Aβ (aggregated) solid-phase sandwich ELISA are designed to measure the amount of the target bound between a matched antibody pair. These assays have an analytical sensitivity of <0.01 ng/mL and are reported to detect a concentration range of 0.09 – 5.7 ng/mL of Aβ aggregates. A serial dilution of standards was prepared using synthetic aggregated Aβ (0ng/ml – 5.7ng/ml) and this was added to appropriate wells (100µL). Samples (collected cell media) were also added to appropriate wells (100µL) and incubated for 2 hours at room temperature. Each well was then washed four times with wash buffer (1x, 300µL). *Hu aggregated Aβ biotin conjugate* (100µL) was added to each well and incubated for 1 hour. A further wash step was carried out, then Streptavidin-HRP working solution (100µL) was added and incubated for 30 minutes. Wells were washed as previously described and stabilised chromogen was added (100µL) with a further 30-minute incubation in the dark at room temperature. Finally, stop solution was added to each well (100µL) and the absorbance was read at 450nm (Fluostar Omega, BMG Labtech). Linear regression was used to calculate sample Aβ (ng/ml) as signal intensity is directly proportional to the concentration of the target protein.

2.4.5 Total 8-isoprostanes

Total 8-isoprostanes were measured using an ELISA kit to assess lipid peroxidation in cell lysates (516351, 8-isoprostane ELISA kit, Cayman Chemical). Immunoprecipitation was performed on cell lysates prior to the assay to ensure maximum specificity of antibody binding. Briefly, samples (100 µL) were added to the 8-isoprostane affinity sorbent (401113,

Cayman Chemical) and incubated for 60 minutes with gentle mixing and then centrifuged at 1500xg for 30 seconds to sediment the sorbent. The supernatant was removed and discarded. Eicosanoid Column Affinity buffer (100µL, 400220, Cayman Chemical) was added and placed in the centrifuge at 1500xg for 30 seconds, the supernatant was then removed. This step was repeated by adding ultrapure water (100µL) before centrifugation and discarding the supernatant. Elution solution (100µL, 95% ethanol) was then added to the sediment and evaporated to dryness under nitrogen. Samples were suspended in the ELISA buffer (100µL). After immunoprecipitation of the samples, standards were prepared from the assay stock solution to create an 8-point standard curve ranging from 0/8 to 500pg/ml, a blank well was used as the 0pg/ml standard. Standard or sample (50µL) was added to the appropriate well with of 8-isoprostane tracer (50µL) and antiserum (50µL). This was incubated for 18hours at 4^{O}C. Ellman's reagent was added to each well (200µL) and left to incubate for 2 hours with gentle agitation. The plate was then read at 420nm (Fluostar Omega, BMG Labtech) and samples were calculated against the logit regression of standards (pg/ml) For cell assays, samples were normalised to total protein concentration of corresponding sample (pg/ml/mg) .

2.4.6 Protein carbonyls

Modification of protein by formation of carbonyl groups was assessed by the method of (Carty et al., 2000). The preparation of carbonyl standards was carried out prior to the assay. Briefly, dialysis tubing was prepared by boiling in sodium bicarbonate (2% v/w) and EDTA (1mM, pH8). Tubing was rinsed and boiled for a further 10 min EDTA (1mM, pH8) before cooling and storing in EtOH at 4 ^{o}C. For oxidized BSA, BSA (10mg/ml) (50ml) was oxidized with AAPH (500mM) for 1h at 37 ^{o}C and dialysed against Tris-buffered Saline (pH7) for 24hours with frequent buffer changes. For reduced BSA, BSA (10mg/ml) was

added to sodium borohydride (1g) in TBS (50ml) and allowed to reduce overnight at 4 °C. The solution was then dialysed against TBS pH7, with frequent buffer changes. Protein concentration was then adjusted following BSA assay measurement and adjusted to equal concentrations (mg/ml). Oxidised and reduced standards were serially mixed to give a range of concentrations. Standards (500ul) were then added to DNPH (10mM, 500ul) and left for 1h with gentle agitation. Controls were made with HCl (2N, 500ul) added to DNPH (10mM, 500ul). Trichloroacetic acid (20%, 500ul) was then added to each standard and mixed before centrifugation for 3 min at 13000g. The supernatant was discarded, and the pellet washed 3 times with ethanol:ethyl acetate (1:1). Following washing, pellets were resuspended in guarnidine HCl (1ml) and after vortexing left for 30 mins at 37 °C. Solutions were vortexed once more before centrifugation for 1min at 13000g. The supernatant was then removed, and absorbance read at 360nm (Fluostar Omega, BMG Labtech). Molarity of the solution was calculated ((abs-blanks)/22000) and normalized to protein content to give standard carbonyl content (nmol/mg).

For determining carbonyl content samples (sodium carbonate 50mM, pH 9.2) were plated into 96 well plates (50µL at 0.05mg/ml). Protein was allowed to bind for 1h at 37°C before washing with TBS–Tween (300µL, 0.5%). DNPH was added in 2M HCl (1mM, 50µL) and allowed to react for 1h at room temperature before washing as before. Non-specific binding sites were blocked overnight at 4°C with TBS-tween (200µL, 1%). After washing, rabbit anti-DNPH primary antibody (50µL, 1:1000) was applied and incubated for 1h at 37°C and, following washing with TBS/Tween, anti-rabbit IgE conjugated to peroxidase (50µL, 1:5000) was also incubated at 37°C for 1h. The reaction was visualised by substrate solution (50µL; o-phenylenediamine tablets with hydrogen peroxide (8µl) in citrate-phosphate buffer (10ml) and stopped by addition of sulphuric acid (50µL, 2N). Absorbance was read at 490nm

(Fluostar Omega, BMG Labtech) and samples were calculated using linear regression. For cell assays, samples were normalised to total protein concentration of corresponding sample (mg/ml).

2.4.7 Total antioxidant capacity

Total antioxidant capacity was measured using a previously described method (Benzie and Strain, 1996). For blood plasma, samples were diluted 1:1 with ultrapure water (Millipore). For cell lysates, no dilution was utlised. Standards were freshly prepared using Ascorbic acid to create a 7-point standard curve ranging from 0µM to 1000µM. Sample or standard (10µl) was then added into wells a 96-well microtiter plate in duplicate. Next, the 'FRAP' reagent (300µl) was made by combining acetate buffer (30ml, 300mM), TPTZ solution (3ml, 10.6mM) and ferric chloride solution (3ml, 20mM) and added to each well. The plate was then incubated for 8 minutes at room temperature. Plate reading was completed at 650nm (Fluostar Omega, BMG Labtech) and values were calculated using linear regression. Values were expressed as µM of antioxidant power relative to ascorbic acid. For cell lysates assays, samples were normalised to total protein concentration of corresponding sample (µM /mg).

2.4.8 Succinate dehydrogenase activity (MTT) assay

HNSC's were seeded (20,000/well) onto 96 well plates coated with poly-L-ornithine (20µg/ml) and Laminin (10 µg/ml) and cultured as previously described for 20 days. Enough wells were cultured to enable triplicate repeats for each control and experimental condition. Treatments were serially diluted and delivered using NMM as the vehicle which was exchanged prior to the assay. Control wells were prepared cells the vehicle alone. After

incubation with the treatment media was removed and cells were wash two times with D-PBS. For the assay, 3-(4,5-Dimethylthiazol-2-Yl)-2,5-Diphenyltetrazolium Bromide (MTT) stock solution was diluted in NMM (1:5), added to each well (100µl) and incubated for three hours (37°C). The MTT solution was then aspirated and DMSO (50µl) was added to each well. Cells were placed on a plate shaker (500rpm) for 30 seconds followed by incubation for 10 minutes (37°C). Finally, absorbance was read at 590nm (Fluostar Omega, BMG Labtech). Percentage viability was calculated from control cells using a Log dose-response curve.

2.5 Statistical Analysis

All statistical analysis was carried out using GraphPad, Prism v8 to produce data figures. Statistics for each chapter are reported specific methods.

CHAPTER 3 - THE EFFECT OF AGE AND OBESITY ON PLATELET AMYLOID PRECURSOR PROTEIN PROCESSING AND PLASMA MARKERS OF OXIDATIVE STRESS AND INFLAMMATION

"Parts of this section are taken verbatim from the following publication in which I am principal author"

Elsworthy, R. J., & Aldred, S. (2020). The effect of age and obesity on platelet amyloid precursor protein processing and plasma markers of oxidative stress and inflammation. *Experimental Gerontology*, 110838.

3.1 Background

This chapter focuses on the identification of an altered physiological state in cognitively healthy individuals who are 'at risk' of developing LOAD. The use of platelet AβPPr and ADAM10 as markers of LOAD has shown promise for identifying people with AD compared to cognitively healthy people (Bianco et al., 2016b, Manzine et al., 2013, Manzine et al., 2014). However, it is not known whether AβPP processing is affected by risk factors for LOAD in cognitively healthy people. Both ageing and obesity are known risk factors for the development of LOAD and are independently associated with elevated circulating biomarkers of oxidative stress and inflammatory cytokines (Fulop et al., 2017, Hauck et al., 2019).

3.1.1 Inflammation and oxidative stress in ageing

Inflammation is a key protective process that is stimulated either by endogenous signalling or invading pathogens to minimise injury, remove necrotic cells and repair damage to tissue (Netea et al., 2017). However, with increasing age there is a shift towards a chronic low-grade inflammatory state. The persistent elevation of inflammatory cytokines has been

termed ‘inflammageing’ and is linked with a high susceptibility to chronic morbidity, disability, frailty, and premature death (Ferrucci and Fabbri, 2018). In addition, the accumulation of genotoxic and oxidative stress can drive cellular senescence which is associated with organelle dysfunction, protein misfolding, dysregulated autophagy/mitophagy and DNA damage (Filomeni et al., 2015). This cellular dysfunction can then generate excess reactive oxygen species (ROS) further elevating oxidative damage, contributing to the chronic inflammatory state seen in ageing (Fulop et al., 2017). Reactive oxygen species are signalling molecules that are fundamental to normal physiology (Sies et al., 2017). To prevent uncontrolled oxidation cascades, antioxidant enzymes and exogenous sources of antioxidant molecules are able to quench ROS to maintain reduction/oxidation (Redox) homeostasis. However, excessive ROS production or reduced antioxidant capacity, as a result of altered metabolic regulation, can have pathophysiological consequences. Chronic inflammation and elevated oxidative stress are intrinsically linked (Blaser et al., 2016). ROS are a central feature of inflammasome signalling and have a role in the regulation of inflammatory pathways including the nuclear factor κ-light-chain-enhancer of activated B cells (NF-κB) (Morgan and Liu, 2011). In addition, ROS generation can lead to secondary oxidative modification of carbohydrates, proteins, lipids and DNA which can have deleterious consequences for cellular function (Radi, 2018). The accumulation of these oxidative modifications have been implicated in the ageing process in the free radical theory of ageing (Harman, 1992) and can be detected as markers of oxidative stress in several diseases such as cardiovascular, metabolic and neurodegenerative disease (Liguori et al., 2018, Forrester et al., 2018, Bisht et al., 2018).

3.1.2 Inflammation and oxidative stress in obesity

Obesity is a global health challenge with over a third of the population overweight or obese. In addition, obesity is becoming more prevalent in younger people (Ng et al., 2014). People who are obese have an elevated risk of metabolic diseases, cardiovascular disease, cancer and neurodegenerative disease in which inflammation and oxidative stress mechanisms have been implicated (Saltiel and Olefsky, 2017). Chronic obesity is associated with a sustained low-grade inflammation which is associated with the development of insulin resistance, hyperglycaemia and dyslipidaemia (Stolarczyk, 2017). The alteration in cytokine signalling can also lead to elevated oxidation of biomolecules which have been found to accumulate in tissue specific sites and globally (Hauck et al., 2019). An excessive supply of energy substrates to metabolic pathways in adipose and non-adipose tissue can lead to elevated ROS production coupled with mitochondrial dysfunction. This can lead to disrupted ROS-mediated signalling pathways such as C-jun N-terminal kinases (JNK) and NF-κB which may play a key role in insulin resistance (Bonomini et al., 2015). Typically, people who are obese consume a diet much lower in vitamins and antioxidants as well as engage in a more sedentary lifestyle which can further promote a pro- oxidative stress state (Hosseini et al., 2017).

Adipose tissue has an important endocrine function controlling the release of several hormones including leptin and adiponectin as well as the secretion of cytokines. Adipose dysfunction caused by excessive adipocyte hypertrophy, impaired lipid metabolism and inadequate vascularisation can further promote a proinflammatory state. In addition, overwhelming adipocytes with lipids can lead to elevated ROS production which prevents 'healthy expansion' and increases ectopic lipid accumulation (Okuno et al., 2018). The combination of elevated adipokines, increased ROS production and reduced antioxidant

enzyme activity seen in obesity can significantly increase the risk of vascular and cognitive comorbidities (Fernández-Sánchez et al., 2011).

3.1.3 Alzheimer's disease in ageing and obesity

Although AD is typically associated with hallmark neuropathology, metabolic dysfunction of peripheral tissue has been identified as contributor to increased risk of the disease. Mid-life obesity, independent of insulin resistance and vascular disease, can significantly increase the risk of AD (Serrano-Pozo and Growdon, 2019). However, the presence of these metabolic comorbidities can further increase the risk of developing AD (Caleyachetty et al., 2017), possibly mediated by low-grade inflammation and increased oxidative stress (Letra et al., 2014, Verdile and Keane, 2015). Elevated inflammatory cytokine signalling cascades are a prevalent feature of AD in both peripheral tissue and brain (Ferreira et al., 2014). Clustering of activated microglia and astrocytes around areas of the brain with amyloid-β (Aβ) plaques enables increased cytokine signalling and innate immunological action, resulting in neuroinflammation (Heneka et al., 2015). Systemic inflammation is thought to interfere and interact with immunological processes in the brain and promote disease progression, therefore, peripheral markers of inflammation have received much attention in the assessment of AD risk.

Increased oxidative stress may also be an early event in the propagation of AD (Caldwell et al., 2015, Nunomura et al., 2001, Zhu et al., 2004). The brain is susceptible to oxidative stress due to its high energy demand, high polyunsaturated fat content and limited antioxidant capacity (Skoumalová and Hort, 2012). Several studies have shown that AD is associated with greater protein carbonyl formation, both in the brain (Butterfield et al., 2006a) and in the periphery on specific proteins linked to cardiovascular dysfunction (Aldred et al.,

2010). This elevation is even seen in mild cognitive impairment (MCI), which is often seen as a precursor to AD (Bermejo et al., 2008, Conrad et al., 2000, Greilberger et al., 2010, Perrotte et al., 2019). The formation of protein carbonyls can be initiated by end products of lipid peroxidation. Due to the brain's high poly-unsaturated fat content, small lipophilic molecules with the capability to cross the blood brain barrier can be produced. These lipophilic molecules are then able to oxidise downstream peripheral targets (Skoumalová and Hort, 2012). F2 isoprostanes are one of the most reliable markers of lipid peroxidation. These prostaglandin-like molecules arise from the non-enzymatic esterification and hydrolysis of the poly-unsaturated fatty acid, Arachidonic acid. F2-isoprostanes have been found to be significantly increased in AD (Sinem et al., 2010).

Although the onset of AD symptoms is typically seen over the age of 65, there is a growing consensus that the underlying biochemical pathology may be present as much as 30 years prior to this. Therefore, it is imperative to develop a greater understanding of how lifestyle factors in younger populations can impact AD. Investigating accessible biomarkers that enable early detection of disease, such as AD is therefore a priority for current and future research.

Due to the prodromal nature of AD development, it is becoming increasing possible to identify biomarkers prior to clinical symptoms of dementia (Dong et al., 2017, Albani et al., 2019). Therefore, it may be possible to detect changes in platelet AβPPr and ADAM10 expression, however, this has not been examined. Interestingly, cognitively healthy older adults have been shown to have increased ADAM10 expression and activity compared to younger individuals (Schuck et al., 2016) however, this is the only evidence of this effect so far. Therefore, the aim of this chapter was to establish whether platelet AβPPr and ADAM10

in addition to plasma markers of inflammation and oxidative stress were altered with advanced age and obesity or a combination of both.

3.2 Methods

3.2.1 Participants

Ninety participants were recruited with a BMI (weight(kg)/height(m)^2) between 17 and 25 (low BMI) or greater than 27 (high BMI) and aged between 21 and 35 years (young) or between 63 and 80 years (old) via online recruitment websites, poster advertisement and participant databases. Individuals who reported a history of gastric banding, eating disorders, neurological or inflammatory disorders (e.g., rheumatoid arthritis, inflammatory bowel disease, multiple sclerosis, periodontitis) or use of anti-depressant, antihistamine, or anti-inflammatory (e.g., antibiotics) medication during the past 7 days were excluded. Participants were invited to make one visit to the lab for anthropometric measures and blood collection. Participants were asked to consume their 'normal' breakfast and refrain from eating or drinking (except water) for a minimum of one hour prior to the visit. Participants were asked to maintain a similar routine before sessions.

Participants were also asked not to engage in strenuous physical exercise or consume alcohol within 12 hours before the test session and reschedule their appointment if they had suspected infection symptoms on the day of testing. On arrival, written informed consent was obtained and it was verified via self-report whether all had complied with instructions. Ethical approval was obtained from the Institutional Science, Technology, Engineering and Mathematics ethics panel.

3.2.2 Blood collection

Blood (6 ml) was collected in Sodium Citrate tubes (Vacutainer, BD). The interval between the collection and the processing was a maximum of 30 minutes. The platelet-rich plasma (PRP) was obtained by centrifugation at 100x*g* for 20 min. Prostaglandin-1 (5µM PGE-1, Sigma-Aldrich) and 1x protease inhibitors were added (Halt protease inhibitor, Thermo Fisher scientific). Platelets were also collected by additional centrifugation of PRP at 7600x*g* for 10 min at room temperature, then washed twice in phosphate buffered saline solution (PBS). Finally, the platelet pellet was suspended in cold lysis buffer (200 mM NaCl, 10 mM EDTA, 10 mM Na_2HPO_4, 0.5% NP40, 0.1% SDS, and 1x protease inhibitors) and incubated for 30 minutes at room temperature. Aliquots of PRP and platelet lysates were then frozen at -80 °C until further use.

3.2.3 SDS-PAGE and Western blotting

The protocols used for SDS-PAGE can be found in the section *2.2.3 Western blotting*. Briefly, the volume of platelet lysate containing 10µg of protein, quantified via BCA assay (Smith et al., 1985), was boiled for 5mins at 95°C and loaded into 10% SDS- PAGE gel. To confirm ADAM10 detection, a purified ADAM10 peptide (Abcam 7868) was used to compare samples. Molecular weight markers (5µl) were loaded at each end of the gels. After the gel running, the proteins were transferred to nitrocellulose membranes for 1 hour. Membranes were blocked with 5% milk in TBST 0.1% for 1 hour and washed in 0.1% TBST. Membranes were then incubated in the primary antibody for ADAM 10 (AB1997), AβPP (Merck MAB348, 22C11) or Actin (Sigma AC40 A3853) followed by incubation with corresponding secondary antibodies (Sigma Anti-mouse IgG FC-specific A0168 or Cell Signalling Anti-rabbit IgG, HRP-linked Antibody 7074). After, the membranes were

developed using ECL substrate, imaged and quantified as previously described. To control for between blot variation in densitometry, samples were normalised to repeated runs of the same participant sample.

3.2.4 Plate-based Assays

PRP samples were analysed for IL-6, Protein Carbonylation, 8-Isoprostanes and total antioxidant capacity as previously described in section *2.4.4 Plate-based assays*.

3.2.5 Statistical Analysis

All quantitative data in the text and figures are presented as Mean ± S.D. unless otherwise stated. To test sample distribution normality the Shapiro-Wilk test was employed. Statistical analysis of between group and between sub-group effects was calculated using Kruskal-Wallis H tests with multiple comparisons of mean rank. This was performed for the total sample (Young/Lean, Young/Obese, Old/Lean and Old/Obese) and for each co-morbidity and medication individually. Spearman's correlation tests were subsequently performed to assess the relationship between plasma markers and platelet protein expression markers. Sensitivity and specificity of plasma markers to predict group characteristics were calculated using receiver operating characteristic (ROC) curves. All data was processed, and figures built using GraphPad Prism Version 8.4.3. The statistical significance level was set at 5%.

3.3 Results

3.3.1 Participant characteristics

Participants were placed into one of four groups based on their age and body mass index (BMI). Inclusion criteria for age was under 40 years for the young groups and over 65 years for the older groups. BMI requirements for the Lean group was below 24.9 $kg.m^2$ and over 29.9 $kg.m^2$ for the participants with obesity. Participants were free from a history of gastric banding, eating disorders, neurological or inflammatory disorders (e.g., rheumatoid arthritis, inflammatory bowel disease, multiple sclerosis, periodontitis) or use of anti-depressant, antihistamine, or anti-inflammatory (e.g., antibiotics) medication during the past 7 days.

Table 3 - *Characteristics and comparison of the participant sample*

Item	Young lean	Young with obesity	Old lean	Old with obesity
PARTICIPANTS (N=90)	21	21	24	24
AGE (YEARS)	24.67 ± 3.38	27.90 ± 4.27	71.67 ± 4.30*	69.67 ± 3.53*
SEX (M/F)	9/12	8/13	9/15	10/14
ETHNICITY %				
- Asian	38.1	47.6	0	0
- Black	4.8	4.8	4.2	4.2
- Hispanic	4.8	0	0	0
- White	52.3	47.6	95.8	95.8
EDUCATION LEVEL %				
- Higher	100	72	75	72
- Middle	0	17	25	28
- Lower	0	11	0	0
SELF REPORTED HEALTH (SCALE 1-10)	8.4 ± 0.9	7.6 ± 1.4	8.7 ± 0.9	8.0 ± 1.2
BMI (kg/m^2)	21.97 ± 2.69	34.02 ± 3.67#	23.51 ± 2.13	32.96 ± 3.66#
EMOTIONAL HEALTH				
- Depression	4.7 ± 6.1	7.4 ± 7.5	1.1 ± 2.0	2.8 ± 3.7
- Anxiety	4.7 ± 5.0	6.0 ± 5.8	0.6 ± 1.3	1.5 ± 2.0
- Stress	10.3 ± 7.5	10.4 ± 7.0	4.8 ± 4.5	5 ± 4.8
- Loneliness	37.2 ± 7.9	37.4 ± 7.5	35.3 ± 6.0	36.5 ± 6.5
COMORBIDITIES				
- CVD	0	0	7	13
- Diabetes	0	0	3	5
- Hypertension	0	0	6	8
MEDICATION				
- Statins	0	0	6	8
- Antihyperglycemic agents	0	0	2	5

(Data shown as mean ± SD)

**Significantly greater than Young Lean and Young with obesity* (p<0.050)

#Significantly greater than Young Lean and Old Lean (p<0.050)

3.3.2 Inflammation

Plasma IL-6 (Figure 4, A) was significantly elevated in young with obesity (2.87 ± 1.69 pg/ml, p=0.007) and old with obesity (2.50 ± 1.10 pg/ml, p=.000) compared to young

lean participants (1.22 ± 0.58 pg/ml). No significant effect of age was detected (p>.05). Simple regression analysis revealed that BMI was the most influential predictor of plasma IL-6 ((F(1,88)= 20.625, p=.000) R^2 = .190). Plasma IL-6 (pg/ml) was found to increase for every .098 kg.m^2 increase in BMI. In addtion, ROC analysis of plasma IL-6 showed an ability to distinguish between participants with obesity and participants without obesity (AUC of 0.80, SE = 0.05, P < 0.001)(Figure 5, **C**).

3.3.3 Oxidative stress

Plasma 8- Isoprostanes (Figure 5, **B**) were significantly elevated in old participants with obesity (52.78 ± 25.09 pg/ml) compared to young lean (25.71 ± 14.51 pg/ml, p < .001), young with obesity (27.97 ± 15.10 pg/ml, p=.000) and old lean (32.87 ± 14.21 pg/ml, p = .001) participants. Both age ((F(1,88) = 12.371, p = .001) R^2 = .123) and BMI ((F(1,88) = 7.413, p = .008) R^2 = .078) were significant predictors of plasma 8-isoprostane concentration. Ageing was associated with an increase in 8-isoprostanes by 1 pg/ml for every .322 increase in years. Obesity was associated with an increase in 8-isoprostanes by 1 pg/ml for every .934 increase in BMI (kg/m^2). Plasma 8-isoprostanes were able to distinguish between both young/ old (AUC of 0.73, SE = 0.05, P < 0.01) (Figure 5, **C**), and participants with obesity and without obesity (AUC of 0.66, SE = 0.01, P < .01) (Figure 5 **D**). Sub-group analysis revealed that plasma 8-isoprostanes were significantly elevated in participants with obesity with a diagnosis of diabetes compared to participants with obesity without diabetes (66.82 ± 29.99 pg/ml, 38.02 ± 17.58 pg/ml, p < .01).

Plasma protein carbonyls were significantly elevated in old participants with obesity (1.44 ± 0.31 nmol/mg) compared to young participants with obesity (1.05 ± 0.13 nmol/mg, p = .000). Further analysis showed that plasma protein carbonyls could distinguish young and

old participants (AUC of 0.69, SE = 0.07 $P < .02$) (*Figure 5,* ***D.***). No significant effects were found for plasma antioxidant status ($p > .05$).

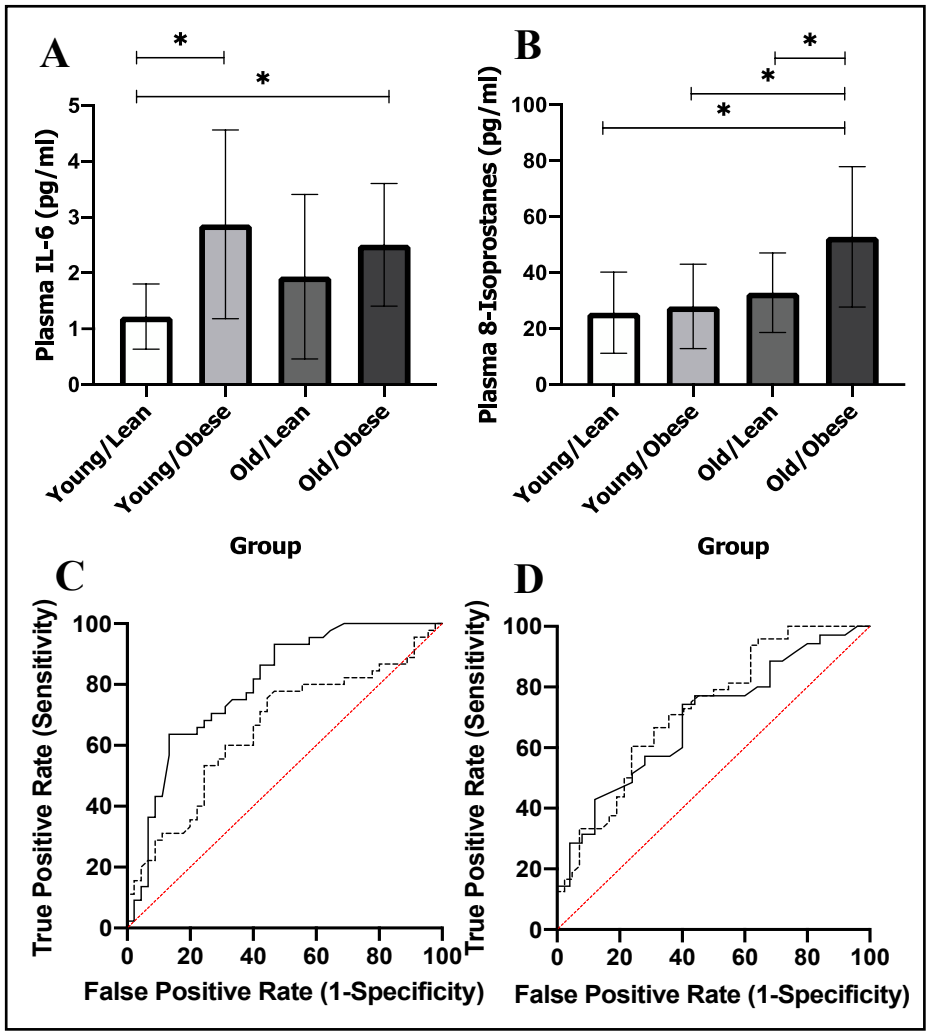

Figure 5 - *Effect of age (years) and BMI (kg/m^2) on plasma markers of inflammation and oxidative stress.* ***A****, Plasma IL-6 (pg/ml) compared between groups.* ***B****, Concentrated plasma 8-isoprostane (pg/ml) compared between groups.* ***C.*** *ROC analysis for predictive capacity of plasma IL-6 (solid line) and isoprostanes (dashed line) to distinguish between obese and non-obese participants.* ***D****, ROC analysis for predictive capacity of plasma protein carbonyls (solid line) and isoprostanes (dashed line) to distinguish between young and old participants. * indicates a significant difference between corresponding groups.*

3.3.4 Platelet AβPP processing markers

A Kruskal-Wallis H test showed that there was a statistically significant difference in Mean Rank platelet mADAM10 protein levels (AU) between groups, $\chi2(3) = 16.734$, $p = 0.001$ (Figure 6, **A)** Old Lean participants had significantly lower platelet mADAM10 protein levels than both Young Lean ($p = 0.017$) and Young participants with obesity ($p = 0.007$). Old participants with obesity also typically showed lower platelet mADAM10 protein levels compared to Young Lean ($p = 0.083$) and Young with obesity ($p = 0.033$). Mean Rank platelet proADAM10 protein levels (AU) was also significantly different between groups, $\chi2(3) = 13.986$, $p = 0.003$ (Figure 6, **B**). Old participants with obesity had significantly lower platelet proADAM10 protein levels compared to both Young Lean ($p = 0.011$) and Young with obesity ($p = 0.030$). Both platelet mADAM10 and proADAM10 were significantly decreased with advancing age ($p<0.05$). Platelet mADAM10 was found to significantly decrease with elevated protein carbonyls. There was no statistically significant difference in platelet AβPPr between groups ($p>0.05$).

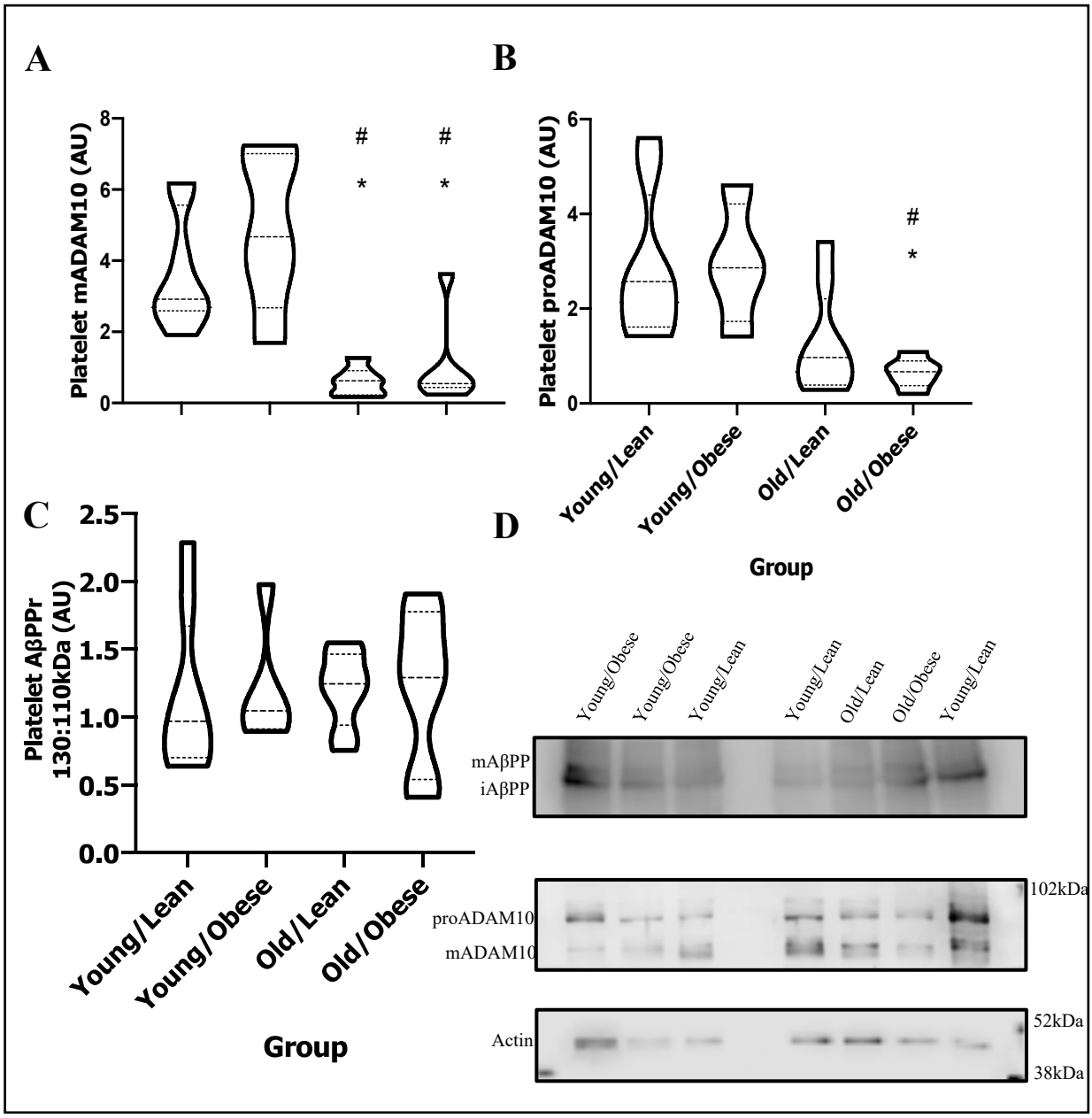

Figure 6 - Effect of age (years) and BMI (kg.m^2) on platelet protein levels of AβPP isoforms and ADAM10 measured via western blotting in a sub sample of participants (Young/Lean n=8, Young with obesity n=6, Old/Lean n=8, Old with obesity n=7). **A**, Platelet protein levels of mADAM10 (AU) normalised to Actin compared between groups. **B**, Platelet protein levels of proADAM10 (AU) normalised to Actin compared between groups. **C.** Platelet protein levels of AβPP (AU) analysed at the ratio between upper and lower band compared between groups. **D**, Images of western blotting for AβPP (Upper box), ADAM10 (middle) and Actin as a control protein (Lower box). *significantly lower than Young/Lean # significantly lower than Young/Obese

3.4 Conclusion

Alterations in platelet ADAM10 expression and AβPPr have been detected in people with AD and MCI. However, it is not known whether these changes are present in people who may be 'at risk' of developing AD despite being cognitively healthy. In this study, IL-6 was significantly associated with increasing BMI whereas lipid peroxidation was more closely related to ageing, with the highest detection in older participants with obesity (Figure 5). mADAM10 was significantly decreased with ageing, with proADAM10 being significantly lower in older participant's with obesity. There were no detected changes in AβPPr between groups (Figure 6).

The results from this study suggest that age and obesity are differentially associated with inflammation and oxidative stress measures. Obesity was associated with elevated inflammation irrespective of age. This finding supports other similar studies suggesting that low-grade inflammation is prevalent in people who are obese and may be linked to the presence of insulin resistance, hyperglycaemia and dyslipidaemia (Stolarczyk, 2017). The alteration in cytokine signalling seen in obesity can also lead to elevated oxidation of biomolecules, which have been found to accumulate in tissue specific sites and globally (Hauck et al., 2019). This is reflected in the current data presented showing that participants with obesity had the greatest accumulation of 8-isoprostanes (figure 5).

Older age, not obesity, was more strongly associated with elevated markers of oxidative stress (Figure 5). Although the production of ROS is essential for normal physiological function, the gradual accumulation of damage as a result of redox imbalance is present in ageing. These oxidative markers are typically further elevated in a number of disease pathologies including neurodegenerative diseases (Liguori et al., 2018, Forrester et al., 2018, Bisht et al., 2018). Interestingly, lipid oxidation was associated with obesity

however, this was not significantly altered in younger participants with obesity (Figure 5). It is possible that younger individuals are able to better tolerate increased ROS production and it is in mid to late-life that obesity significantly impacts oxidative stress (Letra et al., 2014).

This present study is the first to measure changes in ADAM10 protein levels in individuals with obesity. Ageing was linked to lower protein levels of proADAM10, whereas obesity in later life was associated with lower mADAM10 (Figure 6). Alzheimer's disease is argued to exist as a prodromal syndrome long before the onset of clinical symptoms (Dubois et al., 2016). Therefore, a major challenge for researchers is to develop biomarkers capable of detecting AD in 'at-risk' populations to enable effective intervention. People with obesity are one example of an at-risk population (Serrano-Pozo and Growdon, 2019, Caleyachetty et al., 2017). Platelet ADAM10 is an enzyme that acts to preclude Aβ liberation from AβPP and is currently under investigation as a potential biomarker. The protein levels of pro- and mADAM10 were lower in older individuals compared to younger individuals. This contradicts research by (Schuck et al., 2016) who found elevated ADAM10 protein expression and activity in cognitively healthy older adults. A potential explanation for this difference could be that both studies are subject to recruitment bias. The trajectory of ADAM10 expression across the lifespan may be dependent on the individual and therefore, those who age cognitively healthy may have elevated ADAM10 activity from mid-life or younger ages. Further, the effects of diet, exercise and sleep, which are considered neuroprotective against AD, have not been investigated for their impact on ADAM10 protein expression and activity.

In this study there was a significantly lower amount of proADAM10 that was only found in old participants with obesity (Figure 6). This may provide insight into a link between late life-obesity and increased AD risk and warrants further investigation. Although there was

a significant reduction in mADAM10, proADAM10 was not significantly lowered in healthy older participants compared to younger participants (Figure 6). Therefore, ageing may alter the trafficking or pro-domain cleavage of the proADAM10 peptide which are both crucial post-translational steps for generation mature ADAM10. The significant reduction of ProADAM10 was only seen in older participants who were also obese (Figure 6). This may suggest a combinatory effect of ageing and obesity on Pro-ADAM10 protein levels and may reflect changes at a protein transcription level. Whilst changes in ADAM10 expression were identified, there was no change in AβPPr. A reduction in AβPPr has been found in people with MCI and AD as it is indicative of altered maturation of AβPP, which is a crucial event in trafficking to the cell membrane (Colciaghi et al., 2002, Colciaghi et al., 2004). A reduction in maturation may render AβPP to endocytotic vesicles and undergo lysosomal degradation where interaction with BACE-1 is more likely and thus, the generation of Aβ (Cole and Vassar, 2007). Therefore, it is likely that changes in AβPPr is a much later event in the development of AD and perhaps is more closely related to cognitive impairment. Therefore, changes wouldn't appear in this participant group.

Future research into the effect of obesity as a co-factor in the development of AD should examine changes in biomarkers over a longitudinal period. No changes in ADAM10 protein levels were found in young obese participants, it is possible this age range precludes the typical onset of AD pathological changes in AβPP processing and therefore, assessing individuals who are obese as they progress into mid-life may hold valuable information. This research also highlights the potential for ADAM10 to be used as a marker in other high-risk AD populations, such as those with metabolic syndrome.

In conclusion, this study provides evidence that blood-based biomarkers related to the pathology of AD were associated with ageing and obesity in cognitively healthy individuals.

Older age was more strongly associated with elevated markers of oxidative stress whereas obesity was associated with elevated IL-6. Although there was no difference in AβPP, ADAM10 protein levels was significantly reduced in older participants with obesity. This indicates that there may be a reduction in non-amyloidogenic AβPP processing, which has been found to occur in people with AD.

CHAPTER 4 - CHARACTERISATION OF AβPP PROCESSING AND REDOX BALANCE IN SPONTANEOUSLY DIFFERENTIATED HUMAN iPSC-DERIVED NEURON AND ASTROCYTE CO-CULTURES CARRYING PSEN1 GENE MUTATIONS

"Parts of this section are taken verbatim from a publication that is under review in which I am principal author"

4.1 Background

Advances in stem cell biology have enabled the unique ability to manipulate the human central nervous system (CNS), allowing the exploration of regenerative medicine and disease modelling with greater relevance to human tissue than previously possible (Shi et al., 2012). By reprogramming human somatic cells back to a state of induced pluripotency (Takahashi and Yamanaka, 2006) it is possible to direct differentiation towards neural precursor cells and ultimately into functional neuron and astrocytic co-cultures that are more representative of human brain tissue than currently used models (Hill et al., 2016, Gunhanlar et al., 2018). The potential to probe human derived CNS networks is of great interest for developing our understanding of, and exploring the effect of interventions on, the pathological processes underlying Alzheimer's disease (AD). The presentation of key biochemical features, including altered Amyloid-β Precursor Protein (AβPP) processing, hyperphosphorylated tau-protein and increased oxidative stress in induced pluripotent stem cell (iPSC) neural networks derived from people with AD suggests this model may be a useful tool in studying the progression of AD (Kondo et al., 2013, Hossini et al., 2015). Crucially, it has been shown that tissue that has been reprogrammed from people with AD into cortical neurons, exhibited phenotypes that are observed '*in vivo'* (Israel et al., 2012).

The *PSEN1* gene encodes for the protein Presenilin-1 (PS1). Mutations in this gene are the most common cause of familial AD and are known to interfere with activity of the

membrane imbedded γ-secretase complex (Kelleher and Shen, 2017). γ-secretase is comprised of four subunits (Lu et al., 2014) and has an important role in cellular functions, as it cleaves substrates such as Notch and the AβPP. As PS1 forms the catalytic subunit of γ-secretase, mutations in the PSEN1 gene can result in dysregulated substrate cleavage. Alterations in AβPP processing have been of particular interest in research attempting to understand the cause of AD (Selkoe and Hardy, 2016). As previously covered in section 1.6 AβPP is a single-pass transmembrane protein that is present in the cell in multiple isoforms: AβPP695, AβPP751 and AβPP770. Each isoform is differentially expressed depending on the tissue. In the brain, AβPP695 is predominately expressed and is crucial to neuronal growth and maturation, especially during development (Coronel et al., 2019). Each of the AβPP isoforms are proteolytically cleaved in two distinct pathways which are highly dependent on cellular trafficking of AβPP (Figure 1 *See Thesis Introduction*). Post-translational modifications, such as glycosylation, are known to mediate trafficking through the secretory and endo-lysosomal pathways. N-glycosylated AβPP (Immature AβPP) is held in the endoplasmic reticulum, whereas, the modification of O-glycosylation sites promotes AβPP (mature AβPP) movement to the cell membrane (Wang et al., 2017b, Hoffmann et al., 2000). Mature O-glycosylated AβPP is also more likely to be held in the cell membrane (Chun et al., 2015b). This can significantly increase protein interactions which are favourable for non-amyloidogenic AβPP cleavage.

In fact, a reduction in the ratio between mature and immature AβPP forms has been studied as a biomarker of AD in peripheral tissues (Akingbade et al., 2018, Elsworthy and Aldred, 2019). Cleavage of AβPP at the cell membrane can be initiated by an α–secretase of which ADAM10 has been identified as the major physiologically relevant enzyme (Kuhn et al., 2010). This pathway liberates the neuroprotective secreted AβPP-α (sAβPP-α) N-terminal

fragment and an 83-amino acid C-Terminal Fragment (CTF). The cleavage of this CTF by γ-secretase results in the formation of p3 (Chow et al., 2010, O'Brien and Wong, 2011). Alternatively, immature AβPP or reinternalized AβPP can be cleaved through the amyloidogenic pathway in which AβPP is first cleaved by a β-secretase enzyme, BACE-1, in the trans Golgi network and endosomal pathways (Chun et al., 2015a). This releases the soluble N-terminal fragment, sAβPP-β leaving the Amyloid-β (Aβ) -containing C-terminal fragment C99 anchored to the membrane. Subsequent cleavage by γ-secretase, liberates Aβ-peptides and the AβPP intracellular domain.

The generation of Aβ is physiologically normal, however, in fAD a shift towards amyloidogenic AβPP processing can result in an accumulation of longer forms of Aβ peptides (Chen et al., 2017). Longer Aβ peptides have been demonstrated to be more hydrophobic than shorter forms and display an elevated propensity to from soluble oligomeric species, which can significantly disrupt cell membranes and thus are highly cytotoxic (Zoltowska et al., 2016, Selkoe and Hardy, 2016). The accumulation of Aβ is also thought to be critical in the development of late onset AD, however, this may be as a result of reduced Aβ degradation and clearance from the brain as opposed to elevated Aβ generation (Nalivaeva and Turner, 2019). The ratio of Aβ peptides of 42 and 40 amino acids is important and has been shown to distinguish between both fAD and late onset AD compared to cognitively healthy individuals.

As mutations to the PSEN1 gene have been shown to alter the carboxypeptidase-like site of γ-secretase it was initially thought that a ‘gain of toxic function’, leading to elevated Aβ42 production, was critical in the development of AD (Arber et al., 2019). This may also be due to a ‘loss of function’ of the γ-secretase complex resulting in a lowering of total Aβ production, with an increase in the Aβ42:40 ratio and thus, Aβ oligomer formation and altered downstream cell signaling (Xia et al., 2015, Potter et al., 2013, De Strooper, 2007). The

propensity for generating longer forms of Aβ has been demonstrated in both PSEN1 mutations, L286V and R278I which are known to cause fAD (Sun et al., 2017b, Arber et al., 2019). Individuals carrying these mutations have displayed symptom onset before the age of 50, often accompanied with extra pyramidal symptoms (Frommelt et al., 1991, Ryan et al., 2016) and for individuals carrying the R278I mutation, speech impairment is particularly present (Godbolt et al., 2004). It is important however, to consider that the effects on Aβ42:40 production are not ubiquitously found across all known PSEN1 mutations (Sun et al., 2017b). Further, there is some evidence that PSEN1 mutations may impact non-amyloidogenic AβPP processing resulting in the down regulation of sAβPP-α secretion (Ancolio et al., 1997). Although the mechanisms driving this association are unknown. What is clear is that some destabilisation the γ-secretase complex is apparent and can lead to altered substrate interaction and eventually, an AD pathology (Kelleher and Shen, 2017, Oikawa and Walter, 2019, Arber et al., 2019).

There has been considerable interest in the derivation of iPSCs carrying PSEN1 mutations to model AD (Poon et al., 2016, Li et al., 2016b, Li et al., 2016a, Tubsuwan et al., 2016, Pires et al., 2016) and whether these cell models reflect '*in vivo*' phenotype. Neural induction and maturation of these cells into cortical cultures carrying PSEN1 mutations do exhibit pathological features associated with AD during development (Armijo et al., 2017, Ochalek et al., 2017). Neural progenitor cells (NPC) with a PSEN1 mutation have been reported to differentiate prematurely, have decreased proliferation and increased apoptosis (Yang et al., 2017a). Prior to differentiation NPCs carrying a PSEN1 mutation have elevated Aβ42:40 ratio, suggesting this is an early event in familial AD development (Sproul et al., 2014). Further, iPSC derived neurons expressing PSEN1 mutations have been found to exhibit dysfunctional endocytosis linked to an accumulation of β-C-terminal fragments.

Endosomal function was rescued using BACE-1 inhibitors (Kwart et al., 2019). Astrocytes may also play a role in the pathogenesis of AD, not only by a reduced capacity to support surrounding neurons, but also by directly secreting cytotoxic peptides. Astrocytes derived from iPSCs carrying a PSEN1 mutation have shown increased Aβ production and dysregulated calcium homeostasis. In addition, astrocytes may have an altered cytokine profile and increased oxidative stress markers, which are considered major features underlying the progression of AD (Oksanen et al., 2017). Elevated oxidative stress has been implicated in the progression of AD with the brain being particularly susceptible (Oikawa and Walter, 2019). This is due to high energy consumption, a high polyunsaturated fatty acid content and relatively low antioxidant buffering capacity. Elevated oxidative stress and altered mitochondrial function are evident prior to the appearance of Aβ and tau pathology in iPSC derived neurons from people with AD (Birnbaum et al., 2018). This suggests that oxidative stress may be an early pathological feature of AD. Further to this, evidence of PSEN1 mutations altering mitochondrial function may lead to elevated superoxide generation and may compromise cellular redox status (Sarasija and Norman, 2018).

The aim of this chapter was to examine changes proteins associated with AβPP metabolism by measuring the ratio of mature and immature AβPP, the expression of mature ADAM10 (mADAM10) and Aβ production in iPSC-derived neuron and astrocyte cultures carrying PSEN1 (L286V, R278I) mutations. In addition, markers of protein and lipid oxidation in combination with antioxidant capacity was assessed to give insight to the redox status of the cells.

4.2 Methods

4.2.1 Culturing and neuralisation of iPSC's to HNSCs

fAD (R278I) iPSC lines were obtained from Dr Selina Wray. This tissue was provided under the ethical approval of NHS Research Authority NRES Committee London-Central (REC# 08/H0718/54+5). Human iPSC's carrying the *PSEN1* mutation, R278I, were cultured for expansion of cell numbers and monitored for colony size and changes in morphology before undergoing neural induction (*from 2.1.1 Preparation and coating of Geltrex™*).

For neural induction, cells were added to Geltrex™ coated wells and incubated (37°C) with E8 media exchange daily until cells reached 100% confluency as a continuous monolayer. At this point, cell media was removed and neural induction (NIM) media was added. A full media exchange with NIM was carried out for a further 9 days. At day 11 cells were passaged using Accutase™ (1ml). Cells were resuspended in neural maintenance media (NMM) with 10μM ROCK inhibitor (10μM). Cells were incubated for 48hr before a full media exchange with NMM, this was performed every other day for 5 days. To ensure proper neural induction, cultures were checked for rosettes forming around 12-14 days. At day 17 onwards, cells were passaged 2:1 using Accutase™ and maintained with NMM exchange every other day to allow for spontaneous differentiation and maturation.

4.2.2 Expansion and spontaneous differentiation of HNSC's

HNSC's were cultured as previously described to expand cells numbers and achieve neuronal maturation (*2.1.7 Thawing and expansion of HNSC's*). Cells were cultured in 6-well plates for lysates and on 13mm glass coverslips in 12-well plates for ICC. Culture surfaces were coated poly-L-ornithine (20μg/ml) and Laminin (10 μg/ml).

4.2.3 Cell characterisation using ICC

To monitor cell fate and control for successful neural induction and maturation cells were immuno-stained for key protein markers (*2.3.1 Immunocytochemistry*). For the commercial cell lines AX0018 (control) and AX0112 (L286V), iPSC characterisation was supplied in manufacturers information following a previously reported neural induction protocol (Shi et al., 2012).

To monitor the pluripotent state of iPSC's from the R278I line prior to neural induction cells were incubated with primary antibodies for Oct4 (ab19857, Abcam) and Sox2 (MAB2018, R&D Systems). After neural induction, cells were incubated with Pax6 (901301, BioLegend) and Sox2 (MAB2018, R&D systems) to detect early neuronal progenitors. Following 14 days of spontaneous differentiation cell cultures were incubated with S100β (SAB5500172, Sigma-Aldrich) and GFAP (MAB360, Millipore) to identify the astrocyte development. Finally, cell cultures were stained for S100β , TUJ-1 (Ab7751, Abcam) and VGLUT1 (135303, Synaptic Systems), after 45 days to asses cellular maturity. Following primary antibody incubation, appropriate secondary antibodies, Alexa Fluor® 488 AffiniPure Goat Anti-Rabbit IgG (1:2000, 111-545-144, Jackson Laboratories) and Alexa Fluor® 633 Goat anti-Mouse IgG (1:2000, A-21052, ThermoFisher Scientific) were co stained. Cells were mounted in a fixative containing DAPI to glass slides and imaged using a Nikon A1R laser scanning confocal microscope (Nikon EU, Netherlands).

4.2.3 SDS-PAGE and Western blotting

The protocols used for SDS-PAGE were followed as previously described (*2.3.3 Western blotting*). The volume of cell lysate containing 10µg of protein was boiled for 5mins at 95°C and loaded into 8-10% SDS- PAGE gel. Molecular weight markers (5µl) were loaded

at each end of the gels. Membranes were incubated in the primary antibodies, Anti-ADAM 10 (Abcam, AB1997) or anti-AβPP (Merck MAB348, 22C11) followed by incubation with the corresponding secondary antibody (Abcam Anti-rabbit HRP-linked H&L IgG AB6721, Sigma Anti-mouse IgG FC-specific A0168). Membranes were developed using ECL substrate, imaged and quantified as previously described.

4.2.4 Plate-based assays

Cell lysates were analysed for Protein Carbonylation, 8-Isoprostanes and FRAP as previously described. For quantification of Aβ1-40, Aβ1-42 and Aβ- oligomers, spent media was concentrated and analysed for secreted peptides (*2.4 Plate-based assays.*)

4.2.5 Statistical Analysis

All quantitative data in the text and figures are presented as Mean ± S.D. unless otherwise stated. Significance was calculated using ordinary one-way ANOVA with Bonferroni *post hoc* corrections and using linear regression models. All data was processed using GraphPad Prism Version 8.4.3.

4.3 Results

4.3.1 Immunocytochemical cell characterisation

R278I cells were stained to allow immunocytochemical cell characterisation (ICC). Detection of the expression of key markers associated with cell fate is crucial to verify cell development and avoid unwanted differentiation. Positive staining for the transcription factors Oct4 and Sox2 can be seen in figure 7.

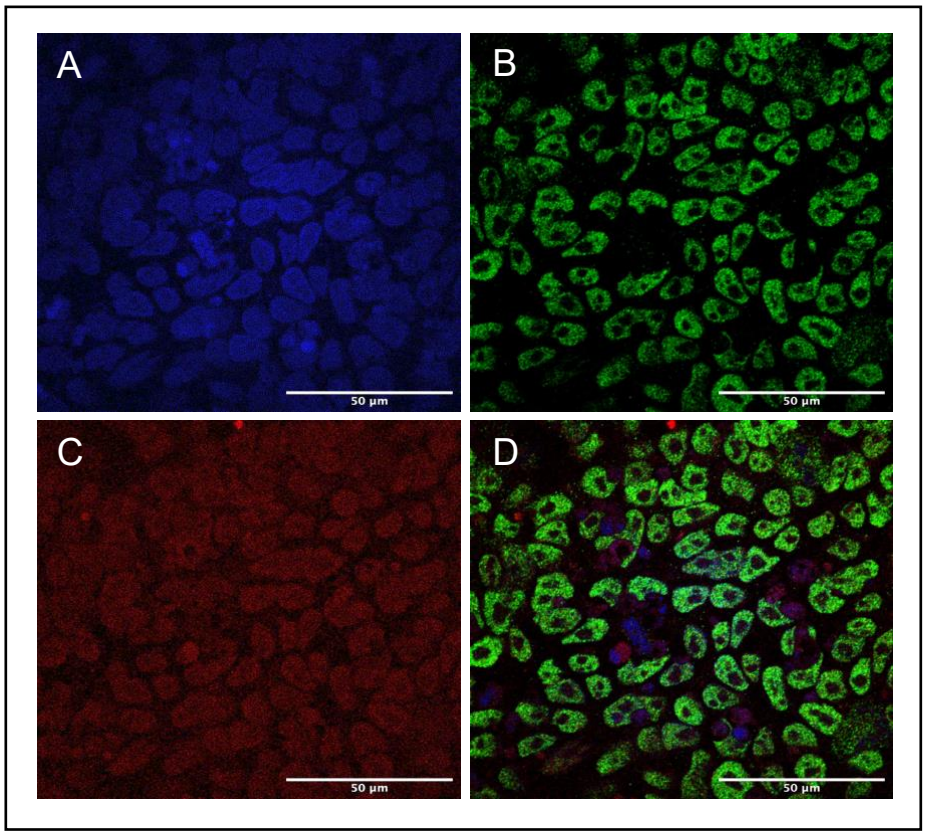

Figure 7 – *Confocal microscopy images of iPSC's with ICC staining taken at 40x magnification. fAD iPSCs were fixed at in PFA and stained for* ***A****. DAPI nuclear stain.* ***B.*** *Oct4 (green)* ***C.*** *Sox2 (red)* ***D.*** *Merge showing co-expression of DAPI, Oct4 and Sox2. (Scale bars to 50µm).*

After neural induction of iPSC's into HNSC's, cells took on a smaller morphology. Following HNSC expansion and final plating cells show a thinning cell soma with axonal protrusions becoming apparent. A crucial rosette pattern is indicative of a neuronal fate as highlighted by the white box in figure 8. HNSC's, although directed towards a cortical lineage suggested by the Pax6 staining, also maintain a pluripotent state with the potential to form a range of cortical cells (Figure 8).

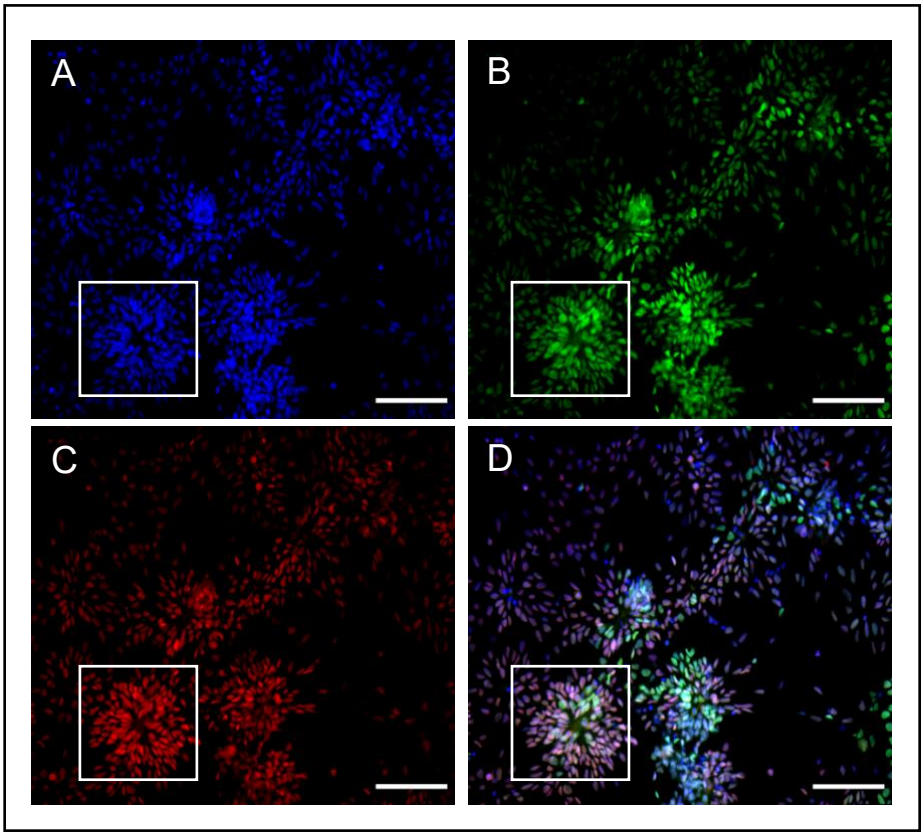

Figure 8 – *Confocal microscopy images of HNSC's with ICC staining taken at 20x magnification. NPCs were fixed in PFA at day 7 following neural induction. The white box indicates an exemplar neural rosette formation* ***A****. DAPI nuclear stain.* ***B.*** *Pax6 (green)* ***C.*** *Sox2 (red)* ***D.*** *Merge showing co-expression of DAPI, Pax6 and Sox2. (Scale bars to 100µm).*

Initially, spontaneous differentiation of HNSC's leads to the development of more mature neuronal cell types. Continual maturation of HNSC cultures began to develop radial glial cell types, surrounding neurons. S100β staining localised to the cell soma is indicative of immature astrocytic development. This is supported by co staining of GFAP which is considered an astrocytic marker (Figure 9).

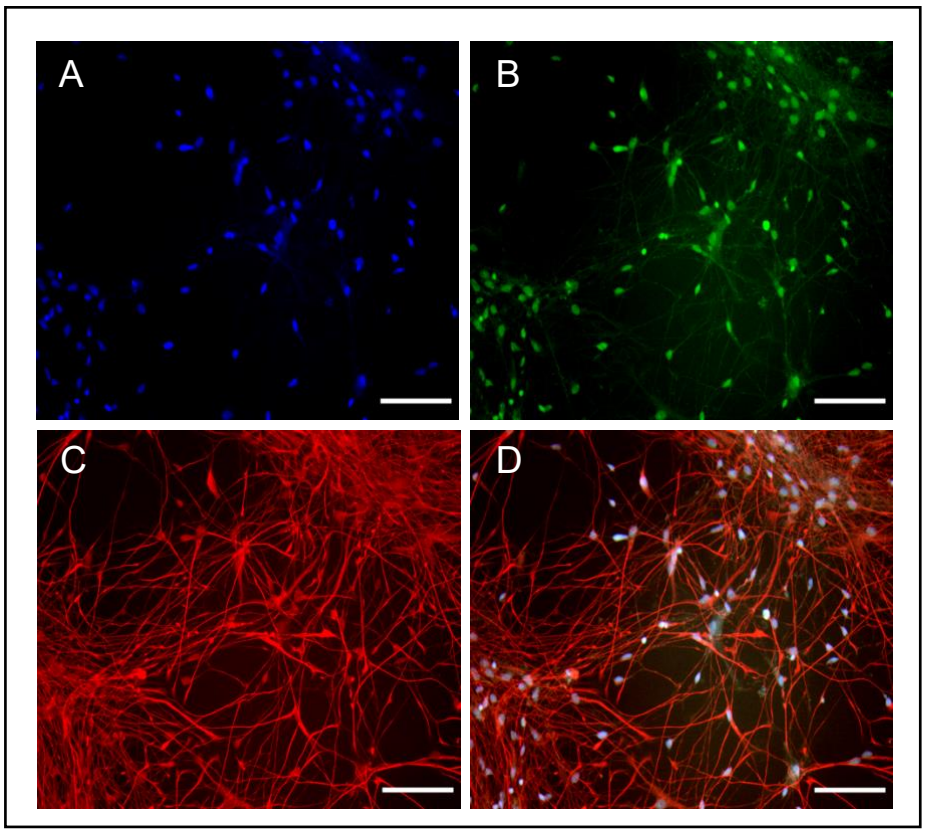

Figure 9 – *Confocal microscopy images of radial glia in co-culture with ICC staining taken at 40x magnification. Formation of immature astrocytes at day 20* ***A****. DAPI nuclear stain.* ***B.*** *S100β (green)* ***C.*** *GFAP (red)* ***D.*** *Merge showing co-expression of DAPI, S100β and GFAP. (Scale bars to 100µm).*

After 45 days of culture, astrocytic cells displayed a much greater S100β expression, throughout both soma and processes. This indicated a more mature astrocytic development. Neurons form more hub-based characteristics with longer axonal processes as can be seen in figure 10.

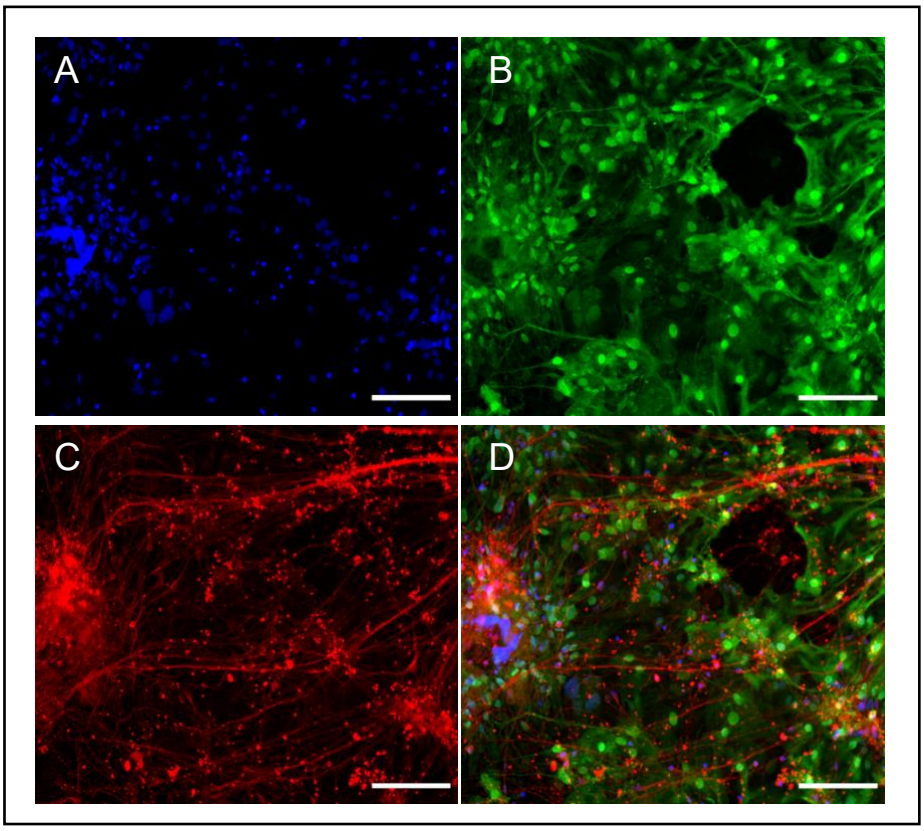

Figure 10– *Confocal microscopy images of neuron and astrocytic co-culture with ICC staining taken at 40x magnification. Neuron and astrocyte co-cultures at day 45.* ***A****. DAPI nuclear stain.* ***B.*** *S100β (green)* ***C****. TUJ1 (red)* ***D****. Merge showing co-expression of DAPI, S100β and TUJ1. (Scale bars to 100µm).*

4.3.2 ADAM10, AβPP and Aβ are altered in PSEN1 mutations

The mature, enzymatically active ADAM10 protein (mADAM10) was significantly lowered in L286V (0.081 ± 0.016 AU, $p = 0.008$) cells compared to healthy control (0.117 ± 0.016 AU). Cells carrying the PSEN1 mutation R278I (0.0465 ± 0.007 AU, p = 0.022) showed a further reduction in mADAM10 expression compared to L286V (*Figure 11,* ***A****.).* There was no significant difference in ProADAM10 between Control (0.126 ± 0.014 AU), L286V (0.187 ± 0.081 AU) and R278I (0.224 ± 0.081AU, $p>0.05$) cells. In addition, the AβPPr was significantly altered with PSEN1 mutations. Both L286V (0.782 ± 0.098 AU, $p =$

0.024) and R278I (0.685 ± 0.208 AU, $p = 0.021$) cells had a significantly lower AβPPr than Control (1.327 ± 0.278 AU). There was no different between PSEN1 mutations ($p > 0.050$) (*Figure 11, **C***.).

To determine the amount of amyloidogenic AβPP processing, Aβ peptides 1-40 and Aβ1-42 were quantified in concentrated cell media. Both Aβ1-40 and Aβ1-42 were significantly elevated in L286V (319.10 ± 59.98 pg/ml, $p = 0.003$ & 191.70 ± 36.17 pg/ml, $p = 0.016$) and R278I cells (300.00 ± 53.28 pg/ml, $p = 0.016$ & 370.40 ± 10.79 pg/ml, $p = 0.001$) compared to healthy control (174.3 ± 35.30 pg/ml & 130.90 ± 23.82 pg/ml) (*Figure 12 **A** & **B.***). The combined Aβ1-40 and Aβ1-42 production was significantly increased in L286V (520.80 ± 84.72 pg/ml, $p = 0.008$) and R278I (670.40 ± 57.11 pg/ml, $p = 0.001$) cells compared to healthy control (305.20 ± 17.74 pg/ml) (*Figure 12 **C.***). The ratio of Aβ1-42:40 was only significantly higher in R278I (1.263 ± 0.2423, $p = 0.022$) cells compared to healthy control (0.7895 ± 0.2440) (*Figure 12 **D***.). Further, Aβ oligomers were significantly elevated in R278I cells (0.8680 ± 0.1077 ng/ml) compared to control (0.4369 ± 0.0361 ng/ml, $p = 0.001$) and L286V cells (0.4712 ± 0.0408 ng/ml, $p = 0.001$).

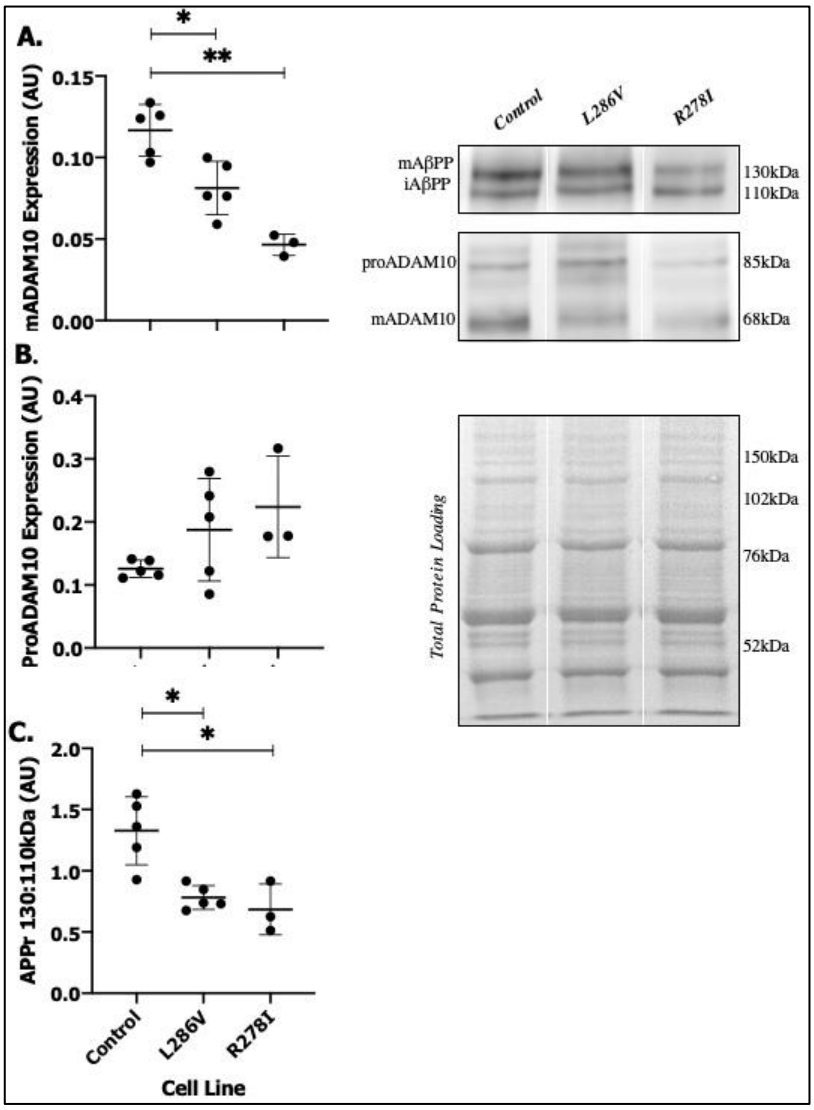

Figure 11 - *Graphs showing the individual data points for cell lysate replicates (45 days old) analysed via western blotting relative to total protein densitometry. Cell lysates from healthy control (n=5), L286V (n=5) and* R278I *(n=3) were separated using SDS-PAGE electrophoresis followed by western blotting. Densitometry was quantified using Licor C-digit and image studio software.* ***A & B.*** *mADAM10 and ProADAM10 expression (AU) normalised to total protein densitometry which can be seen on the right. Representative blot images show both the immature 85kDa proADAM10 and mature/active 68kDa mADAM10 detected by Ab1997 antibody corresponding to table above.* ***B.*** *AβPPr quantified by the ratio of bands at 130kDa to 110kDa. Representative blotting images of AβPP bands detected using Mab348 antibody corresponding to table above. *Significantly different to matched Cell Line ($p<0.05$) **($p<0.01$)*

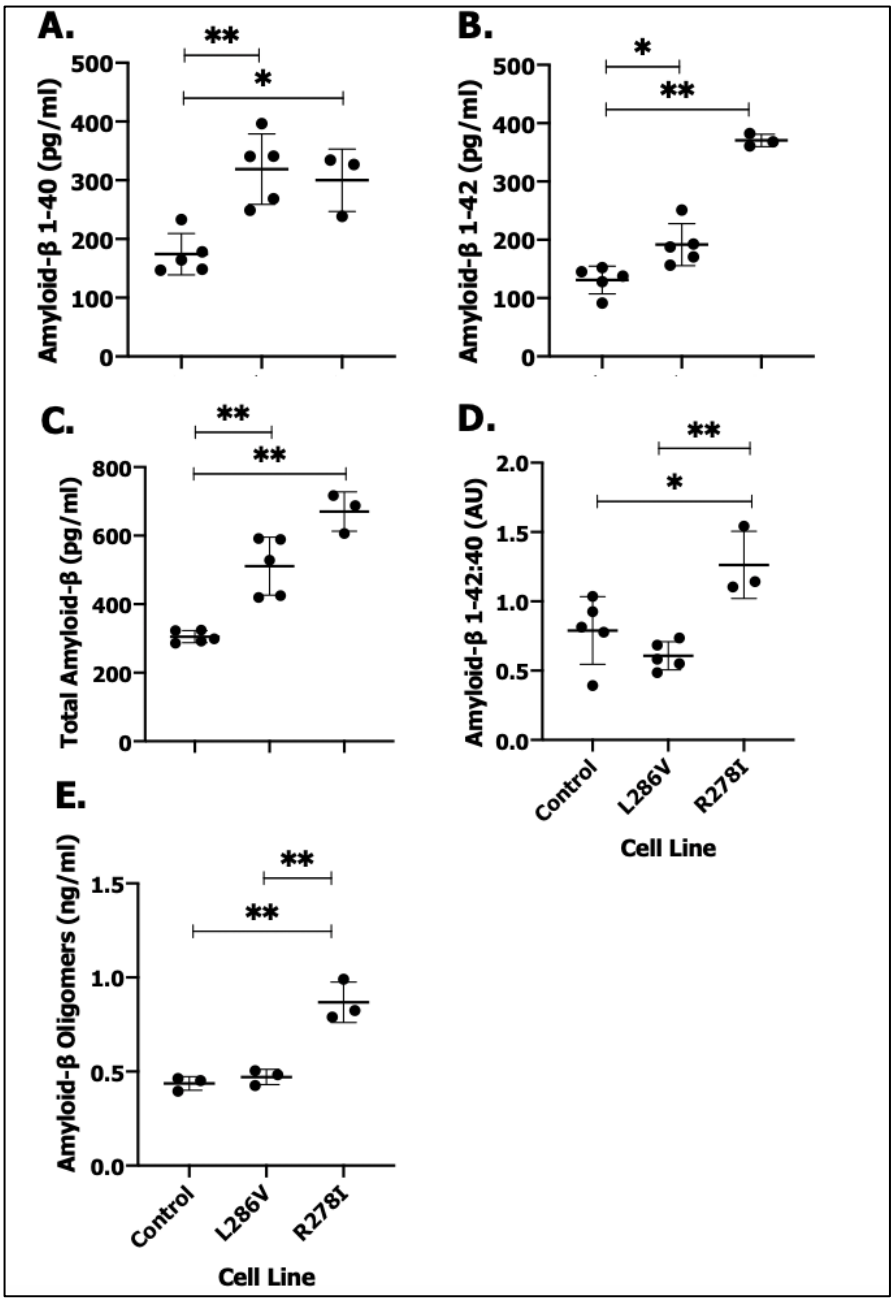

Figure 12 - *Graphs showing the individual data points for media concentration replicates of* ***A.*** *Aβ1:40 and* ***B.*** *Aβ1-42 (pg/ml) analysed via ELISA in Healthy control (n=5), L268V (n=5) and* R278I *(n=3) at day 45 post neural induction.* **C.** *Shows the sum of Aβ1:40+1:42 peptides to give total amyloid Aβ1:40 and 1:42 secretion.* **D.** *The ratio of Aβ1:42 to Aβ1:40 is shown in Arbitrary units (AU).* **E.** *Aβ oligomers (ng/ml) (n=3 for each cell line) *Significantly different to matched Cell Line (p<0.05) **(p<0.01)*

4.3.3 Redox balance is perturbed in cocultures carrying PSEN1 mutations

To quantify cellular redox balance markers of oxidative stress and cellular antioxidant capacity were measured. Protein carbonylation was significantly elevated in both L286V (27.87 ± 8.800 mg/ml), $p = 0.004$) and R278I (39.10 ± 4.088 mg/ml), $p = 0.001$) cells compared to Control (13.06 ± 5.365 mg/ml)) (*Figure 13, **A***.). In addition, total 8-isoprostanes was elevated in L286V (3.867 ± 0.7670 pg/mg/ml) cells compared to both Control (1.210 ± 0.6283 pg/mg/ml, $p = 0.001$) and R278I (2.477 ± 0.1964 pg/mg/ml, $p = 0.034$) cells (*Figure 13, **B***.). Cellular antioxidant capacity was significantly lowered in R278I (48.37 ± 7.447 µM/mg)) cells compared to Control (141.3 ± 38.22 µM/mg), $p = 0.003$) and L286V (135.1 ± 34.18 µM/mg), $p = 0.005$) cells (*Figure 13, **C***.). Further analysis across all cell lines showed higher amounts of protein carbonylation was significantly associated with lower mADAM10 expression ($(F(1,11)=19.020, P = 0.001) R^2 = 0.634)$ and with AβPPr ($(F(1,11)=10.670, P = 0.001) R^2 = 0.492)$ (*Figure 13, **D** & **E***.).

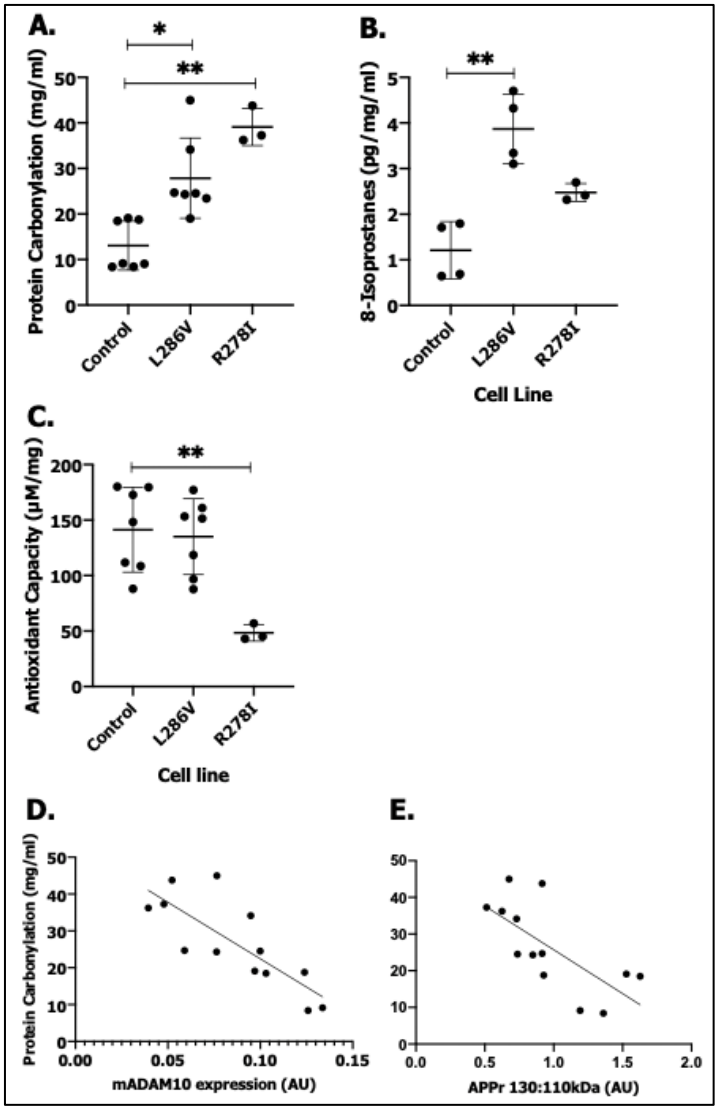

Figure 13 - *Graphs showing the individual data point replicates for markers of redox balance in cell lysates (45 days old) normalised to cellular protein content.* ***A.*** *Protein carbonylation in healthy control (n=7), L286V (n=7) and R278I (n=3) measured via ELISA* (mg/ml) *B. Total 8-isoprostanes in immunopurified lysate preparations from healthy control (n=4), L286V (n=4) and R278I (n=3) quantified by ELISA* (pg/mg/ml) ***C****. Cellular antioxidant capacity relative to ascorbic acid measured in healthy control (n=7), L286V (n=7) and R278I (n=3) using colorimetric assay* (µg/mg)*. Regression analysis between markers of oxidative stress and AβPP processing.* ***D.*** *Protein carbonylation (mg/ml) and mADAM10 expression (AU) measured via ELISA and Western blot respectively.* ***E.*** *Protein carbonylation (mg/ml) and AβPPr (AU) measured via ELISA and Western blot respectively. *Significantly different to matched Cell Line ($p<0.05$) **($p<0.01$)*

4.4 Conclusion

The continued development of iPSC technology has the potential to enable detailed investigation into disease pathology and drug screening. However, for this to be possible it is essential that iPSC-derived models display a phenotype similar to that seen '*in vivo'*. A crucial step in this process is to characterise and closely monitor cellular development to achieve the desired cell fate. Data presented herein demonstrated that proteins involved in AβPP processing were significantly altered in *PSEN1* co-cultures (Figure 11 & 12). In this chapter, *PSEN1* co-cultures also had altered redox status compared to control co-cultures (Figure 13). These features are important characteristics of AD and therefore, this '*in vitro'* model represents a functional system to study the early pathological features of AD.

After differentiation of iPSC's into co-cultures of neurons and astrocytes, markers indicative of altered AβPP processing were quantified (Figures 7-10). Interestingly, both *PSEN1* mutations showed a reduction in mADAM10 protein expression, matched by a lower AβPPr in both *PSEN1*mutations (Figure 11). A reduction in the AβPPr is supported by several studies into potential biomarkers of AD in both central and peripheral tissues (Akingbade et al., 2018). An altered AβPPr may be indicative of a reduced amount of AβPP reaching the cell membrane. This may be due to the changes in the glycosylation of the protein and may therefore result in a reduced interaction of mature AβPP with mADAM10 (Akasaka-Manya et al., 2017, Wang et al., 2017b). To further clarify whether the reduction in ADAM10 and AβPPr are indeed indicative of a difference in non-amyloidogenic AβPP processing, future research should quantify products of direct ADAM10 mediated AβPP cleavage such as sAβPPα. This could be further analysed by measuring ADAM10 activity directly and is a limitation of this study.

The nature of *PSEN1* mutations directly impacts the function of the catalytic subunit of the γ-secretase enzyme. However, whether such mutations lead to a gain of toxic function or a loss of normal γ-secretase function is still under debate (Kelleher and Shen, 2017, De Strooper, 2007). Interestingly, the two *PSEN1* mutations characterised herein highlight this problem. In *PSEN1* L286V cells, the total Aβ generated from both Aβ1-40 and Aβ1-42 was significantly higher than the *PSEN1* R278I mutation, so in this case R278I cells were more similar to 'Healthy' control cells. Yet, the ratio of Aβ1-42:40 was shifted towards Aβ1-42 generation in the PSEN1 mutation R278I, which was more different to controls than L286V cells, where the ratio of Aβ1-42:40 was unchanged compared to control (Figure 12). The findings from this chapter alone are limited by the small number of cells lines utilised that provide only a small view of the effects that *PSEN1* mutations have on Aβ generation. However, these findings are supported by studies including larger panels of iPSC derived cultures carrying fAD mutation (Kwart et al., 2019). Other research has shown the PSEN1 mutation R278I, has a significantly higher Aβ1-42:40 ratio compared to other fAD mutations (Arber et al., 2019). This shift is indicative of an altered AβPP cleavage site preference by γ-secretase. Aβ1-42:40 ratio is often used as a CSF marker to aid diagnosis of AD (Pannee et al., 2016, Hansson et al., 2019). An increase in longer forms of Aβ is associated with a greater propensity for aggregation, this was supported by the finding of increase Aβ oliogerms in R278I cells, which has the most elevated Aβ1-42. Thus, there is understandably growing attention around the hypothesis that different *PSEN1* mutations can lead to varied Aβ production (Woodruff et al., 2013, Kwart et al., 2019, Arber et al., 2019).

Oxidative stress is common feature of neurodegenerative diseases, metabolic disorders and even healthy ageing (Butterfield and Halliwell, 2019). However, understanding the cellular redox balance of specific cell populations may be critical to understanding

pathological processes. Neurons are particularly susceptible to oxidative stress due to their high energy demand with astrocytes playing a key role in neuroprotection by supporting cell metabolism (Butterfield, 2018, Allen and Eroglu, 2017). Therefore, co-culturing neuron and astrocytes can replicate a closer model to monitor '*in vivo*' cell stress. Both *PSEN1* mutations used in the study herein displayed elevated protein carbonylation and this was significantly associated with a reduction in both mADAM10 and mature AβPP relative to immature AβPP (Figure 13). This link may be explained by the addition of protein carbonyl groups directly effecting normal protein function or trafficking, which is crucial for the maturation of both ADAM10 and AβPP. This highlights an interesting direction for future research. Elevated oxidative stress could be further seen in R278I cells, which had a significantly lowered antioxidant capacity, however, lipid oxidation was only significantly elevated in L286V cell compared to both R278I and 'Healthy' control cells (Figure 13).

The insertion and interaction of Aβ1-42 with lipid membranes has been linked to ROS propagation of oxidised lipids and proteins (Butterfield and Halliwell, 2019). The tendency of cells carrying the *PSEN1* mutation to generate longer Aβ peptides relative to shorter forms of Aβ can increase the likelihood of oligomerisation. This may in part explain the association of *PSEN1* mutations with elevated oxidative damage markers. However, there was no difference seen for Aβ oligomers in L286V cells suggesting an oxidative stress may occur independently from Aβ oligomer formation. As F8-isoprostanes was the only marker of lipid peroxidation measured it may be possible that other modified lipids are more closely linked to Aβ oligomers such as, 4-hydroxynonenal adducts (Butterfield, 2020). Further, it should be noted that this study only focuses on Aβ1-42/40, whereas Aβ exists in a number of deferent C- and N- terminally truncated forms (Arber et al., 2019). More data on a larger number of Aβ

peptides of varying length in *PSEN1* mutations is warranted to further investigate the link between Aβ-cell membrane interaction and lipid oxidation.

The utlisation of co-cultures containing both neurons and astrocytes is an important step in producing better models of AD. Astrocytes play a key role in supporting in maintaining neuronal function, substrate transport/ metabolism and neuroprotection (Rodríguez-Arellano et al., 2016). This research shows that such co-cultures carrying a *PSEN1* mutation display perturbed features associated with AβPP processing and redox balance. However, from this data it is not possible to distinguish the contribution of each cell type to the observed phenotype. This highlights an interesting avenue for future research comparing both mono-cultures and co-cultures of neurons and astrocytes. The use of isogenic cell lines may also strengthen conclusions on Aβ-cell membrane interaction by controlling for other confounding genetic variance impacting lipid transport and Aβ dynamics. Taken together, these findings highlight the need for more research into ROS production and how *PSEN1* mutations may result in perturbed to oxidative stress cascades.

In conclusion, this study provides evidence that *PSEN1* mutations in iPSC-derived neuron and astrocyte co-cultures can lead to significant alterations in AβPP processing accompanied by a change in the redox status of the cell. These changes are present in the pathology of AD. A reduction in both the AβPP ratio and mature ADAM10 protein levels, in combination with altered generation of Aβ1-40 and Aβ1-42 was found in cells carrying *PSEN1* mutations compared to 'healthy' control. Notably, levels of Aβ in monomeric and oligomeric forms also varied between *PSEN1* mutations. In addition, elevated oxidative stress was apparent in cells with a *PSEN1* mutation compared to control. This study provides data to suggest that iPSC-derived cell networks are a valuable tool to investigate genetic mutations associated with AD, however it is crucial consider the differential effects individual *PSEN1*

mutations may have on different cell types during the progression of the AD. Future studies will help to better understand the causative mechanisms associated with *PSEN1* mutations and fAD which in turn, will facilitate the development of therapeutic inventions.

CHAPTER 5 - THE 5HT4 RECEPTOR IN iPSC-DERIVED NEURON AND ASTROCYTES

5.1 Background

The potential benefits of increasing ADAM10 activity in people at risk of, or with a diagnosis of AD is reliant on therapeutic targets that are both selective and carry minimal risk of side effects. ADAM10 is present in multiple cells and tissues and is involved in a number of key processes including tissue growth and repair, inflammation and cell signalling (Maurer et al., 2020, Kuhn et al., 2016, Mizuno et al., 2020). Therefore, non-specific increases in ADAM10 activity could potentially disrupt normal cellular processes. In addition, the association of ADAM10 over activity with other diseases such as cancer (Smith et al., 2020), further highlights the need for controlled and specific ADAM10 activity promotion.

As previously stated, SSRI medication may hold beneficial effects for reducing the severity of AD pathological progression and slowing cognitive decline (Elsworthy and Aldred, 2019). Treatment with SSRI's has been linked to increased neurogenesis and neurotropic growth factors as well as reduced neuroinflammation and oxidative stress (See '*mechanisms of action*', 1.9.1). In addition, AβPP processing may be affected by SSRI treatment with evidence showing lowered cerebral and CSF Aβ load (Cirrito et al., 2011, Sheline et al., 2014). However, there is little evidence to suggest SSRI treatment blunts the generation of Aβ directly. Instead, these effects may be in part explained by an increase in sAβPP-α secretion which is produced after cleavage of AβPP by α-secretase enzymes. This is supported by the finding that blocking all α-secretase activity, stops the Aβ-lowering action of SSRI treatment (Fisher et al., 2016). If this is correct, the effect of SSRI treatment to lower Aβ generation could be mediated by increased ADAM10 enzyme activity by precluding the interaction of available AβPP with BACE-1. Whether SSRI treatment stimulates the

ADAM10 enzyme directly, through increasing 5HTr ligand binding or by other mechanisms has been under investigation.

The 5HT4r was identified as a seven transmembrane G-protein coupled receptor in 1988 and since then has been shown to have eight splice variants in humans (Dumuis et al., 1988). These C-terminal variants are thought to have a key role in the activity of the receptor (De Deurwaerdère et al., 2020). The 5HT4r is coupled to the Adenylyl cyclase enzyme and therefore the production of Cyclic-AMP (cAMP) has been used as a readout for identifying ligands of the receptor. Although the presence of constitutive activity of the receptor is unclear, several potent and selective agonists have been identified to enable further interrogation of basal and ligand induced activity. Interestingly, 5HT4r agonists have been suggested to exert neuroprotective effects and may have a beneficial impact on learning and memory in rodent models (Hagena and Manahan-Vaughan, 2017, Bianco et al., 2016a, Darcet et al., 2016). Research has shown that ADAM10 co-localizes with the 5HT4r and that stimulation of the receptor may increase sAβPP-α secretion. Taken together these findings point towards an indirect pathway to stimulate ADAM10 activity (Cochet et al., 2013, Baranger et al., 2017, Robert et al., 2005). Notably, there was no change in Aβ secretion after 48hr treatment with serotonin (5HT) or prucalopride, a selective 5HT4r agonist (Robert et al., 2005). This link between 5HT4r and ADAM10 activity may be a mechanistic mode of action for the therapeutic effects of SSRI's on AβPP processing (see figure 14).

Advancements in stem cell technology have enabled the generation of functional serotoninergic neurons (Licinio and Wong, 2016). As introduced in Chapter 1, section 1.11, and further investigated in chapter 4, iPSC derived neurons provide an excellent model to study the association of ADAM10, APP processing and the 5HT4r. These iPSC-derived neurons display spontaneous activity and they have been shown to respond to bath application

of 5HT, measured via the detection of calcium transients. This measure of neuronal activity is an important tool in determining culture maturity, as functional networks develop at later stages of culture. When 5HT1 and 2 receptors have been specifically targeted with agonist or antagonists functional responses have also been seen (Wang et al., 2016a). Further, serotoninergic neurons have also been shown to respond to treatment with SSRI's (Vadodaria et al., 2016). However, there is currently no research investigating the presence of functional 5HT4r receptors in iPSC-derived cortical networks. In our previous review paper we hypothesise that SSRI's can increase non-amyloidogenic AβPP as described in chapter 1 section 1.10.1 and if this mechanism is to be investigated further, then 5HT4 receptors must be present and display functional activity (Elsworthy and Aldred, 2019).

The aim of this chapter was to interrogate the localisation and activity of the 5HT4r receptor in iPSC-derived neuron and astrocyte cocultures. Further, the activity of ADAM10 in response to 5HT4r modulation was investigated.

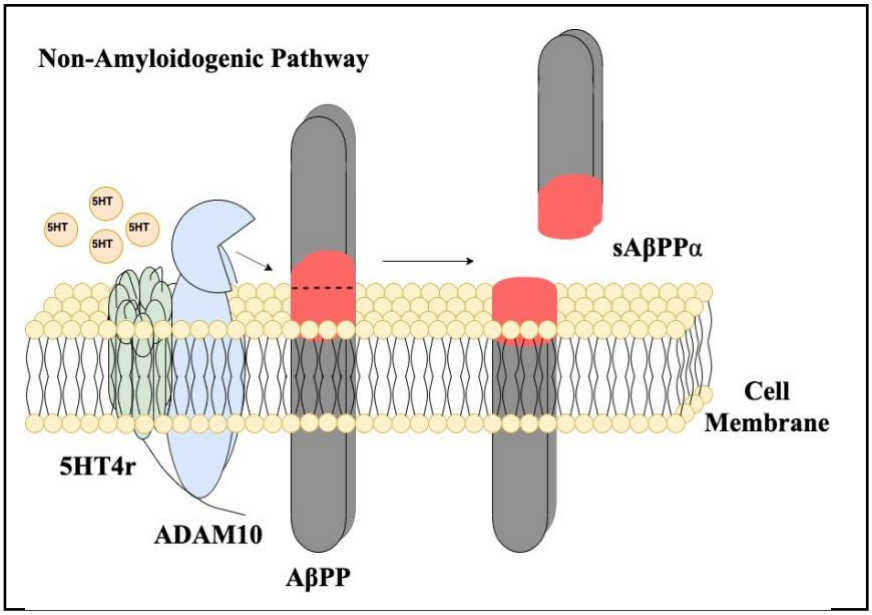

Figure 14 – *Diagram showing the potential interaction of 5HT4 receptor with ADAM10 at the cell membrane. Agonist binding, shown here by 5HT, stimulates ADAM10 activity and therefore, increases non-amyloidogenic AβPP processing.*

5.2 Methods

5.2.1 Cell culture and immunodetection of 5HT4r

Human Neuronal Stem Cells (HNSC) (AX0018 & AX0113) were kindly provided by Dr Eric J Hill from Aston University and cultured as previously described to achieve neuronal maturation whereby spontaneous calcium signalling activity can be detected (*2.1.8 Spontaneous differentiation of HNSC's into neuron and astrocyte co-cultures*). Cells were cultured in 6-well plates for lysates and on 13mm glass coverslips in 12-well plates for ICC. Culture surfaces were coated poly-L-ornithine (20µg/ml) and Laminin (10 µg/ml).

For immunodetection of 5HT4r by western blotting, cells were lysed and probed with a rabbit anti-5HT4r antibody (ab60359, Abcam) followed by Goat Anti-Rabbit IgG H&L secondary (ab205718, Abcam). Protein mass of 5HT4r is 42kDa and therefore band detection was expected in this region (*2.3.3 Western blotting*). For ICC staining, coverslips were co-stained in blocking buffer with rabbit anti-5HT4r (1:100, ab60359, Abcam) and mouse anti-AβPP (1:100, Merck, Mab348) antibodies followed by Alexa Fluor® 488 AffiniPure Goat Anti-Rabbit IgG (1:1000, 111-545-144, Jackson Laboratories) and Alexa Fluor® 633 Goat anti-Mouse IgG (1:1000, A-21052, ThermoFisher Scientific) secondary antibodies (*2.3.1 Immunocytochemistry*). Cells were mounted to glass slides and imaged using a Nikon A1R laser scanning confocal microscope (Nikon EU, Netherlands).

5.2.2 Calcium imaging

Fluo-4AM labelled calcium imaging was undertaken on cells cultured on 13mm glass coverslips coated with poly-L-ornithine (20µg/ml) and Laminin (10 µg/ml) (*2.2.1 Fluo-4AM imaging*). For baseline measurements of calcium signalling, artificial CSF (aCSF) was perfused over the cells for 5 minutes (see table 3). Experimental compounds were applied in

5-minute intervals suspended in aCSF as follows; 5HT (20µM, Sigma-Aldrich, 14927). Prucalopride (10µM, Sigma-Aldrich, SML1371), GR113808 (5µM, Sigma-Aldrich, G5918). A minimum time-course of 3-minutes has been used in previous research to investigate 5HT induced calcium dynamics at similar compound concentrations (Vadodaria et al., 2019, Cochet et al., 2013).

Table 4 – aCSF constituents used for baseline calcium signalling measurements and experimental compounds.

COMPONENT	**FINAL CONCENTRATION (mM)**
NaCl	126
KCl	2.5
$NaHCO_3$	26
KH_2PO_4	1.25
$MgSO_4$	1
$CaCl_2$	2
Glucose	10

Note*: pH 7.3 – Continuous bubbling with CO_2 throughout experiment. All components were supplied by Sigma-Aldrich.*

5.2.3 ADAM10 activity

The enzymatic activity of ADAM10 was quantified by FRET assay (*2.4.2 ADAM10 enzyme activity*). Control (AX0018) and L286V (AX0112) cells were cultured in 96 well plates coated with poly-L-ornithine (20µg/ml) and Laminin (10 µg/ml). Treatment with experimental compounds were at matched concentrations to those used for calcium imaging,

however, for this assay pre-treatment was 2 hours (37°C) with NMM as the vehicle. All values were normalised to total protein content measured via BCA assay.

5.2.4 Statistical Analysis

All quantitative data in the text and figures are presented as Mean ± S.D. unless otherwise stated. Calcium image data was processed as change in fluorescence from baseline recordings. To test data distribution normality the Shapiro-Wilk test was employed. Statistical analysis of between conditions was calculated using Kruskal-Wallis H tests with multiple comparisons of mean rank. ADAM10 activity data was assessed using unpaired Mann-Whitney tests to compare mean ranks. All data was processed using GraphPad Prism Version 8.4.3. Significant values were set at 0.05%.

5.3 Results

5.3.1 Immuno-based detection of 5HT4r

ICC staining of cells (Figure 15, A2 & A4) revealed distinct binding (green colour) suggesting the presence of 5HT4r in iPSC-derived neuron and astrocyte co-cultures. Fluorescence was predominately localised to cell bodies with weaker staining suggesting lower 5HT4r expression in axons. This is emphasised by the intensity of the counterstain for AβPP, which is expressed throughout the cell (Figure 15, A3). Further, 5HT4r was detected at protein bands corresponding to the predicted molecular weight ~ 44kDa in cell lysate (Figure 15, B). This band was not present when only the secondary antibody was incubated with cell lysates.

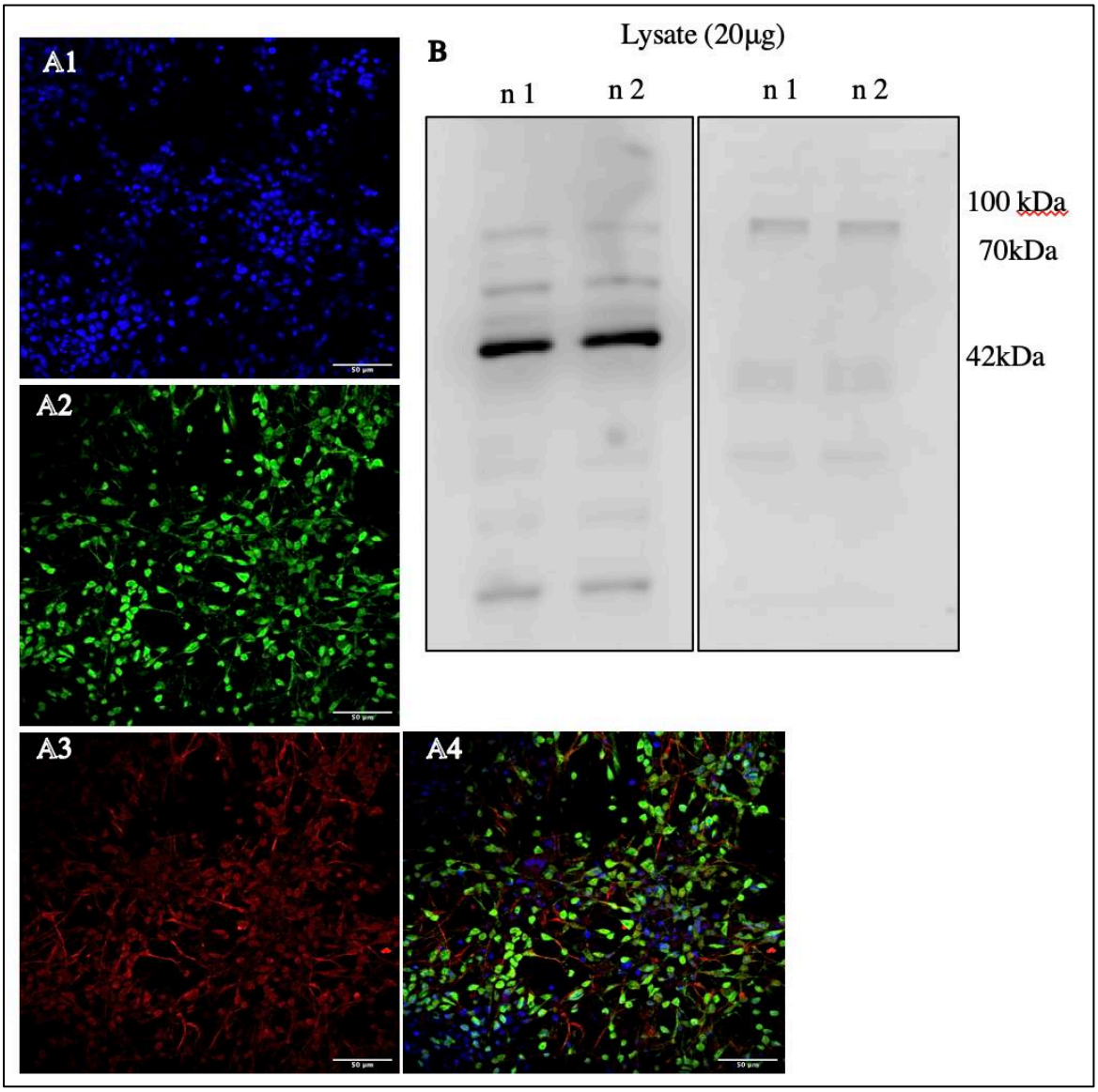

Figure 15 – *ICC images of control cells 45 days post differentiation taken at 40x magnification (scale bars at 50µm) and protein expression via western blotting.* ***A1*** *- DAPI (blue) nuclear stain.* ***A2*** *- 5HT4r (green).* ***A3*** *- AβPP (red).* ***A4*** *- Merge of A1, A2 and A3 to show co-staining. B. Two identical bands ~ 44kDa after detection with anti-5HT4r antibody in 20µg cell lysate (n=2). Right panel shows identical samples after detection with secondary antibody only.*

5.3.2 Functional 5HT4r respond to selective agonists

In order to investigate whether the 5HT4r was functionally active, calcium transients were monitored under agonist or antagonist treatment conditions. After 45-days of maturation, iPSC-derived neuron and astrocyte cocultures displayed spontaneous activity as shown by calcium fluctuations under resting conditions (see figure 16, **A-B**, aCSF only). The addition of 5HT as a blanket agonist that binds to all 5HT receptors (see figure 16, A) elicited a significant increase in calcium transients (dF/F) relative to basal levels (4.392 ± 1.908 RFU, $p = 0.020$). This effect appeared to be sustained even after a five-minute wash-out period with aCSF, although in some cases the response was no-longer significant ($p > 0.050$).

Next, cells were treated with Prucalopride to test selective 5HT4r agonist stimulation. An increase in peak fluorescence (RFU) (17.19 ± 7.014 RFU, $p = 0.003$) compared to baseline (2.832 ± 0.765 RFU) was observed. The addition of 5HT in addition to Prucalopride further increased calcium responses with calcium transients (dF/F) significantly elevated relative to baseline (7.707 ± 0.605 RFU, $p = 0.002$) and a significant increase in peak fluorescence (17.76 ± 8.431 RFU, $p = 0.046$) compared to baseline (2.832 ± 0.765 RFU, $p = 0.046$). Subsequent addition of GR113808, a selective 5HT4r antagonist, blunted the calcium response to 5HT and Prucalopride, although this was non-significant ($p > 0.050$) (see figure 16, **B**).

Finally, cells were treated with GR113808 and showed a significant decrease in peak calcium signalling fluorescence (RFU) (0.902 ± 0.164 RFU, $p = 0.001$) compared to baseline (1.488 ± 0.065 RFU). Average fluorescence (RFU) over the five-minute bath application period with GR113808 was also significantly lower (5.778 ± 0.375 RFU, $p = 0.003$) compared to control (10.92 ± 2.211 RFU). Prucalopride treatment in addition to GR113808

was unable to rescue this decline in calcium signalling fluorescence ($p > 0.050$) (see figure 16, **C**).

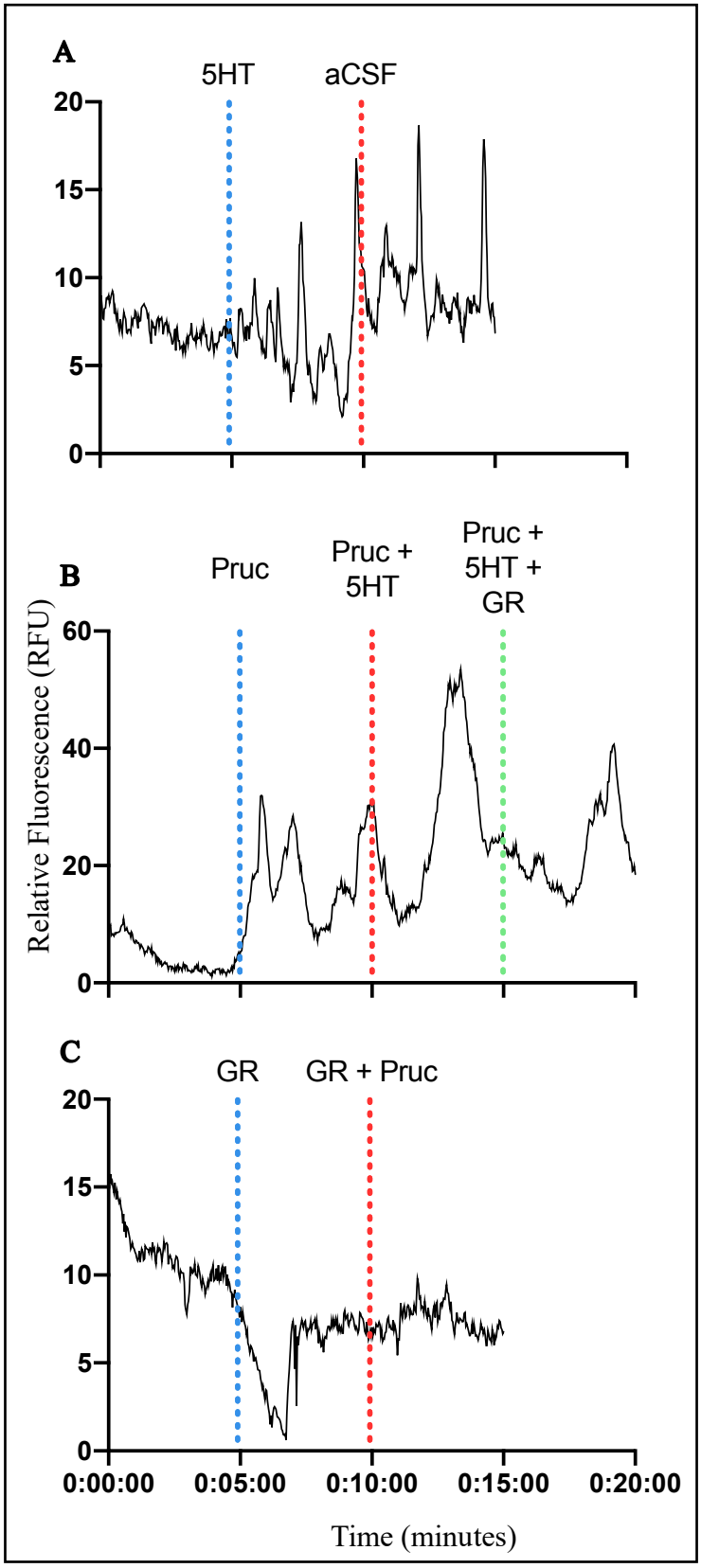

Figure 16 – *Traces displaying baseline adjusted relative fluorescence (RFU) of Fluo-4AM calcium binding averaged over time in five ROIs (N=3). In all conditions from 0-5 minutes aCSF was perfused over cells to allow for baseline measurements* ***A.*** *Shows a calcium trace at baseline followed by 5HT (20μM) perfusion (blue line) and then aCSF (red line).* ***B.*** *Shows a calcium trace at baseline, with Prucalopride (10μM) (blue line), Prucalopride and 5HT (red line) and Prucalopride, 5HT and GR113808 (50μM) (green line).* ***C.*** *Shows a calcium trace at baseline, with GR113808 (blue line) and GR113808 and Prucalopride (red line).*

5.3.3 Effect of 5HT4r agonist treatment ADAM10 activity in Control and *PSEN1* mutation cells

After identifying the functional activity of 5HT4r in iPSC derived neuron and astrocyte co-cultures, ADAM10 activity (RFU) was assessed in response to incubation with agonist or antagonist ligands. To test the specificity of the assay, ADAM10 activity was compared at baseline and after treatment with the specific ADAM10 inhibitor, GI254023X in control cells. ADAM10 activity significantly reduced after GI254023X (0.068± 0.027 RFU) treatment compared to baseline (0.307± 0.096 RFU, $p = 0.0026$) (Figure 17, **A**.). At baseline ADAM10 activity was also significantly lower in L286V (0.105± 0.0107 RFU, $p = 0.001$) cells compared to control (Figure 17),

ADAM10 activity in control cells showed no significant response to pre incubation with 5HT or Prucalopride ($p > 0.050$ (Figure 17 **A**). Further, cells carrying the *PSEN1* mutation, L286V, which had previously been shown to exhibit reduced basal ADAM10 activity, showed no change in ADAM10 activity with 5HT treatment ($p > 0.05$). (figure 17, **B**). However, Prucalopride treatment also increased ADAM10 activity (0.175 ± 0.053 RFU, $p = 0.005$) and this effect was blunted by co-treatment with GR113808 (0.093 ± 0.015 RFU, $p = 0.002$) (see figure 17, **B**).

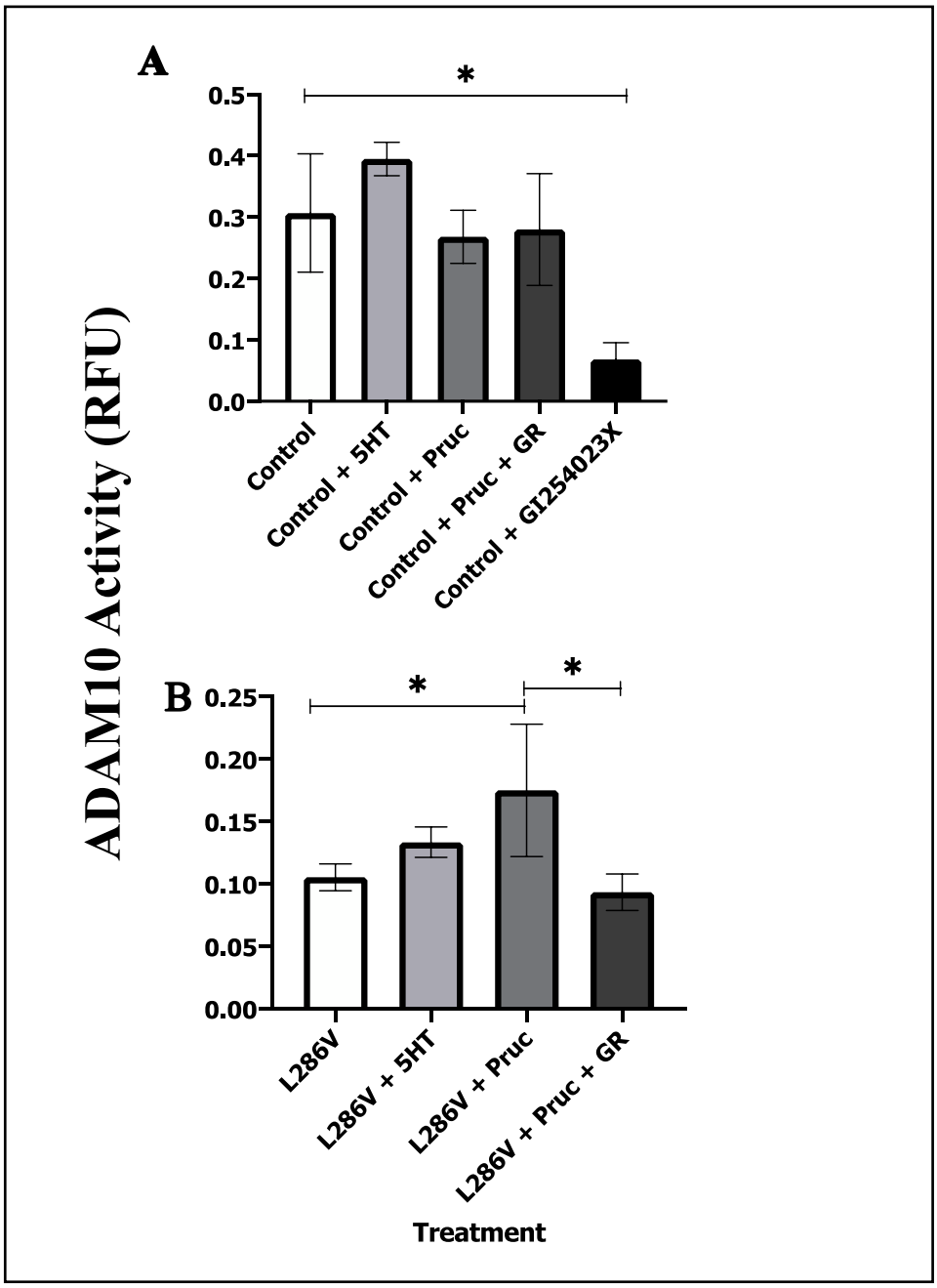

Figure 17 – *Comparison of ADAM10 activity measured via FRET assay in iPSC derived neuron and astrocyte co-cultures (day 45 post induction).* ***A.*** *Baseline ADAM10 activity in control cells (n=6) compared to treatment with 5HT (n=2), Prucalopride (n=6) and GI254023X (n=2).* ***B.*** *Baseline ADAM10 activity in L286V cells compared to L286V cells treated with 5HT (n=2) and Prucalopride (n=6). Al treatments were for 2 hours prior to assay. *Significantly different to matched condition.*

5.4 Conclusion

The identification of functional 5HT4r's in iPSC-derived neuron and astrocyte co-cultures highlights the potential for these cell models to be used to study the action of serotonin. Specifically, this research is of interest to the work of this thesis as it provides an opportunity to investigate the relationship between agonist stimulation of 5HT4r and elevated secretion of sAβPP-α. The bath application of 5HT in this study evoked significant calcium responses seen with specific serotoninergic neuron models (Wang et al., 2016a) which represents an increase in the depolarisation of neuronal synapses (Figure 16). This event is indicative of increased 5HT mediated signalling between cortical cells and shows 5HTr must be present in the cultures. If the proposed hypothesis that SSRI's may promote ADAM10 activity through the 5HT4r, and therefore be a therapeutic option for the treatment of AD, it is essential to establish that this specific 5HTr is present and functional.

The 5HT4r specific agonist, Prucalopride, evoked calcium transients when applied to cell cultures. Further, bath application with the compound, GR113808, led to a significant decrease in average fluorescence and the peak fluorescence intensity compared to baseline measurements. However, there was no change in the calcium transients of GR113808 application compared to baseline (Figure 16). As GR113808 is both a neutral antagonist and inverse agonist of subtypes of 5HT4r it is possible this compound had a direct effect on calcium signalling (De Deurwaerdère et al., 2020). Crucially, adding Prucalopride and GR113808 restored calcium transients to baseline levels, yet only the excitatory response seen with Prucalopride alone was blunted. This supports the finding that 5HT4r's are able to functionally respond to ligands and that iPSC neuron and astrocyte co-cultures are suitable models for investigation the effects of SSRI's on the ADAM10 activity through the 5HT4r receptor.

Importantly, treatment of co-cultures with both 5HT and Prucalopride were able to increase ADAM10 activity in cells carrying the *PSEN1* mutation, L286V (Figure 17). This research adds support to the previous findings that agonist binding to 5HT4r can significantly increase non-amyloidogenic AβPP processing through increasing ADAM10 activity (Cochet et al., 2013). This effect was not seen in control cells where ADAM10 activity was relatively higher at baseline compared to cells with a *PSEN1* mutation (Figure 17). This is interesting as may suggest that agonist action on 5HT4r can only act to limited capacity. As ADAM10 activity was measured directly via cleavage of a fluorescent peptide the absence of this effect is not likely to be due to a lack of available substrate. Perhaps one explanation for this is that 5HT signalling is reduced in cells carrying a *PSEN1* mutation, and agonist stimulation was able to rescue this phenotype. This would in part explain the finding that SSRI treatment can improve pathobiological markers of AD (See '*mechanisms of action*', 1.9.1). It cannot be ruled out however, that cells carrying the PSEN1 mutation respond differently to stimulation of the 5HT4r, or that downstream signalling, perhaps through cAMP signalling, is impacted. This highlights a limitation of the methods used to identify functional 5HT4r in this model. Although, calcium signalling provides a measure of neuronal activity, and also as an indication of culture maturity, it is not a specific readout for 5HT4r activation. Further research should examine the relative expression and function of 5HT4r's in cells carrying PSEN1 mutations. This should also be carried out in a larger number of fAD mutations and control cells to address donor/ culture specific effects. Interestingly, an increased expression of 5HT4r's has been associated with the early pathology of AD, potentially as a compensatory mechanism for decreased 5HT levels in the brain (Madsen et al., 2011). To gain a better understanding the role of 5HT4r in AD pathology and the potential for modulating ADAM10

activity, it is critical that 5HT4r knockdown iPSC models are developed to enable specific mechanism to be investigated.

The data presented herein provides clear rationale for the further investigation of modulated 5HT signalling on ADAM10 activity and AβPP processing. Previous research identifying perturbed AβPP processing and elevated oxidative stress in cells carrying a *PSEN1* mutation (see *chapter 4*) also provides rationale to investigate the mechanism of action of SSRI treatments on the pathology of AD.

CHAPTER 6 - THE EFFECT OF CITALOPRAM TREATMENT ON AβPP PROCESSING AND REDOX BALANCE

"Parts of this section is taken verbatim from the following publication in which I am principal author (Elsworthy and Aldred, 2019)".

6.1 Background

In chapter 5, evidence of functional serotonin receptors was found in iPSC-derived neuron and astrocyte co-cultures. Thus, to extend this work the aim of the research presented in this chapter was to examine the effect of Selective Serotonin Reuptake Inhibitor (SSRI) treatment on AβPP processing. SSRIs target the serotonin receptor transporters (SERT), preventing serotonin re-uptake from the synapse and therefore, increase signalling and ligand-receptor binding. Initially, SSRIs were assumed to possess therapeutic effects based on the 'monoamine hypothesis' of depression which postulates that defective neurotransmitter signalling is a central feature (Haase and Brown, 2015). However, multiple downstream effects have been suggested. In a recent review, the potential therapeutic benefits of SSRI treatment, to delay the progression of AD, was highlighted (Elsworthy and Aldred, 2019). The potential actions of SSRIs in AD may include elevated neurogenesis, reduced oxidative stress and favourable alterations in AβPP processing (Elsworthy and Aldred, 2019). These alterations in AβPP processing are shown by elevated sAβPP-α secretion in addition to lowered Aβ1-42:Aβ1-40 ratio (Cirrito et al., 2011, Sheline et al., 2014), supporting the idea that AβPP processing is being shifted towards the non-amyloidogenic pathway. However, the mechanisms by which these changes occur are not yet known. As previously highlighted, the activity of ADAM10, the main α-secretase enzyme in the AβPP processing pathway, may be

altered by SSRI treatment. If ADAM10 activity is increased due to 5HT, then it might be sensible to suggest that elevated serotonin receptor ligand binding may also stimulate ADAM10 activity. In particular, agonist binding of the 5HT4r, which is one receptor that SSRIs act via, has been associated with altered ADAM10 activity (Robert et al., 2005, Cochet et al., 2013). In addition, the elevations seen in sAβPP-α may be in part explained by increased trafficking and retention of AβPP at the cell membrane. In AD, the ratio of AβPP (130kDa:110kDa) protein is reduced, suggesting lowered maturation of AβPP. Treatment with SSRI's may restore 'normal' AβPP trafficking by increasing the AβPP interaction with ADAM10. In turn, this may reduce AβPP interaction with BACE-1. Further, SSRI treatment is likely to improve cell health through restored physiological signalling (Mdawar et al., 2020). Increasing synaptic serotonin can act as a 'trophic-factor', promote antioxidant-like actions and improve mitochondrial functioning (Fanibunda and Vaidya, 2020). Further to this, reduced neuroinflammation and elevated brain-derived neurotrophic factor are all potential mechanisms by which SSRI treatment may contribute to the delayed progression of AD (Bartels et al., 2018). This can significantly reduce cellular stress and enable the maintenance of cell function. The production of ROS is closely linked to cellular respiration, which when perturbed, can result in excess superoxide leak. The resulting ROS cascades can significantly alter biomolecular actions (Butterfield and Halliwell, 2019). Neurons are particularly susceptible to these redox cascades due to a high capacity for aerobic respiration and large energy demand. Hypometabolism and increased oxidative stress, which are seen in the AD brain, may therefore be rescued in part by treatment with SSRIs (Elsworthy and Aldred, 2019). Thus, treatment with SSRIs may hold therapeutic benefit.

In previous chapters of this thesis, co-cultures carrying the *PSEN1* mutation, L286V, have been found to exhibit pathophysiological similarities to those seen '*in vivo'* in AD.

Therefore, the aim of this chapter is to investigate the effect of SSRI treatment on the AβPP processing and redox balance in these iPSC-derived neuron and astrocyte co-cultures compared to healthy control cells.

6.2 Methods

6.2.1 Optimising Citalopram treatments

In order to assess cell viability after acute incubation with Citalopram, control cells (AX0018) were cultured for 45 days on a poly-L-ornithine (20µg/ml) and Laminin (10 µg/ml) coated 96 well plate before being treated with Citalopram hydrobromide (Sigma-Aldrich, C7861) at a range of concentrations (0-1280µM). Citalopram treatment was delivered in NMM for 48 hours under normal cell culture conditions. Following this, cells were analysed using the MTT assay (*2.4.7 Succinate dehydrogenase activity (MTT) assay*) to determine the dose-response effect on cell viability. Data was collected by plotting percentage viability using a sigmoidal four-parameter variable slope to determine IC50.

6.2.2 Longitudinal delivery of Citalopram treatments

HNSC's were cultured for 45 days on poly-L-ornithine (20µg/ml) and Laminin (10µg/ml) coated 96 well (ADAM10 activity) or 12 well plates (MitoSOX/lysate/media). Both Control (AX0018) and L286V(AX0112) cells were used in this study (*2.1.8 Spontaneous differentiation of HNSC's into neuron and astrocyte co-cultures*).

Following expansion, HNSC's cells were seeded at a final density of 150,000 cells/cm^2. Cells were incubated with ROCK inhibitor (10µM/ml) for 24 hours post passage and a further 24 hours in NMM only. Treatment with Citalopram began 48 hours after final passage and was delivered in NMM as per usual feeding schedule. Citalopram was delivered

at 0.8μM, 5μM and 10μM concentrations for 43 days giving a total culture period of 45 days. From day 39, spent media was collected totalling 3 collection points. At day 45, cells were lysed and stored for analysis.

6.2.3 ADAM10 activity

The enzymatic activity of ADAM10 was quantified by FRET assay following the culture and treatment protocol detailed above (*2.4.2 ADAM10 enzyme activity*). All values were normalised to total protein content measured via BCA assay.

6.2.4 AβPPr measured by Western Blotting

The protocols used for SDS-PAGE can be found in the section (*2.3.3 Western blotting*). The volume of cell lysate containing 10μg of protein was boiled for 5mins at 95°C and loaded into 8% SDS- PAGE gel. Molecular weight markers (5μl) were loaded at each end of the gels. Membranes were incubated in the primary antibody for AβPP (Merck MAB348, 22C11) followed by incubation with the corresponding secondary antibody (Sigma Anti-mouse IgG FC-specific A0168). Membranes were developed using ECL substrate, imaged and quantified as previously described.

6.2.5 Mitochondrial ROS production

Control and L286V cells were cultured for 45 days followed by staining with MitoSOX Red mitochondrial superoxide indicator at a final concentration of 5μM (*2.2.2 MitoSOX Red assay*). Initially, control cell ROS production quantified at baseline and with incubation of H_2O_2 (100μM) over 10 minutes to measure any time-related increases in fluorescence and monitor the sensitivity of the assay to oxidative insult. Next, ROS

production in Citalopram treated Control and L286V cells was measured over 5 minutes (Baseline, 150 seconds, 300 seconds). Quantification of the fluorescence intensity from oxidized MitoSOX reagent was performed as a measure of ROS production over time and peak fluorescence.

6.2.6 Plate-based assays

Cell lysates were analysed for, Protein Carbonylation, 8-Isoprostanes and FRAP as previously described (*2.4 Plate-based assays*). For quantification of Aβ1-40 and Aβ1-42 spent media was concentrated and analysed for secreted peptides.

6.2.7 Statistical Analysis

All quantitative data in the text and figures are presented as Mean ± S.D. unless otherwise stated. The best fit model for prediction IC50 and maximum viability response was calculated using graph pad dose-response curve parameters. To test data distribution normality the Shapiro-Wilk test was employed. Statistical analysis of between Citalopram treatments conditions was calculated using Kruskal-Wallis H tests with multiple comparisons of mean rank. For comparison of control and PSEN1 MitoSox Red fluorescence, Mann-Whitney mean ranks was applied. All data was processed using GraphPad Prism Version 8.4.3. Significant values were set at 0.05%.

6.3 Results

6.3.1 Optimisation of Citalopram doses

In order to optimise the dose of Citalopram treatment, cell viability was measured via MTT assay. The best fit model predicted a maximum viability response (EMAX) of 113.1% and a minimum viability 2.559% under the range of Citalopram treatments used. The predicted IC50, or the concentration of Citalopram to elicit a 50% loss in viability was at a concentration of 150.9µM with a hill slope of -3.169 (Figure 18, **A**). Thus showing, lower doses of Citalopram had a trending protective effects with no apparent viability loss at doses up to 80µM. Grouped analysis showed a decline in cell viability around 40µM; however, this was only significant at concentrations at or above 320µM (Figure 18, **B**). From this, dosages giving maximum cell viability yet closest to physiological blood concentration of 0.8µM were selected for further assay.

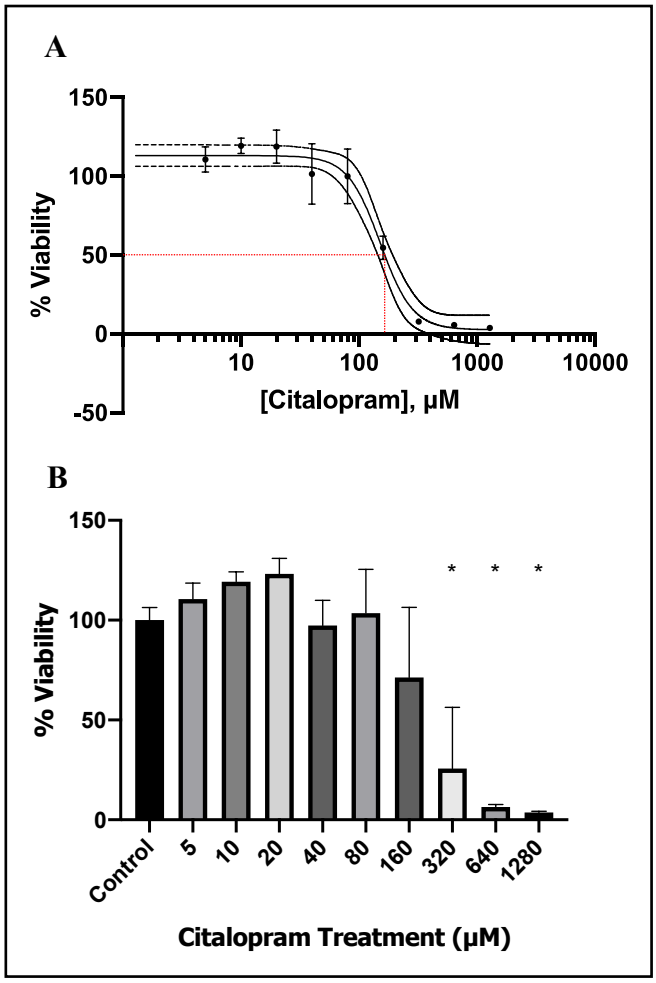

Figure 18 – Percentage viability after treatment with Citalopram (µM) measured via MTT assay in control cells at 45 days post differentiation. Each dose was replicated 3 times **A.** Sigmoidal four-parameter variable slope of percentage viability against $\log^{10}$ Citalopram concentration (µM). Red line shows IC50. **B.** Bar graph representation of percentage viability to highlight significant decrease from baseline shown by * ($p<0.05$), (n = 3).

6.3.2 AβPP processing

In control cells, Citalopram treatment had no significant effect on ADAM10 activity (RFU) at any of the tested concentrations ($p > 0.050$) (Figure 19, **A**). Interestingly, in L286V cells ADAM10 activity was significantly elevated after treatment with 0.8μM (0.408 ± 0.063 RFU), 5μM (0.359 ± 0.046 RFU) and 10μM (0.284 ± 0.066 RFU) Citalopram, compared to baseline (0.145 ± 0.063 RFU, $p = 0.003$) (Figure 19, **B**). To further investigate changes associated with AβPP processing, the ratio of AβPP (130:110kDa) expression was quantified. In the control group there was no significant effect of Citalopram treatment from baseline (1.327 ± 0.288 AU, $p > 0.050$) (Figure 19, **C**). In L286V cells, AβPPr was significantly elevated with both 0.8μM (1.326 ± 0.385 AU) and 5μM (1.336 ± 0.011 AU) Citalopram treatment compared to baseline (0.782 ± 0.098 AU, $p = 0.011$) (Figure 19, **D**).

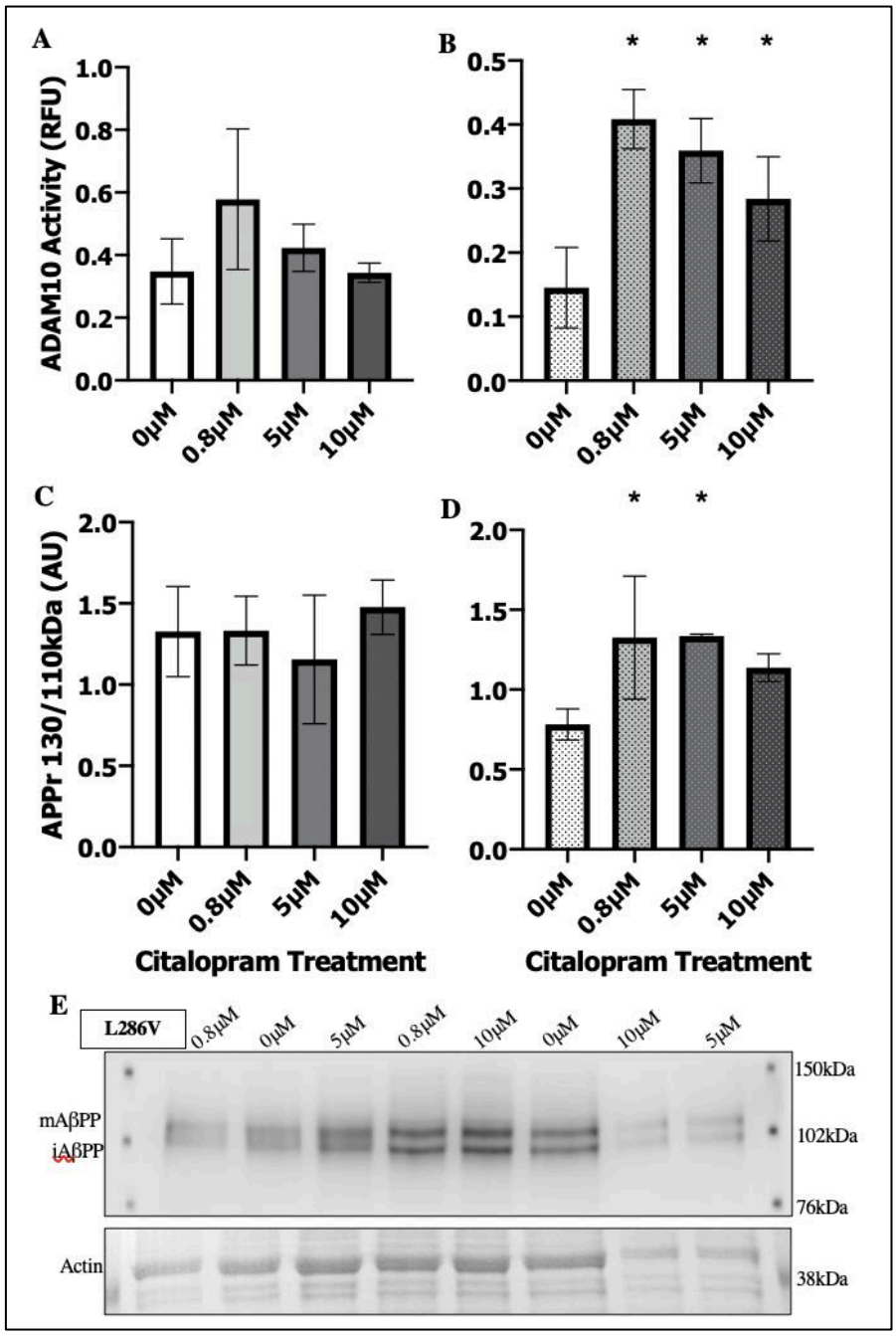

Figure 19 – *Data displaying ADAM10 activity and APPr in control (solid bars) and L286V (spotted bars) cells after continuous treatment with 0μM (n=5), 0.8μM (n=2), 5μM (n=2), 10μM (n=2) of Citalopram for 45 days post differentiation. ADAM10 activity (n=3 all conditions) measured via FRET assay (**A&B**) and AβPPr measured by western blotting (**C&D**). Example loading of western blots in L286V cells displayed in **E**. *Significantly different to 0μM treatment condition.*

To monitor changes in amyloidogenic AβPP processing after Citalopram treatment, Aβ1-40 and Aβ1-42 secretion was measured by ELISA in media collected 48hr hours after the final treatment/ media exchange 45 days after differentiation. In control cells Aβ1-40 was significantly elevated after treatment with 10μM Citalopram (140.40 ± 39.08 pg/mg/ml) compared to baseline (60.14 ± 12.82 pg/mg/ml, $p = 0.001$) (See figure 20 **A**). In addition, the total Aβ secretion was elevated after 10μM Citalopram treatment (163.7 ± 44.65 pg/mg/ml) compared to baseline (104.5 ± 16.30 pg/mg/ml, $p = 0.040$) (See figure 20 **C**). However, treatment with 0.8μM Citalopram significantly reduced total Aβ secretion (40.13 ± 4.459 pg/mg/ml, $p = 0.027$). No significant effects were seen for Aβ1-42 or the Aβ1-42:Aβ1-40 ratio in control cells ($p > 0.050$) despite a trend towards lower Aβ1-42:Aβ1-40 after 10μM treatment (*$p=0.09$)*. There was no significant effect of Citalopram treatment on any measures of Aβ peptides in L286V cells ($p > 0.050$) (See figures 20 **E, F, G** & **H**).

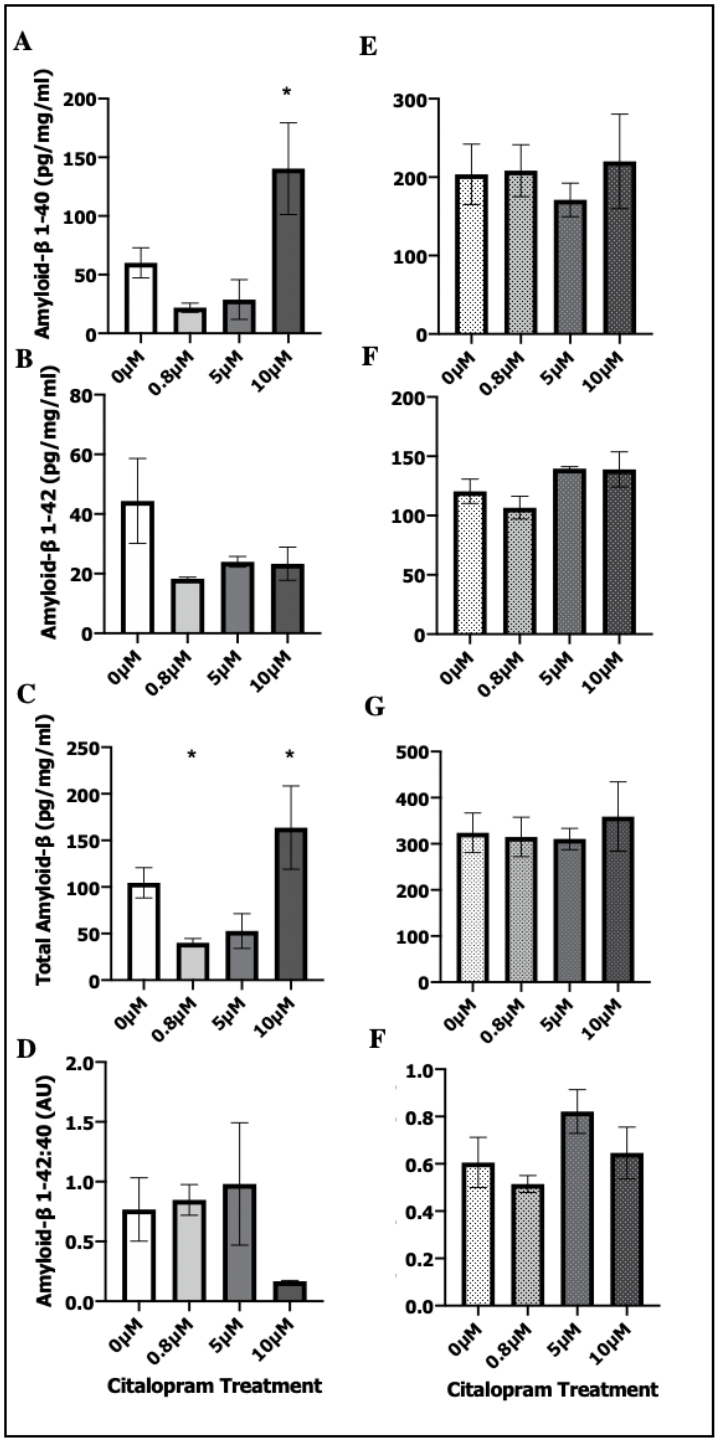

Figure 20 - *Data displaying Aβ secretion into spent media from control (solid bars) and L286V (spotted bars) cells after continuous treatment with 0μM (n=5), 0.8μM (n=2), 5μM (n=2), 10μM (n=2) of Citalopram for 45 days post differentiation.* ***A-D*** *shows data for control cells,* ***E-F*** *shows data for L286V cells. *Significantly different to 0μM treatment condition.*

6.3.3 Oxidative stress

Mitochondrial ROS production was quantified by repeated measurements under control conditions and in the presence H_2O_2 (100μM) to test the sensitivity of the assay to detect changes in ROS production. This also served as a time control for change in fluorescence with time. Under control conditions there was no significant change in fluorescence with time indicating there was no elevation in ROS production as an artefact of time between measurements (*p>0.05)*. Incubation with H_2O_2 (100μM) led to a significant elevation in ROS production (RFU) after 450 seconds (1.052 ± 0.011 RFU, $p = 0.001$) and 600 seconds (1.082 ± 0.006 RFU, $p = 0.001$) compared to time matched control (1.002 ± 0.002 RFU & 1.003 ± 0.002 RFU respectively) (Figure 21, **A)**. Next, Mitochondrial ROS production was assessed in control and L286V cells at baseline and with Citalopram treatment. Baseline Mitochondrial ROS production was significantly higher in L286V cells (0.171 ± 0.015 RFU) compared to control cells (0.055 ± 0.008 RFU, $p = 0.001$) (Figure 21, **B**). No significant effects were found in control cells with Citalopram treatments ($p > 0.050$) (Figure 21, **C)**. In L286V cells, Citalopram treatments of 0.8μM (0.122 ± 0.008 RFU, $p = 0.003$), 5μM (0.094 ± 0.014 RFU $p = 0.002$) and 10μM (0.096 ± 0.002 RFU, $p = 0.003$) significantly reduced mitochondrial ROS production compared to baseline (0.171 ± 0.015 RFU) (Figure 21, **D**).

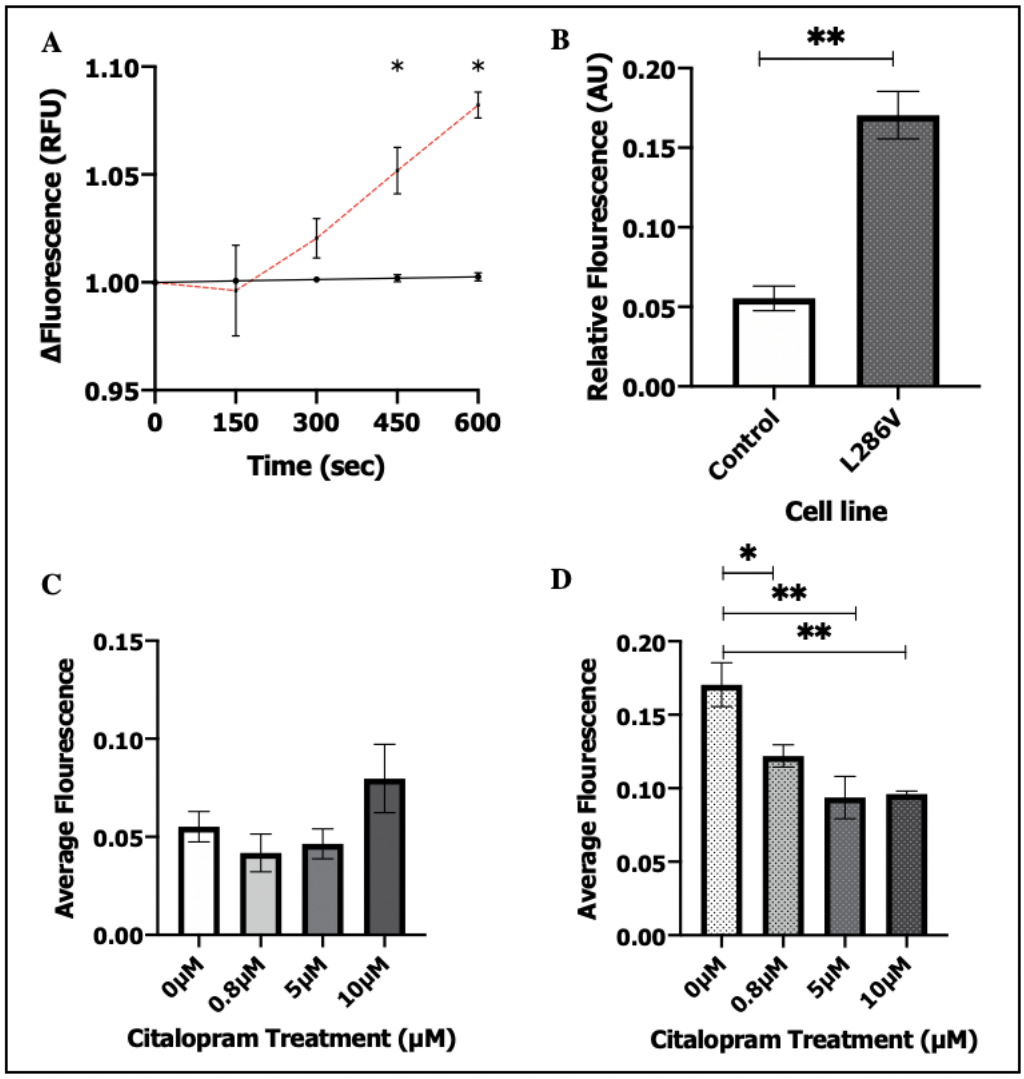

Figure 21 – *Figures displaying MitoSOX Red assay data in cells 45 days post differentiation (N=3).* ***A.*** *Change in fluorescence over time in control (AX0018) cells at basal rates. Red line depicts the change in fluorescence (RFU) with the addition of with H_2O_2 (100μM) indicating increased ROS production.* ***B.*** *Comparison of basal ROS production from MitoSOX Probe binding between control and L286V (n=3).* ***C-D****. Change in ROS generation after being treated continuously for 45 days with Citalopram at different doses (μM) *Significantly different to L286V cells under no treatment condition ($p<0.05$) (**$p<0.01$).*

To further monitor the redox status of the cells in response to Citalopram treatment, markers of protein and lipid oxidation were measured. In both control and L286V cells, Citalopram treatment did not affect protein carbonylation ($p > 0.050$) (Figure 22, **A-B)**.

Lipid peroxidation, quantified by total 8-isoprostanes, was significantly elevated in control cells at Citalopram treatment concentrations of 5μM (4.654 ± 1.475 pg/ml, $p = 0.005$) and 10μM (3.770 ± 0.165 pg/ml, $p = 0.021$) compared to baseline (1.210 ± 0.628 pg/ml) (Figure 22, **C**). In contrast, Citalopram treatment at concentrations of 0.8μM (0.910 ± 0.146 pg/ml, $p = 0.002$) and 5μM (1.732 ± 0.192 pg/ml, $p = 0.011$) was associated with significantly lower total 8-isoprostanes compared to baseline L286V cells (3.867 ± 0.767 pg/ml) (Figure 22, **D**). In control cells, total antioxidant capacity was not changed significantly with Citalopram treatment ($p > 0.050$) (Figure 22, **E)**. In L286V cells, antioxidant capacity was significantly elevated with 5μM treatment of citalopram (257.7 ± 13.04 μM/mg, $p = 0.001$) compared to baseline (135.1 ± 34.18 μM/mg). This effect was not seen with 0.8μM or 10μM treatment ($p > 0.050$) (Figure 22, **F**).

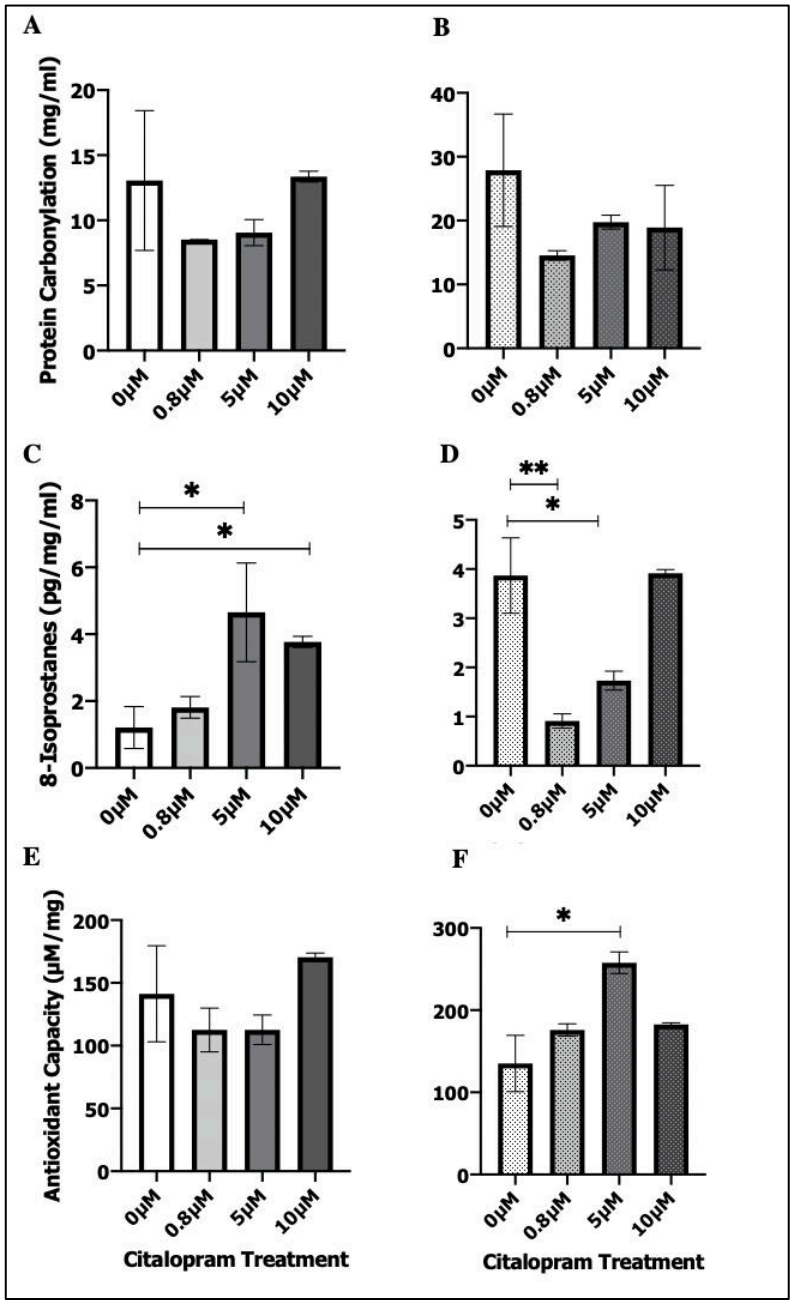

Figure 22 – *Figures displaying markers of oxidative stress data in cell lysates 45 days post differentiation after different treatments with Citalopram, 0μM (n=7) 0.8μM (n=2), 5μM (n=2) and 10μM (n=2).* ***A-B*** *Protein carbonylation (mg/ml) in Control cells (Left, solid bars) and L286V cells (Right, spotted bars).* ***C-D*** *Total 8-isoprostanes (pg/mg/ml) in Control cells (Left, solid bars) and L286V cells (Right, spotted bars).* ***E-F*** *Antioxidant capacity (μM/mg) in Control cells (Left, solid bars) and L286V cells (Right, spotted bars). *Significantly different to L286V cells under no treatment condition ($p<0.05$) (**$p<0.01$).*

6.4 Conclusion

The data presented herein suggest that longitudinal Citalopram treatment at concentrations of 0.8μM and 5μM can have a neuroprotective effect in cells carrying the *PSEN1* mutation L286V. However, Citalopram treatment at a concentration of 10μM did not show benefits in the measured outcomes. In control cells, the protective effect of Citalopram treatment was absent and higher doses of Citalopram (5μM and 10μM) caused an increase in 8-isoprostanes (Figure 22). Our initial experiments to determine the optimal doses of Citalopram, undertaken in iPSC-derived neuron and astrocytes, showed that cell viability was maintained across doses up to around 20μM (Figure 18). This suggests iPSC-derived neuron and astrocyte co-cultures are a feasible model to study the effects of Citalopram on AβPP processing.

The proposed potential therapeutic role of SSRI's to delay the progression of AD is partially based on the ability of elevated 5HT signalling to boost non-amyloidogenic AβPP processing. Crucially, both ADAM10 activity and AβPPr were elevated with Citalopram treatment in L286V cells supporting this hypothesis (Figure 20). Whilst the exact mechanism of Citalopram treatment in increasing non-amyloidogenic processing cannot be determined from the current research alone, combining this data with the previous chapter (See *Chapter 5*) it could be suggested that increased 5HT4r agonist binding may be responsible for some of the beneficial effects of Citalopram in slowing AD progression. In control cells this effect of was not seen following SSRI treatment. This may be explained by the already 'higher' baseline AβPPr and expression of ADAM10 as determined previously in chapter 4 compared to L286V cells.

To gain a further understanding of how amyloidogenic AβPP processing may be altered in response to Citalopram treatment, Aβ1-40 and Aβ1-42 was measured in cell media.

Interestingly, L286V cells, there was no significant impact of Citalopram treatment on Aβ generation (Figure 20). This perhaps makes sense as agonist stimulation of 5HTr has been shown to have no effect on Aβ generation (Robert et al., 2005) and therefore increasing 5HT availability through Citalopram treatment may not impact amyloidogenic processing. Instead, this places the beneficial effects of SSRI's for treating AD on increasing non-amyloidogenic processing. However, in Control cells both Aβ1-40 and total AβPP were increased after treatment with 10μM Citalopram. Yet, total Aβ was significantly lower with 0.8μM treatment (Figure 20). This suggests that continuous treatment above 5μM Citalopram may promote the generation of Aβ1-40, without impacting longer Aβ1-42 production.

Data presented showing mitochondrial ROS production was reduced, in combination with a reduction in markers of downstream oxidative stress, provide further evidence of the neuroprotective effects of SSRIs (Figure 21 & 22). The brain is particularly susceptible to ROS damage, which is elevated in AD (Butterfield and Halliwell, 2019), and therefore highlights another potential mechanism of action for Citalopram as an effective treatment in AD. Although this study is limited by a small number of repeats in treatment conditions, the overall trends with Citalopram treatment highlight the need for further research into these effects. As cells carrying *PSEN1* mutations have perturbed development, treatment with SSRI's may restore 'normal function' and this research therefore highlights a key consideration that should be taken into account when designing future studies using SSRI's as a treatment for AD. It is also critical that the effects of citalopram treatment are investigated in a larger number of fAD mutations to control for donor specific effects. This is also a consideration for the control donor samples as some individuals display SSRI resistance and therefore, reprogrammed cells may also be resistant. This, however, has not be tested and should be conducted in future work.

Overall, Citalopram treatment may hold therapeutic benefits for promoting non-amyloidogenic AβPPr processing and reducing oxidative stress. Whilst SSRI's are unlikely to recover Aβ pathology in vivo completely, they may have a vital role in delaying the progression of AD.

CHAPTER 7 - GENERAL DISCUSSION

The overarching theme of this collection of work was to investigate AβPP processing and redox balance in the development of AD. More specifically, chapter one aimed to gather a better understanding of how ageing and obesity can alter to pathological markers associated with AD in cognitively healthy individuals, including the ADAM10, the AβPPr, IL-6 and oxidative damage to lipids and proteins. In chapter two, these markers were characterised in iPSC-derived cortical models of fAD carrying PSEN1 mutations to test whether these cells represent similar phenotype to people with AD. In chapter 5, the research aimed to investigate the presence and functionality of 5HT4r receptors in iPSC-derived cortical cultures and whether modulation of the receptor could impact ADAM10 activity. In the final empirical chapter, iPSC derived cell models were treated with the SSRI, Citalopram, and markers associated with AβPP processing and oxidative stress were monitored.

Early detection of key biochemical changes is critical if better therapeutic interventions are to be successfully developed for LOAD. Being able to assess the risk of LOAD in a cognitively 'normal' person is one such avenue for research. Both advancing age and obesity are known risk factors for the development LOAD and have been associated with a chronic inflammatory state and perturbed redox balance. However, less is known about how peripheral markers influencing AβPP processing might be affected by age and obesity. Initially, research was undertaken to identify whether changes in blood-based biomarkers associated AβPP processing, inflammation and oxidative stress could be detected in cognitively healthy people who may be 'at risk' of LOAD. This research presented in chapter 3 supports previous research showing that ageing and obesity are associated with an altered inflammatory and redox balance state (Ferrucci and Fabbri, 2018, Stolarczyk, 2017, Hauck et al., 2019). Data was also presented to show that ADAM10 protein expression was also

significantly lowered with ageing and obesity, even in cognitively healthy individuals. These findings are novel, and this is the first study to suggest that ADAM10 protein expression may be altered in AD 'at risk' but otherwise cognitively healthy individuals. Expression of the full-length zymogen, ProADAM10, was more strongly associated with ageing whereas, expression of mADAM10 was associated with obesity in later life. There was no change in AβPPr in any of the participant groups. These findings are in agreement with other studies that have shown that blood-based markers associated with LOAD are altered in ageing and obesity. The changes observed in protein expression of the different ADAM10 proteins may be indicative of lowered non-amyloidogenic AβPP processing, which is associated with an elevated risk of LOAD. Therefore, highlighting a potential link between redox status, inflammation, AβPP processing and LOAD. Further, a previous research has shown that the C-terminal fragment associated with alpha-secretase activity was reduced with age in healthy individuals (Nistor et al., 2007). Although the protein levels of ADAM10 have been shown to decrease in people with AD (Manzine et al., 2013, Manzine et al., 2014, Colciaghi et al., 2002, Colciaghi et al., 2004) it is not a direct measure of ADAM10 activity. Although there is some evidence that mADAM10 protein levels and activity are related in platelets (Schuck et al., 2016), the outcomes of this study are limited, and it is not possible to conclude on whether amyloidogenic AβPP processing is altered. Further research measuring sAβPP-α would provide a more direct analysis. The findings from this study are in contradiction to a research study that showed elevated ADAM10 activity in cognitively healthy older adults (Schuck et al., 2016). An important consideration when comparing the results of these studies is that cross-sectional analysis is subject to a selection bias. By nature, older adults who maintain cognitively healthy as they age may have greater ADAM10 activity throughout their lifespan compared to those who experience cognitive deficits. Therefore, this analysis is unable to

detect changes in ADAM10 activity from 'baseline' to older age. Further, the effects of diet, exercise and sleep, which are considered neuroprotective against AD, have not been investigated for their impact on ADAM10 protein expression and activity and may explain differences between these study findings.

Research is warranted to monitor ADAM10 protein expression and activity across the lifespan to see if reduced expression in younger or mid-life is a factor associated with a future diagnosis of LOAD. This research is further supported by identification of the *ADAM10* as a susceptibility gene for AD (Jansen et al., 2019). Although rare, ADAM10 missense mutations functionally impair ADAM10 prodomain chaperone function, leading to a shift in AβPP towards the amyloidogenic pathway and increase reactive gliosis in mouse brain (Suh et al., 2013). Irrespective of the conflicting findings for altered mADAM10 platelet expression with cognitively healthy ageing, ADAM10 and AβPP may be excellent targets for therapeutic intervention in AD. By increasing ADAM10 activity, perhaps via intervention, it may be possible to reduce amyloidogenic AβPP processing and therefore preclude the generation of Aβ. This approach to treatment would also result in the release of sAβPP-α which is considered neuroprotective. There is, however, a key issue. Strategies aimed at increasing 'global' ADAM10 activity are likely to cause significant unwanted side effects. ADAM10 is expressed on a number of different cells types and is known to cleave a number of substrates (Wetzel et al., 2017). This problem is similar to that seen with current attempts to treat AD by the use of both BACE-1 and γ-secretase inhibitors. However, the finding that ADAM10 can associate with partner proteins at the cell membrane (Matthews et al., 2017, Cochet et al., 2013) may enable a more targeted approach to increasing non-amyloidogenic AβPP processing. Several lines of evidence suggest that modulating serotonin signalling, possibly through agonist binding of the 5HT4r receptor can increase ADAM10 activity (Robert et al.,

2005, Cochet et al., 2013, Bianco et al., 2016b). This highlights a potential therapeutic avenue for treating AD. In order to further investigate this, it was first critical to establish physiologically relevant model. The recent advancements in iPSC technology, enabling the generation of cortical cell models could provide a suitable platform for this research.

In chapter 4 iPSC-derived neuron and astrocyte co-cultures carrying *PSEN1* mutations were characterised for markers of AβPP processing and oxidative stress and compared to a healthy control cell line. Although *PSEN1* mutations cause fAD, the pathological features are nearly identical in presentation to LOAD and therefore, modelling AD in iPSC-derived cortical models may represent a powerful research tool. The aim of this research was to establish whether the iPSC-derived neuron and astrocytes co-cultures also displayed a phenotype similar to that seen in LOAD, in particular whether ADAM10 protein expression and cellular redox balance was altered. The results of this study showed that iPSC-derived neuron and astrocyte co-cultures with either the *PSEN1* mutation L286V or R278I had significantly lower mADAM10 expression compared to controls. In addition, the AβPPr was also significantly lower in both *PSEN1* mutation cell lines. Further, alterations in Aβ peptide secretion were detected in both lines. Although, the L286V mutation had an overall increase in Aβ accumulation, whereas, the R278I mutation had an alteration in the Aβ1-42:Aβ1-40 ratio. Further, the R278I mutation also had an elevation in Aβ oligomers. This makes sense as increasing longer Aβ species, such as Aβ1:42, are more prone to aggregation (Qiu et al., 2015). The lowered mADAM10 expression in *PSEN1* mutation carrying cells compared to control cells may make this a viable model for exploring the effects of therapeutic treatments aimed at restoring ADAM10 activity. Further, markers of oxidative stress were also altered in cells carrying a *PSEN1* mutation. Although the involvement of disrupted redox balance has not been precisely elucidated, it is a prevalent and early pathological feature in LOAD and

fAD (Smith et al., 2000, Nunomura et al., 2001, Butterfield and Boyd-Kimball, 2018a). As shown in chapter 3 elevated oxidative stress is also seen in people who may be at risk of developing LOAD. However, it is important to consider the limitations of these findings as only two mutations were used in comparison to the relatively large number of known *PSEN1* mutations identified. It is possible that different mutations each display a distinct phenotype, and this is currently an area of investigation. The findings from chapter 4 do compliment previous research showing that both AβPP processing and the species of Aβ generated is significantly altered in neurons and astrocytes carrying *PSEN1* (Kwart et al., 2019, Arber et al., 2019, Sproul et al., 2014). Therefore, iPSC-derived cells models will likely provide invaluable insight as a tool to investigate the pathogenesis of AD in future work.

In chapter 5, the research aimed to further examine the potential use of iPSC-derived neuron and astrocyte co-cultures as a model to study the interaction of ADAM10 activity with the 5HT4r. A key criticism of iPSC-derived cortical cells models is that they represent a very early developmental stage of cell growth which may not be a relevant model to study a disease like LOAD that is thought to develop gradually in later life. In addition, the maturation of neuronal circuits is critical for network signalling activity and may not have taken place in the iPSC model. As such, to test therapeutic compounds that may modify ADAM10 activity though modulating neurotransmitter release, such as SSRI's, cell networks need to be able to functionally respond to treatments. Evidence supporting the presence of functional 5HT4r receptors is presented in chapter 5 following bath application of 5HT and selective agonist and antagonist compounds evoking calcium potentials, which is indicative of signalling activity. Further to this, the treatment of co-cultures with Prucalopride significantly elevated ADAM10 activity, and this effect was subsequently blunted by the addition of the 5HT4r inhibitor GR113808. Interestingly, this effect was only seen in cells carrying the

L286V *PSEN1* mutation which was seen to have a lower baseline ADAM10 activity. This provided further support to existing evidence suggesting agonist binding of the 5HT4r may be a target for increasing ADAM10 activity (Robert et al., 2005, Cochet et al., 2013).

This apparent link between 5HTr agonists and ADAM10 activity has led to a hypothesis that proposes that SSRIs may have a beneficial role in the delaying the progression of AD (Elsworthy and Aldred, 2019). Whilst there is some evidence suggesting SSRI's may protect against cognitive decline in people with AD (Pelton et al., 2016, Bartels et al., 2018), the ability of SSRIs to affect the pathology of AD is far from proven (Sepehry et al., 2012). The evidence from animal models supports a disease modifying effect of SSRI's on AD pathology and cognition (Huang et al., 2018, Kim et al., 2018), however, this effect appears to be less apparent in modifying established amyloid pathology (von Linstow et al., 2017, Severino et al., 2018). There is a clear need for more research into these effects.

In chapter 6, iPSC-derived neuron and astrocyte co-cultures from healthy control and the *PSEN1* mutation, L286V were used to examine the effects of Citalopram on AβPP processing and redox status. In L286V cells, Citalopram treatment at concentrations of 0.8μM, 5μM and 10μM resulted in a significant elevation in ADAM10 activity. The AβPPr was also increased with 0.8μM and 5μM treatments. There was no effect of Citalopram treatments in Control cells. This finding strongly supports the previous finding that 5HT4r agonist stimulation only altered ADAM10 activity in disease (L286V) cells. One explanation for this may be that 5HT signalling is disrupted in cortical cells carrying a *PSEN1* mutation, which is then restored by Citalopram treatment. Whilst there is some evidence to support dysfunctional 5HT signalling in AD (Geldenhuys and Van der Schyf, 2011) it is an area that warrants further investigation.

The elevation of ADAM10 activity and increased AβPPr after treatment with Citalopram point towards an increase in the non-amyloidogenic AβPP pathway, however without directly measuring sAβPP-α generation this cannot be confirmed. Several studies looking at the effects of SSRI treatment in animal models of AD have shown reductions in Aβ production, however, the data presented in chapter 6 did not suggest that Aβ production was lower in L286V cells. The release of Aβ into cell media was only impacted in Control cells, where a reduction of total Aβ concentration was observed with Citalopram treatment (at a concentration of 0.8μM) and Aβ concentration was increased when cells were treated with 10μM Citalopram treatment. A crucial consideration when interpreting this data is that the nature of the *PSEN1* mutation that was present in the model system used herein causes altered γ-secretase activity, and the mechanisms by which this occurs are poorly understood. Therefore, any effects of Citalopram on L286V cells may be significantly affected by the specific mutations' effect on baseline Aβ cleavage. However, in chapter 4, the L286V cells were shown to have elevated Aβ generation at baseline compared to both control and a second *PSEN1* mutation R278I. Therefore, it likely if Citalopram treatment could directly modulate Aβ production it would likely be highlighted in this model. From this data it instead points towards Citalopram treatment acting through the non-amyloidogenic, ADAM10, pathway.

One limiting factor in this study is the small number of repeats in the Citalopram treatment groups. This may cause subtle changes in outcome measures to be lost. Alternatively, outcome measures with high variation can be subject to more type 1 error, i.e. a false positive. However, after grouping Citalopram treatments against the control group for each of the Aβ generation outcome measures, there was little to no change in statistical power (Cohens d below 0.1) suggesting that there is no effect of Citalopram treatment on Aβ generation in this study.

To understand the effects of Citalopram on cellular redox balance, ROS production, markers of oxidative stress and antioxidant capacity were measured. In L286V cells, which were previously shown to have perturbed basal redox balance (chapter 4), Citalopram treatment reduced oxidative stress. This was supported by both a significant reduction in mitochondrial ROS production in all Citalopram treatment conditions and a reduction in lipid peroxidation with 0.8μM and 5μM treatments. Further, treatment with Citalopram treatment typically elevated antioxidant capacity, reaching statistical significance in only the 5μM condition. This points to a redox favourable role of Citalopram treatments in conditions where oxidative stress is elevated.

Throughout this research, markers of oxidative stress have been monitored predominantly though end-point oxidation products to lipids and proteins. Further, direct superoxide generation using the MitoSOX red probe was utilised in chapter 6. Whilst these are commonly used method of assessing redox balance, this approach only presents a limited view of redox balance. To compliment this work and strengthen the conclusions on redox balance disruption in both the participants in chapter 3 and iPSC models in subsequent chapters, a number of alternative measures could have been made. Specific oxidation adducts to proteins have been shown to better reflect AD symptomology than global markers of carbonylation (Aldred et al., 2010). Measuring redox couples/ cycles such as the glutathione cycle, could also provide further insight to cellular oxidative stress, in addition to antioxidant enzymes and genes associated with maintain redox homeostasis. Superoxide dismutase -1 is one such enzyme that is commonly associated with AD (Cao et al., 2018). Generating a full redox profile of *PSEN1* mutation carrying iPSCs is perhaps an area for further work.

The research presented in chapter 6 highlights another important mechanism by which SSRI's may exert neuroprotective effects to delay some of the neurodegenerative processes

that are seen in AD. Current research suggests that long-term treatment with SSRIs may delay the progression from MCI to AD (Pelton et al., 2016, Bartels et al., 2018). Further, effective treatment with SSRIs can induce neurogenesis, delay hippocampal atrophy (Dale et al., 2016, Eliwa et al., 2017), reduced neuroinflammatory processes and increase neurotrophic factors (Bartels et al., 2018, Alboni et al., 2016). SSRIs may also be effective in lowering oxidative stress. This may be due to either increased endogenous antioxidant capacity or activity, or through possible antioxidant properties of the drugs itself suggesting alternative protective action (Lee et al., 2013, Chang et al., 2015). As previously discussed in section *1.10.1 'mechanisms of action'* the beneficial effects of SSRI treatment in people with AD has translated into a reduced mortality rate at two-year follow up, although this effect dissipates after four years (Sepehry et al., 2016). Therefore, it may be critical for effective intervention to begin much earlier in disease pathology, perhaps even prior to clinical symptoms appear. This is crucial as once the clinical symptoms of AD become apparent the associated neurodegeneration is irreversible. Therefore, the treatment of AD with SSRIs is not curative or necessarily able restore a loss of function but may delay the disease process and crucially, prolong cognitive function into older age.

In order to achieve this therapeutic effect, SSRIs must act through mechanisms that interfere with aberrant pathological processes seen in people with AD and there is emerging evidence to support this effect. The results in chapter 6 demonstrate that SSRIs may be beneficial as a treatment for AD by increasing ADAM10 activity and reducing oxidative stress. These beneficial effects may however be independent of Aβ pathology. This should be investigated further in a larger number of biological repeats and fAD mutations in iPSC derived co-cultures for more powerful data collection. Some of the possible mechanisms by which SSRIs could alter the processing of AβPP are via altered AβPP expression or increased

trafficking of AβPP to the cellular membrane, increased ADAM10 activity and/or reduced BACE-1 activity. Two of these mechanisms, increased ADAM10 activity and altered AβPP expression, were identified in chapter 6 however, BACE-1 was not investigated and is a limitation of the research presented.

Based on the findings presented in this thesis, there is clearly scope for further research into the modulation of serotoninergic systems to delay the progression of AD. Perhaps most crucially, it is important to understand the mechanisms of action of 5HT4r agonists on ADAM10 activity to be able to develop specific novel compounds for use as a disease modifying options for AD. Current clinical trials of selective 5HT4r and 5HT6r agonists and antagonists respectively will elucidate whether such modulation holds therapeutic effects (Hung and Fu, 2017). In addition to the physiological relevance of iPSC-derived neuron and astrocyte co-cultures to humans, this cell model provides a platform for rigorous control and manipulation of cell conditions. Applying gene editing techniques, for example, would enable the specific interactions of 5HT4r and ADAM10 to be probed. To test the hypothesis that 5HT4r receptors are crucial for the effect of Citalopram on ADAM10 activity, knockout models of 5HT4r could be used to shed light into this mechanism of action. Further, the relatively new finding that ADAM10 is chaperoned by members of the TSPAN family could be a critical factor in the co-localisation of 5HT4r and ADAM10 at the cell membrane (Matthews et al., 2017). Developing TSPAN knockout models could be an interesting tool applied to this area of research. Whilst this body of research provides supporting evidence for perturbed features associated with AD pathology in iPSC derived cortical models, in addition to novel findings for the beneficial impact of SSRI treatment for AD, it is crucial that larger number mutations are investigated. Modelling AD using iPSC derived cortical cells is proving a highly valuable research tool, yet the relatively limited

neurodevelopmental components cannot fully explain the more multifactorial nature of LOAD. Therefore, novel findings from research including this work, need to be transitioned into human studies to allow our understanding of AD to develop more effectively.

Overall, this research has highlighted that biochemical changes associated with AD are detectable in the blood of older individuals with obesity who may be at considered at risk of LOAD. Further, iPSC-derived neuron and astrocyte co-cultures carrying *PSEN1* mutations display phenotypic features consistent with the diagnosis of AD and are a viable model to study the mechanisms of SSRI treatment on AβPP processing. The findings from this research suggest that more large-scale studies to examine the effects of SSRI's in people at risk of LOAD or in close proximity post-diagnosis are warranted in the near future.

REFERENCES

ABOLHASSANI, N., LEON, J., SHENG, Z., OKA, S., HAMASAKI, H., IWAKI, T. & NAKABEPPU, Y. 2017. Molecular pathophysiology of impaired glucose metabolism, mitochondrial dysfunction, and oxidative DNA damage in Alzheimer's disease brain. *Mech Ageing Dev,* 161**,** 95-104.

ABOUKHATWA, M. & LUO, Y. 2011. Antidepressants modulate intracellular amyloid peptide species in N2a neuroblastoma cells. *J Alzheimers Dis,* 24**,** 221-34.

AHMED, R. R., HOLLER, C. J., WEBB, R. L., LI, F., BECKETT, T. L. & MURPHY, M. P. 2010. BACE1 and BACE2 enzymatic activities in Alzheimer's disease. *J Neurochem,* 112**,** 1045-53.

AKASAKA-MANYA, K., KAWAMURA, M., TSUMOTO, H., SAITO, Y., TACHIDA, Y., KITAZUME, S., HATSUTA, H., MIURA, Y., HISANAGA, S. I., MURAYAMA, S., HASHIMOTO, Y., MANYA, H. & ENDO, T. 2017. Excess APP O-glycosylation by GalNAc-T6 decreases Aβ production. *J Biochem,* 161**,** 99-111.

AKINGBADE, O. E. S., GIBSON, C., KALARIA, R. N. & MUKAETOVA-LADINSKA, E. B. 2018. Platelets: Peripheral Biomarkers of Dementia? *J Alzheimers Dis,* 63**,** 1235-1259.

ALBANI, D., MARIZZONI, M., FERRARI, C., FUSCO, F., BOERI, L., RAIMONDI, I., JOVICICH, J., BABILONI, C., SORICELLI, A., LIZIO, R., GALLUZZI, S., CAVALIERE, L., DIDIC, M., SCHÖNKNECHT, P., MOLINUEVO, J. L., NOBILI, F., PARNETTI, L., PAYOUX, P., BOCCHIO, L., SALVATORE, M., ROSSINI, P. M., TSOLAKI, M., VISSER, P. J., RICHARDSON, J. C., WILTFANG, J., BORDET, R., BLIN, O., FORLONI, G., FRISONI, G. B. & CONSORTIUM, P. 2019. Plasma Aβ42 as a Biomarker of Prodromal Alzheimer's Disease Progression in Patients with Amnestic Mild Cognitive Impairment: Evidence from the PharmaCog/E-ADNI Study. *J Alzheimers Dis,* 69**,** 37-48.

ALBONI, S., POGGINI, S., GAROFALO, S., MILIOR, G., EL HAJJ, H., LECOURS, C., GIRARD, I., GAGNON, S., BOISJOLY-VILLENEUVE, S., BRUNELLO, N., WOLFER, D. P., LIMATOLA, C., TREMBLAY, M., MAGGI, L. & BRANCHI, I. 2016. Fluoxetine treatment affects the inflammatory response and microglial function according to the quality of the living environment. *Brain Behav Immun,* 58**,** 261-271.

ALDRED, S., BENNETT, S. & MECOCCI, P. 2010. Increased low-density lipoprotein oxidation, but not total plasma protein oxidation, in Alzheimer's disease. *Clin Biochem,* 43**,** 267-71.

ALFORD, S., PATEL, D., PERAKAKIS, N. & MANTZOROS, C. S. 2018. Obesity as a risk factor for Alzheimer's disease: weighing the evidence. *Obes Rev,* 19**,** 269-280.

ALLEN, N. J. & EROGLU, C. 2017. Cell Biology of Astrocyte-Synapse Interactions. *Neuron,* 96**,** 697-708.

ALLINSON, T. M., PARKIN, E. T., TURNER, A. J. & HOOPER, N. M. 2003. ADAMs family members as amyloid precursor protein alpha-secretases. *J Neurosci Res,* 74**,** 342-52.

ALMEIDA, O. P., FORD, A. H., HANKEY, G. J., YEAP, B. B., GOLLEDGE, J. & FLICKER, L. 2019. Risk of dementia associated with psychotic disorders in later life: the health in men study (HIMS). *Psychol Med,* 49**,** 232-242.

ALZHEIMER, A., STELZMANN, R. A., SCHNITZLEIN, H. N. & MURTAGH, F. R. 1995. An English translation of Alzheimer's 1907 paper, "Uber eine eigenartige Erkankung der Hirnrinde". *Clin Anat,* 8**,** 429-31.

AMARO, M., ŠACHL, R., AYDOGAN, G., MIKHALYOV, I. I., VÁCHA, R. & HOF, M. 2016. GM1 Ganglioside Inhibits β-Amyloid Oligomerization Induced by Sphingomyelin. *Angew Chem Int Ed Engl,* 55**,** 9411-5.

ANCOLIO, K., MARAMBAUD, P., DAUCH, P. & CHECLER, F. 1997. Alpha-secretase-derived product of beta-amyloid precursor protein is decreased by presenilin 1 mutations linked to familial Alzheimer's disease. *J Neurochem,* 69**,** 2494-9.

ANDERS, A., GILBERT, S., GARTEN, W., POSTINA, R. & FAHRENHOLZ, F. 2001. Regulation of the alpha-secretase ADAM10 by its prodomain and proprotein convertases. *FASEB J,* 15**,** 1837-9.

ANDREOTTI, J., DIERKS, T., WAHLUND, L. O. & GRIEDER, M. 2017. Diverging Progression of Network Disruption and Atrophy in Alzheimer's Disease and Semantic Dementia. *J Alzheimers Dis,* 55**,** 981-993.

ANDREWS, S. J., FULTON-HOWARD, B. & GOATE, A. 2020. Interpretation of risk loci from genome-wide association studies of Alzheimer's disease. *Lancet Neurol*.

ANGELOVA, P. R. & ABRAMOV, A. Y. 2018. Role of mitochondrial ROS in the brain: from physiology to neurodegeneration. *FEBS Lett,* 592**,** 692-702.

ANSARI, M. A. & SCHEFF, S. W. 2010. Oxidative stress in the progression of Alzheimer disease in the frontal cortex. *J Neuropathol Exp Neurol,* 69**,** 155-67.

ANSTEY, K. J., CHERBUIN, N., BUDGE, M. & YOUNG, J. 2011. Body mass index in midlife and late-life as a risk factor for dementia: a meta-analysis of prospective studies. *Obes Rev,* 12**,** e426-37.

ARBER, C., TOOMBS, J., LOVEJOY, C., RYAN, N. S., PATERSON, R. W., WILLUMSEN, N., GKANATSIOU, E., PORTELIUS, E., BLENNOW, K., HESLEGRAVE, A., SCHOTT, J. M., HARDY, J., LASHLEY, T., FOX, N. C., ZETTERBERG, H. & WRAY, S. 2019. Familial Alzheimer's disease patient-derived neurons reveal distinct mutation-specific effects on amyloid beta. *Mol Psychiatry*.

ARMIJO, E., GONZALEZ, C., SHAHNAWAZ, M., FLORES, A., DAVIS, B. & SOTO, C. 2017. Increased susceptibility to Aβ toxicity in neuronal cultures derived from familial Alzheimer's disease (PSEN1-A246E) induced pluripotent stem cells. *Neurosci Lett,* 639**,** 74-81.

BARANGER, K., GIANNONI, P., GIRARD, S. D., GIROT, S., GAVEN, F., STEPHAN, D., MIGLIORATI, M., KHRESTCHATISKY, M., BOCKAERT, J., MARCHETTI-GAUTHIER, E., RIVERA, S., CLAEYSEN, S. & ROMAN, F. S. 2017. Chronic treatments with a 5-HT. *Neuropharmacology,* 126**,** 128-141.

BARTELS, C., WAGNER, M., WOLFSGRUBER, S., EHRENREICH, H., SCHNEIDER, A. & INITIATIVE, A. S. D. N. 2018. Impact of SSRI Therapy on Risk of Conversion From Mild Cognitive Impairment to Alzheimer's Dementia in Individuals With Previous Depression. *Am J Psychiatry,* 175**,** 232-241.

BARÃO, S., MOECHARS, D., LICHTENTHALER, S. F. & DE STROOPER, B. 2016. BACE1 Physiological Functions May Limit Its Use as Therapeutic Target for Alzheimer's Disease. *Trends Neurosci,* 39**,** 158-169.

BELLOY, M. E., NAPOLIONI, V. & GREICIUS, M. D. 2019. A Quarter Century of APOE and Alzheimer's Disease: Progress to Date and the Path Forward. *Neuron,* 101**,** 820-838.

BENNETT, B. D., DENIS, P., HANIU, M., TEPLOW, D. B., KAHN, S., LOUIS, J. C., CITRON, M. & VASSAR, R. 2000. A furin-like convertase mediates propeptide cleavage of BACE, the Alzheimer's beta -secretase. *J Biol Chem,* 275**,** 37712-7.

BENZIE, I. F. & STRAIN, J. J. 1996. The ferric reducing ability of plasma (FRAP) as a measure of "antioxidant power": the FRAP assay. *Anal Biochem,* 239**,** 70-6.

BERMEJO, P., MARTÍN-ARAGÓN, S., BENEDÍ, J., SUSÍN, C., FELICI, E., GIL, P., RIBERA, J. M. & VILLAR, A. M. 2008. Peripheral levels of glutathione and protein oxidation as markers in the development of Alzheimer's disease from Mild Cognitive Impairment. *Free Radic Res,* 42**,** 162-70.

BERNSTEIN, S. L., DUPUIS, N. F., LAZO, N. D., WYTTENBACH, T., CONDRON, M. M., BITAN, G., TEPLOW, D. B., SHEA, J. E., RUOTOLO, B. T., ROBINSON, C. V. & BOWERS, M. T. 2009. Amyloid-β protein oligomerization and the importance of tetramers and dodecamers in the aetiology of Alzheimer's disease. *Nat Chem,* 1**,** 326-31.

BERTI, V., WALTERS, M., STERLING, J., QUINN, C. G., LOGUE, M., ANDREWS, R., MATTHEWS, D. C., OSORIO, R. S., PUPI, A., VALLABHAJOSULA, S., ISAACSON, R. S., DE LEON, M. J. & MOSCONI, L. 2018. Mediterranean diet and 3-year Alzheimer brain biomarker changes in middle-aged adults. *Neurology,* 90**,** e1789-e1798.

BETTHAUSER, T. J., KOSCIK, R. L., JONAITIS, E. M., ALLISON, S. L., CODY, K. A., ERICKSON, C. M., ROWLEY, H. A., STONE, C. K., MUELLER, K. D., CLARK, L. R., CARLSSON, C. M., CHIN, N. A., ASTHANA, S., CHRISTIAN, B. T. & JOHNSON, S. C. 2020. Amyloid and tau imaging biomarkers explain cognitive decline from late middle-age. *Brain,* 143**,** 320-335.

BEZPROZVANNY, I. & HIESINGER, P. R. 2013. The synaptic maintenance problem: membrane recycling, Ca2+ homeostasis and late onset degeneration. *Mol Neurodegener,* 8**,** 23.

BHARADWAJ, P., SOLOMON, T., MALAJCZUK, C. J., MANCERA, R. L., HOWARD, M., ARRIGAN, D. W. M., NEWSHOLME, P. & MARTINS, R. N. 2018. Role of the cell membrane interface in modulating production and uptake of Alzheimer's beta amyloid protein. *Biochim Biophys Acta Biomembr*.

BIANCO, F., BONORA, E., NATARAJAN, D., VARGIOLU, M., THAPAR, N., TORRESAN, F., GIANCOLA, F., BOSCHETTI, E., VOLTA, U., BAZZOLI, F., MAZZONI, M., SERI, M., CLAVENZANI, P., STANGHELLINI, V., STERNINI, C. & DE GIORGIO, R. 2016a. Prucalopride exerts neuroprotection in human enteric neurons. *Am J Physiol Gastrointest Liver Physiol,* 310**,** G768-75.

BIANCO, O. A., MANZINE, P. R., NASCIMENTO, C. M., VALE, F. A., PAVARINI, S. C. & COMINETTI, M. R. 2016b. Serotoninergic antidepressants positively affect platelet ADAM10 expression in patients with Alzheimer's disease. *Int Psychogeriatr,* 28**,** 939-44.

BIRKS, J. 2006. Cholinesterase inhibitors for Alzheimer's disease. *Cochrane Database Syst Rev***,** CD005593.

BIRNBAUM, J. H., WANNER, D., GIETL, A. F., SAAKE, A., KÜNDIG, T. M., HOCK, C., NITSCH, R. M. & TACKENBERG, C. 2018. Oxidative stress and altered mitochondrial protein expression in the absence of amyloid-β and tau pathology in iPSC-derived neurons from sporadic Alzheimer's disease patients. *Stem Cell Res,* 27**,** 121-130.

BISHT, K., SHARMA, K. & TREMBLAY, M. 2018. Chronic stress as a risk factor for Alzheimer's disease: Roles of microglia-mediated synaptic remodeling, inflammation, and oxidative stress. *Neurobiol Stress,* 9**,** 9-21.

BLASER, H., DOSTERT, C., MAK, T. W. & BRENNER, D. 2016. TNF and ROS Crosstalk in Inflammation. *Trends Cell Biol,* 26**,** 249-261.

BONOMINI, F., RODELLA, L. F. & REZZANI, R. 2015. Metabolic syndrome, aging and involvement of oxidative stress. *Aging Dis,* 6**,** 109-20.

BORGHI, R., PATRIARCA, S., TRAVERSO, N., PICCINI, A., STORACE, D., GARUTI, A., GABRIELLA CIRMENA, PATRIZIO ODETTI & MASSIMO TABATON 2007. The increased activity of BACE1 correlates with oxidative stress in Alzheimer's disease. *Neurobiol Aging,* 28**,** 1009-14.

BORRONI, B., AGOSTI, C., MARCELLO, E., DI LUCA, M. & PADOVANI, A. 2010. Blood cell markers in Alzheimer Disease: Amyloid Precursor Protein form ratio in platelets. *Exp Gerontol,* 45**,** 53-6.

BRAAK, H., BRAAK, E., BOHL, J. & REINTJES, R. 1996. Age, neurofibrillary changes, A beta-amyloid and the onset of Alzheimer's disease. *Neurosci Lett,* 210**,** 87-90.

BRAM, J. M. F., TALIB, L. L., JOAQUIM, H. P. G., SARNO, T. A., GATTAZ, W. F. & FORLENZA, O. V. 2018. Protein levels of ADAM10, BACE1, and PSEN1 in platelets and leukocytes of Alzheimer's disease patients. *Eur Arch Psychiatry Clin Neurosci*.

BROTHERS, H. M., GOSZTYLA, M. L. & ROBINSON, S. R. 2018. The Physiological Roles of Amyloid-β Peptide Hint at New Ways to Treat Alzheimer's Disease. *Front Aging Neurosci,* 10**,** 118.

BRUMMER, T., PIGONI, M., ROSSELLO, A., WANG, H., NOY, P. J., TOMLINSON, M. G., BLOBEL, C. P. & LICHTENTHALER, S. F. 2018. The metalloprotease ADAM10 (a disintegrin and metalloprotease 10) undergoes rapid, postlysis autocatalytic degradation. *FASEB J,* 32**,** 3560-3573.

BURSAVICH, M. G., HARRISON, B. A. & BLAIN, J. F. 2016. Gamma Secretase Modulators: New Alzheimer's Drugs on the Horizon? *J Med Chem,* 59**,** 7389-409.

BUTTERFIELD, D. A. 2018. Perspectives on Oxidative Stress in Alzheimer's Disease and Predictions of Future Research Emphases. *J Alzheimers Dis,* 64**,** S469-S479.

BUTTERFIELD, D. A. 2020. BRAIN LIPID PEROXIDATION AND ALZHEIMER DISEASE: SYNERGY BETWEEN THE BUTTERFIELD AND MATTSON LABORATORIES. *Ageing Res Rev***,** 101049.

BUTTERFIELD, D. A. & BOYD-KIMBALL, D. 2018a. Oxidative Stress, Amyloid-β Peptide, and Altered Key Molecular Pathways in the Pathogenesis and Progression of Alzheimer's Disease. *J Alzheimers Dis,* 62**,** 1345-1367.

BUTTERFIELD, D. A. & BOYD-KIMBALL, D. 2018b. Redox proteomics and amyloid β-peptide: insights into Alzheimer disease. *J Neurochem*.

BUTTERFIELD, D. A. & HALLIWELL, B. 2019. Oxidative stress, dysfunctional glucose metabolism and Alzheimer disease. *Nat Rev Neurosci,* 20**,** 148-160.

BUTTERFIELD, D. A., PERLUIGI, M. & SULTANA, R. 2006a. Oxidative stress in Alzheimer's disease brain: new insights from redox proteomics. *Eur J Pharmacol,* 545**,** 39-50.

BUTTERFIELD, D. A., REED, T., PERLUIGI, M., DE MARCO, C., COCCIA, R., CINI, C. & SULTANA, R. 2006b. Elevated protein-bound levels of the lipid peroxidation product, 4-hydroxy-

2-nonenal, in brain from persons with mild cognitive impairment. *Neurosci Lett,* 397**,** 170-3.

CABRAL, D. F., RICE, J., MORRIS, T. P., RUNDEK, T., PASCUAL-LEONE, A. & GOMES-OSMAN, J. 2019. Exercise for Brain Health: An Investigation into the Underlying Mechanisms Guided by Dose. *Neurotherapeutics,* 16**,** 580-599.

CAETANO, F. A., BERALDO, F. H., HAJJ, G. N., GUIMARAES, A. L., JÜRGENSEN, S., WASILEWSKA-SAMPAIO, A. P., HIRATA, P. H., SOUZA, I., MACHADO, C. F., WONG, D. Y., DE FELICE, F. G., FERREIRA, S. T., PRADO, V. F., RYLETT, R. J., MARTINS, V. R. & PRADO, M. A. 2011. Amyloid-beta oligomers increase the localization of prion protein at the cell surface. *J Neurochem,* 117**,** 538-53.

CAI, H., WANG, Y., MCCARTHY, D., WEN, H., BORCHELT, D. R., PRICE, D. L. & WONG, P. C. 2001. BACE1 is the major beta-secretase for generation of Abeta peptides by neurons. *Nat Neurosci,* 4**,** 233-4.

CAILLET-BOUDIN, M. L., BUÉE, L., SERGEANT, N. & LEFEBVRE, B. 2015. Regulation of human MAPT gene expression. *Mol Neurodegener,* 10**,** 28.

CALDWELL, C. C., YAO, J. & BRINTON, R. D. 2015. Targeting the prodromal stage of Alzheimer's disease: bioenergetic and mitochondrial opportunities. *Neurotherapeutics,* 12**,** 66-80.

CALEYACHETTY, R., THOMAS, G. N., TOULIS, K. A., MOHAMMED, N., GOKHALE, K. M., BALACHANDRAN, K. & NIRANTHARAKUMAR, K. 2017. Metabolically Healthy Obese and Incident Cardiovascular Disease Events Among 3.5 Million Men and Women. *J Am Coll Cardiol,* 70**,** 1429-1437.

CALVO-RODRIGUEZ, M., HERNANDO-PEREZ, E., NUÑEZ, L. & VILLALOBOS, C. 2019. Amyloid β Oligomers Increase ER-Mitochondria Ca. *Front Cell Neurosci,* 13**,** 22.

CAMFIELD, D. A., NOLIDIN, K., SAVAGE, K., TIMMER, J., CROFT, K., TANGESTANI FARD, M., SIMPSON, T., DOWNEY, L., SCHOLEY, A., PIPINGAS, A., DELEUIL, S. & STOUGH, C. 2019. Higher plasma levels of F. *Free Radic Res,* 53**,** 377-386.

CAO, K., DONG, Y. T., XIANG, J., XU, Y., HONG, W., SONG, H. & GUAN, Z. Z. 2018. Reduced expression of SIRT1 and SOD-1 and the correlation between these levels in various regions of the brains of patients with Alzheimer's disease. *J Clin Pathol,* 71**,** 1090-1099.

CARROLL, C. M. & LI, Y. M. 2016. Physiological and pathological roles of the γ-secretase complex. *Brain Res Bull,* 126**,** 199-206.

CARSWELL, C. J., WIN, Z., MUCKLE, K., KENNEDY, A., WALDMAN, A., DAWE, G., BARWICK, T. D., KHAN, S., MALHOTRA, P. A. & PERRY, R. J. 2018. Clinical utility of amyloid PET imaging with (18)F-florbetapir: a retrospective study of 100 patients. *J Neurol Neurosurg Psychiatry,* 89**,** 294-299.

CARTY, J. L., BEVAN, R., WALLER, H., MISTRY, N., COOKE, M., LUNEC, J. & GRIFFITHS, H. R. 2000. The effects of vitamin C supplementation on protein oxidation in healthy volunteers. *Biochem Biophys Res Commun,* 273**,** 729-35.

CASELLI, R. J., WALKER, D., SUE, L., SABBAGH, M. & BEACH, T. 2010. Amyloid load in nondemented brains correlates with APOE e4. *Neurosci Lett,* 473**,** 168-71.

CASTILLO-MORALES, A., MONZÓN-SANDOVAL, J., URRUTIA, A. O. & GUTIÉRREZ, H. 2019. Postmitotic cell longevity-associated genes: a transcriptional signature of postmitotic maintenance in neural tissues. *Neurobiol Aging,* 74**,** 147-160.

CHAMBERS, S. M., FASANO, C. A., PAPAPETROU, E. P., TOMISHIMA, M., SADELAIN, M. & STUDER, L. 2009. Highly efficient neural conversion of human ES and iPS cells by dual inhibition of SMAD signaling. *Nat Biotechnol,* 27**,** 275-80.

CHANG, C. C., LEE, C. T., LAN, T. H., JU, P. C., HSIEH, Y. H. & LAI, T. J. 2015. Effects of antidepressant treatment on total antioxidant capacity and free radical levels in patients with major depressive disorder. *Psychiatry Res,* 230**,** 575-80.

CHARTIER-HARLIN, M. C., CRAWFORD, F., HOULDEN, H., WARREN, A., HUGHES, D., FIDANI, L., GOATE, A., ROSSOR, M., ROQUES, P. & HARDY, J. 1991. Early-onset Alzheimer's disease caused by mutations at codon 717 of the beta-amyloid precursor protein gene. *Nature,* 353**,** 844-6.

CHATTERJEE, P., ELMI, M., GOOZEE, K., SHAH, T., SOHRABI, H. R., DIAS, C. B., PEDRINI, S., SHEN, K., ASIH, P. R., DAVE, P., TADDEI, K., VANDERSTICHELE, H., ZETTERBERG, H., BLENNOW, K. & MARTINS, R. N. 2019. Ultrasensitive Detection of Plasma Amyloid-β as a Biomarker for Cognitively Normal Elderly Individuals at Risk of Alzheimer's Disease. *J Alzheimers Dis,* 71**,** 775-783.

CHAUDHURY, S., BROOKES, K. J., PATEL, T., FALLOWS, A., GUETTA-BARANES, T., TURTON, J. C., GUERREIRO, R., BRAS, J., HARDY, J., FRANCIS, P. T., CROUCHER, R., HOLMES, C., MORGAN, K. & THOMAS, A. J. 2019. Alzheimer's disease polygenic risk score as a predictor of conversion from mild-cognitive impairment. *Transl Psychiatry,* 9**,** 154.

CHEIGNON, C., TOMAS, M., BONNEFONT-ROUSSELOT, D., FALLER, P., HUREAU, C. & COLLIN, F. 2018. Oxidative stress and the amyloid beta peptide in Alzheimer's disease. *Redox Biol,* 14**,** 450-464.

CHEN, A. C., KIM, S., SHEPARDSON, N., PATEL, S., HONG, S. & SELKOE, D. J. 2015. Physical and functional interaction between the α- and γ-secretases: A new model of regulated intramembrane proteolysis. *J Cell Biol,* 211**,** 1157-76.

CHEN, G. F., XU, T. H., YAN, Y., ZHOU, Y. R., JIANG, Y., MELCHER, K. & XU, H. E. 2017. Amyloid beta: structure, biology and structure-based therapeutic development. *Acta Pharmacol Sin,* 38**,** 1205-1235.

CHENG, Y. & BAI, F. 2018. The Association of Tau With Mitochondrial Dysfunction in Alzheimer's Disease. *Front Neurosci,* 12**,** 163.

CHO, Y. Y., KWON, O. H., PARK, M. K., KIM, T. W. & CHUNG, S. 2019. Elevated cellular cholesterol in Familial Alzheimer's presenilin 1 mutation is associated with lipid raft localization of β-amyloid precursor protein. *PLoS One,* 14**,** e0210535.

CHOW, V. W., MATTSON, M. P., WONG, P. C. & GLEICHMANN, M. 2010. An overview of APP processing enzymes and products. *Neuromolecular Med,* 12**,** 1-12.

CHUANG, Y. F., AN, Y., BILGEL, M., WONG, D. F., TRONCOSO, J. C., O'BRIEN, R. J., BREITNER, J. C., FERRUCI, L., RESNICK, S. M. & THAMBISETTY, M. 2016. Midlife adiposity predicts earlier onset of Alzheimer's dementia, neuropathology and presymptomatic cerebral amyloid accumulation. *Mol Psychiatry,* 21**,** 910-5.

CHUN, Y. S., KWON, O. H., OH, H. G., KIM, T. W., MCINTIRE, L. B., PARK, M. K. & CHUNG, S. 2015a. Threonine 576 residue of amyloid-β precursor protein regulates its trafficking and processing. *Biochem Biophys Res Commun,* 467**,** 955-60.

CHUN, Y. S., PARK, Y., OH, H. G., KIM, T. W., YANG, H. O., PARK, M. K. & CHUNG, S. 2015b. O-GlcNAcylation promotes non-amyloidogenic processing of amyloid-β protein

precursor via inhibition of endocytosis from the plasma membrane. *J Alzheimers Dis,* 44**,** 261-75.

CIABATTONI, G., PORRECA, E., DI FEBBO, C., DI IORIO, A., PAGANELLI, R., BUCCIARELLI, T., PESCARA, L., DEL RE, L., GIUSTI, C., FALCO, A., SAU, A., PATRONO, C. & DAVÌ, G. 2007. Determinants of platelet activation in Alzheimer's disease. *Neurobiol Aging,* 28**,** 336-42.

CIRRITO, J. R., DISABATO, B. M., RESTIVO, J. L., VERGES, D. K., GOEBEL, W. D., SATHYAN, A., HAYREH, D., D'ANGELO, G., BENZINGER, T., YOON, H., KIM, J., MORRIS, J. C., MINTUN, M. A. & SHELINE, Y. I. 2011. Serotonin signaling is associated with lower amyloid-β levels and plaques in transgenic mice and humans. *Proc Natl Acad Sci U S A,* 108**,** 14968-73.

CLARK, R. F., HUTTON, M., FULDNER, R. A., FROELICH, S., KARRAN, E., TALBOT, C. & CROOK R, L. C., PRIHAR G, HE C, KORENBLAT K, MARTINEZ A, WRAGG M, BUSFIELD F, BEHRENS MI, MYERS A, NORTON J, MORRIS J, MEHTA N, PEARSON C, LINCOLN S, BAKER M, DUFF K, ZEHR C, PEREZ-TUR J, HOULDEN H, RUIZ A, OSSA J, LOPERA F, ARCOS M, MADRIGAL L, COLLINGE J, HUMPHREYS C, ASHWORTH A, SARNER S, FOX N, HARVEY R, KENNEDY A, ROQUES P, CLINE RT, PHILLIPS CA, VENTER JC, FORSELL L, AXELMAN K, LILIUS L, JOHNSTON J, COWBURN R, VITANEN M, WINBLAD B, KOSIK K, HALTIA M, POYHONEN M, DICKSON D, MANN D, NEARY D, SNOWDEN J, LANTOS P, LANNFELT L, ROSSOR M, ROBERTS GW, ADAMS MD, HARDY J, GOATE A. 1995. The structure of the presenilin 1 (S182) gene and identification of six novel mutations in early onset AD families. *Nat Genet,* 11**,** 219-22.

COCHET, M., DONNEGER, R., CASSIER, E., GAVEN, F., LICHTENTHALER, S. F., MARIN, P., BOCKAERT, J., DUMUIS, A. & CLAEYSEN, S. 2013. 5-HT4 receptors constitutively promote the non-amyloidogenic pathway of APP cleavage and interact with ADAM10. *ACS Chem Neurosci,* 4**,** 130-40.

COLCIAGHI, F., BORRONI, B., PASTORINO, L., MARCELLO, E., ZIMMERMANN, M., CATTABENI, F., PADOVANI, A. & DI LUCA, M. 2002. [alpha]-Secretase ADAM10 as well as [alpha]APPs is reduced in platelets and CSF of Alzheimer disease patients. *Mol Med,* 8**,** 67-74.

COLCIAGHI, F., MARCELLO, E., BORRONI, B., ZIMMERMANN, M., CALTAGIRONE, C., CATTABENI, F., PADOVANI, A. & DI LUCA, M. 2004. Platelet APP, ADAM 10 and BACE alterations in the early stages of Alzheimer disease. *Neurology,* 62**,** 498-501.

COLE, S. L. & VASSAR, R. 2007. The Alzheimer's disease beta-secretase enzyme, BACE1. *Mol Neurodegener,* 2**,** 22.

CONRAD, C. C., MARSHALL, P. L., TALENT, J. M., MALAKOWSKY, C. A., CHOI, J. & GRACY, R. W. 2000. Oxidized proteins in Alzheimer's plasma. *Biochem Biophys Res Commun,* 275**,** 678-81.

CORDER, E. H., SAUNDERS, A. M., STRITTMATTER, W. J., SCHMECHEL, D. E., GASKELL, P. C., SMALL, G. W., ROSES, A. D., HAINES, J. L. & PERICAK-VANCE, M. A. 1993. Gene dose of apolipoprotein E type 4 allele and the risk of Alzheimer's disease in late onset families. *Science,* 261**,** 921-3.

CORONEL, R., LACHGAR, M., BERNABEU-ZORNOZA, A., PALMER, C., DOMÍNGUEZ-ALVARO, M., REVILLA, A., OCAÑA, I., FERNÁNDEZ, A., MARTÍNEZ-SERRANO, A., CANO, E. &

LISTE, I. 2019. Neuronal and Glial Differentiation of Human Neural Stem Cells Is Regulated by Amyloid Precursor Protein (APP) Levels. *Mol Neurobiol,* 56**,** 1248-1261.
CORRADA, M. M., BROOKMEYER, R., BERLAU, D., PAGANINI-HILL, A. & KAWAS, C. H. 2008. Prevalence of dementia after age 90: results from the 90+ study. *Neurology,* 71**,** 337-43.
COWAN, C. A., ATIENZA, J., MELTON, D. A. & EGGAN, K. 2005. Nuclear reprogramming of somatic cells after fusion with human embryonic stem cells. *Science,* 309**,** 1369-73.
DALE, E., PEHRSON, A. L., JEYARAJAH, T., LI, Y., LEISER, S. C., SMAGIN, G., OLSEN, C. K. & SANCHEZ, C. 2016. Effects of serotonin in the hippocampus: how SSRIs and multimodal antidepressants might regulate pyramidal cell function. *CNS Spectr,* 21**,** 143-61.
DARCET, F., GARDIER, A. M., DAVID, D. J. & GUILLOUX, J. P. 2016. Chronic 5-HT4 receptor agonist treatment restores learning and memory deficits in a neuroendocrine mouse model of anxiety/depression. *Neurosci Lett,* 616**,** 197-203.
DAS, U., SCOTT, D. A., GANGULY, A., KOO, E. H., TANG, Y. & ROY, S. 2013. Activity-induced convergence of APP and BACE-1 in acidic microdomains via an endocytosis-dependent pathway. *Neuron,* 79**,** 447-60.
DAY, G. S., MUSIEK, E. S., ROE, C. M., NORTON, J., GOATE, A. M., CRUCHAGA, C., CAIRNS, N. J. & MORRIS, J. C. 2016. Phenotypic Similarities Between Late-Onset Autosomal Dominant and Sporadic Alzheimer Disease: A Single-Family Case-Control Study. *JAMA Neurol,* 73**,** 1125-32.
DE ANTONIO CORRADI, M., LISBOA, A. B. & FRAGUAS JUNIOR, R. 2017. Inflammatory markers as predictive factors for selective serotonin reuptake inhibitors (SSRI) antidepressant effect. Revista de Medicina.
DE DEURWAERDÈRE, P., BHARATIYA, R., CHAGRAOUI, A. & DI GIOVANNI, G. 2020. Constitutive activity of 5-HT receptors: Factual analysis. *Neuropharmacology***,** 107967.
DE JAGER, C. A., HONEY, T. E., BIRKS, J. & WILCOCK, G. K. 2010. Retrospective evaluation of revised criteria for the diagnosis of Alzheimer's disease using a cohort with post-mortem diagnosis. *Int J Geriatr Psychiatry,* 25**,** 988-97.
DE STROOPER, B. 2007. Loss-of-function presenilin mutations in Alzheimer disease. Talking Point on the role of presenilin mutations in Alzheimer disease. *EMBO Rep,* 8**,** 141-6.
DE STROOPER, B. 2014. Lessons from a failed γ-secretase Alzheimer trial. *Cell,* 159**,** 721-6.
DEL TREDICI, K. & BRAAK, H. 2019. To stage, or not to stage. *Curr Opin Neurobiol,* 61**,** 10-22.
DEL-FAVERO, J., GOOSSENS, D., VAN DEN BOSSCHE, D. & VAN BROECKHOVEN, C. 1999. YAC fragmentation with repetitive and single-copy sequences: detailed physical mapping of the presenilin 1 gene on chromosome 14. *Gene,* 229**,** 193-201.
DENG, J., HABIB, A., OBREGON, D. F., BARGER, S. W., GIUNTA, B., WANG, Y. J., HOU, H., SAWMILLER, D. & TAN, J. 2015. Soluble amyloid precursor protein alpha inhibits tau phosphorylation through modulation of GSK3β signaling pathway. *J Neurochem,* 135**,** 630-7.
DETURE, M. A. & DICKSON, D. W. 2019. The neuropathological diagnosis of Alzheimer's disease. *Mol Neurodegener,* 14**,** 32.

DI DOMENICO, F., COCCIA, R., BUTTERFIELD, D. A. & PERLUIGI, M. 2011. Circulating biomarkers of protein oxidation for Alzheimer disease: expectations within limits. *Biochim Biophys Acta,* 1814**,** 1785-95.

DI DOMENICO, F., TRAMUTOLA, A. & BUTTERFIELD, D. A. 2017. Role of 4-hydroxy-2-nonenal (HNE) in the pathogenesis of alzheimer disease and other selected age-related neurodegenerative disorders. *Free Radic Biol Med,* 111**,** 253-261.

DOAN, N. T., ENGVIG, A., ZASKE, K., PERSSON, K., LUND, M. J., KAUFMANN, T., CORDOVA-PALOMERA, A., ALNÆS, D., MOBERGET, T., BRÆKHUS, A., BARCA, M. L., NORDVIK, J. E., ENGEDAL, K., AGARTZ, I., SELBÆK, G., ANDREASSEN, O. A., WESTLYE, L. T. & INITIATIVE, A. S. D. N. 2017. Distinguishing early and late brain aging from the Alzheimer's disease spectrum: consistent morphological patterns across independent samples. *Neuroimage,* 158**,** 282-295.

DONG, A., TOLEDO, J. B., HONNORAT, N., DOSHI, J., VAROL, E., SOTIRAS, A., WOLK, D., TROJANOWSKI, J. Q., DAVATZIKOS, C. & INITIATIVE, A. S. D. N. 2017. Heterogeneity of neuroanatomical patterns in prodromal Alzheimer's disease: links to cognition, progression and biomarkers. *Brain,* 140**,** 735-747.

DOODY, R. S., RAMAN, R., FARLOW, M., IWATSUBO, T., VELLAS, B., JOFFE, S., KIEBURTZ, K., HE, F., SUN, X., THOMAS, R. G., AISEN, P. S., SIEMERS, E., SETHURAMAN, G., MOHS, R., COMMITTEE, A. S. D. C. S. S. & GROUP, S. S. 2013. A phase 3 trial of semagacestat for treatment of Alzheimer's disease. *N Engl J Med,* 369**,** 341-50.

DORNIER, E., COUMAILLEAU, F., OTTAVI, J. F., MORETTI, J., BOUCHEIX, C., MAUDUIT, P., SCHWEISGUTH, F. & RUBINSTEIN, E. 2012. TspanC8 tetraspanins regulate ADAM10/Kuzbanian trafficking and promote Notch activation in flies and mammals. *J Cell Biol,* 199**,** 481-96.

DREWS, A., FLINT, J., SHIVJI, N., JÖNSSON, P., WIRTHENSOHN, D., DE GENST, E., VINCKE, C., MUYLDERMANS, S., DOBSON, C. & KLENERMAN, D. 2016. Individual aggregates of amyloid beta induce temporary calcium influx through the cell membrane of neuronal cells. *Sci Rep,* 6**,** 31910.

DUBOIS, B., HAMPEL, H., FELDMAN, H. H., SCHELTENS, P., AISEN, P., ANDRIEU, S., BAKARDJIAN, H., BENALI, H., BERTRAM, L., BLENNOW, K., BROICH, K., CAVEDO, E., CRUTCH, S., DARTIGUES, J. F., DUYCKAERTS, C., EPELBAUM, S., FRISONI, G. B., GAUTHIER, S., GENTHON, R., GOUW, A. A., HABERT, M. O., HOLTZMAN, D. M., KIVIPELTO, M., LISTA, S., MOLINUEVO, J. L., O'BRYANT, S. E., RABINOVICI, G. D., ROWE, C., SALLOWAY, S., SCHNEIDER, L. S., SPERLING, R., TEICHMANN, M., CARRILLO, M. C., CUMMINGS, J., JACK, C. R., AD", P. O. T. M. O. T. I. W. G. I. A. T. A. A. S. A. O. T. P. S. O., JULY 23 & WASHINGTON DC, U. S. A. 2016. Preclinical Alzheimer's disease: Definition, natural history, and diagnostic criteria. *Alzheimers Dement,* 12**,** 292-323.

DUMUIS, A., BOUHELAL, R., SEBBEN, M., CORY, R. & BOCKAERT, J. 1988. A nonclassical 5-hydroxytryptamine receptor positively coupled with adenylate cyclase in the central nervous system. *Mol Pharmacol,* 34**,** 880-7.

EDWARDS III, G. A., GAMEZ, N., ESCOBEDO, G., CALDERON, O. & MORENO-GONZALEZ, I. 2019. Modifiable Risk Factors for Alzheimer's Disease. *Front Aging Neurosci,* 11**,** 146.

EHEHALT, R., KELLER, P., HAASS, C., THIELE, C. & SIMONS, K. 2003. Amyloidogenic processing of the Alzheimer beta-amyloid precursor protein depends on lipid rafts. *J Cell Biol,* 160**,** 113-23.

ELIWA, H., BELZUNG, C. & SURGET, A. 2017. Adult hippocampal neurogenesis: Is it the alpha and omega of antidepressant action? *Biochem Pharmacol,* 141**,** 86-99.
ELSWORTHY, R. J. & ALDRED, S. 2019. Depression in Alzheimer's Disease: An Alternative Role for Selective Serotonin Reuptake Inhibitors? *J Alzheimers Dis,* 69**,** 651-661.
ELSWORTHY, R. J. & ALDRED, S. 2020. The effect of age and obesity on platelet amyloid precursor protein processing and plasma markers of oxidative stress and inflammation. *Exp Gerontol***,** 110838.
FABELO, N., MARTÍN, V., MARÍN, R., MORENO, D., FERRER, I. & DÍAZ, M. 2014. Altered lipid composition in cortical lipid rafts occurs at early stages of sporadic Alzheimer's disease and facilitates APP/BACE1 interactions. *Neurobiol Aging,* 35**,** 1801-12.
FANIBUNDA, S. E. & VAIDYA, V. A. 2020. Serotonin minting new mitochondria in cortical neurons: implications for psychopathology. *Neuropsychopharmacology*.
FERNANDEZ MONTENEGRO, J. M. & ARGYRIOU, V. 2017. Cognitive evaluation for the diagnosis of Alzheimer's disease based on Turing Test and Virtual Environments. *Physiol Behav,* 173**,** 42-51.
FERNÁNDEZ-SÁNCHEZ, A., MADRIGAL-SANTILLÁN, E., BAUTISTA, M., ESQUIVEL-SOTO, J., MORALES-GONZÁLEZ, A., ESQUIVEL-CHIRINO, C., DURANTE-MONTIEL, I., SÁNCHEZ-RIVERA, G., VALADEZ-VEGA, C. & MORALES-GONZÁLEZ, J. A. 2011. Inflammation, oxidative stress, and obesity. *Int J Mol Sci,* 12**,** 3117-32.
FERREIRA, S. T., CLARKE, J. R., BOMFIM, T. R. & DE FELICE, F. G. 2014. Inflammation, defective insulin signaling, and neuronal dysfunction in Alzheimer's disease. *Alzheimers Dement,* 10**,** S76-83.
FERRERO, J., WILLIAMS, L., STELLA, H., LEITERMANN, K., MIKULSKIS, A., O'GORMAN, J. & SEVIGNY, J. 2016. First-in-human, double-blind, placebo-controlled, single-dose escalation study of aducanumab (BIIB037) in mild-to-moderate Alzheimer's disease. *Alzheimers Dement (N Y),* 2**,** 169-176.
FERRUCCI, L. & FABBRI, E. 2018. Inflammageing: chronic inflammation in ageing, cardiovascular disease, and frailty. *Nat Rev Cardiol,* 15**,** 505-522.
FESTA, G., MALLAMACE, F., SANCESARIO, G. M., CORSARO, C., MALLAMACE, D., FAZIO, E., ARCIDIACONO, L., GARCIA SAKAI, V., SENESI, R., PREZIOSI, E., SANCESARIO, G. & ANDREANI, C. 2019. Aggregation States of A. *Int J Mol Sci,* 20.
FILOMENI, G., DE ZIO, D. & CECCONI, F. 2015. Oxidative stress and autophagy: the clash between damage and metabolic needs. *Cell Death Differ,* 22**,** 377-88.
FINDER, V. H., VODOPIVEC, I., NITSCH, R. M. & GLOCKSHUBER, R. 2010. The recombinant amyloid-beta peptide Abeta1-42 aggregates faster and is more neurotoxic than synthetic Abeta1-42. *J Mol Biol,* 396**,** 9-18.
FISHER, J. R., WALLACE, C. E., TRIPOLI, D. L., SHELINE, Y. I. & CIRRITO, J. R. 2016. Redundant Gs-coupled serotonin receptors regulate amyloid-β metabolism in vivo. *Mol Neurodegener,* 11**,** 45.
FIŠAR, Z., HANSÍKOVÁ, H., KŘÍŽOVÁ, J., JIRÁK, R., KITZLEROVÁ, E., ZVĚŘOVÁ, M., HROUDOVÁ, J., WENCHICH, L., ZEMAN, J. & RABOCH, J. 2019. Activities of mitochondrial respiratory chain complexes in platelets of patients with Alzheimer's disease and depressive disorder. *Mitochondrion,* 48**,** 67-77.

FOLSTEIN, M. F., FOLSTEIN, S. E. & MCHUGH, P. R. 1975. "Mini-mental state". A practical method for grading the cognitive state of patients for the clinician. *J Psychiatr Res,* 12**,** 189-98.

FORLONI, G. & BALDUCCI, C. 2018. Alzheimer's Disease, Oligomers, and Inflammation. *J Alzheimers Dis,* 62**,** 1261-1276.

FORNY-GERMANO, L., DE FELICE, F. G. & VIEIRA, M. N. D. N. 2018. The Role of Leptin and Adiponectin in Obesity-Associated Cognitive Decline and Alzheimer's Disease. *Front Neurosci,* 12**,** 1027.

FORRESTER, S. J., KIKUCHI, D. S., HERNANDES, M. S., XU, Q. & GRIENDLING, K. K. 2018. Reactive Oxygen Species in Metabolic and Inflammatory Signaling. *Circ Res,* 122**,** 877-902.

FRISONI, G. B., BOCCARDI, M., BARKHOF, F., BLENNOW, K., CAPPA, S., CHIOTIS, K., DÉMONET, J. F., GARIBOTTO, V., GIANNAKOPOULOS, P., GIETL, A., HANSSON, O., HERHOLZ, K., JACK, C. R., NOBILI, F., NORDBERG, A., SNYDER, H. M., TEN KATE, M., VARRONE, A., ALBANESE, E., BECKER, S., BOSSUYT, P., CARRILLO, M. C., CERAMI, C., DUBOIS, B., GALLO, V., GIACOBINI, E., GOLD, G., HURST, S., LÖNNEBORG, A., LOVBLAD, K. O., MATTSSON, N., MOLINUEVO, J. L., MONSCH, A. U., MOSIMANN, U., PADOVANI, A., PICCO, A., PORTERI, C., RATIB, O., SAINT-AUBERT, L., SCERRI, C., SCHELTENS, P., SCHOTT, J. M., SONNI, I., TEIPEL, S., VINEIS, P., VISSER, P. J., YASUI, Y. & WINBLAD, B. 2017. Strategic roadmap for an early diagnosis of Alzheimer's disease based on biomarkers. *Lancet Neurol,* 16**,** 661-676.

FRISONI, G. B., FOX, N. C., JACK, C. R., SCHELTENS, P. & THOMPSON, P. M. 2010. The clinical use of structural MRI in Alzheimer disease. *Nat Rev Neurol,* 6**,** 67-77.

FROMMELT, P., SCHNABEL, R., KÜHNE, W., NEE, L. E. & POLINSKY, R. J. 1991. Familial Alzheimer disease: a large, multigeneration German kindred. *Alzheimer Dis Assoc Disord,* 5**,** 36-43.

FULOP, T., LARBI, A., DUPUIS, G., LE PAGE, A., FROST, E. H., COHEN, A. A., WITKOWSKI, J. M. & FRANCESCHI, C. 2017. Immunosenescence and Inflamm-Aging As Two Sides of the Same Coin: Friends or Foes? *Front Immunol,* 8**,** 1960.

GABR, M. T. & ABDEL-RAZIQ, M. S. 2018. Design and synthesis of donepezil analogues as dual AChE and BACE-1 inhibitors. *Bioorg Chem,* 80**,** 245-252.

GAMBA, P., STAURENGHI, E., TESTA, G., GIANNELLI, S., SOTTERO, B. & LEONARDUZZI, G. 2019. A Crosstalk Between Brain Cholesterol Oxidation and Glucose Metabolism in Alzheimer's Disease. *Front Neurosci,* 13**,** 556.

GARIBOTTO, V., HERHOLZ, K., BOCCARDI, M., PICCO, A., VARRONE, A., NORDBERG, A., NOBILI, F., RATIB, O. & BIOMARKERS, G. T. F. F. T. R. O. A. S. 2017. Clinical validity of brain fluorodeoxyglucose positron emission tomography as a biomarker for Alzheimer's disease in the context of a structured 5-phase development framework. *Neurobiol Aging,* 52**,** 183-195.

GARWOOD, C. J., RATCLIFFE, L. E., SIMPSON, J. E., HEATH, P. R., INCE, P. G. & WHARTON, S. B. 2017. Review: Astrocytes in Alzheimer's disease and other age-associated dementias: a supporting player with a central role. *Neuropathol Appl Neurobiol,* 43**,** 281-298.

GAŁECKI, P., MOSSAKOWSKA-WÓJCIK, J. & TALAROWSKA, M. 2018. The anti-inflammatory mechanism of antidepressants - SSRIs, SNRIs. *Prog Neuropsychopharmacol Biol Psychiatry,* 80**,** 291-294.

GELDENHUYS, W. J. & VAN DER SCHYF, C. J. 2011. Role of serotonin in Alzheimer's disease: a new therapeutic target? *CNS Drugs,* 25**,** 765-81.

GHIDONI, R., SQUITTI, R., SIOTTO, M. & BENUSSI, L. 2018. Innovative Biomarkers for Alzheimer's Disease: Focus on the Hidden Disease Biomarkers. *J Alzheimers Dis,* 62**,** 1507-1518.

GLENNER, G. G. & WONG, C. W. 1984. Alzheimer's disease: initial report of the purification and characterization of a novel cerebrovascular amyloid protein. *Biochem Biophys Res Commun,* 120**,** 885-90.

GOATE, A. & HARDY, J. 2012. Twenty years of Alzheimer's disease-causing mutations. *J Neurochem,* 120 Suppl 1**,** 3-8.

GODBOLT, A. K., BECK, J. A., COLLINGE, J., GARRARD, P., WARREN, J. D., FOX, N. C. & ROSSOR, M. N. 2004. A presenilin 1 R278I mutation presenting with language impairment. *Neurology,* 63**,** 1702-4.

GOODGER, Z. V., RAJENDRAN, L., TRUTZEL, A., KOHLI, B. M., NITSCH, R. M. & KONIETZKO, U. 2009. Nuclear signaling by the APP intracellular domain occurs predominantly through the amyloidogenic processing pathway. *J Cell Sci,* 122**,** 3703-14.

GRALLE, M., OLIVEIRA, C. L., GUERREIRO, L. H., MCKINSTRY, W. J., GALATIS, D., MASTERS, C. L., CAPPAI, R., PARKER, M. W., RAMOS, C. H., TORRIANI, I. & FERREIRA, S. T. 2006. Solution conformation and heparin-induced dimerization of the full-length extracellular domain of the human amyloid precursor protein. *J Mol Biol,* 357**,** 493-508.

GREEN, D. J. & SMITH, K. J. 2018. Effects of Exercise on Vascular Function, Structure, and Health in Humans. *Cold Spring Harb Perspect Med,* 8.

GREILBERGER, J., FUCHS, D., LEBLHUBER, F., GREILBERGER, M., WINTERSTEIGER, R. & TAFEIT, E. 2010. Carbonyl proteins as a clinical marker in Alzheimer's disease and its relation to tryptophan degradation and immune activation. *Clin Lab,* 56**,** 441-8.

GULISANO, W., MAUGERI, D., BALTRONS, M. A., FÀ, M., AMATO, A., PALMERI, A., D'ADAMIO, L., GRASSI, C., DEVANAND, D. P., HONIG, L. S., PUZZO, D. & ARANCIO, O. 2018. Role of Amyloid-β and Tau Proteins in Alzheimer's Disease: Confuting the Amyloid Cascade. *J Alzheimers Dis,* 64**,** S611-S631.

GUNHANLAR, N., SHPAK, G., VAN DER KROEG, M., GOUTY-COLOMER, L. A., MUNSHI, S. T., LENDEMEIJER, B., GHAZVINI, M., DUPONT, C., HOOGENDIJK, W. J. G., GRIBNAU, J., DE VRIJ, F. M. S. & KUSHNER, S. A. 2018. A simplified protocol for differentiation of electrophysiologically mature neuronal networks from human induced pluripotent stem cells. *Mol Psychiatry,* 23**,** 1336-1344.

GUPTA, M., NEAVIN, D., LIU, D., BIERNACKA, J., HALL-FLAVIN, D., BOBO, W. V., FRYE, M. A., SKIME, M., JENKINS, G. D., BATZLER, A., KALARI, K., MATSON, W., BHASIN, S. S., ZHU, H., MUSHIRODA, T., NAKAMURA, Y., KUBO, M., WANG, L., KADDURAH-DAOUK, R. & WEINSHILBOUM, R. M. 2016. TSPAN5, ERICH3 and selective serotonin reuptake inhibitors in major depressive disorder: pharmacometabolomics-informed pharmacogenomics. *Mol Psychiatry,* 21**,** 1717-1725.

GURDON, J. B., ELSDALE, T. R. & FISCHBERG, M. 1958. Sexually mature individuals of Xenopus laevis from the transplantation of single somatic nuclei. *Nature,* 182**,** 64-5.
GUZIK, T. J. & TOUYZ, R. M. 2017. Oxidative Stress, Inflammation, and Vascular Aging in Hypertension. *Hypertension,* 70**,** 660-667.
GÜNER, G. & LICHTENTHALER, S. F. 2020. The substrate repertoire of γ-secretase/presenilin. *Semin Cell Dev Biol,* 105**,** 27-42.
HAASE, J. & BROWN, E. 2015. Integrating the monoamine, neurotrophin and cytokine hypotheses of depression--a central role for the serotonin transporter? *Pharmacol Ther,* 147**,** 1-11.
HAASS, C., KAETHER, C., THINAKARAN, G. & SISODIA, S. 2012. Trafficking and proteolytic processing of APP. *Cold Spring Harb Perspect Med,* 2**,** a006270.
HAASS, C. & SELKOE, D. J. 2007. Soluble protein oligomers in neurodegeneration: lessons from the Alzheimer's amyloid beta-peptide. *Nat Rev Mol Cell Biol,* 8**,** 101-12.
HAGENA, H. & MANAHAN-VAUGHAN, D. 2017. The serotonergic 5-HT4 receptor: A unique modulator of hippocampal synaptic information processing and cognition. *Neurobiol Learn Mem,* 138**,** 145-153.
HALLER, S., MONTANDON, M. L., RODRIGUEZ, C., GARIBOTTO, V., LILJA, J., HERRMANN, F. R. & GIANNAKOPOULOS, P. 2019. Amyloid Load, Hippocampal Volume Loss, and Diffusion Tensor Imaging Changes in Early Phases of Brain Aging. *Front Neurosci,* 13**,** 1228.
HALLIDAY, G. 2017. Pathology and hippocampal atrophy in Alzheimer's disease. *Lancet Neurol,* 16**,** 862-864.
HALLIKAINEN, I., HONGISTO, K., VÄLIMÄKI, T., HÄNNINEN, T., MARTIKAINEN, J. & KOIVISTO, A. M. 2018. The Progression of Neuropsychiatric Symptoms in Alzheimer's Disease During a Five-Year Follow-Up: Kuopio ALSOVA Study. *J Alzheimers Dis,* 61**,** 1367-1376.
HANSSON, O., LEHMANN, S., OTTO, M., ZETTERBERG, H. & LEWCZUK, P. 2019. Advantages and disadvantages of the use of the CSF Amyloid β (Aβ) 42/40 ratio in the diagnosis of Alzheimer's Disease. *Alzheimers Res Ther,* 11**,** 34.
HARDY, J. A. & HIGGINS, G. A. 1992. Alzheimer's disease: the amyloid cascade hypothesis. *Science,* 256**,** 184-5.
HARMAN, D. 1992. Free radical theory of aging. *Mutat Res,* 275**,** 257-66.
HAUCK, A. K., HUANG, Y., HERTZEL, A. V. & BERNLOHR, D. A. 2019. Adipose oxidative stress and protein carbonylation. *J Biol Chem,* 294**,** 1083-1088.
HAWKINS, K. E. & DUCHEN, M. 2019. Modelling mitochondrial dysfunction in Alzheimer's disease using human induced pluripotent stem cells. *World J Stem Cells,* 11**,** 236-253.
HENEKA, M. T., CARSON, M. J., EL KHOURY, J., LANDRETH, G. E., BROSSERON, F., FEINSTEIN, D. L., JACOBS, A. H., WYSS-CORAY, T., VITORICA, J., RANSOHOFF, R. M., HERRUP, K., FRAUTSCHY, S. A., FINSEN, B., BROWN, G. C., VERKHRATSKY, A., YAMANAKA, K., KOISTINAHO, J., LATZ, E., HALLE, A., PETZOLD, G. C., TOWN, T., MORGAN, D., SHINOHARA, M. L., PERRY, V. H., HOLMES, C., BAZAN, N. G., BROOKS, D. J., HUNOT, S., JOSEPH, B., DEIGENDESCH, N., GARASCHUK, O., BODDEKE, E., DINARELLO, C. A., BREITNER, J. C., COLE, G. M., GOLENBOCK, D. T. & KUMMER, M. P. 2015. Neuroinflammation in Alzheimer's disease. *Lancet Neurol,* 14**,** 388-405.

HENLEY, D. B., SUNDELL, K. L., SETHURAMAN, G., DOWSETT, S. A. & MAY, P. C. 2014. Safety profile of semagacestat, a gamma-secretase inhibitor: IDENTITY trial findings. *Curr Med Res Opin,* 30**,** 2021-32.

HICK, M., HERRMANN, U., WEYER, S. W., MALLM, J. P., TSCHÄPE, J. A., BORGERS, M., MERCKEN, M., ROTH, F. C., DRAGUHN, A., SLOMIANKA, L., WOLFER, D. P., KORTE, M. & MÜLLER, U. C. 2015. Acute function of secreted amyloid precursor protein fragment APPsα in synaptic plasticity. *Acta Neuropathol,* 129**,** 21-37.

HILL, E., NAGEL, D., PARRI, R. & COLEMAN, M. 2016. Stem cell-derived astrocytes: are they physiologically credible? *J Physiol,* 594**,** 6595-6606.

HILLS, I. D. & VACCA, J. P. 2007. Progress toward a practical BACE-1 inhibitor. *Curr Opin Drug Discov Devel,* 10**,** 383-91.

HOFFMANN, J., TWIESSELMANN, C., KUMMER, M. P., ROMAGNOLI, P. & HERZOG, V. 2000. A possible role for the Alzheimer amyloid precursor protein in the regulation of epidermal basal cell proliferation. *Eur J Cell Biol,* 79**,** 905-14.

HONG, S., OSTASZEWSKI, B. L., YANG, T., O'MALLEY, T. T., JIN, M., YANAGISAWA, K., LI, S., BARTELS, T. & SELKOE, D. J. 2014. Soluble Aβ oligomers are rapidly sequestered from brain ISF in vivo and bind GM1 ganglioside on cellular membranes. *Neuron,* 82**,** 308-19.

HONIG, L. S., VELLAS, B., WOODWARD, M., BOADA, M., BULLOCK, R., BORRIE, M., HAGER, K., ANDREASEN, N., SCARPINI, E., LIU-SEIFERT, H., CASE, M., DEAN, R. A., HAKE, A., SUNDELL, K., POOLE HOFFMANN, V., CARLSON, C., KHANNA, R., MINTUN, M., DEMATTOS, R., SELZLER, K. J. & SIEMERS, E. 2018. Trial of Solanezumab for Mild Dementia Due to Alzheimer's Disease. *N Engl J Med,* 378**,** 321-330.

HOSSEINI, B., SAEDISOMEOLIA, A. & ALLMAN-FARINELLI, M. 2017. Association Between Antioxidant Intake/Status and Obesity: a Systematic Review of Observational Studies. *Biol Trace Elem Res,* 175**,** 287-297.

HOSSINI, A. M., MEGGES, M., PRIGIONE, A., LICHTNER, B., TOLIAT, M. R., WRUCK, W., SCHRÖTER, F., NUERNBERG, P., KROLL, H., MAKRANTONAKI, E., ZOUBOULIS, C. C., ZOUBOULISS, C. C. & ADJAYE, J. 2015. Induced pluripotent stem cell-derived neuronal cells from a sporadic Alzheimer's disease donor as a model for investigating AD-associated gene regulatory networks. *BMC Genomics,* 16**,** 84.

HOU, Y., DAN, X., BABBAR, M., WEI, Y., HASSELBALCH, S. G., CROTEAU, D. L. & BOHR, V. A. 2019. Ageing as a risk factor for neurodegenerative disease. *Nat Rev Neurol,* 15**,** 565-581.

HUANG, M., LIANG, Y., CHEN, H., XU, B., CHAI, C. & XING, P. 2018. The Role of Fluoxetine in Activating Wnt/β-Catenin Signaling and Repressing β-Amyloid Production in an Alzheimer Mouse Model. *Front Aging Neurosci,* 10**,** 164.

HUANG, Y. R. & LIU, R. T. 2020. The Toxicity and Polymorphism of β-Amyloid Oligomers. *Int J Mol Sci,* 21.

HUGHES, C. P., BERG, L., DANZIGER, W. L., COBEN, L. A. & MARTIN, R. L. 1982. A new clinical scale for the staging of dementia. *Br J Psychiatry,* 140**,** 566-72.

HUGO, J. & GANGULI, M. 2014. Dementia and cognitive impairment: epidemiology, diagnosis, and treatment. *Clin Geriatr Med,* 30**,** 421-42.

HUNG, S. Y. & FU, W. M. 2017. Drug candidates in clinical trials for Alzheimer's disease. *J Biomed Sci,* 24**,** 47.

IQBAL, K., ALONSO, A. E. C., CHEN, S., CHOHAN, M. O., EL-AKKAD, E., GONG, C. X., KHATOON, S., LI, B., LIU, F., RAHMAN, A., TANIMUKAI, H. & GRUNDKE-IQBAL, I. 2005. Tau pathology in Alzheimer disease and other tauopathies. *Biochim Biophys Acta,* 1739**,** 198-210.

ISRAEL, M. A., YUAN, S. H., BARDY, C., REYNA, S. M., MU, Y., HERRERA, C., HEFFERAN, M. P., VAN GORP, S., NAZOR, K. L., BOSCOLO, F. S., CARSON, C. T., LAURENT, L. C., MARSALA, M., GAGE, F. H., REMES, A. M., KOO, E. H. & GOLDSTEIN, L. S. 2012. Probing sporadic and familial Alzheimer's disease using induced pluripotent stem cells. *Nature,* 482**,** 216-20.

ITTNER, A. & ITTNER, L. M. 2018. Dendritic Tau in Alzheimer's Disease. *Neuron,* 99**,** 13-27.

JACKSON, P. A., PIALOUX, V., CORBETT, D., DROGOS, L., ERICKSON, K. I., ESKES, G. A. & POULIN, M. J. 2016. Promoting brain health through exercise and diet in older adults: a physiological perspective. *J Physiol,* 594**,** 4485-98.

JACOBS, K. R., LIM, C. K., BLENNOW, K., ZETTERBERG, H., CHATTERJEE, P., MARTINS, R. N., BREW, B. J., GUILLEMIN, G. J. & LOVEJOY, D. B. 2019. Correlation between plasma and CSF concentrations of kynurenine pathway metabolites in Alzheimer's disease and relationship to amyloid-β and tau. *Neurobiol Aging,* 80**,** 11-20.

JAHN, H. 2013. Memory loss in Alzheimer's disease. *Dialogues Clin Neurosci,* 15**,** 445-54.

JANELIDZE, S., STOMRUD, E., PALMQVIST, S., ZETTERBERG, H., VAN WESTEN, D., JEROMIN, A., SONG, L., HANLON, D., TAN HEHIR, C. A., BAKER, D., BLENNOW, K. & HANSSON, O. 2016. Plasma β-amyloid in Alzheimer's disease and vascular disease. *Sci Rep,* 6**,** 26801.

JANSEN, I. E., SAVAGE, J. E., WATANABE, K., BRYOIS, J., WILLIAMS, D. M., STEINBERG, S., SEALOCK, J., KARLSSON, I. K., HÄGG, S., ATHANASIU, L., VOYLE, N., PROITSI, P., WITOELAR, A., STRINGER, S., AARSLAND, D., ALMDAHL, I. S., ANDERSEN, F., BERGH, S., BETTELLA, F., BJORNSSON, S., BRÆKHUS, A., BRÅTHEN, G., DE LEEUW, C., DESIKAN, R. S., DJUROVIC, S., DUMITRESCU, L., FLADBY, T., HOHMAN, T. J., JONSSON, P. V., KIDDLE, S. J., RONGVE, A., SALTVEDT, I., SANDO, S. B., SELBÆK, G., SHOAI, M., SKENE, N. G., SNAEDAL, J., STORDAL, E., ULSTEIN, I. D., WANG, Y., WHITE, L. R., HARDY, J., HJERLING-LEFFLER, J., SULLIVAN, P. F., VAN DER FLIER, W. M., DOBSON, R., DAVIS, L. K., STEFANSSON, H., STEFANSSON, K., PEDERSEN, N. L., RIPKE, S., ANDREASSEN, O. A. & POSTHUMA, D. 2019. Genome-wide meta-analysis identifies new loci and functional pathways influencing Alzheimer's disease risk. *Nat Genet,* 51**,** 404-413.

JAROSZ-GRIFFITHS, H. H., CORBETT, N. J., ROWLAND, H. A., FISHER, K., JONES, A. C., BARON, J., HOWELL, G. J., COWLEY, S. A., CHINTAWAR, S., CADER, M. Z., KELLETT, K. A. B. & HOOPER, N. M. 2019. Proteolytic shedding of the prion protein via activation of metallopeptidase ADAM10 reduces cellular binding and toxicity of amyloid-β oligomers. *J Biol Chem,* 294**,** 7085-7097.

JEON, S. W. & KIM, Y. K. 2016. Neuroinflammation and cytokine abnormality in major depression: Cause or consequence in that illness? *World J Psychiatry,* 6**,** 283-93.

JONES, V. C., ATKINSON-DELL, R., VERKHRATSKY, A. & MOHAMET, L. 2017. Aberrant iPSC-derived human astrocytes in Alzheimer's disease. *Cell Death Dis,* 8**,** e2696.

JOUANNET, S., SAINT-POL, J., FERNANDEZ, L., NGUYEN, V., CHARRIN, S., BOUCHEIX, C., BROU, C., MILHIET, P. E. & RUBINSTEIN, E. 2016. TspanC8 tetraspanins differentially

regulate the cleavage of ADAM10 substrates, Notch activation and ADAM10 membrane compartmentalization. *Cell Mol Life Sci,* 73**,** 1895-915.

KACÍŘOVÁ, M., ZMEŠKALOVÁ, A., KOŘÍNKOVÁ, L., ŽELEZNÁ, B., KUNEŠ, J. & MALETÍNSKÁ, L. 2020. Inflammation: major denominator of obesity, Type 2 diabetes and Alzheimer's disease-like pathology? *Clin Sci (Lond),* 134**,** 547-570.

KANG, J., LEMAIRE, H. G., UNTERBECK, A., SALBAUM, J. M., MASTERS, C. L., GRZESCHIK, K. H., MULTHAUP, G., BEYREUTHER, K. & MÜLLER-HILL, B. 1987. The precursor of Alzheimer's disease amyloid A4 protein resembles a cell-surface receptor. *Nature,* 325**,** 733-6.

KATZMARSKI, N., ZIEGLER-WALDKIRCH, S., SCHEFFLER, N., WITT, C., ABOU-AJRAM, C., NUSCHER, B., PRINZ, M., HAASS, C. & MEYER-LUEHMANN, M. 2020. Aβ oligomers trigger and accelerate Aβ seeding. *Brain Pathol,* 30**,** 36-45.

KELLEHER, R. J. & SHEN, J. 2017. Presenilin-1 mutations and Alzheimer's disease. *Proc Natl Acad Sci U S A,* 114**,** 629-631.

KEMPURAJ, D., THANGAVEL, R., SELVAKUMAR, G. P., ZAHEER, S., AHMED, M. E., RAIKWAR, S. P., ZAHOOR, H., SAEED, D., NATTERU, P. A., IYER, S. & ZAHEER, A. 2017. Brain and Peripheral Atypical Inflammatory Mediators Potentiate Neuroinflammation and Neurodegeneration. *Front Cell Neurosci,* 11**,** 216.

KERMANI, P. & HEMPSTEAD, B. 2019. BDNF Actions in the Cardiovascular System: Roles in Development, Adulthood and Response to Injury. *Front Physiol,* 10**,** 455.

KHOSRAVI, M., PETER, J., WINTERING, N. A., SERRUYA, M., SHAMCHI, S. P., WERNER, T. J., ALAVI, A. & NEWBERG, A. B. 2019. 18F-FDG Is a Superior Indicator of Cognitive Performance Compared to 18F-Florbetapir in Alzheimer's Disease and Mild Cognitive Impairment Evaluation: A Global Quantitative Analysis. *J Alzheimers Dis*.

KIM, H. J., CHAE, S. C., LEE, D. K., CHROMY, B., LEE, S. C., PARK, Y. C., KLEIN, W. L., KRAFFT, G. A. & HONG, S. T. 2003. Selective neuronal degeneration induced by soluble oligomeric amyloid beta protein. *FASEB J,* 17**,** 118-20.

KIM, M., SUH, J., ROMANO, D., TRUONG, M. H., MULLIN, K., HOOLI, B., NORTON, D., TESCO, G., ELLIOTT, K., WAGNER, S. L., MOIR, R. D., BECKER, K. D. & TANZI, R. E. 2009. Potential late-onset Alzheimer's disease-associated mutations in the ADAM10 gene attenuate {alpha}-secretase activity. *Hum Mol Genet,* 18**,** 3987-96.

KIM, W. S., FU, Y., DOBSON-STONE, C., HSIAO, J. T., SHANG, K., HALLUPP, M., SCHOFIELD, P. R., GARNER, B., KARL, T. & KWOK, J. B. J. 2018. Effect of Fluvoxamine on Amyloid-β Peptide Generation and Memory. *J Alzheimers Dis,* 62**,** 1777-1787.

KINNUNEN, K. M., CASH, D. M., POOLE, T., FROST, C., BENZINGER, T. L. S., AHSAN, R. L., LEUNG, K. K., CARDOSO, M. J., MODAT, M., MALONE, I. B., MORRIS, J. C., BATEMAN, R. J., MARCUS, D. S., GOATE, A., SALLOWAY, S. P., CORREIA, S., SPERLING, R. A., CHHATWAL, J. P., MAYEUX, R. P., BRICKMAN, A. M., MARTINS, R. N., FARLOW, M. R., GHETTI, B., SAYKIN, A. J., JACK, C. R., SCHOFIELD, P. R., MCDADE, E., WEINER, M. W., RINGMAN, J. M., THOMPSON, P. M., MASTERS, C. L., ROWE, C. C., ROSSOR, M. N., OURSELIN, S., FOX, N. C. & (DIAN), D. I. A. N. 2018. Presymptomatic atrophy in autosomal dominant Alzheimer's disease: A serial magnetic resonance imaging study. *Alzheimers Dement,* 14**,** 43-53.

KISHI, T., MATSUNAGA, S., OYA, K., NOMURA, I., IKUTA, T. & IWATA, N. 2017. Memantine for Alzheimer's Disease: An Updated Systematic Review and Meta-analysis. *J Alzheimers Dis,* 60**,** 401-425.

KOFFIE, R. M., MEYER-LUEHMANN, M., HASHIMOTO, T., ADAMS, K. W., MIELKE, M. L., GARCIA-ALLOZA, M., MICHEVA, K. D., SMITH, S. J., KIM, M. L., LEE, V. M., HYMAN, B. T. & SPIRES-JONES, T. L. 2009. Oligomeric amyloid beta associates with postsynaptic densities and correlates with excitatory synapse loss near senile plaques. *Proc Natl Acad Sci U S A,* 106**,** 4012-7.

KOJRO, E., GIMPL, G., LAMMICH, S., MARZ, W. & FAHRENHOLZ, F. 2001. Low cholesterol stimulates the nonamyloidogenic pathway by its effect on the alpha -secretase ADAM 10. *Proc Natl Acad Sci U S A,* 98**,** 5815-20.

KONDO, T., ASAI, M., TSUKITA, K., KUTOKU, Y., OHSAWA, Y., SUNADA, Y., IMAMURA, K., EGAWA, N., YAHATA, N., OKITA, K., TAKAHASHI, K., ASAKA, I., AOI, T., WATANABE, A., WATANABE, K., KADOYA, C., NAKANO, R., WATANABE, D., MARUYAMA, K., HORI, O., HIBINO, S., CHOSHI, T., NAKAHATA, T., HIOKI, H., KANEKO, T., NAITOH, M., YOSHIKAWA, K., YAMAWAKI, S., SUZUKI, S., HATA, R., UENO, S., SEKI, T., KOBAYASHI, K., TODA, T., MURAKAMI, K., IRIE, K., KLEIN, W. L., MORI, H., ASADA, T., TAKAHASHI, R., IWATA, N., YAMANAKA, S. & INOUE, H. 2013. Modeling Alzheimer's disease with iPSCs reveals stress phenotypes associated with intracellular Aβ and differential drug responsiveness. *Cell Stem Cell,* 12**,** 487-96.

KUDO, W., LEE, H. P., ZOU, W. Q., WANG, X., PERRY, G., ZHU, X., SMITH, M. A., PETERSEN, R. B. & LEE, H. G. 2012. Cellular prion protein is essential for oligomeric amyloid-β-induced neuronal cell death. *Hum Mol Genet,* 21**,** 1138-44.

KUHN, P. H., COLOMBO, A. V., SCHUSSER, B., DREYMUELLER, D., WETZEL, S., SCHEPERS, U., HERBER, J., LUDWIG, A., KREMMER, E., MONTAG, D., MÜLLER, U., SCHWEIZER, M., SAFTIG, P., BRÄSE, S. & LICHTENTHALER, S. F. 2016. Systematic substrate identification indicates a central role for the metalloprotease ADAM10 in axon targeting and synapse function. *Elife,* 5.

KUHN, P. H., WANG, H., DISLICH, B., COLOMBO, A., ZEITSCHEL, U., ELLWART, J. W., KREMMER, E., ROSSNER, S. & LICHTENTHALER, S. F. 2010. ADAM10 is the physiologically relevant, constitutive alpha-secretase of the amyloid precursor protein in primary neurons. *EMBO J,* 29**,** 3020-32.

KUNKLE, B. W., GRENIER-BOLEY, B., SIMS, R., BIS, J. C., DAMOTTE, V., NAJ, A. C., BOLAND, A., VRONSKAYA, M., VAN DER LEE, S. J., AMLIE-WOLF, A., BELLENGUEZ, C., FRIZATTI, A., CHOURAKI, V., MARTIN, E. R., SLEEGERS, K., BADARINARAYAN, N., JAKOBSDOTTIR, J., HAMILTON-NELSON, K. L., MORENO-GRAU, S., OLASO, R., RAYBOULD, R., CHEN, Y., KUZMA, A. B., HILTUNEN, M., MORGAN, T., AHMAD, S., VARDARAJAN, B. N., EPELBAUM, J., HOFFMANN, P., BOADA, M., BEECHAM, G. W., GARNIER, J. G., HAROLD, D., FITZPATRICK, A. L., VALLADARES, O., MOUTET, M. L., GERRISH, A., SMITH, A. V., QU, L., BACQ, D., DENNING, N., JIAN, X., ZHAO, Y., DEL ZOMPO, M., FOX, N. C., CHOI, S. H., MATEO, I., HUGHES, J. T., ADAMS, H. H., MALAMON, J., SANCHEZ-GARCIA, F., PATEL, Y., BRODY, J. A., DOMBROSKI, B. A., NARANJO, M. C. D., DANIILIDOU, M., EIRIKSDOTTIR, G., MUKHERJEE, S., WALLON, D., UPHILL, J., ASPELUND, T., CANTWELL, L. B., GARZIA, F., GALIMBERTI, D., HOFER, E., BUTKIEWICZ, M., FIN, B., SCARPINI, E., SARNOWSKI, C., BUSH, W. S., MESLAGE, S., KORNHUBER, J.,

WHITE, C. C., SONG, Y., BARBER, R. C., ENGELBORGHS, S., SORDON, S., VOIJNOVIC, D., ADAMS, P. M., VANDENBERGHE, R., MAYHAUS, M., CUPPLES, L. A., ALBERT, M. S., DE DEYN, P. P., GU, W., HIMALI, J. J., BEEKLY, D., SQUASSINA, A., HARTMANN, A. M., ORELLANA, A., BLACKER, D., RODRIGUEZ-RODRIGUEZ, E., LOVESTONE, S., GARCIA, M. E., DOODY, R. S., MUNOZ-FERNADEZ, C., SUSSAMS, R., LIN, H., FAIRCHILD, T. J., BENITO, Y. A., et al. 2019. Genetic meta-analysis of diagnosed Alzheimer's disease identifies new risk loci and implicates Aβ, tau, immunity and lipid processing. *Nat Genet,* 51**,** 414-430.

KWAK, S. S., WASHICOSKY, K. J., BRAND, E., VON MAYDELL, D., ARONSON, J., KIM, S., CAPEN, D. E., CETINBAS, M., SADREYEV, R., NING, S., BYLYKBASHI, E., XIA, W., WAGNER, S. L., CHOI, S. H., TANZI, R. E. & KIM, D. Y. 2020. Amyloid-β42/40 ratio drives tau pathology in 3D human neural cell culture models of Alzheimer's disease. *Nat Commun,* 11**,** 1377.

KWAK, Y. D., BRANNEN, C. L., QU, T., KIM, H. M., DONG, X., SOBA, P., MAJUMDAR, A., KAPLAN, A., BEYREUTHER, K. & SUGAYA, K. 2006. Amyloid precursor protein regulates differentiation of human neural stem cells. *Stem Cells Dev,* 15**,** 381-9.

KWART, D., GREGG, A., SCHECKEL, C., MURPHY, E., PAQUET, D., DUFFIELD, M., FAK, J., OLSEN, O., DARNELL, R. & TESSIER-LAVIGNE, M. 2019. A Large Panel of Isogenic APP and PSEN1 Mutant Human iPSC Neurons Reveals Shared Endosomal Abnormalities Mediated by APP β-CTFs, Not Aβ. *Neuron,* 104**,** 256-270.e5.

KÖGEL, D., DELLER, T. & BEHL, C. 2012. Roles of amyloid precursor protein family members in neuroprotection, stress signaling and aging. *Exp Brain Res,* 217**,** 471-9.

KÖHLER, C. 2016. Granulovacuolar degeneration: a neurodegenerative change that accompanies tau pathology. *Acta Neuropathol,* 132**,** 339-59.

LALKOVIČOVÁ, M. & DANIELISOVÁ, V. 2016. Neuroprotection and antioxidants. *Neural Regen Res,* 11**,** 865-74.

LAMB, S. E., SHEEHAN, B., ATHERTON, N., NICHOLS, V., COLLINS, H., MISTRY, D., DOSANJH, S., SLOWTHER, A. M., KHAN, I., PETROU, S., LALL, R. & INVESTIGATORS, D. T. 2018. Dementia And Physical Activity (DAPA) trial of moderate to high intensity exercise training for people with dementia: randomised controlled trial. *BMJ,* 361**,** k1675.

LANZILLOTTA, C., DI DOMENICO, F., PERLUIGI, M. & BUTTERFIELD, D. A. 2019. Targeting Mitochondria in Alzheimer Disease: Rationale and Perspectives. *CNS Drugs,* 33**,** 957-969.

LARSON, M., SHERMAN, M. A., AMAR, F., NUVOLONE, M., SCHNEIDER, J. A., BENNETT, D. A., AGUZZI, A. & LESNÉ, S. E. 2012. The complex PrP(c)-Fyn couples human oligomeric Aβ with pathological tau changes in Alzheimer's disease. *J Neurosci,* 32**,** 16857-71a.

LEE, J. H., YU, W. H., KUMAR, A., LEE, S., MOHAN, P. S., PETERHOFF, C. M., WOLFE, D. M., MARTINEZ-VICENTE, M., MASSEY, A. C., SOVAK, G., UCHIYAMA, Y., WESTAWAY, D., CUERVO, A. M. & NIXON, R. A. 2010. Lysosomal proteolysis and autophagy require presenilin 1 and are disrupted by Alzheimer-related PS1 mutations. *Cell,* 141**,** 1146-58.

LEE, S. J., NAM, E., LEE, H. J., SAVELIEFF, M. G. & LIM, M. H. 2017. Towards an understanding of amyloid-β oligomers: characterization, toxicity mechanisms, and inhibitors. *Chem Soc Rev,* 46**,** 310-323.

LEE, S. Y., LEE, S. J., HAN, C., PATKAR, A. A., MASAND, P. S. & PAE, C. U. 2013. Oxidative/nitrosative stress and antidepressants: targets for novel antidepressants. *Prog Neuropsychopharmacol Biol Psychiatry,* 46**,** 224-35.

LESNÉ, S., KOTILINEK, L. & ASHE, K. H. 2008. Plaque-bearing mice with reduced levels of oligomeric amyloid-beta assemblies have intact memory function. *Neuroscience,* 151**,** 745-9.

LETRA, L., SANTANA, I. & SEIÇA, R. 2014. Obesity as a risk factor for Alzheimer's disease: the role of adipocytokines. *Metab Brain Dis,* 29**,** 563-8.

LEUNER, K., SCHÜTT, T., KURZ, C., ECKERT, S. H., SCHILLER, C., OCCHIPINTI, A., MAI, S., JENDRACH, M., ECKERT, G. P., KRUSE, S. E., PALMITER, R. D., BRANDT, U., DRÖSE, S., WITTIG, I., WILLEM, M., HAASS, C., REICHERT, A. S. & MÜLLER, W. E. 2012. Mitochondrion-derived reactive oxygen species lead to enhanced amyloid beta formation. *Antioxid Redox Signal,* 16**,** 1421-33.

LEUZY, A., CHIOTIS, K., HASSELBALCH, S. G., RINNE, J. O., DE MENDONÇA, A., OTTO, M., LLEÓ, A., CASTELO-BRANCO, M., SANTANA, I., JOHANSSON, J., ANDERL-STRAUB, S., VON ARNIM, C. A., BEER, A., BLESA, R., FORTEA, J., HERUKKA, S. K., PORTELIUS, E., PANNEE, J., ZETTERBERG, H., BLENNOW, K. & NORDBERG, A. 2016. Pittsburgh compound B imaging and cerebrospinal fluid amyloid-β in a multicentre European memory clinic study. *Brain,* 139**,** 2540-53.

LEVY-LAHAD, E., WASCO, W., POORKAJ, P., ROMANO, D. M., OSHIMA, J., PETTINGELL, W. H., YU, C. E., JONDRO, P. D., SCHMIDT, S. D. & WANG, K. 1995. Candidate gene for the chromosome 1 familial Alzheimer's disease locus. *Science,* 269**,** 973-7.

LEWCZUK, P., MATZEN, A., BLENNOW, K., PARNETTI, L., MOLINUEVO, J. L., EUSEBI, P., KORNHUBER, J., MORRIS, J. C. & FAGAN, A. M. 2017. Cerebrospinal Fluid Aβ42/40 Corresponds Better than Aβ42 to Amyloid PET in Alzheimer's Disease. *J Alzheimers Dis,* 55**,** 813-822.

LI, R., LINDHOLM, K., YANG, L. B., YUE, X., CITRON, M., YAN, R., BEACH, T., SUE, L., SABBAGH, M., CAI, H., WONG, P., PRICE, D. & SHEN, Y. 2004. Amyloid beta peptide load is correlated with increased beta-secretase activity in sporadic Alzheimer's disease patients. *Proc Natl Acad Sci U S A,* 101**,** 3632-7.

LI, S. & SELKOE, D. J. 2020. A mechanistic hypothesis for the impairment of synaptic plasticity by soluble Aβ oligomers from Alzheimer's brain. *J Neurochem*.

LI, T., PIRES, C., NIELSEN, T. T., WALDEMAR, G., HJERMIND, L. E., NIELSEN, J. E., DINNYES, A., HOLST, B., HYTTEL, P. & FREUDE, K. K. 2016a. Generation of induced pluripotent stem cells (iPSCs) from an Alzheimer's disease patient carrying a M146I mutation in PSEN1. *Stem Cell Res,* 16**,** 334-7.

LI, T., PIRES, C., NIELSEN, T. T., WALDEMAR, G., HJERMIND, L. E., NIELSEN, J. E., DINNYES, A., HYTTEL, P. & FREUDE, K. K. 2016b. Generation of induced pluripotent stem cells (iPSCs) from an Alzheimer's disease patient carrying an A79V mutation in PSEN1. *Stem Cell Res,* 16**,** 229-32.

LI, X. L., HU, N., TAN, M. S., YU, J. T. & TAN, L. 2014. Behavioral and psychological symptoms in Alzheimer's disease. *Biomed Res Int,* 2014**,** 927804.

LICHTENTHALER, S. F., HAASS, C. & STEINER, H. 2011. Regulated intramembrane proteolysis--lessons from amyloid precursor protein processing. *J Neurochem,* 117**,** 779-96.

LICINIO, J. & WONG, M. L. 2016. Serotonergic neurons derived from induced pluripotent stem cells (iPSCs): a new pathway for research on the biology and pharmacology of major depression. *Mol Psychiatry,* 21**,** 1-2.

LIGUORI, I., RUSSO, G., CURCIO, F., BULLI, G., ARAN, L., DELLA-MORTE, D., GARGIULO, G., TESTA, G., CACCIATORE, F., BONADUCE, D. & ABETE, P. 2018. Oxidative stress, aging, and diseases. *Clin Interv Aging,* 13**,** 757-772.

LINDQVIST, D., DHABHAR, F. S., JAMES, S. J., HOUGH, C. M., JAIN, F. A., BERSANI, F. S., REUS, V. I., VERHOEVEN, J. E., EPEL, E. S., MAHAN, L., ROSSER, R., WOLKOWITZ, O. M. & MELLON, S. H. 2017. Oxidative stress, inflammation and treatment response in major depression. *Psychoneuroendocrinology,* 76**,** 197-205.

LINSENMEIER, L., MOHAMMADI, B., WETZEL, S., PUIG, B., JACKSON, W. S., HARTMANN, A., UCHIYAMA, K., SAKAGUCHI, S., ENDRES, K., TATZELT, J., SAFTIG, P., GLATZEL, M. & ALTMEPPEN, H. C. 2018. Structural and mechanistic aspects influencing the ADAM10-mediated shedding of the prion protein. *Mol Neurodegener,* 13**,** 18.

LIVINGSTON, G., SOMMERLAD, A., ORGETA, V., COSTAFREDA, S. G., HUNTLEY, J., AMES, D., BALLARD, C., BANERJEE, S., BURNS, A., COHEN-MANSFIELD, J., COOPER, C., FOX, N., GITLIN, L. N., HOWARD, R., KALES, H. C., LARSON, E. B., RITCHIE, K., ROCKWOOD, K., SAMPSON, E. L., SAMUS, Q., SCHNEIDER, L. S., SELBÆK, G., TERI, L. & MUKADAM, N. 2017. Dementia prevention, intervention, and care. *Lancet,* 390**,** 2673-2734.

LOBO, A., LAUNER, L. J., FRATIGLIONI, L., ANDERSEN, K., DI CARLO, A., BRETELER, M. M., COPELAND, J. R., DARTIGUES, J. F., JAGGER, C., MARTINEZ-LAGE, J., SOININEN, H. & HOFMAN, A. 2000. Prevalence of dementia and major subtypes in Europe: A collaborative study of population-based cohorts. Neurologic Diseases in the Elderly Research Group. *Neurology,* 54**,** S4-9.

LU, P., BAI, X. C., MA, D., XIE, T., YAN, C., SUN, L., YANG, G., ZHAO, Y., ZHOU, R., SCHERES, S. H. W. & SHI, Y. 2014. Three-dimensional structure of human γ-secretase. *Nature,* 512**,** 166-170.

LUO, Y., BOLON, B., KAHN, S., BENNETT, B. D., BABU-KHAN, S., DENIS, P., FAN, W., KHA, H., ZHANG, J., GONG, Y., MARTIN, L., LOUIS, J. C., YAN, Q., RICHARDS, W. G., CITRON, M. & VASSAR, R. 2001. Mice deficient in BACE1, the Alzheimer's beta-secretase, have normal phenotype and abolished beta-amyloid generation. *Nat Neurosci,* 4**,** 231-2.

MA, J., GAO, Y., JIANG, L., CHAO, F. L., HUANG, W., ZHOU, C. N., TANG, W., ZHANG, L., HUANG, C. X., ZHANG, Y., LUO, Y. M., XIAO, Q., YU, H. R., JIANG, R. & TANG, Y. 2017. Fluoxetine attenuates the impairment of spatial learning ability and prevents neuron loss in middle-aged APPswe/PSEN1dE9 double transgenic Alzheimer's disease mice. *Oncotarget,* 8**,** 27676-27692.

MA, L. Z., HUANG, Y. Y., WANG, Z. T., LI, J. Q., HOU, X. H., SHEN, X. N., OU, Y. N., DONG, Q., TAN, L., YU, J. T. & INITIATIVE, A. D. N. 2019. Metabolically healthy obesity reduces the risk of Alzheimer's disease in elders: a longitudinal study. *Aging (Albany NY),* 11**,** 10939-10951.

MAAROUF, C. L., DAUGS, I. D., KOKJOHN, T. A., KALBACK, W. M., PATTON, R. L., LUEHRS, D. C., MASLIAH, E., NICOLL, J. A., SABBAGH, M. N., BEACH, T. G., CASTAÑO, E. M. & ROHER, A. E. 2010. The biochemical aftermath of anti-amyloid immunotherapy. *Mol Neurodegener,* 5**,** 39.

MADSEN, K., NEUMANN, W. J., HOLST, K., MARNER, L., HAAHR, M. T., LEHEL, S., KNUDSEN, G. M. & HASSELBALCH, S. G. 2011. Cerebral serotonin 4 receptors and amyloid-β in early Alzheimer's disease. *J Alzheimers Dis,* 26**,** 457-66.

MAHLEY, R. W. 1988. Apolipoprotein E: cholesterol transport protein with expanding role in cell biology. *Science,* 240**,** 622-30.

MANZINE, P. R., BARHAM, E. J., VALE, F. A., SELISTRE-DE-ARAÚJO, H. S., PAVARINI, S. C. & COMINETTI, M. R. 2014. Platelet a disintegrin and metallopeptidase 10 expression correlates with clock drawing test scores in Alzheimer's disease. *Int J Geriatr Psychiatry,* 29**,** 414-20.

MANZINE, P. R., BARHAM, E. J., VALE, F. E. A., SELISTRE-DE-ARAÚJO, H. S., IOST PAVARINI, S. C. & COMINETTI, M. R. 2013. Correlation between mini-mental state examination and platelet ADAM10 expression in Alzheimer's disease. *J Alzheimers Dis,* 36**,** 253-60.

MANZINE, P. R., ETTCHETO, M., CANO, A., BUSQUETS, O., MARCELLO, E., PELUCCHI, S., DI LUCA, M., ENDRES, K., OLLOQUEQUI, J., CAMINS, A. & COMINETTI, M. R. 2019. ADAM10 in Alzheimer's disease: Pharmacological modulation by natural compounds and its role as a peripheral marker. *Biomed Pharmacother,* 113**,** 108661.

MARCINKIEWICZ, M. & SEIDAH, N. G. 2000. Coordinated expression of beta-amyloid precursor protein and the putative beta-secretase BACE and alpha-secretase ADAM10 in mouse and human brain. *J Neurochem,* 75**,** 2133-43.

MARIONI, R. E., HARRIS, S. E., ZHANG, Q., MCRAE, A. F., HAGENAARS, S. P., HILL, W. D., DAVIES, G., RITCHIE, C. W., GALE, C. R., STARR, J. M., GOATE, A. M., PORTEOUS, D. J., YANG, J., EVANS, K. L., DEARY, I. J., WRAY, N. R. & VISSCHER, P. M. 2018. GWAS on family history of Alzheimer's disease. *Transl Psychiatry,* 8**,** 99.

MARKESBERY, W. R. 1997. Oxidative stress hypothesis in Alzheimer's disease. *Free Radic Biol Med,* 23**,** 134-47.

MARKSTEINER, J., KEMMLER, G., WEISS, E. M., KNAUS, G., ULLRICH, C., MECHTCHERIAKOV, S., OBERBAUER, H., AUFFINGER, S., HINTERHÖLZL, J., HINTERHUBER, H. & HUMPEL, C. 2011. Five out of 16 plasma signaling proteins are enhanced in plasma of patients with mild cognitive impairment and Alzheimer's disease. *Neurobiol Aging,* 32**,** 539-40.

MARSHALL, G. A., FAIRBANKS, L. A., TEKIN, S., VINTERS, H. V. & CUMMINGS, J. L. 2007. Early-onset Alzheimer's disease is associated with greater pathologic burden. *J Geriatr Psychiatry Neurol,* 20**,** 29-33.

MATTHEWS, A. L., SZYROKA, J., COLLIER, R., NOY, P. J. & TOMLINSON, M. G. 2017. Scissor sisters: regulation of ADAM10 by the TspanC8 tetraspanins. *Biochem Soc Trans,* 45**,** 719-730.

MATÍAS-GUIU, J. A., VALLES-SALGADO, M., ROGNONI, T., HAMRE-GIL, F., MORENO-RAMOS, T. & MATÍAS-GUIU, J. 2017. Comparative Diagnostic Accuracy of the ACE-III, MIS, MMSE, MoCA, and RUDAS for Screening of Alzheimer Disease. *Dement Geriatr Cogn Disord,* 43**,** 237-246.

MAURER, S., KOPP, H. G., SALIH, H. R. & KROPP, K. N. 2020. Modulation of Immune Responses by Platelet-Derived ADAM10. *Front Immunol,* 11**,** 44.

MCGURRAN, H., GLENN, J. M., MADERO, E. N. & BOTT, N. T. 2019. Prevention and Treatment of Alzheimer's Disease: Biological Mechanisms of Exercise. *J Alzheimers Dis,* 69**,** 311-338.

MDAWAR, B., GHOSSOUB, E. & KHOURY, R. 2020. Selective serotonin reuptake inhibitors and Alzheimer's disease. *Neural Regen Res,* 15**,** 41-46.

MECOCCI, P., BOCCARDI, V., CECCHETTI, R., BASTIANI, P., SCAMOSCI, M., RUGGIERO, C. & BARONI, M. 2018. A Long Journey into Aging, Brain Aging, and Alzheimer's Disease Following the Oxidative Stress Tracks. *J Alzheimers Dis,* 62**,** 1319-1335.

MEINECK, M., SCHUCK, F., ABDELFATAH, S., EFFERTH, T. & ENDRES, K. 2016. Identification of Phlogacantholide C as a Novel ADAM10 Enhancer from Traditional Chinese Medicinal Plants. *Medicines (Basel),* 3.

MELIS, R. J. F., HAAKSMA, M. L. & MUNIZ-TERRERA, G. 2019. Understanding and predicting the longitudinal course of dementia. *Curr Opin Psychiatry,* 32**,** 123-129.

MENDEZ, M. F. 2019. Early-onset Alzheimer Disease and Its Variants. *Continuum (Minneap Minn),* 25**,** 34-51.

MIELKE, M. M., HAGEN, C. E., WENNBERG, A. M. V., AIREY, D. C., SAVICA, R., KNOPMAN, D. S., MACHULDA, M. M., ROBERTS, R. O., JACK, C. R., PETERSEN, R. C. & DAGE, J. L. 2017. Association of Plasma Total Tau Level With Cognitive Decline and Risk of Mild Cognitive Impairment or Dementia in the Mayo Clinic Study on Aging. *JAMA Neurol,* 74**,** 1073-1080.

MILNE, G. L. 2017. Classifying oxidative stress by F. *Redox Biol,* 12**,** 897-898.

MINTER, M. R., TAYLOR, J. M. & CRACK, P. J. 2016. The contribution of neuroinflammation to amyloid toxicity in Alzheimer's disease. *J Neurochem,* 136**,** 457-74.

MIZUNO, S., YODA, M., KIMURA, T., SHIMODA, M., AKIYAMA, H., CHIBA, K., NAKAMURA, M. & HORIUCHI, K. 2020. ADAM10 is indispensable for longitudinal bone growth in mice. *Bone,* 134**,** 115273.

MONTINE, T. J., QUINN, J. F., MILATOVIC, D., SILBERT, L. C., DANG, T., SANCHEZ, S., TERRY, E., ROBERTS, L. J., KAYE, J. A. & MORROW, J. D. 2002. Peripheral F2-isoprostanes and F4-neuroprostanes are not increased in Alzheimer's disease. *Ann Neurol,* 52**,** 175-9.

MORENAS-RODRÍGUEZ, E., ALCOLEA, D., SUÁREZ-CALVET, M., MUÑOZ-LLAHUNA, L., VILAPLANA, E., SALA, I., SUBIRANA, A., QUEROL-VILASECA, M., CARMONA-IRAGUI, M., ILLÁN-GALA, I., RIBOSA-NOGUÉ, R., BLESA, R., HAASS, C., FORTEA, J. & LLEÓ, A. 2019. Different pattern of CSF glial markers between dementia with Lewy bodies and Alzheimer's disease. *Sci Rep,* 9**,** 7803.

MORGAN, M. J. & LIU, Z. G. 2011. Crosstalk of reactive oxygen species and NF-κB signaling. *Cell Res,* 21**,** 103-15.

MOUSSA-PACHA, N. M., ABDIN, S. M., OMAR, H. A., ALNISS, H. & AL-TEL, T. H. 2020. BACE1 inhibitors: Current status and future directions in treating Alzheimer's disease. *Med Res Rev,* 40**,** 339-384.

MROCZKO, B., GROBLEWSKA, M., LITMAN-ZAWADZKA, A., KORNHUBER, J. & LEWCZUK, P. 2018. Cellular Receptors of Amyloid β Oligomers (AβOs) in Alzheimer's Disease. *Int J Mol Sci,* 19.

MUELLER, C., PERERA, G., HAYES, R. D., SHETTY, H. & STEWART, R. 2018. Associations of acetylcholinesterase inhibitor treatment with reduced mortality in Alzheimer's disease: a retrospective survival analysis. *Age Ageing,* 47**,** 88-94.

MURRAY, I. V., SINDONI, M. E. & AXELSEN, P. H. 2005. Promotion of oxidative lipid membrane damage by amyloid beta proteins. *Biochemistry,* 44**,** 12606-13.

MURRELL, J., FARLOW, M., GHETTI, B. & BENSON, M. D. 1991. A mutation in the amyloid precursor protein associated with hereditary Alzheimer's disease. *Science,* 254**,** 97-9.

MÜLLER, U. C., DELLER, T. & KORTE, M. 2017. Not just amyloid: physiological functions of the amyloid precursor protein family. *Nat Rev Neurosci,* 18**,** 281-298.

NALIVAEVA, N. N. & TURNER, A. J. 2019. Targeting amyloid clearance in Alzheimer's disease as a therapeutic strategy. *Br J Pharmacol,* 176**,** 3447-3463.

NETEA, M. G., BALKWILL, F., CHONCHOL, M., COMINELLI, F., DONATH, M. Y., GIAMARELLOS-BOURBOULIS, E. J., GOLENBOCK, D., GRESNIGT, M. S., HENEKA, M. T., HOFFMAN, H. M., HOTCHKISS, R., JOOSTEN, L. A. B., KASTNER, D. L., KORTE, M., LATZ, E., LIBBY, P., MANDRUP-POULSEN, T., MANTOVANI, A., MILLS, K. H. G., NOWAK, K. L., O'NEILL, L. A., PICKKERS, P., VAN DER POLL, T., RIDKER, P. M., SCHALKWIJK, J., SCHWARTZ, D. A., SIEGMUND, B., STEER, C. J., TILG, H., VAN DER MEER, J. W. M., VAN DE VEERDONK, F. L. & DINARELLO, C. A. 2017. A guiding map for inflammation. *Nat Immunol,* 18**,** 826-831.

NEUNER, S. M., TCW, J. & GOATE, A. M. 2020. Genetic architecture of Alzheimer's disease. *Neurobiol Dis,* 143**,** 104976.

NG, M., FLEMING, T., ROBINSON, M., THOMSON, B., GRAETZ, N., MARGONO, C., MULLANY, E. C., BIRYUKOV, S., ABBAFATI, C., ABERA, S. F., ABRAHAM, J. P., ABU-RMEILEH, N. M., ACHOKI, T., ALBUHAIRAN, F. S., ALEMU, Z. A., ALFONSO, R., ALI, M. K., ALI, R., GUZMAN, N. A., AMMAR, W., ANWARI, P., BANERJEE, A., BARQUERA, S., BASU, S., BENNETT, D. A., BHUTTA, Z., BLORE, J., CABRAL, N., NONATO, I. C., CHANG, J. C., CHOWDHURY, R., COURVILLE, K. J., CRIQUI, M. H., CUNDIFF, D. K., DABHADKAR, K. C., DANDONA, L., DAVIS, A., DAYAMA, A., DHARMARATNE, S. D., DING, E. L., DURRANI, A. M., ESTEGHAMATI, A., FARZADFAR, F., FAY, D. F., FEIGIN, V. L., FLAXMAN, A., FOROUZANFAR, M. H., GOTO, A., GREEN, M. A., GUPTA, R., HAFEZI-NEJAD, N., HANKEY, G. J., HAREWOOD, H. C., HAVMOELLER, R., HAY, S., HERNANDEZ, L., HUSSEINI, A., IDRISOV, B. T., IKEDA, N., ISLAMI, F., JAHANGIR, E., JASSAL, S. K., JEE, S. H., JEFFREYS, M., JONAS, J. B., KABAGAMBE, E. K., KHALIFA, S. E., KENGNE, A. P., KHADER, Y. S., KHANG, Y. H., KIM, D., KIMOKOTI, R. W., KINGE, J. M., KOKUBO, Y., KOSEN, S., KWAN, G., LAI, T., LEINSALU, M., LI, Y., LIANG, X., LIU, S., LOGROSCINO, G., LOTUFO, P. A., LU, Y., MA, J., MAINOO, N. K., MENSAH, G. A., MERRIMAN, T. R., MOKDAD, A. H., MOSCHANDREAS, J., NAGHAVI, M., NAHEED, A., NAND, D., NARAYAN, K. M., NELSON, E. L., NEUHOUSER, M. L., NISAR, M. I., OHKUBO, T., OTI, S. O., PEDROZA, A., et al. 2014. Global, regional, and national prevalence of overweight and obesity in children and adults during 1980-2013: a systematic analysis for the Global Burden of Disease Study 2013. *Lancet,* 384**,** 766-81.

NIKOLAC PERKOVIC, M. & PIVAC, N. 2019. Genetic Markers of Alzheimer's Disease. *Adv Exp Med Biol,* 1192**,** 27-52.

NIKOLAEV, A., MCLAUGHLIN, T., O'LEARY, D. D. & TESSIER-LAVIGNE, M. 2009. APP binds DR6 to trigger axon pruning and neuron death via distinct caspases. *Nature,* 457**,** 981-9.

NIRMALRAJ, P. N., LIST, J., BATTACHARYA, S., HOWE, G., XU, L., THOMPSON, D. & MAYER, M. 2020. Complete aggregation pathway of amyloid β (1-40) and (1-42) resolved on an atomically clean interface. *Sci Adv,* 6**,** eaaz6014.

NISBET, R. M., POLANCO, J. C., ITTNER, L. M. & GÖTZ, J. 2015. Tau aggregation and its interplay with amyloid-β. *Acta Neuropathol,* 129**,** 207-20.

NISTOR, M., DON, M., PAREKH, M., SARSOZA, F., GOODUS, M., LOPEZ, G. E., KAWAS, C., LEVERENZ, J., DORAN, E., LOTT, I. T., HILL, M. & HEAD, E. 2007. Alpha- and beta-secretase activity as a function of age and beta-amyloid in Down syndrome and normal brain. *Neurobiol Aging,* 28**,** 1493-506.

NOY, P. J., YANG, J., REYAT, J. S., MATTHEWS, A. L., CHARLTON, A. E., FURMSTON, J., ROGERS, D. A., RAINGER, G. E. & TOMLINSON, M. G. 2016. TspanC8 Tetraspanins and A Disintegrin and Metalloprotease 10 (ADAM10) Interact via Their Extracellular Regions: EVIDENCE FOR DISTINCT BINDING MECHANISMS FOR DIFFERENT TspanC8 PROTEINS. *J Biol Chem,* 291**,** 3145-57.

NUNOMURA, A., PERRY, G., ALIEV, G., HIRAI, K., TAKEDA, A., BALRAJ, E. K., JONES, P. K., GHANBARI, H., WATAYA, T., SHIMOHAMA, S., CHIBA, S., ATWOOD, C. S., PETERSEN, R. B. & SMITH, M. A. 2001. Oxidative damage is the earliest event in Alzheimer disease. *J Neuropathol Exp Neurol,* 60**,** 759-67.

O'BRIEN, R. J. & WONG, P. C. 2011. Amyloid precursor protein processing and Alzheimer's disease. *Annu Rev Neurosci,* 34**,** 185-204.

O'BRYANT, S. E., GUPTA, V., HENRIKSEN, K., EDWARDS, M., JEROMIN, A., LISTA, S., BAZENET, C., SOARES, H., LOVESTONE, S., HAMPEL, H., MONTINE, T., BLENNOW, K., FOROUD, T., CARRILLO, M., GRAFF-RADFORD, N., LASKE, C., BRETELER, M., SHAW, L., TROJANOWSKI, J. Q., SCHUPF, N., RISSMAN, R. A., FAGAN, A. M., OBEROI, P., UMEK, R., WEINER, M. W., GRAMMAS, P., POSNER, H., MARTINS, R. & GROUPS, S.-B. A. B. W. 2015. Guidelines for the standardization of preanalytic variables for blood-based biomarker studies in Alzheimer's disease research. *Alzheimers Dement,* 11**,** 549-60.

O'BRYANT, S. E., MIELKE, M. M., RISSMAN, R. A., LISTA, S., VANDERSTICHELE, H., ZETTERBERG, H., LEWCZUK, P., POSNER, H., HALL, J., JOHNSON, L., FONG, Y. L., LUTHMAN, J., JEROMIN, A., BATRLA-UTERMANN, R., VILLARREAL, A., BRITTON, G., SNYDER, P. J., HENRIKSEN, K., GRAMMAS, P., GUPTA, V., MARTINS, R., HAMPEL, H. & AREA, B. B. B. P. I. 2017. Blood-based biomarkers in Alzheimer disease: Current state of the science and a novel collaborative paradigm for advancing from discovery to clinic. *Alzheimers Dement,* 13**,** 45-58.

O'CONNOR, A., KARIKARI, T. K., POOLE, T., ASHTON, N. J., LANTERO RODRIGUEZ, J., KHATUN, A., SWIFT, I., HESLEGRAVE, A. J., ABEL, E., CHUNG, E., WESTON, P. S. J., PAVISIC, I. M., RYAN, N. S., BARKER, S., ROSSOR, M. N., POLKE, J. M., FROST, C., MEAD, S., BLENNOW, K., ZETTERBERG, H. & FOX, N. C. 2020. Plasma phospho-tau181 in presymptomatic and symptomatic familial Alzheimer's disease: a longitudinal cohort study. *Mol Psychiatry*.

OCHALEK, A., MIHALIK, B., AVCI, H. X., CHANDRASEKARAN, A., TÉGLÁSI, A., BOCK, I., GIUDICE, M. L., TÁNCOS, Z., MOLNÁR, K., LÁSZLÓ, L., NIELSEN, J. E., HOLST, B., FREUDE, K., HYTTEL, P., KOBOLÁK, J. & DINNYÉS, A. 2017. Neurons derived from sporadic Alzheimer's disease iPSCs reveal elevated TAU hyperphosphorylation, increased amyloid levels, and GSK3B activation. *Alzheimers Res Ther,* 9**,** 90.

OIKAWA, N. & WALTER, J. 2019. Presenilins and γ-Secretase in Membrane Proteostasis. *Cells,* 8.

OKITA, K., MATSUMURA, Y., SATO, Y., OKADA, A., MORIZANE, A., OKAMOTO, S., HONG, H., NAKAGAWA, M., TANABE, K., TEZUKA, K., SHIBATA, T., KUNISADA, T., TAKAHASHI, M.,

TAKAHASHI, J., SAJI, H. & YAMANAKA, S. 2011. A more efficient method to generate integration-free human iPS cells. *Nat Methods,* 8**,** 409-12.

OKSANEN, M., PETERSEN, A. J., NAUMENKO, N., PUTTONEN, K., LEHTONEN, Š., GUBERT OLIVÉ, M., SHAKIRZYANOVA, A., LESKELÄ, S., SARAJÄRVI, T., VIITANEN, M., RINNE, J. O., HILTUNEN, M., HAAPASALO, A., GINIATULLIN, R., TAVI, P., ZHANG, S. C., KANNINEN, K. M., HÄMÄLÄINEN, R. H. & KOISTINAHO, J. 2017. PSEN1 Mutant iPSC-Derived Model Reveals Severe Astrocyte Pathology in Alzheimer's Disease. *Stem Cell Reports,* 9**,** 1885-1897.

OKU, Y., MURAKAMI, K., IRIE, K., HOSEKI, J. & SAKAI, Y. 2017. Synthesized Aβ42 Caused Intracellular Oxidative Damage, Leading to Cell Death, via Lysosome Rupture. *Cell Struct Funct,* 42**,** 71-79.

OKUNO, Y., FUKUHARA, A., HASHIMOTO, E., KOBAYASHI, H., KOBAYASHI, S., OTSUKI, M. & SHIMOMURA, I. 2018. Oxidative Stress Inhibits Healthy Adipose Expansion Through Suppression of SREBF1-Mediated Lipogenic Pathway. *Diabetes,* 67**,** 1113-1127.

OLSSON, B., LAUTNER, R., ANDREASSON, U., ÖHRFELT, A., PORTELIUS, E., BJERKE, M., HÖLTTÄ, M., ROSÉN, C., OLSSON, C., STROBEL, G., WU, E., DAKIN, K., PETZOLD, M., BLENNOW, K. & ZETTERBERG, H. 2016. CSF and blood biomarkers for the diagnosis of Alzheimer's disease: a systematic review and meta-analysis. *Lancet Neurol,* 15**,** 673-684.

OSTROWITZKI, S., LASSER, R. A., DORFLINGER, E., SCHELTENS, P., BARKHOF, F., NIKOLCHEVA, T., ASHFORD, E., RETOUT, S., HOFMANN, C., DELMAR, P., KLEIN, G., ANDJELKOVIC, M., DUBOIS, B., BOADA, M., BLENNOW, K., SANTARELLI, L., FONTOURA, P. & INVESTIGATORS, S. R. 2017. A phase III randomized trial of gantenerumab in prodromal Alzheimer's disease. *Alzheimers Res Ther,* 9**,** 95.

OSWALD, M. C. W., GARNHAM, N., SWEENEY, S. T. & LANDGRAF, M. 2018. Regulation of neuronal development and function by ROS. *FEBS Lett,* 592**,** 679-691.

PAGANI, M., DE CARLI, F., MORBELLI, S., ÖBERG, J., CHINCARINI, A., FRISONI, G. B., GALLUZZI, S., PERNECZKY, R., DRZEZGA, A., VAN BERCKEL, B. N., OSSENKOPPELE, R., DIDIC, M., GUEDJ, E., BRUGNOLO, A., PICCO, A., ARNALDI, D., FERRARA, M., BUSCHIAZZO, A., SAMBUCETI, G. & NOBILI, F. 2015. Volume of interest-based [18F]fluorodeoxyglucose PET discriminates MCI converting to Alzheimer's disease from healthy controls. A European Alzheimer's Disease Consortium (EADC) study. *Neuroimage Clin,* 7**,** 34-42.

PALMQVIST, S., INSEL, P. S., ZETTERBERG, H., BLENNOW, K., BRIX, B., STOMRUD, E., MATTSSON, N., HANSSON, O., INITIATIVE, A. S. D. N. & STUDY, S. B. 2019. Accurate risk estimation of β-amyloid positivity to identify prodromal Alzheimer's disease: Cross-validation study of practical algorithms. *Alzheimers Dement,* 15**,** 194-204.

PALTA, P., SHARRETT, A. R., DEAL, J. A., EVENSON, K. R., GABRIEL, K. P., FOLSOM, A. R., GROSS, A. L., WINDHAM, B. G., KNOPMAN, D., MOSLEY, T. H. & HEISS, G. 2019. Leisure-time physical activity sustained since midlife and preservation of cognitive function: The Atherosclerosis Risk in Communities Study. *Alzheimers Dement,* 15**,** 273-281.

PANNEE, J., PORTELIUS, E., MINTHON, L., GOBOM, J., ANDREASSON, U., ZETTERBERG, H., HANSSON, O. & BLENNOW, K. 2016. Reference measurement procedure for CSF amyloid beta (Aβ). *J Neurochem,* 139**,** 651-658.

PASE, M. P., BEISER, A. S., HIMALI, J. J., SATIZABAL, C. L., APARICIO, H. J., DECARLI, C., CHÊNE, G., DUFOUIL, C. & SESHADRI, S. 2019. Assessment of Plasma Total Tau Level as a Predictive Biomarker for Dementia and Related Endophenotypes. *JAMA Neurol,* 76**,** 598-606.

PATTERSON, D., GARDINER, K., KAO, F. T., TANZI, R., WATKINS, P. & GUSELLA, J. F. 1988. Mapping of the gene encoding the beta-amyloid precursor protein and its relationship to the Down syndrome region of chromosome 21. *Proc Natl Acad Sci U S A,* 85**,** 8266-70.

PELTON, G. H., HARPER, O. L., ROOSE, S. P., MARDER, K., D'ANTONIO, K. & DEVANAND, D. P. 2016. Combined treatment with memantine/es-citalopram for older depressed patients with cognitive impairment: a pilot study. *Int J Geriatr Psychiatry,* 31**,** 648-55.

PEREZ ORTIZ, J. M. & SWERDLOW, R. H. 2019. Mitochondrial dysfunction in Alzheimer's disease: Role in pathogenesis and novel therapeutic opportunities. *Br J Pharmacol,* 176**,** 3489-3507.

PERLUIGI, M., SULTANA, R., CENINI, G., DI DOMENICO, F., MEMO, M., PIERCE, W. M., COCCIA, R. & BUTTERFIELD, D. A. 2009. Redox proteomics identification of 4-hydroxynonenal-modified brain proteins in Alzheimer's disease: Role of lipid peroxidation in Alzheimer's disease pathogenesis. *Proteomics Clin Appl,* 3**,** 682-693.

PERROTTE, M., LE PAGE, A., FOURNET, M., LE SAYEC, M., RASSART, E., FULOP, T. & RAMASSAMY, C. 2019. Blood-based redox-signature and their association to the cognitive scores in MCI and Alzheimer's disease patients. *Free Radical Biology and Medicine,* 130**,** 499-511.

PERRY, G., CASH, A. D. & SMITH, M. A. 2002. Alzheimer Disease and Oxidative Stress. *J Biomed Biotechnol,* 2**,** 120-123.

PETERS, C., BASCUÑÁN, D., OPAZO, C. & AGUAYO, L. G. 2016. Differential Membrane Toxicity of Amyloid-β Fragments by Pore Forming Mechanisms. *J Alzheimers Dis,* 51**,** 689-99.

PETERS-LIBEU, C., CAMPAGNA, J., MITSUMORI, M., POKSAY, K. S., SPILMAN, P., SABOGAL, A., BREDESEN, D. E. & JOHN, V. 2015. sAβPPα is a Potent Endogenous Inhibitor of BACE1. *J Alzheimers Dis,* 47**,** 545-55.

PETERSEN, R. C., LUNDT, E. S., THERNEAU, T. M., WEIGAND, S. D., KNOPMAN, D. S., MIELKE, M. M., ROBERTS, R. O., LOWE, V. J., MACHULDA, M. M., KREMERS, W. K., GEDA, Y. E. & JACK, C. R. 2019. Predicting Progression to Mild Cognitive Impairment. *Ann Neurol,* 85**,** 155-160.

PEÑA-BAUTISTA, C., BAQUERO, M., LÓPEZ-NOGUEROLES, M., VENTO, M., HERVÁS, D. & CHÁFER-PERICÁS, C. 2020. Isoprostanoids Levels in Cerebrospinal Fluid Do Not Reflect Alzheimer's Disease. *Antioxidants (Basel),* 9.

PEÑA-BAUTISTA, C., VIGOR, C., GALANO, J. M., OGER, C., DURAND, T., FERRER, I., CUEVAS, A., LÓPEZ-CUEVAS, R., BAQUERO, M., LÓPEZ-NOGUEROLES, M., VENTO, M., HERVÁS, D., GARCÍA-BLANCO, A. & CHÁFER-PERICÁS, C. 2018. Plasma lipid peroxidation biomarkers for early and non-invasive Alzheimer Disease detection. *Free Radic Biol Med,* 124**,** 388-394.

PICKETT, E. K., KOFFIE, R. M., WEGMANN, S., HENSTRIDGE, C. M., HERRMANN, A. G., COLOM-CADENA, M., LLEO, A., KAY, K. R., VAUGHT, M., SOBERMAN, R., WALSH, D. M., HYMAN, B. T. & SPIRES-JONES, T. L. 2016. Non-Fibrillar Oligomeric Amyloid-β within Synapses. *J Alzheimers Dis,* 53**,** 787-800.

PICONE, P., DI CARLO, M. & NUZZO, D. 2020. Obesity and Alzheimer's disease: Molecular bases. *Eur J Neurosci*.

PIMENOVA, A. A., RAJ, T. & GOATE, A. M. 2018. Untangling Genetic Risk for Alzheimer's Disease. *Biol Psychiatry,* 83**,** 300-310.

PIRES, C., SCHMID, B., PETRÆUS, C., POON, A., NIMSANOR, N., NIELSEN, T. T., WALDEMAR, G., HJERMIND, L. E., NIELSEN, J. E., HYTTEL, P. & FREUDE, K. K. 2016. Generation of a gene-corrected isogenic control cell line from an Alzheimer's disease patient iPSC line carrying a A79V mutation in PSEN1. *Stem Cell Res,* 17**,** 285-288.

PLASSMAN, B. L., LANGA, K. M., FISHER, G. G., HEERINGA, S. G., WEIR, D. R., OFSTEDAL, M. B., BURKE, J. R., HURD, M. D., POTTER, G. G., RODGERS, W. L., STEFFENS, D. C., WILLIS, R. J. & WALLACE, R. B. 2007. Prevalence of dementia in the United States: the aging, demographics, and memory study. *Neuroepidemiology,* 29**,** 125-32.

PLUMMER, S., VAN DEN HEUVEL, C., THORNTON, E., CORRIGAN, F. & CAPPAI, R. 2016. The Neuroprotective Properties of the Amyloid Precursor Protein Following Traumatic Brain Injury. *Aging Dis,* 7**,** 163-79.

POON, A., LI, T., PIRES, C., NIELSEN, T. T., NIELSEN, J. E., HOLST, B., DINNYES, A., HYTTEL, P. & FREUDE, K. K. 2016. Derivation of induced pluripotent stem cells from a familial Alzheimer's disease patient carrying the L282F mutation in presenilin 1. *Stem Cell Res,* 17**,** 470-473.

POON, W. W., CARLOS, A. J., AGUILAR, B. L., BERCHTOLD, N. C., KAWANO, C. K., ZOGRABYAN, V., YAOPRUKE, T., SHELANSKI, M. & COTMAN, C. W. 2013. β-Amyloid (Aβ) oligomers impair brain-derived neurotrophic factor retrograde trafficking by down-regulating ubiquitin C-terminal hydrolase, UCH-L1. *J Biol Chem,* 288**,** 16937-48.

POSTINA, R., SCHROEDER, A., DEWACHTER, I., BOHL, J., SCHMITT, U., KOJRO, E., PRINZEN, C., ENDRES, K., HIEMKE, C., BLESSING, M., FLAMEZ, P., DEQUENNE, A., GODAUX, E., VAN LEUVEN, F. & FAHRENHOLZ, F. 2004. A disintegrin-metalloproteinase prevents amyloid plaque formation and hippocampal defects in an Alzheimer disease mouse model. *J Clin Invest,* 113**,** 1456-64.

POTTER, R., PATTERSON, B. W., ELBERT, D. L., OVOD, V., KASTEN, T., SIGURDSON, W., MAWUENYEGA, K., BLAZEY, T., GOATE, A., CHOTT, R., YARASHESKI, K. E., HOLTZMAN, D. M., MORRIS, J. C., BENZINGER, T. L. & BATEMAN, R. J. 2013. Increased in vivo amyloid-β42 production, exchange, and loss in presenilin mutation carriers. *Sci Transl Med,* 5**,** 189ra77.

POULSEN, E. T., IANNUZZI, F., RASMUSSEN, H. F., MAIER, T. J., ENGHILD, J. J., JØRGENSEN, A. L. & MATRONE, C. 2017. An Aberrant Phosphorylation of Amyloid Precursor Protein Tyrosine Regulates Its Trafficking and the Binding to the Clathrin Endocytic Complex in Neural Stem Cells of Alzheimer's Disease Patients. *Front Mol Neurosci,* 10**,** 59.

PRATICÒ, D., MY LEE, V., TROJANOWSKI, J. Q., ROKACH, J. & FITZGERALD, G. A. 1998. Increased F2-isoprostanes in Alzheimer's disease: evidence for enhanced lipid peroxidation in vivo. *FASEB J,* 12**,** 1777-83.

PRINCE, M., ALI, G., GUERCHET, M., PRINA, A. M., ALBANESE, E. & WU, Y. 2016. Recent global trends in the prevalence and incidence of dementia, and survival with dementia. *Alzheimer's Research & Therapy,* 8**,** 23.

PROX, J., WILLENBROCK, M., WEBER, S., LEHMANN, T., SCHMIDT-ARRAS, D., SCHWANBECK, R., SAFTIG, P. & SCHWAKE, M. 2012. Tetraspanin15 regulates cellular trafficking and activity of the ectodomain sheddase ADAM10. *Cell Mol Life Sci,* 69**,** 2919-32.

PÁKÁSKI, M., BJELIK, A., HUGYECZ, M., KÁSA, P., JANKA, Z. & KÁLMÁN, J. 2005. Imipramine and citalopram facilitate amyloid precursor protein secretion in vitro. *Neurochem Int,* 47**,** 190-5.

QIAN, M., SHEN, X. & WANG, H. 2016. The Distinct Role of ADAM17 in APP Proteolysis and Microglial Activation Related to Alzheimer's Disease. *Cell Mol Neurobiol,* 36**,** 471-82.

QIU, T., LIU, Q., CHEN, Y. X., ZHAO, Y. F. & LI, Y. M. 2015. Aβ42 and Aβ40: similarities and differences. *J Pept Sci,* 21**,** 522-9.

RACINE, A. M., KOSCIK, R. L., BERMAN, S. E., NICHOLAS, C. R., CLARK, L. R., OKONKWO, O. C., ROWLEY, H. A., ASTHANA, S., BENDLIN, B. B., BLENNOW, K., ZETTERBERG, H., GLEASON, C. E., CARLSSON, C. M. & JOHNSON, S. C. 2016. Biomarker clusters are differentially associated with longitudinal cognitive decline in late midlife. *Brain,* 139**,** 2261-74.

RADI, R. 2018. Oxygen radicals, nitric oxide, and peroxynitrite: Redox pathways in molecular medicine. *Proc Natl Acad Sci U S A,* 115**,** 5839-5848.

RAFII, M. S. & AISEN, P. S. 2019. Alzheimer's Disease Clinical Trials: Moving Toward Successful Prevention. *CNS Drugs,* 33**,** 99-106.

RANA, M. & SHARMA, A. K. 2019. Cu and Zn interactions with Aβ peptides: consequence of coordination on aggregation and formation of neurotoxic soluble Aβ oligomers. *Metallomics,* 11**,** 64-84.

RAY, S., BRITSCHGI, M., HERBERT, C., TAKEDA-UCHIMURA, Y., BOXER, A., BLENNOW, K., FRIEDMAN, L. F., GALASKO, D. R., JUTEL, M., KARYDAS, A., KAYE, J. A., LESZEK, J., MILLER, B. L., MINTHON, L., QUINN, J. F., RABINOVICI, G. D., ROBINSON, W. H., SABBAGH, M. N., SO, Y. T., SPARKS, D. L., TABATON, M., TINKLENBERG, J., YESAVAGE, J. A., TIBSHIRANI, R. & WYSS-CORAY, T. 2007. Classification and prediction of clinical Alzheimer's diagnosis based on plasma signaling proteins. *Nat Med,* 13**,** 1359-62.

REED, T., PERLUIGI, M., SULTANA, R., PIERCE, W. M., KLEIN, J. B., TURNER, D. M., COCCIA, R., MARKESBERY, W. R. & BUTTERFIELD, D. A. 2008. Redox proteomic identification of 4-hydroxy-2-nonenal-modified brain proteins in amnestic mild cognitive impairment: insight into the role of lipid peroxidation in the progression and pathogenesis of Alzheimer's disease. *Neurobiol Dis,* 30**,** 107-20.

RESENDE, R., FERREIRO, E., PEREIRA, C. & RESENDE DE OLIVEIRA, C. 2008. Neurotoxic effect of oligomeric and fibrillar species of amyloid-beta peptide 1-42: involvement of endoplasmic reticulum calcium release in oligomer-induced cell death. *Neuroscience,* 155**,** 725-37.

REYNOLDS, D. S. 2019. A short perspective on the long road to effective treatments for Alzheimer's disease. *Br J Pharmacol,* 176**,** 3636-3648.

REZAZADEH, M., HOSSEINZADEH, H., MORADI, M., SALEK ESFAHANI, B., TALEBIAN, S., PARVIN, S. & GHARESOURAN, J. 2019. Genetic discoveries and advances in late-onset Alzheimer's disease. *J Cell Physiol*.

RIDHA, B. H., BARNES, J., BARTLETT, J. W., GODBOLT, A., PEPPLE, T., ROSSOR, M. N. & FOX, N. C. 2006. Tracking atrophy progression in familial Alzheimer's disease: a serial MRI study. *Lancet Neurol,* 5**,** 828-34.

RINGMAN, J. M., COPPOLA, G., ELASHOFF, D., RODRIGUEZ-AGUDELO, Y., MEDINA, L. D., GYLYS, K., CUMMINGS, J. L. & COLE, G. M. 2012a. Cerebrospinal fluid biomarkers and proximity to diagnosis in preclinical familial Alzheimer's disease. *Dement Geriatr Cogn Disord,* 33**,** 1-5.

RINGMAN, J. M., TOMIC, J. L., COPPOLA, G., ELASHOFF, D., GYLYS, K. H. & GLABE, C. G. 2012b. Conformation-dependent oligomers in cerebrospinal fluid of presymptomatic familial Alzheimer's disease mutation carriers. *Dement Geriatr Cogn Dis Extra,* 2**,** 652-7.

ROBERT, S., MAILLET, M., MOREL, E., LAUNAY, J. M., FISCHMEISTER, R., MERCKEN, L. & LEZOUALC'H, F. 2005. Regulation of the amyloid precursor protein ectodomain shedding by the 5-HT4 receptor and Epac. *FEBS Lett,* 579**,** 1136-42.

ROBINSON, S. R., BISHOP, G. M., LEE, H. G. & MÜNCH, G. 2004. Lessons from the AN 1792 Alzheimer vaccine: lest we forget. *Neurobiol Aging,* 25**,** 609-15.

RODRÍGUEZ-ARELLANO, J. J., PARPURA, V., ZOREC, R. & VERKHRATSKY, A. 2016. Astrocytes in physiological aging and Alzheimer's disease. *Neuroscience,* 323**,** 170-82.

ROGAEV, E. I., SHERRINGTON, R., ROGAEVA, E. A., LEVESQUE, G., IKEDA, M., LIANG, Y., CHI, H., LIN, C., HOLMAN, K. & TSUDA, T. 1995. Familial Alzheimer's disease in kindreds with missense mutations in a gene on chromosome 1 related to the Alzheimer's disease type 3 gene. *Nature,* 376**,** 775-8.

ROSENBLUM, W. I. 2014. Why Alzheimer trials fail: removing soluble oligomeric beta amyloid is essential, inconsistent, and difficult. *Neurobiol Aging,* 35**,** 969-74.

ROSES, A. D. 1994. Apolipoprotein E affects the rate of Alzheimer disease expression: beta-amyloid burden is a secondary consequence dependent on APOE genotype and duration of disease. *J Neuropathol Exp Neurol,* 53**,** 429-37.

ROVELET-LECRUX, A., HANNEQUIN, D., RAUX, G., LE MEUR, N., LAQUERRIÈRE, A., VITAL, A., DUMANCHIN, C., FEUILLETTE, S., BRICE, A., VERCELLETTO, M., DUBAS, F., FREBOURG, T. & CAMPION, D. 2006. APP locus duplication causes autosomal dominant early-onset Alzheimer disease with cerebral amyloid angiopathy. *Nat Genet,* 38**,** 24-6.

RUDENKO, L. K., WALLRABE, H., PERIASAMY, A., SILLER, K. H., SVINDRYCH, Z., SEWARD, M. E., BEST, M. N. & BLOOM, G. S. 2019. Intraneuronal Tau Misfolding Induced by Extracellular Amyloid-β Oligomers. *J Alzheimers Dis,* 71**,** 1125-1138.

RUSHWORTH, J. V. & HOOPER, N. M. 2010. Lipid Rafts: Linking Alzheimer's Amyloid-β Production, Aggregation, and Toxicity at Neuronal Membranes. *Int J Alzheimers Dis,* 2011**,** 603052.

RYAN, N. S., NICHOLAS, J. M., WESTON, P. S. J., LIANG, Y., LASHLEY, T., GUERREIRO, R., ADAMSON, G., KENNY, J., BECK, J., CHAVEZ-GUTIERREZ, L., DE STROOPER, B., REVESZ, T., HOLTON, J., MEAD, S., ROSSOR, M. N. & FOX, N. C. 2016. Clinical phenotype and genetic associations in autosomal dominant familial Alzheimer's disease: a case series. *Lancet Neurol,* 15**,** 1326-1335.

SAKONO, M. & ZAKO, T. 2010. Amyloid oligomers: formation and toxicity of Abeta oligomers. *FEBS J,* 277**,** 1348-58.

SALAHUDDIN, P., FATIMA, M. T., ABDELHAMEED, A. S., NUSRAT, S. & KHAN, R. H. 2016. Structure of amyloid oligomers and their mechanisms of toxicities: Targeting amyloid oligomers using novel therapeutic approaches. *Eur J Med Chem,* 114**,** 41-58.

SALAZAR, S. V. & STRITTMATTER, S. M. 2017. Cellular prion protein as a receptor for amyloid-β oligomers in Alzheimer's disease. *Biochem Biophys Res Commun,* 483**,** 1143-1147.

SALTIEL, A. R. & OLEFSKY, J. M. 2017. Inflammatory mechanisms linking obesity and metabolic disease. *J Clin Invest,* 127**,** 1-4.

SAMPAIO, A., MARQUES, E. A., MOTA, J. & CARVALHO, J. 2019. Effects of a multicomponent exercise program in institutionalized elders with Alzheimer's disease. *Dementia (London),* 18**,** 417-431.

SANDELIUS, Å., PORTELIUS, E., KÄLLÉN, Å., ZETTERBERG, H., ROT, U., OLSSON, B., TOLEDO, J. B., SHAW, L. M., LEE, V. M. Y., IRWIN, D. J., GROSSMAN, M., WEINTRAUB, D., CHEN-PLOTKIN, A., WOLK, D. A., MCCLUSKEY, L., ELMAN, L., KOSTANJEVECKI, V., VANDIJCK, M., MCBRIDE, J., TROJANOWSKI, J. Q. & BLENNOW, K. 2019. Elevated CSF GAP-43 is Alzheimer's disease specific and associated with tau and amyloid pathology. *Alzheimers Dement,* 15**,** 55-64.

SARASIJA, S. & NORMAN, K. R. 2018. Role of Presenilin in Mitochondrial Oxidative Stress and Neurodegeneration in. *Antioxidants (Basel),* 7.

SATLIN, A., WANG, J., LOGOVINSKY, V., BERRY, S., SWANSON, C., DHADDA, S. & BERRY, D. A. 2016. Design of a Bayesian adaptive phase 2 proof-of-concept trial for BAN2401, a putative disease-modifying monoclonal antibody for the treatment of Alzheimer's disease. *Alzheimers Dement (N Y),* 2**,** 1-12.

SCHEDIN-WEISS, S., WINBLAD, B. & TJERNBERG, L. O. 2014. The role of protein glycosylation in Alzheimer disease. *FEBS J,* 281**,** 46-62.

SCHEFF, S. W., ANSARI, M. A. & MUFSON, E. J. 2016. Oxidative stress and hippocampal synaptic protein levels in elderly cognitively intact individuals with Alzheimer's disease pathology. *Neurobiol Aging,* 42**,** 1-12.

SCHELLENBERG, G. D., BIRD, T. D., WIJSMAN, E. M., ORR, H. T., ANDERSON, L., NEMENS, E., WHITE, J. A., BONNYCASTLE, L., WEBER, J. L. & ALONSO, M. E. 1992. Genetic linkage evidence for a familial Alzheimer's disease locus on chromosome 14. *Science,* 258**,** 668-71.

SCHUCK, F., WOLF, D., FELLGIEBEL, A. & ENDRES, K. 2016. Increase of α-Secretase ADAM10 in Platelets Along Cognitively Healthy Aging. *J Alzheimers Dis,* 50**,** 817-26.

SCIACCA, M. F., KOTLER, S. A., BRENDER, J. R., CHEN, J., LEE, D. K. & RAMAMOORTHY, A. 2012. Two-step mechanism of membrane disruption by Aβ through membrane fragmentation and pore formation. *Biophys J,* 103**,** 702-10.

SEIFERT, A., DÜSTERHÖFT, S., WOZNIAK, J., KOO, C. Z., TOMLINSON, M. G., NUTI, E., ROSSELLO, A., CUFFARO, D., YILDIZ, D. & LUDWIG, A. 2020. The metalloproteinase ADAM10 requires its activity to sustain surface expression. *Cell Mol Life Sci*.

SEIPOLD, L., DAMME, M., PROX, J., RABE, B., KASPAREK, P., SEDLACEK, R., ALTMEPPEN, H., WILLEM, M., BOLAND, B., GLATZEL, M. & SAFTIG, P. 2017. Tetraspanin 3: A central endocytic membrane component regulating the expression of ADAM10, presenilin and the amyloid precursor protein. *Biochim Biophys Acta Mol Cell Res,* 1864**,** 217-230.

SEIPOLD, L. & SAFTIG, P. 2016. The Emerging Role of Tetraspanins in the Proteolytic Processing of the Amyloid Precursor Protein. *Front Mol Neurosci,* 9**,** 149.

SEITZ, D. P., CHAN, C. C., NEWTON, H. T., GILL, S. S., HERRMANN, N., SMAILAGIC, N., NIKOLAOU, V. & FAGE, B. A. 2018. Mini-Cog for the diagnosis of Alzheimer's disease dementia and other dementias within a primary care setting. *Cochrane Database Syst Rev,* 2**,** CD011415.

SELKOE, D. J. & HARDY, J. 2016. The amyloid hypothesis of Alzheimer's disease at 25 years. *EMBO Mol Med,* 8**,** 595-608.

SEPEHRY, A. A., LEE, P. E., HSIUNG, G. Y., BEATTIE, B. L. & JACOVA, C. 2012. Effect of selective serotonin reuptake inhibitors in Alzheimer's disease with comorbid depression: a meta-analysis of depression and cognitive outcomes. *Drugs Aging,* 29**,** 793-806.

SEPEHRY, A. A., LIU, G., DUJELA, C., KEDLAC, H., BEATTIE, B. L., CHAPPELL, N. L. & HSIUNG, G. Y. R. 2016. Medications for depression in alzheimer's and risk of mortality: a longitudinal observational study from the adti. *Alzheimer's and Dementia,* 12**,** 801.

SERRANO-POZO, A. & GROWDON, J. H. 2019. Is Alzheimer's Disease Risk Modifiable? *J Alzheimers Dis,* 67**,** 795-819.

SEVERINO, M., SIVASARAVANAPARAN, M., OLESEN, L., VON LINSTOW, C. U., METAXAS, A., BOUZINOVA, E. V., KHAN, A. M., LAMBERTSEN, K. L., BABCOCK, A. A., GRAMSBERGEN, J. B., WIBORG, O. & FINSEN, B. 2018. Established amyloid-β pathology is unaffected by chronic treatment with the selective serotonin reuptake inhibitor paroxetine. *Alzheimers Dement (N Y),* 4**,** 215-223.

SHANBHAG, N. M., EVANS, M. D., MAO, W., NANA, A. L., SEELEY, W. W., ADAME, A., RISSMAN, R. A., MASLIAH, E. & MUCKE, L. 2019. Early neuronal accumulation of DNA double strand breaks in Alzheimer's disease. *Acta Neuropathol Commun,* 7**,** 77.

SHELINE, Y. I., WEST, T., YARASHESKI, K., SWARM, R., JASIELEC, M. S., FISHER, J. R., FICKER, W. D., YAN, P., XIONG, C., FREDERIKSEN, C., GRZELAK, M. V., CHOTT, R., BATEMAN, R. J., MORRIS, J. C., MINTUN, M. A., LEE, J. M. & CIRRITO, J. R. 2014. An antidepressant decreases CSF Aβ production in healthy individuals and in transgenic AD mice. *Sci Transl Med,* 6**,** 236re4.

SHERRINGTON, R., FROELICH, S., SORBI, S., CAMPION, D., CHI, H., ROGAEVA, E. A., LEVESQUE, G., ROGAEV, E. I., LIN, C., LIANG, Y., IKEDA, M., MAR, L., BRICE, A., AGID, Y., PERCY, M. E., CLERGET-DARPOUX, F., PIACENTINI, S., MARCON, G., NACMIAS, B., AMADUCCI, L., FREBOURG, T., LANNFELT, L., ROMMENS, J. M. & ST GEORGE-HYSLOP, P. H. 1996. Alzheimer's disease associated with mutations in presenilin 2 is rare and variably penetrant. *Hum Mol Genet,* 5**,** 985-8.

SHI, Y., KIRWAN, P. & LIVESEY, F. J. 2012. Directed differentiation of human pluripotent stem cells to cerebral cortex neurons and neural networks. *Nat Protoc,* 7**,** 1836-46.

SIES, H., BERNDT, C. & JONES, D. P. 2017. Oxidative Stress. *Annu Rev Biochem,* 86**,** 715-748.

SIES, H. & JONES, D. P. 2020. Reactive oxygen species (ROS) as pleiotropic physiological signalling agents. *Nat Rev Mol Cell Biol*.

SINEM, F., DILDAR, K., GÖKHAN, E., MELDA, B., ORHAN, Y. & FILIZ, M. 2010. The serum protein and lipid oxidation marker levels in Alzheimer's disease and effects of cholinesterase inhibitors and antipsychotic drugs therapy. *Curr Alzheimer Res,* 7**,** 463-9.

SINGH, M., DANG, T. N., ARSENEAULT, M. & RAMASSAMY, C. 2010. Role of by-products of lipid oxidation in Alzheimer's disease brain: a focus on acrolein. *J Alzheimers Dis,* 21**,** 741-56.

SIVERA, R., DELINGETTE, H., LORENZI, M., PENNEC, X., AYACHE, N. & INITIATIVE, A. S. D. N. 2019. A model of brain morphological changes related to aging and Alzheimer's disease from cross-sectional assessments. *Neuroimage,* 198**,** 255-270.

SKOUMALOVÁ, A. & HORT, J. 2012. Blood markers of oxidative stress in Alzheimer's disease. *J Cell Mol Med,* 16**,** 2291-300.

SMALL, D. H. & CAPPAI, R. 2006. Alois Alzheimer and Alzheimer's disease: a centennial perspective. *J Neurochem,* 99**,** 708-10.

SMITH, L. M. & STRITTMATTER, S. M. 2017. Binding Sites for Amyloid-β Oligomers and Synaptic Toxicity. *Cold Spring Harb Perspect Med,* 7.

SMITH, M. A., ATWOOD, C. S., JOSEPH, J. A. & PERRY, G. 2002. Predicting the failure of amyloid-beta vaccine. *Lancet,* 359**,** 1864-5.

SMITH, M. A., ROTTKAMP, C. A., NUNOMURA, A., RAINA, A. K. & PERRY, G. 2000. Oxidative stress in Alzheimer's disease. *Biochim Biophys Acta,* 1502**,** 139-44.

SMITH, P. K., KROHN, R. I., HERMANSON, G. T., MALLIA, A. K., GARTNER, F. H., PROVENZANO, M. D., FUJIMOTO, E. K., GOEKE, N. M., OLSON, B. J. & KLENK, D. C. 1985. Measurement of protein using bicinchoninic acid. *Anal Biochem,* 150**,** 76-85.

SMITH, T. M., THARAKAN, A. & MARTIN, R. K. 2020. Targeting ADAM10 in Cancer and Autoimmunity. *Front Immunol,* 11**,** 499.

SPERLING, R. A., MORMINO, E. C., SCHULTZ, A. P., BETENSKY, R. A., PAPP, K. V., AMARIGLIO, R. E., HANSEEUW, B. J., BUCKLEY, R., CHHATWAL, J., HEDDEN, T., MARSHALL, G. A., QUIROZ, Y. T., DONOVAN, N. J., JACKSON, J., GATCHEL, J. R., RABIN, J. S., JACOBS, H., YANG, H. S., PROPERZI, M., KIRN, D. R., RENTZ, D. M. & JOHNSON, K. A. 2019. The impact of amyloid-beta and tau on prospective cognitive decline in older individuals. *Ann Neurol,* 85**,** 181-193.

SPROUL, A. A., JACOB, S., PRE, D., KIM, S. H., NESTOR, M. W., NAVARRO-SOBRINO, M., SANTA-MARIA, I., ZIMMER, M., AUBRY, S., STEELE, J. W., KAHLER, D. J., DRANOVSKY, A., ARANCIO, O., CRARY, J. F., GANDY, S. & NOGGLE, S. A. 2014. Characterization and molecular profiling of PSEN1 familial Alzheimer's disease iPSC-derived neural progenitors. *PLoS One,* 9**,** e84547.

STEINER, H., FUKUMORI, A., TAGAMI, S. & OKOCHI, M. 2018. Making the final cut: pathogenic amyloid-β peptide generation by γ-secretase. *Cell Stress,* 2**,** 292-310.

STELLOS, K., PANAGIOTA, V., KÖGEL, A., LEYHE, T., GAWAZ, M. & LASKE, C. 2010. Predictive value of platelet activation for the rate of cognitive decline in Alzheimer's disease patients. *J Cereb Blood Flow Metab,* 30**,** 1817-20.

STOLARCZYK, E. 2017. Adipose tissue inflammation in obesity: a metabolic or immune response? *Curr Opin Pharmacol,* 37**,** 35-40.

STRITTMATTER, W. J., SAUNDERS, A. M., SCHMECHEL, D., PERICAK-VANCE, M., ENGHILD, J., SALVESEN, G. S. & ROSES, A. D. 1993. Apolipoprotein E: high-avidity binding to beta-amyloid and increased frequency of type 4 allele in late-onset familial Alzheimer disease. *Proc Natl Acad Sci U S A,* 90**,** 1977-81.

STROBEL, S., GRÜNBLATT, E., HEINSEN, H., RIEDERER, P., ESPACH, T., MEDER, M. & MONORANU, C. M. 2019. Astrocyte- and Microglia-Specific Mitochondrial DNA Deletions Levels in Sporadic Alzheimer's Disease. *J Alzheimers Dis,* 67**,** 149-157.

SUH, J., CHOI, S. H., ROMANO, D. M., GANNON, M. A., LESINSKI, A. N., KIM, D. Y. & TANZI, R. E. 2013. ADAM10 missense mutations potentiate β-amyloid accumulation by impairing prodomain chaperone function. *Neuron,* 80**,** 385-401.

SULTANA, R., PERLUIGI, M., NEWMAN, S. F., PIERCE, W. M., CINI, C., COCCIA, R. & BUTTERFIELD, D. A. 2010. Redox proteomic analysis of carbonylated brain proteins in mild cognitive impairment and early Alzheimer's disease. *Antioxid Redox Signal,* 12**,** 327-36.

SUN, D. S., GAO, L. F., JIN, L., WU, H., WANG, Q., ZHOU, Y., FAN, S., JIANG, X., KE, D., LEI, H., WANG, J. Z. & LIU, G. P. 2017a. Fluoxetine administration during adolescence attenuates cognitive and synaptic deficits in adult 3×TgAD mice. *Neuropharmacology,* 126**,** 200-212.

SUN, J. & ROY, S. 2018. The physical approximation of APP and BACE-1: A key event in alzheimer's disease pathogenesis. *Dev Neurobiol,* 78**,** 340-347.

SUN, L., ZHOU, R., YANG, G. & SHI, Y. 2017b. Analysis of 138 pathogenic mutations in presenilin-1 on the in vitro production of Aβ42 and Aβ40 peptides by γ-secretase. *Proc Natl Acad Sci U S A,* 114**,** E476-E485.

SUN, X., WANG, Y., QING, H., CHRISTENSEN, M. A., LIU, Y., ZHOU, W., TONG, Y., XIAO, C., HUANG, Y., ZHANG, S., LIU, X. & SONG, W. 2005. Distinct transcriptional regulation and function of the human BACE2 and BACE1 genes. *FASEB J,* 19**,** 739-49.

SUN, Z., WANG, Z. T., SUN, F. R., SHEN, X. N., XU, W., MA, Y. H., DONG, Q., TAN, L., YU, J. T. & INITIATIVE, A. S. D. N. 2020. Late-life obesity is a protective factor for prodromal Alzheimer's disease: a longitudinal study. *Aging (Albany NY),* 12**,** 2005-2017.

SWERDLOW, R. H. & KHAN, S. M. 2004. A "mitochondrial cascade hypothesis" for sporadic Alzheimer's disease. *Med Hypotheses,* 63**,** 8-20.

TAGAMI, S., YANAGIDA, K., KODAMA, T. S., TAKAMI, M., MIZUTA, N., OYAMA, H., NISHITOMI, K., CHIU, Y. W., OKAMOTO, T., IKEUCHI, T., SAKAGUCHI, G., KUDO, T., MATSUURA, Y., FUKUMORI, A., TAKEDA, M., IHARA, Y. & OKOCHI, M. 2017. Semagacestat Is a Pseudo-Inhibitor of γ-Secretase. *Cell Rep,* 21**,** 259-273.

TAJEDDINN, W., FERESHTEHNEJAD, S. M., SEED AHMED, M., YOSHITAKE, T., KEHR, J., SHAHNAZ, T., MILOVANOVIC, M., BEHBAHANI, H., HÖGLUND, K., WINBLAD, B., CEDAZO-MINGUEZ, A., JELIC, V., JÄREMO, P. & AARSLAND, D. 2016. Association of Platelet Serotonin Levels in Alzheimer's Disease with Clinical and Cerebrospinal Fluid Markers. *J Alzheimers Dis,* 53**,** 621-30.

TAKAHASHI, K., TANABE, K., OHNUKI, M., NARITA, M., ICHISAKA, T., TOMODA, K. & YAMANAKA, S. 2007. Induction of pluripotent stem cells from adult human fibroblasts by defined factors. *Cell,* 131**,** 861-72.

TAKAHASHI, K. & YAMANAKA, S. 2006. Induction of pluripotent stem cells from mouse embryonic and adult fibroblast cultures by defined factors. *Cell,* 126**,** 663-76.

TAMAGNO, E., BARDINI, P., GUGLIELMOTTO, M., DANNI, O. & TABATON, M. 2006. The various aggregation states of beta-amyloid 1-42 mediate different effects on oxidative stress, neurodegeneration, and BACE-1 expression. *Free Radic Biol Med,* 41**,** 202-12.

TAMAYEV, R., MATSUDA, S., ARANCIO, O. & D'ADAMIO, L. 2012. β- but not γ-secretase proteolysis of APP causes synaptic and memory deficits in a mouse model of dementia. *EMBO Mol Med,* 4**,** 171-9.

TAN, B. L., NORHAIZAN, M. E. & LIEW, W. P. 2018. Nutrients and Oxidative Stress: Friend or Foe? *Oxid Med Cell Longev,* 2018**,** 9719584.

TAN, J. L., LI, Q. X., CICCOTOSTO, G. D., CROUCH, P. J., CULVENOR, J. G., WHITE, A. R. & EVIN, G. 2013. Mild oxidative stress induces redistribution of BACE1 in non-apoptotic conditions and promotes the amyloidogenic processing of Alzheimer's disease amyloid precursor protein. *PLoS One,* 8**,** e61246.

TATEBE, H., KASAI, T., OHMICHI, T., KISHI, Y., KAKEYA, T., WARAGAI, M., KONDO, M., ALLSOP, D. & TOKUDA, T. 2017. Quantification of plasma phosphorylated tau to use as a biomarker for brain Alzheimer pathology: pilot case-control studies including patients with Alzheimer's disease and down syndrome. *Mol Neurodegener,* 12**,** 63.

TESTA, G., STAURENGHI, E., ZERBINATI, C., GARGIULO, S., IULIANO, L., GIACCONE, G., FANTÒ, F., POLI, G., LEONARDUZZI, G. & GAMBA, P. 2016. Changes in brain oxysterols at different stages of Alzheimer's disease: Their involvement in neuroinflammation. *Redox Biol,* 10**,** 24-33.

THAL, D. R. & BRAAK, H. 2005. [Post-mortem diagnosis of Alzheimer's disease]. *Pathologe,* 26**,** 201-13.

THEOFILAS, P., EHRENBERG, A. J., NGUY, A., THACKREY, J. M., DUNLOP, S., MEJIA, M. B., ALHO, A. T., PARAIZO LEITE, R. E., RODRIGUEZ, R. D., SUEMOTO, C. K., NASCIMENTO, C. F., CHIN, M., MEDINA-CLEGHORN, D., CUERVO, A. M., ARKIN, M., SEELEY, W. W., MILLER, B. L., NITRINI, R., PASQUALUCCI, C. A., FILHO, W. J., RUEB, U., NEUHAUS, J., HEINSEN, H. & GRINBERG, L. T. 2018. Probing the correlation of neuronal loss, neurofibrillary tangles, and cell death markers across the Alzheimer's disease Braak stages: a quantitative study in humans. *Neurobiol Aging,* 61**,** 1-12.

TRAMUTOLA, A., LANZILLOTTA, C., PERLUIGI, M. & BUTTERFIELD, D. A. 2017. Oxidative stress, protein modification and Alzheimer disease. *Brain Res Bull,* 133**,** 88-96.

TUBSUWAN, A., PIRES, C., RASMUSSEN, M. A., SCHMID, B., NIELSEN, J. E., HJERMIND, L. E., HALL, V., NIELSEN, T. T., WALDEMAR, G., HYTTEL, P., CLAUSEN, C., KITIYANANT, N., FREUDE, K. K. & HOLST, B. 2016. Generation of induced pluripotent stem cells (iPSCs) from an Alzheimer's disease patient carrying a L150P mutation in PSEN-1. *Stem Cell Res,* 16**,** 110-2.

UM, J. W., NYGAARD, H. B., HEISS, J. K., KOSTYLEV, M. A., STAGI, M., VORTMEYER, A., WISNIEWSKI, T., GUNTHER, E. C. & STRITTMATTER, S. M. 2012. Alzheimer amyloid-β oligomer bound to postsynaptic prion protein activates Fyn to impair neurons. *Nat Neurosci,* 15**,** 1227-35.

UMEDA, T., TOMIYAMA, T., SAKAMA, N., TANAKA, S., LAMBERT, M. P., KLEIN, W. L. & MORI, H. 2011. Intraneuronal amyloid β oligomers cause cell death via endoplasmic reticulum stress, endosomal/lysosomal leakage, and mitochondrial dysfunction in vivo. *J Neurosci Res,* 89**,** 1031-42.

VADODARIA, K. C., JI, Y., SKIME, M., PAQUOLA, A., NELSON, T., HALL-FLAVIN, D., FREDLENDER, C., HEARD, K. J., DENG, Y., LE, A. T., DAVE, S., FUNG, L., LI, X., MARCHETTO, M. C., WEINSHILBOUM, R. & GAGE, F. H. 2019. Serotonin-induced hyperactivity in SSRI-resistant major depressive disorder patient-derived neurons. *Mol Psychiatry,* 24**,** 795-807.

VADODARIA, K. C., MERTENS, J., PAQUOLA, A., BARDY, C., LI, X., JAPPELLI, R., FUNG, L., MARCHETTO, M. C., HAMM, M., GORRIS, M., KOCH, P. & GAGE, F. H. 2016.

Generation of functional human serotonergic neurons from fibroblasts. *Mol Psychiatry,* 21**,** 49-61.

VAN 'T ERVE, T. J., KADIISKA, M. B., LONDON, S. J. & MASON, R. P. 2017. Classifying oxidative stress by F. *Redox Biol,* 12**,** 582-599.

VAN DER LEE, S. J., WOLTERS, F. J., IKRAM, M. K., HOFMAN, A., IKRAM, M. A., AMIN, N. & VAN DUIJN, C. M. 2018. The effect of APOE and other common genetic variants on the onset of Alzheimer's disease and dementia: a community-based cohort study. *Lancet Neurol,* 17**,** 434-444.

VAN DYCK, C. H. 2018. Anti-Amyloid-β Monoclonal Antibodies for Alzheimer's Disease: Pitfalls and Promise. *Biol Psychiatry,* 83**,** 311-319.

VASSAR, R. 2001. The beta-secretase, BACE: a prime drug target for Alzheimer's disease. *J Mol Neurosci,* 17**,** 157-70.

VASSAR, R., BENNETT, B. D., BABU-KHAN, S., KAHN, S., MENDIAZ, E. A., DENIS, P., TEPLOW, D. B., ROSS, S., AMARANTE, P., LOELOFF, R., LUO, Y., FISHER, S., FULLER, J., EDENSON, S., LILE, J., JAROSINSKI, M. A., BIERE, A. L., CURRAN, E., BURGESS, T., LOUIS, J. C., COLLINS, F., TREANOR, J., ROGERS, G. & CITRON, M. 1999. Beta-secretase cleavage of Alzheimer's amyloid precursor protein by the transmembrane aspartic protease BACE. *Science,* 286**,** 735-41.

VASSILAKI, M., AAKRE, J. A., SYRJANEN, J. A., MIELKE, M. M., GEDA, Y. E., KREMERS, W. K., MACHULDA, M. M., ALHURANI, R. E., STAUBO, S. C., KNOPMAN, D. S., PETERSEN, R. C., LOWE, V. J., JACK, C. R. & ROBERTS, R. O. 2018. Mediterranean Diet, Its Components, and Amyloid Imaging Biomarkers. *J Alzheimers Dis,* 64**,** 281-290.

VERBERK, I. M. W., SLOT, R. E., VERFAILLIE, S. C. J., HEIJST, H., PRINS, N. D., VAN BERCKEL, B. N. M., SCHELTENS, P., TEUNISSEN, C. E. & VAN DER FLIER, W. M. 2018. Plasma Amyloid as Prescreener for the Earliest Alzheimer Pathological Changes. *Ann Neurol,* 84**,** 648-658.

VERDILE , G. & KEANE, K. C., VINICIUS MEDIC, SANDRA SABALE, MIHEER ROWLES, JOANNE WIJESEKARA, NADEEJA MARTINS, RALPH FRASER, PAUL NEWSHOLME, PHILIP 2015. Inflammation and Oxidative Stress: The Molecular Connectivity between Insulin Resistance, Obesity, and Alzheimer's Disease. *Mediators of Inflammation,* 26**,** 1-17.

VERGALLO, A., MÉGRET, L., LISTA, S., CAVEDO, E., ZETTERBERG, H., BLENNOW, K., VANMECHELEN, E., DE VOS, A., HABERT, M. O., POTIER, M. C., DUBOIS, B., NERI, C., HAMPEL, H., GROUP, I.-P. S. & (APMI), A. P. M. I. 2019. Plasma amyloid β 40/42 ratio predicts cerebral amyloidosis in cognitively normal individuals at risk for Alzheimer's disease. *Alzheimers Dement,* 15**,** 764-775.

VILLENEUVE, S., RABINOVICI, G. D., COHN-SHEEHY, B. I., MADISON, C., AYAKTA, N., GHOSH, P. M., LA JOIE, R., ARTHUR-BENTIL, S. K., VOGEL, J. W., MARKS, S. M., LEHMANN, M., ROSEN, H. J., REED, B., OLICHNEY, J., BOXER, A. L., MILLER, B. L., BORYS, E., JIN, L. W., HUANG, E. J., GRINBERG, L. T., DECARLI, C., SEELEY, W. W. & JAGUST, W. 2015. Existing Pittsburgh Compound-B positron emission tomography thresholds are too high: statistical and pathological evaluation. *Brain,* 138**,** 2020-33.

VLASSENKO, A. G., BENZINGER, T. L. & MORRIS, J. C. 2012. PET amyloid-beta imaging in preclinical Alzheimer's disease. *Biochim Biophys Acta,* 1822**,** 370-9.

VON LINSTOW, C. U., WAIDER, J., GREBING, M., METAXAS, A., LESCH, K. P. & FINSEN, B. 2017. Serotonin augmentation therapy by escitalopram has minimal effects on amyloid-β levels in early-stage Alzheimer's-like disease in mice. *Alzheimers Res Ther,* 9**,** 74.

VOS, S. J., XIONG, C., VISSER, P. J., JASIELEC, M. S., HASSENSTAB, J., GRANT, E. A., CAIRNS, N. J., MORRIS, J. C., HOLTZMAN, D. M. & FAGAN, A. M. 2013. Preclinical Alzheimer's disease and its outcome: a longitudinal cohort study. *Lancet Neurol,* 12**,** 957-65.

VOYTYUK, I., DE STROOPER, B. & CHÁVEZ-GUTIÉRREZ, L. 2018a. Modulation of γ- and β-Secretases as Early Prevention Against Alzheimer's Disease. *Biol Psychiatry,* 83**,** 320-327.

VOYTYUK, I., MUELLER, S. A., HERBER, J., SNELLINX, A., MOECHARS, D., VAN LOO, G., LICHTENTHALER, S. F. & DE STROOPER, B. 2018b. BACE2 distribution in major brain cell types and identification of novel substrates. *Life Sci Alliance,* 1**,** e201800026.

WANG, C. & HOLTZMAN, D. M. 2020. Bidirectional relationship between sleep and Alzheimer's disease: role of amyloid, tau, and other factors. *Neuropsychopharmacology,* 45**,** 104-120.

WANG, H., HU, L., LIU, C., SU, Z., WANG, L., PAN, G., GUO, Y. & HE, J. 2016a. 5-HT2 receptors mediate functional modulation of GABAa receptors and inhibitory synaptic transmissions in human iPS-derived neurons. *Sci Rep,* 6**,** 20033.

WANG, H. X., MACDONALD, S. W., DEKHTYAR, S. & FRATIGLIONI, L. 2017a. Association of lifelong exposure to cognitive reserve-enhancing factors with dementia risk: A community-based cohort study. *PLoS Med,* 14**,** e1002251.

WANG, X., ZHOU, X., LI, G., ZHANG, Y., WU, Y. & SONG, W. 2017b. Modifications and Trafficking of APP in the Pathogenesis of Alzheimer's Disease. *Front Mol Neurosci,* 10**,** 294.

WANG, Y. & MANDELKOW, E. 2016. Tau in physiology and pathology. *Nat Rev Neurosci,* 17**,** 5-21.

WANG, Y. J., REN, Q. G., GONG, W. G., WU, D., TANG, X., LI, X. L., WU, F. F., BAI, F., XU, L. & ZHANG, Z. J. 2016b. Escitalopram attenuates β-amyloid-induced tau hyperphosphorylation in primary hippocampal neurons through the 5-HT1A receptor mediated Akt/GSK-3β pathway. *Oncotarget,* 7**,** 13328-39.

WESTON, P. S., NICHOLAS, J. M., LEHMANN, M., RYAN, N. S., LIANG, Y., MACPHERSON, K., MODAT, M., ROSSOR, M. N., SCHOTT, J. M., OURSELIN, S. & FOX, N. C. 2016. Presymptomatic cortical thinning in familial Alzheimer disease: A longitudinal MRI study. *Neurology,* 87**,** 2050-2057.

WETZEL, S., SEIPOLD, L. & SAFTIG, P. 2017. The metalloproteinase ADAM10: A useful therapeutic target? *Biochim Biophys Acta Mol Cell Res,* 1864**,** 2071-2081.

WINBLAD, B., AMOUYEL, P., ANDRIEU, S., BALLARD, C., BRAYNE, C., BRODATY, H., CEDAZO-MINGUEZ, A., DUBOIS, B., EDVARDSSON, D., FELDMAN, H., FRATIGLIONI, L., FRISONI, G. B., GAUTHIER, S., GEORGES, J., GRAFF, C., IQBAL, K., JESSEN, F., JOHANSSON, G., JÖNSSON, L., KIVIPELTO, M., KNAPP, M., MANGIALASCHE, F., MELIS, R., NORDBERG, A., RIKKERT, M. O., QIU, C., SAKMAR, T. P., SCHELTENS, P., SCHNEIDER, L. S., SPERLING, R., TJERNBERG, L. O., WALDEMAR, G., WIMO, A. & ZETTERBERG, H. 2016. Defeating Alzheimer's disease and other dementias: a priority for European science and society. *Lancet Neurol,* 15**,** 455-532.

WOLFE, M. S. 2020. Substrate recognition and processing by γ-secretase. *Biochim Biophys Acta Biomembr,* 1862**,** 183016.

WOODRUFF, G., YOUNG, J. E., MARTINEZ, F. J., BUEN, F., GORE, A., KINAGA, J., LI, Z., YUAN, S. H., ZHANG, K. & GOLDSTEIN, L. S. 2013. The presenilin-1 ΔE9 mutation results in reduced γ-secretase activity, but not total loss of PS1 function, in isogenic human stem cells. *Cell Rep,* 5**,** 974-85.

WU, H. Y., KUO, P. C., WANG, Y. T., LIN, H. T., ROE, A. D., WANG, B. Y., HAN, C. L., HYMAN, B. T., CHEN, Y. J. & TAI, H. C. 2018. β-Amyloid Induces Pathology-Related Patterns of Tau Hyperphosphorylation at Synaptic Terminals. *J Neuropathol Exp Neurol,* 77**,** 814-826.

XIA, D., WATANABE, H., WU, B., LEE, S. H., LI, Y., TSVETKOV, E., BOLSHAKOV, V. Y., SHEN, J. & KELLEHER, R. J. 2015. Presenilin-1 knockin mice reveal loss-of-function mechanism for familial Alzheimer's disease. *Neuron,* 85**,** 967-81.

XU, D., SHARMA, C. & HEMLER, M. E. 2009. Tetraspanin12 regulates ADAM10-dependent cleavage of amyloid precursor protein. *FASEB J,* 23**,** 3674-81.

XU, T. H., YAN, Y., KANG, Y., JIANG, Y., MELCHER, K. & XU, H. E. 2016. Alzheimer's disease-associated mutations increase amyloid precursor protein resistance to γ-secretase cleavage and the Aβ42/Aβ40 ratio. *Cell Discov,* 2**,** 16026.

XU, W., TAN, L., WANG, H. F., JIANG, T., TAN, M. S., ZHAO, Q. F., LI, J. Q., WANG, J. & YU, J. T. 2015. Meta-analysis of modifiable risk factors for Alzheimer's disease. *J Neurol Neurosurg Psychiatry,* 86**,** 1299-306.

YANG, J., ZHAO, H., MA, Y., SHI, G., SONG, J., TANG, Y., LI, S., LI, T., LIU, N., TANG, F., GU, J., ZHANG, L., ZHANG, Z., ZHANG, X., JIN, Y. & LE, W. 2017a. Early pathogenic event of Alzheimer's disease documented in iPSCs from patients with PSEN1 mutations. *Oncotarget,* 8**,** 7900-7913.

YANG, L., RIEVES, D. & GANLEY, C. 2012. Brain amyloid imaging--FDA approval of florbetapir F18 injection. *N Engl J Med,* 367**,** 885-7.

YANG, L. B., LINDHOLM, K., YAN, R., CITRON, M., XIA, W., YANG, X. L., BEACH, T., SUE, L., WONG, P., PRICE, D., LI, R. & SHEN, Y. 2003. Elevated beta-secretase expression and enzymatic activity detected in sporadic Alzheimer disease. *Nat Med,* 9**,** 3-4.

YANG, T., LI, S., XU, H., WALSH, D. M. & SELKOE, D. J. 2017b. Large Soluble Oligomers of Amyloid β-Protein from Alzheimer Brain Are Far Less Neuroactive Than the Smaller Oligomers to Which They Dissociate. *J Neurosci,* 37**,** 152-163.

YARIBEYGI, H., PANAHI, Y., JAVADI, B. & SAHEBKAR, A. 2018. The Underlying Role of Oxidative Stress in Neurodegeneration: A Mechanistic Review. *CNS Neurol Disord Drug Targets,* 17**,** 207-215.

YUAN, X. Z., SUN, S., TAN, C. C., YU, J. T. & TAN, L. 2017. The Role of ADAM10 in Alzheimer's Disease. *J Alzheimers Dis,* 58**,** 303-322.

YUN, S. H., SIM, E. H., GOH, R. Y., PARK, J. I. & HAN, J. Y. 2016. Platelet Activation: The Mechanisms and Potential Biomarkers. *Biomed Res Int,* 2016**,** 9060143.

YUN, S. M., CHO, S. J., JO, C., PARK, M. H., HAN, C. & KOH, Y. H. 2019. Elevation of plasma soluble amyloid precursor protein beta in Alzheimer's disease. *Arch Gerontol Geriatr,* 87**,** 103995.

ZABEL, M., NACKENOFF, A., KIRSCH, W. M., HARRISON, F. E., PERRY, G. & SCHRAG, M. 2018. Markers of oxidative damage to lipids, nucleic acids and proteins and antioxidant

enzymes activities in Alzheimer's disease brain: A meta-analysis in human pathological specimens. *Free Radic Biol Med,* 115**,** 351-360.

ZANNIS, V. I., BRESLOW, J. L., UTERMANN, G., MAHLEY, R. W., WEISGRABER, K. H., HAVEL, R. J., GOLDSTEIN, J. L., BROWN, M. S., SCHONFELD, G., HAZZARD, W. R. & BLUM, C. 1982. Proposed nomenclature of apoE isoproteins, apoE genotypes, and phenotypes. *J Lipid Res,* 23**,** 911-4.

ZETTERBERG, H. 2019. Blood-based biomarkers for Alzheimer's disease-An update. *J Neurosci Methods,* 319**,** 2-6.

ZETTERBERG, H., ANDREASSON, U., HANSSON, O., WU, G., SANKARANARAYANAN, S., ANDERSSON, M. E., BUCHHAVE, P., LONDOS, E., UMEK, R. M., MINTHON, L., SIMON, A. J. & BLENNOW, K. 2008. Elevated cerebrospinal fluid BACE1 activity in incipient Alzheimer disease. *Arch Neurol,* 65**,** 1102-7.

ZETTERBERG, H. & BLENNOW, K. 2018. From Cerebrospinal Fluid to Blood: The Third Wave of Fluid Biomarkers for Alzheimer's Disease. *J Alzheimers Dis,* 64**,** S271-S279.

ZETTERBERG, H., WILSON, D., ANDREASSON, U., MINTHON, L., BLENNOW, K., RANDALL, J. & HANSSON, O. 2013. Plasma tau levels in Alzheimer's disease. *Alzheimers Res Ther,* 5**,** 9.

ZHANG, D., QI, Y., KLYUBIN, I., ONDREJCAK, T., SARELL, C. J., CUELLO, A. C., COLLINGE, J. & ROWAN, M. J. 2017. Targeting glutamatergic and cellular prion protein mechanisms of amyloid β-mediated persistent synaptic plasticity disruption: Longitudinal studies. *Neuropharmacology,* 121**,** 231-246.

ZHANG, H., SUN, S., HERREMAN, A., DE STROOPER, B. & BEZPROZVANNY, I. 2010. Role of presenilins in neuronal calcium homeostasis. *J Neurosci,* 30**,** 8566-80.

ZHANG, X., LI, Y., XU, H. & ZHANG, Y. W. 2014. The γ-secretase complex: from structure to function. *Front Cell Neurosci,* 8**,** 427.

ZHAO, Q. F., TAN, L., WANG, H. F., JIANG, T., TAN, M. S., XU, W., LI, J. Q., WANG, J., LAI, T. J. & YU, J. T. 2016. The prevalence of neuropsychiatric symptoms in Alzheimer's disease: Systematic review and meta-analysis. *J Affect Disord,* 190**,** 264-271.

ZHAO, Y. & ZHAO, B. 2013. Oxidative stress and the pathogenesis of Alzheimer's disease. *Oxid Med Cell Longev,* 2013**,** 316523.

ZHENG, W., TSAI, M. Y. & WOLYNES, P. G. 2017. Comparing the Aggregation Free Energy Landscapes of Amyloid Beta(1-42) and Amyloid Beta(1-40). *J Am Chem Soc,* 139**,** 16666-16676.

ZHOU, R., YANG, G., GUO, X., ZHOU, Q., LEI, J. & SHI, Y. 2019. Recognition of the amyloid precursor protein by human γ-secretase. *Science,* 363.

ZHU, X., RAINA, A. K., PERRY, G. & SMITH, M. A. 2004. Alzheimer's disease: the two-hit hypothesis. *Lancet Neurol,* 3**,** 219-26.

ZOLLO, A., ALLEN, Z., RASMUSSEN, H. F., IANNUZZI, F., SHI, Y., LARSEN, A., MAIER, T. J. & MATRONE, C. 2017. Sortilin-Related Receptor Expression in Human Neural Stem Cells Derived from Alzheimer's Disease Patients Carrying the APOE Epsilon 4 Allele. *Neural Plast,* 2017**,** 1892612.

ZOLTOWSKA, K. M., MAESAKO, M. & BEREZOVSKA, O. 2016. Interrelationship between Changes in the Amyloid β 42/40 Ratio and Presenilin 1 Conformation. *Mol Med,* 22**,** 329-337.

ZOTCHEVA, E., BERGH, S., SELBÆK, G., KROKSTAD, S., HÅBERG, A. K., STRAND, B. H. & ERNSTSEN, L. 2018. Midlife Physical Activity, Psychological Distress, and Dementia Risk: The HUNT Study. *J Alzheimers Dis,* 66**,** 825-833.